Energy & Environmental Research Center
15 North 23rd Street, Stop 9018 • Grand Forks, ND 58202-9018 • P. 701.777.5000 • F. 701.777.5181
www.undeerc.org

June 26, 2024

Mr. Reice Haase
Deputy Director
North Dakota Industrial Commission
State Capitol, 14th Floor
600 East Boulevard Avenue, Department 405
Bismarck, ND 58505-0840

Dear Mr. Haase:

Subject: Final Report Entitled "Unitized Legacy Oil Fields: Prototypes for Revitalizing Conventional Oil Fields in North Dakota"; Contract No. G-045-086
EERC Fund 26645

Attached please find the subject final report along with the required one-page summary. If you have any questions, please contact me by phone at (701) 777-5343 or by email at tjiang@undeerc.org.

Sincerely,

DocuSigned by:
Jim Sorensen for
0671D00C8437443...
Todd Jiang
Principal Reservoir Engineer

TJ/ro

Attachment

c: Brent Brannan, North Dakota Industrial Commission
Erin Stieg, North Dakota Industrial Commission

UNITIZED LEGACY OIL FIELDS: PROTOTYPES FOR REVITALIZING CONVENTIONAL OIL FIELDS IN NORTH DAKOTA

Final Report

Prepared for:

Reice Haase

North Dakota Industrial Commission
600 East Boulevard Avenue, Department 405
State Capitol, 14th Floor
Bismarck, ND 58505-0840

Contract No. G-045-086

Prepared by:

Tao (Todd) Jiang
Lu Jin
Stephen N. Guillot
Michael P. Warmack
Xincheng Wan
Chenyu Wu
Nidhal Badrouchi
Neil W. Dotzenrod
Motaz Saeed
Lawrance J. Pekot
Steven A. Smith
Nicholas W. Bosshart
Jamie A. Schod
James A. Sorensen
John A. Hamling

Energy & Environmental Research Center
University of North Dakota
15 North 23rd Street, Stop 9018
Grand Forks, ND 58202-9018

2024-EERC-06-02

June 2024

EERC DISCLAIMER

LEGAL NOTICE: This research report was prepared by the Energy & Environmental Research Center of the University of North Dakota (UND EERC) as an account of work sponsored by the North Dakota Industrial Commission (NDIC) (SPONSOR). Because of the research nature of the work performed, neither UND EERC, nor any of its employees makes any warranty, express or implied, or assumes any legal liability or responsibility for the accuracy, completeness, or usefulness of any information, apparatus, product, or process disclosed, or represents that its use would not infringe privately owned rights. Reference herein to any specific commercial product, process, or service by trade name, trademark, manufacturer, or otherwise does not necessarily constitute or imply its endorsement or recommendation by UND EERC. SPONSOR understands and accepts that this research report and any associated deliverables are intended for a specific project. Any modifications of the report or of any associated deliverables or use or reuse other than for the intended project is at the sole risk of the SPONSOR and without liability or legal exposure to UND EERC or to its directors, officers, or employees.

NDIC DISCLAIMER

LEGAL NOTICE: This research report was prepared by UND EERC as an account of work sponsored by NDIC through the Oil and Gas Research Program. To the best of UND EERC's knowledge and belief, this report is true, complete, and accurate; however, because of the research nature of the work performed, neither UND EERC, NDIC, nor any of their directors, officers, or employees makes any warranty, express or implied, or assumes any legal liability or responsibility for the use of any information, apparatus, product, method, process, or similar item disclosed or represents that its use would not infringe privately owned rights. Reference herein to any specific commercial product, process, or service by trade name, trademark, manufacturer, or otherwise does not necessarily constitute or imply its endorsement or recommendation by UND EERC or NDIC. NDIC understands and accepts that this research report and any associated deliverables are intended for a specific project. Any reuse, extensions, or modifications of the report or any associated deliverables by NDIC or others will be at such party's sole risk and without liability or legal exposure to UND EERC or to their directors, officers, and employees.

ACKNOWLEDGMENT

The EERC would like to thank project partner Eagle Energy Partners Tundra, LLC for its in-kind support and active engagement, which has made the successful execution of this project possible.

TABLE OF CONTENTS

Continued . . .

TABLE OF CONTENTS (continued)

LIST OF FIGURES

Continued . . .

LIST OF FIGURES (continued)

Continued . . .

LIST OF FIGURES (continued)

LIST OF TABLES

UNITIZED LEGACY OIL FIELDS: PROTOTYPES FOR REVITALIZING CONVENTIONAL OIL FIELDS IN NORTH DAKOTA

EXECUTIVE SUMMARY

North Dakota has abundant oil and gas resources in both conventional and unconventional formations, with oil and gas production serving as a mainstay industrial activity since the 1950s. Over 1935 million barrels (MMbbl) of oil have been produced from the conventional formations through 2020.[1] Many conventional reservoirs have undergone primary production and water-flooding operations over the past 70 years, leading to a decline in oil production rates since the 1990s. This research aims to enable revitalization of conventional oil fields in North Dakota, with the ultimate goal of increasing oil production and prolonging the operational lifetime of fields, contributing to the development of North Dakota's endowment of oil and benefiting areas of the state beyond the extent of current Bakken petroleum system production.

The funding provided to the Energy & Environmental Research Center (EERC) was used for evaluating (secondary) improved oil recovery (IOR) potential and tertiary enhanced oil recovery (EOR) techniques for the Foreman Butte Field, which produces from the Madison Group. This evaluation was conducted with in-kind support from our project partner, Eagle Energy Partners Tundra, LLC (EEPT). The EERC collaborated closely with EEPT on various aspects, including the following:

- Field Production Performance Evaluation: Assessing historical and current production data to understand trends and identify opportunities for improvement.
- Field Facility Assessment: Evaluating existing infrastructure to determine its suitability for EOR operations.
- Water Injection Pilot Study: Evaluating a pilot project to test the efficacy of water injection in increasing oil recovery.
- Collection of Additional Data from Stratigraphic Well: Gathering new data from the legacy field to inform reservoir characterization and modeling.
- Rock and Fluid Characterization Analysis: Analyzing reservoir rocks and fluids to determine their properties and behavior under different EOR scenarios.
- Laboratory Evaluations of EOR Methods: Testing various EOR techniques in the lab to identify those most suitable for the Madison Group and other similar reservoirs.
- Detailed Site Characterization and Geologic Model Construction: Creating detailed static geologic models of the reservoir to guide EOR evaluation through predictive simulations.

[1] North Dakota Industrial Commission, 2024. Department of Mineral Resources, Oil and Gas Division: https://www.dmr.nd.gov/oilgas/ (accessed March 26, 2024).

- History Matching of Field Historical Production, and Evaluation of EOR Methods Using Field-Scale Simulation: Comparing simulation results with historical production data to validate models, and assessing the potential of different EOR techniques.

- Development of a Machine Learning-Based CO_2 EOR Screening Tool: Creating a tool to rank potential CO_2 EOR candidates and reservoirs in North Dakota based on various criteria.

The results of the research effort suggest that the widely distributed carbonate reservoirs in the area, including the Madison Group and other producing horizons, are among the main oil-producing formations. While water flooding and CO_2 flooding show potential for improving the oil recovery, water flooding acts as a precursor to CO_2 EOR and may not be as effective as using CO_2 directly because of factors such as the high initial water saturation in the reservoir, tight formation matrix petrophysical properties, and the presence of the natural fracture networks. Those are confirmed from both simulation and laboratory evaluations. Additional challenges for IOR and EOR implementations are identified, which include aging equipment and techniques used such as open hole completion, and also complicate the direct implementation of some of the EOR techniques. Upgrading equipment to reduce the producing pressure and using stimulation to reduce the skin factor near the wellbore may also be effective in improving the production performance. In addition to the CO_2 EOR method, other EOR methods such as surfactant EOR and engineered water injection also offer viable options for revitalizing conventional oil fields. Those methods could provide immediate benefits to operators and the state and facilitate the extension of the CO_2 transportation infrastructure, thus making the CO_2 source more accessible for future field CO_2 EOR implementation.

UNITIZED LEGACY OIL FIELDS: PROTOTYPES FOR REVITALIZING CONVENTIONAL OIL FIELDS IN NORTH DAKOTA

1.0 INTRODUCTION

North Dakota has abundant oil and gas resources in both conventional and unconventional formations. Oil and gas production has been one of the main industrial activities in North Dakota since the 1950s. Over 1935 million barrels (MMbbl) of oil have been produced from conventional formations through the 2020s (North Dakota Industrial Commission, 2024), as shown in Table 1-1. Most conventional reservoirs have gone through primary production and water-flooding operations in the past 70 years. The oil production rates continue to decline in these conventional reservoirs, as illustrated in Figure 1-1. However, studies indicated that an additional 280 MMbbl to over 630 MMbbl of oil could be recovered from the 86 unitized conventional oil fields through CO_2 enhanced oil recovery (EOR) (North Dakota Legislative Management, 2014). Peck and others (2019) determined that potential incremental oil recovery from CO_2 injection across North Dakota could be as much as one billion barrels.

Prior to 2022, there has been limited CO_2 flooding-related activities in the Williston Basin. A small-spacing injection pilot was conducted in the Mission Canyon Formation at the Little Knife Field in 1981 (Gulf Oil, 1983). This paper provides a comprehensive petrophysical and reservoir engineering evaluation in preparation for CO_2 flooding. The pilot results provide useful references for others considering CO_2 flooding within the Williston Basin; however, they do not incorporate integrated petrographic techniques for carbonate reservoir description, where pore types are characterized and used to define reservoir flow units. Other work has provided important approaches to the discourse for the development of Williston Basin with CO_2 EOR. Christman and Gorell (1990) and Good and Downer (1988) focused on predicting CO_2 injectivity, which presently can be predicted with greater certainty than when these studies were undertaken. Ruzyla and Friedman (1982) provided insights on the geological heterogeneity of carbonates. Bethel and Welbourn (1959) documented a process for a thorough reservoir description and petrophysical

Table 1-1. Summary of Oil Production from the Main Conventional Formations in North Dakota (North Dakota Industrial Commission, 2024)

No.	Group/Formation	Cumulative Oil, bbl	%	Active Wells
1	Madison	980,361,163	50.65	5647
2	Red River B	187,856,067	9.70	560
3	Red River	118,830,837	6.14	769
4	Sanish	117,717,862	6.08	380
5	Devonian	103,983,324	5.37	146
6	Heath	67,516,761	3.49	198
7	Silurian	65,996,855	3.41	223
8	Lodgepole	63,238,275	3.27	52
9	Duperow	54,013,796	2.79	353
10	Spearfish/Charles	52,625,326	2.72	238
11	Others	123,597,657	6.39	934
Total		**1,935,737,923**	**100.00**	**9500**

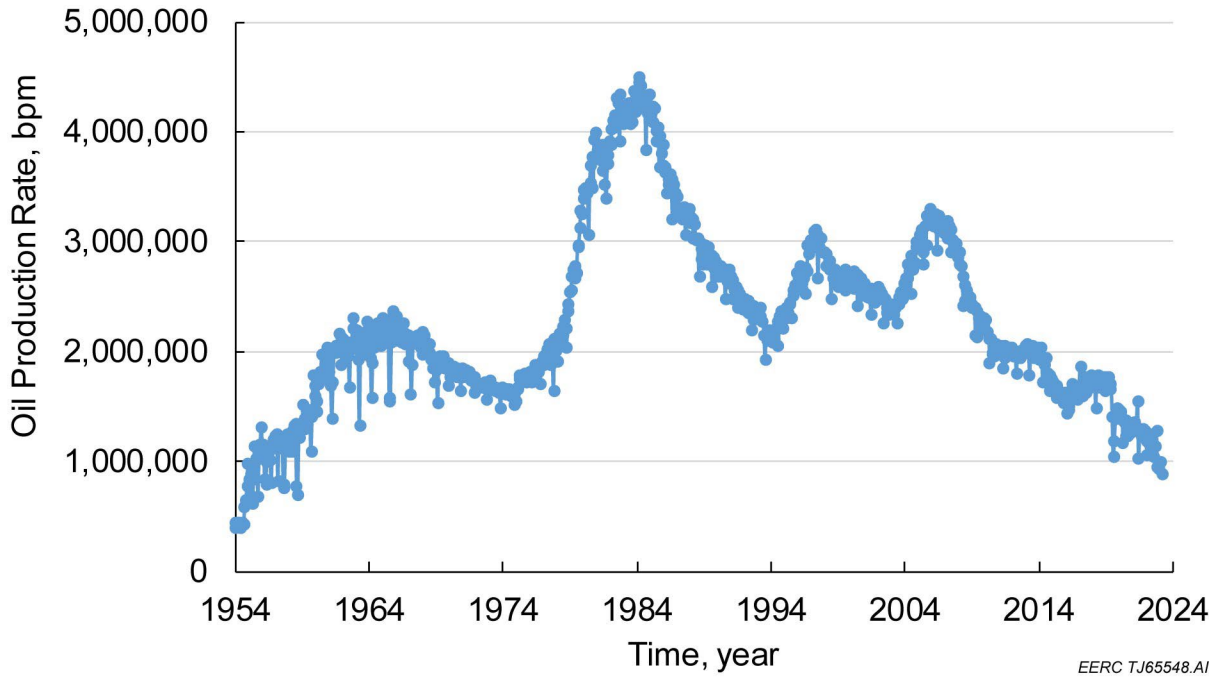

Figure 1-1. Oil production history of conventional reservoirs in North Dakota (North Dakota Industrial Commission, 2024).

study based on well log and core analysis technology that has since been vastly improved. However, it was written before digital reservoir simulation was practiced; therefore, it was not written with that end in mind. Reviewing the literature illuminates the need for an updated template for assessing CO_2 flood feasibility in the Williston Basin, and this template should be flexible enough to provide guidance for analyzing not just CO_2 flooding but any other production enhancement opportunity.

The objective of the research is closely collaborating with our project partner, Eagle Energy Partners Tundra, LLC (EEPT), to investigate waterflooding feasibility, potential CO_2 EOR and other revitalization strategies for Foreman Butte Field, producing from the Madison Group. The workflow template that has been developed can be applied for evaluating other EOR methods and their implementations to the Madison Group and other suitable production horizons, which include those carbonate reservoirs that contribute most of the oil productions. The methodology used herein is primarily a generic approach applicable to many fields but is tailored to conventional Williston Basin reservoirs and includes testing and evaluation relative to CO_2 confinement and retention that recently became more relevant with the passage of incentives for carbon sequestration. Other means of reviving oil production in these fields will also be addressed, such as well recompletion and stimulation and drilling of infill vertical or horizontal wells, but assessing CO_2 EOR potential is the focal point. These additional methods are addressed individually, though economic considerations have not been investigated in detail.

2.0 KEY LESSONS LEARNED AND RECOMMENDATIONS

The key lessons learned by the Energy & Environmental Research Center's (EERC's) assessment of revitalizing conventional oil fields in North Dakota include technical evaluations of Foreman Butte Field, producing from Madison Group, and its water flooding and potential CO_2 or other EOR methods performance; development of a comprehensive technical workflow that can be applicable for assessing other conventional oil fields in North Dakota; and applicability to another conventional oil field producing from the Red River Formation.

Regarding Foreman Butte Field, the study showed that a tight rock matrix, natural fractures, and residual oil were observed in core samples acquired from a newly drilled stratigraphic test well, with data collection targeting the Ratcliffe interval of the Charles Formation of the Madison Group. The recovery factors remain low and oil production rates decline fast during primary production. Core-flooding experiments indicated the effectiveness of various EOR methods, including water flooding and CO_2 flooding, in improving oil recovery. However, due to the reservoir's natural fracture network, high water saturation, and the rock's oil-wet and mixed-wet characteristics and heterogeneity, CO_2 flooding was more effective in extracting oil compared to water flooding.

Carbonate reservoirs are widely distributed among the main oil-producing formations, such as the Charles, Mission Canyon, Lodgepole, Red River, and others. These reservoirs exhibit a broad spectrum of pore types and sizes, ranging from micropores in mudstones to large vugs and caves. This heterogeneity in pore structure significantly influences the flow of hydrocarbons. Because of this complexity, developing alternative approaches and EOR techniques is crucial to reviving different types of legacy oil field reservoirs. A thorough review of various EOR techniques for carbonate reservoirs has been conducted to provide a deeper understanding of the methods available for improving oil production. This review highlights the importance of selecting the appropriate EOR method based on the specific characteristics of each reservoir. Understanding critical reservoir characteristics, such as porosity, permeability, fluid saturation, and rock wettability, is key to successfully implementing cost-effective techniques for enhancing oil recovery and prolonging production.

Detailed geologic modeling and high-efficiency field-scale simulation workflows have been developed to effectively assess the performance of different EOR methods in various types of reservoirs. The workflow applied to the Foreman Butte Field modeling and simulation and another carbonate reservoir producing from the Red River Formation. These tools allow for a better characterization of the reservoir, facilitating the selection and optimization of EOR techniques at the various operation conditions. Those can be evaluated and tailored to the specific reservoir and fluid properties of the reservoirs.

In addition, the facility and operability assessment suggests careful evaluation of the operational conditions and challenges for the different EOR techniques' implementation. Those evaluations include facility upgrade needs, integrity of existing and new infrastructure, and facilities' compatibility of different injection fluids with a reservoir and capability of managing the reservoir pressure and fluid dynamic changes and differences compared to the primary production. Upgrading the equipment and employing completion techniques can enhance oil

production, prior to effectively implementing the new improved oil recovery (IOR) and/or EOR strategies.

The study results on the feasibility of water flooding and CO_2 EOR in North Dakota's conventional oil fields have spurred discussions within the industry and have been presented at several prominent conferences. These include the Williston Basin Petroleum Conference, SPE Western Regional Meeting, SPE Improved Oil Recovery Conference, International Energy Agency EOR Technical Collaboration Program Meeting, CO_2 Conference, and the American Institute of Chemical Engineers Annual Meeting. Additionally, a peer-reviewed journal article detailing the findings was published in Geoenergy Science and Engineering.

3.0 EOR IN CONVENTIONAL RESERVOIRS IN WILLISTON BASIN

3.1 Carbonate Reservoirs in the Williston Basin

Carbonate reservoirs are widely distributed among the main oil-producing formations listed in Table 1-1. Characteristically different from sandstone reservoirs, carbonates are primarily composed of sedimentary rocks like limestone and dolostone, formed from the skeletal remains of marine organisms and precipitation of minerals from seawater. These reservoirs are deposited in a wide range of marine environments, leading to their diverse porosity and permeability characteristics. Unlike sandstones, which are typically more uniform in their porosity and permeability, carbonate reservoirs exhibit a broad spectrum of pore types and sizes, ranging from micropores in mudstones to large vugs and caves. This heterogeneity in pore structure significantly influences the storage and flow of hydrocarbons (Xu and others, 2020).

The Madison Group consists of sedimentary rocks primarily from the Mississippian period. It is well-known for its carbonate reservoirs, which include limestone and dolostone. The Lodgepole, Mission Canyon, and Charles Formations are the primary units within this group (Gaswirth and others, 2010). The Lodgepole Formation is known for its unique Waulsortian mound reservoirs (locally known as the Lodgepole Mounds), which are considered tight reservoirs, largely concentrated in Stark County, North Dakota. These mounds are primarily carbonate buildups that began as organic material accumulation on paleo-topographic highs (Burke and Lasemi, 1995). However, they exhibit some degree of porosity and permeability enhancements through fracturing and dissolution processes (Johnson, 1995). For example, within these mounds, the carbonate rocks typically have lower porosity unless enhanced by vuggy porosity and natural fractures. The fractures can notably improve the reservoir quality, making portions of the Lodgepole Formation effective for hydrocarbon production despite its overall tight nature (Montgomery, 1996). These structures are mostly sealed by impermeable limestone, which restricts lateral migration and effectively traps the oil within the mounds (Gaswirth and others, 2010).

In contrast, the Mission Canyon and Charles Formations account for the majority of oil production within the Madison Group. Unlike the Lodgepole, these formations are sourced by organic-rich carbonates and marly shales within their strata. They feature complex stratigraphy with multiple depositional cycles influenced by sea-level changes, creating diverse reservoir

architectures such as dolomitized mudstones, wackestones, and grainy limestones (Gerhard and others, 1991; Kerr, 1988). These intervals have conventional reservoir characteristics with significant oil production deriving from both matrix porosity and enhanced fracture networks. Fracturing is particularly crucial along structural features such as anticlines where increased permeability due to natural fractures facilitates hydrocarbon flow (Lindsay 1988). The presence of anhydrite layers interbedded with carbonate reservoirs can act as barriers to fluid flow. Notable oil-producing structures include the Nesson Anticline and the Billings Nose Anticline, which are characterized by extensive development and the use of advanced recovery techniques such as horizontal drilling (Gaswirth and others, 2010).

The oils of the Mission Canyon and Ratcliffe intervals of the Charles Formation are characterized by high sulfur content and aromatic hydrocarbons (Jarvie, 2001). The high aromaticity is indicative of limited migration, which tends to strip lighter aromatic compounds during movement through rocks with variable mineralogy. This contrasts with the Lodgepole mound fields, where the oil is believed to be sourced from the Bakken Formation (Jarvie 2001). For the Mission Canyon and Charles Formations, there is extensive production across major structures and in stratigraphic-structural traps, with the largest fields located on the Little Knife, Billings Nose, and Nesson anticlines (Jarvie 2001).

3.2 Field Applications of EOR in the Williston Basin

Since most conventional oil fields in North Dakota are near the end of their primary production phase, or have gone through the secondary oil recovery, EOR has become an important research topic to revitalizing these fields. The diversity of available EOR methods calls for careful selection and strategic design of the EOR technique to be employed, adapted to the unique characteristics of each field. A significant portion of the EOR projects and tests in the Williston Basin has concentrated on gas injection methods, including the use of air, CO_2, rich gas, and hydrocarbon (HC) gas injections (Ling and others, 2014). A notable majority of gas injection projects within the basin have utilized high-pressure air injection (HPAI). This method involves injecting air at elevated pressures to achieve two primary objectives: 1) for the air to serve as an immiscible gas that sweeps the oil and increases reservoir pressure and 2) to initiate an in situ combustion by facilitating a reaction between the oxygen in the injected air and the oil at high pressures, generating heat that in turn decreases the oil viscosity. Furthermore, the CO_2 produced during the combustion process acts as a solvent to the oil, decreasing the oil's viscosity and consequently enhancing the efficiency of the sweep through the reservoir (Moore and others, 2002; Denney 2011). Documented cases of HPAI experiments have been observed in the Red River Formation, specifically within the Horse Creek, Medicine Pole Hills, and Cedar Hills Fields, as well as in the Mission Canyon Formation at the Glass Bluff Field (Watts and others, 1997; Kumar and others, 1995; Ling and others, 2014). These field tests targeted reservoirs with porosities ranging from 5% to 25% and permeabilities from 0.0001 mD to 97 mD, with oil viscosities between 0.33 and 1.4 cP. These characteristics classify these formations as tight light oil plays. The outcomes of these field tests have exhibited incremental oil recoveries varying from 7% to 15%.

In addition to HPAI, miscible flooding EOR methods have also been tested across a variety of fields in the Williston Basin in North Dakota. These applications have incorporated both CO_2

and HC gas injections, implemented either as standalone gas injection or a water-alternating-gas (WAG) injection strategy. A CO_2 WAG test was reported in an inverted four-spot pattern at the Little Knife Field. The process commenced with reservoir pressurization from 2750 psi to 3400 psi via water injection, followed by a 1:1 CO_2 WAG injection, which yielded 18% oil recovery of 18% incremental to a 12.5% primary recovery factor (Thakur and others, 1984; Advanced Resources International, 2006a). The application of a propane-enriched HC gas mixture for EOR in the Dolphin Field resulted in noticeable improvements in oil recovery rates in the months following treatment (Straight and Fallin, 1992). HC injection conducted in the Red Wing Creek oil field in 1982 reported a 20% incremental oil recovery, compared to a 30% recovery rate from primary recovery (Pickard, 1994).

3.3 EOR for Carbonate Reservoirs

3.3.1 Challenges of Performing EOR in Carbonate Reservoirs

Carbonate reservoirs are generally characterized by low porosities and permeabilities, with 80% of the carbonate reservoirs worldwide possessing porosities between 4% and 16% and permeabilities between 1 and 500 mD. Because of these characteristics, the main contributions of fluid flow come from the natural fractures and dissolution vugs as opposed to flow through the carbonate rock matrix (Xu and others, 2020). Therefore, one of the main technologies used for oil production in carbonate reservoirs is near-wellbore stimulation through hydraulic fracturing and matrix acidization. These two methods lead to the enhancement of permeabilities and flow properties around the wellbore, leading to improved fluid flow from the reservoir to the wellbore (Gdanski, 2005). In addition to strong reservoir heterogeneity, the high-salinity nature of carbonate brines results in unfavorable rock wettability for oil flow in the reservoirs. The depth of prospective target reservoirs in the Williston Basin also yields a high temperature, which not only makes it more difficult to develop miscibility between oil and gas but also makes other EOR methods become challenging, such as chemical EOR.

For carbonate reservoirs with low-permeability matrix but high-permeability fractures, the deployment of gas EOR could be facing conformance issues, i.e., gas channels from injection wells to production wells through fractures instead of sweeping the rock matrix owing to the higher gas mobility than oil. This phenomenon adversely affects the EOR operations and reduces sweep efficiency across the reservoir, ultimately reducing the oil recovery of the field (Sorensen and Hamling, 2016). Furthermore, the high capital expenditure (CAPEX) nature of gas EOR operations makes economic assessment a key component to consider for each field. To overcome these obstacles, exploration of alternative EOR strategies is imperative to promote EOR in the Williston Basin.

3.3.2 Gas EOR

Gas EOR includes miscible or immiscible gas injection to improve oil recovery. Miscible gases, mainly HC and CO_2, are injected inside the reservoir at a pressure greater than the minimum miscibility pressure (MMP), leading the injected gas to become miscible in the crude oil. HC gas injection may involve produced gas from the same field or an outside source, at a pressure higher than the MMP, leading the gas to dissolve into the crude oil and improve oil mobility. HC injection

projects have been performed in several carbonate fields. In Levelland Field in Texas, an enriched gas mixture of methane, ethane, propane, CO_2, and nitrogen was injected into the dolostones of the San Andres Formation. The field tests indicated good sweep efficiency and improved oil production from the offset wells (Brannan and Whitington, 1977). Dawoud and others (2010) reported on an HC gas injection in a carbonate reservoir in Abu Dhabi, UAE. The reservoir is characterized with a low permeability and a porosity in the range of 13%–18%. At the time of the paper, the project had achieved its initial targets of injection and production rates as well as pressure support because of a successful voidage replacement process.

CO_2 injection has been one of the main EOR methods used in carbonate reservoirs since the 1980s (Manrique and others, 2007). Some of these projects included the continuous injection of CO_2, and others utilized a WAG mode. Numerous successful field applications have been reported in the literature. In Abu Dhabi, UAE, CO_2 was injected into a carbonate reservoir with low permeability and moderate porosity. Field results indicated that the oil production rate increased during the CO_2 injection and immediately decreased after the CO_2 breakthrough, highlighting the impact of conformance issues on CO_2 EOR performance (Al Basry and others, 2011). Recently, a published study showed that two pilots of CO_2 flooding in a giant oil field in Abu Dhabi resulted in favorable outcomes (Mabkhout AlSeiari and others, 2022). The CO_2 injection was performed in a WAG mode into a carbonate formation. Each pilot consisted of one horizontal producer and two horizontal injectors. Field results indicated the potential of high incremental oil recovery compared to water injection. Moreover, after several years, no increase in gas-to-oil ratio (GOR) or water cut was recorded in the producers as a result of the pilots. In addition, no loss in injectivity was observed between the different WAG cycles. In another field application, CO_2 injection was performed in a carbonate formation of the Wellington Field in 2015 (Holubnyak and others, 2018). The formation had permeabilities less than 10 mD and porosities between 10% and 12%. An average incremental oil production of 34 bpd was observed after the injection. In West Virginia, a pilot test of CO_2 flood in a tight dolomitized limestone reservoir in the Hilly Upland Field showed an incremental oil recovery of 5% (Watts and others, 1982). It is worth noting that the CO_2 injection was preferred to water injection in this case because of the tight nature of the reservoir that severely limited the water injection at an economic rate. In another field case, CO_2 was injected into a heterogeneous carbonate reservoir in a field in Texas. The oil production rate was increased from 250 bpd to 800 bpd, which indicates a successful implementation. However, it was observed that early CO_2 breakthrough occurred in nearby wells, which led to a poor volumetric sweep efficiency, indicating a conformance issue (Sharma and others, 2020). Various other CO_2 carbonate field projects have been reported in the literature such as Slaughter, Slaughter Frazier, Wasson Willard, South Welch, and Hanford East, among others in Texas that were performed in the San Andres Formation (Manrique and others, 2007).

3.3.3 Chemical EOR

Chemical EOR using polymer, surfactant, or alkaline are all options to improve oil recovery from carbonate oil reservoirs. The use of these traditional chemicals is usually challenged by the reservoir conditions of carbonates, especially the common high salinities and the occasional high temperatures. These two factors lead to chemicals degrading during flooding if not properly designed, leading to an inefficient process.

Polymer flooding is the injection of water containing dissolved polymer, which results in increasing the viscosity of the injected water, creating a more stable displacement of the in situ oil and improving the overall sweep efficiency of the flooding process. Various types of polymers are used in polymer flooding, some of which are synthetic, and others are natural. However, the most widely used polymer is hydrolyzed polyacrylamide (HPAM), which is a synthetic polymer (Sheng and others, 2010). The employment of polymer flooding generally requires light to intermediate oil, as high-viscosity oil will require higher concentrations and viscosities of polymer, which would result in a costly operation and difficulties of injectivity because of the high polymer viscosity required for the sweep efficiency to be favorable. Polymer flooding can also be used in heterogenous reservoirs that suffer from water channeling problems by improving conformance (Sheng and others, 2010).

One of the challenges related to polymer flooding in carbonate reservoirs is the high polymer retention expected because of the surface charge nature of the carbonate rocks that attracts the negative charges on the polymer structure's ends. For example, in the case of HPAM, the polymer is characterized by deprotonated carboxylic groups (-COO-) at the ends of its structure that get attached to the positively charged ions at the carbonate rock surface, increasing the polymer adsorption and reducing the effective polymer concentration in the injected aqueous phase (Saeed and Jadhawar, 2023). Another challenge is dictated by the high brine salinities encountered in many carbonate reservoirs. The polymer increases the viscosity of the injected brine by improving the repulsion between its negatively charged (-COO-) groups, which causes the polymer to stretch in a string-like manner, thus increasing the water viscosity. In the case of high salinity, the negative charges on the polymers are screened as a result of the high concentration of positive ions in the in situ reservoir brine. This consequently leads to a decreased viscosity of the injected aqueous phase and reduces the overall efficiency of the process (Saeed and Jadhawar, 2023). Therefore, it is generally favorable to use low-salinity water as the make-up brine of the injected polymer slug, which reduces the polymer degradation, reduces the polymer adsorption on reservoir rock, and improves the wettability of the reservoir, which leads to changes in the reservoir wettability from oil-wet toward more favorable wettability (Jadhawar and Saeed, 2023).

Polymer flooding field applications have been reported in many sandstone reservoirs; however, it was estimated that less than 5% of the total polymer flooding projects were conducted in carbonate reservoirs (Standnes and Skjevrak, 2014). This can be attributed to the potential thermal and salinity degradations as explained above. However, research is ongoing to develop temperature and salinity-resistant polymers that can withstand high salinity and high-temperature conditions. One application was reported in Wyoming's North Oregon Basin and Byron Fields using partially hydrolyzed polyacrylamide (PHPA). Results showed that the oil production increased with a decrease in the water cut over the following months (Hekker and others, 1986). Another polymer injection application was reported in the Eliasville Caddo Unit in Stephens County Field in Texas. The field results indicated a positive response from the polymer injection, with an estimated incremental oil recovery of 4.2% (Weiss, 1992).

Surfactant flooding improves oil recovery by lowering the interfacial tension (IFT) between oil and water, facilitating the formation of microemulsions, and thereby enhancing the mobility of oil within the water phase. Certain surfactants can also modify the reservoir rock's wettability, shifting it from oil-wet or mixed-wet to water-wet, which is beneficial for oil recovery (Sheng,

2010). Surfactants can be classified to anionic, cationic, nonionic, and zwitterionic based on the charge on the polar head group. Surfactant flooding has been performed in a few carbonate reservoirs. Yang and Waldeigh (2000) reported the utilization of nonionic and ionic surfactants in a dolostone reservoir in Yates Field, a reservoir characterized by low temperature, 15% porosity, and 100 mD permeability. An incremental oil recovery of 15% was observed in the field. Rilian and others (2010) reported an application of a nonionic surfactant in a carbonate reservoir in Semoga Field in Indonesia. Oil recovery was improved by 20%, the average oil production increased from 425 to 928 bpd, and the water cut decreased from 96% to 88% as a result of using the surfactant. Another application of an anionic surfactant was later reported in Yates Field by Cheng and Kwan (2012), where the incremental oil production rate was estimated to range between 29% and 71%.

Al-Sinani and others (2016) conducted a surfactant huff 'n' puff (alternate injection and production cycles in the same well) field test in a carbonate reservoir in Oman under high-temperature and high-salinity (HTHS) conditions, observing an increase in oil production coupled with a reduction in water cut over a 6-month period. Shuler and others (2016) also reported on a surfactant huff 'n' puff field test in China, targeting a reservoir characterized by high-salinity brine and temperatures exceeding 120°C. This test resulted in additional oil production from the wells under investigation. Moreover, a nonionic surfactant was applied in a Russian field with reservoir salinity at 217,500 ppm and a relatively low temperature of 23°C, as documented by Varfolomeev and others (2020). The outcomes indicated not only enhanced oil production following surfactant use but also improved injectivity.

In other instances, surfactants have been employed in HTHS carbonate reservoirs in conjunction with other chemicals, such as polymers or alkaline solutions, to enhance EOR efficiency. Al-Amerie and others (2015) described a one-spot surfactant-polymer (SP) pilot test in a carbonate reservoir with high-temperature (83°C) and high-salinity (190,000 ppm) conditions. The pilot observed a 36% reduction in oil saturation around the test well, indicating a positive response to the SP slug injection. Alkaline-surfactant-polymer (ASP) combinations have been utilized in HTHS sandstone reservoirs as well, with a field pilot in Kuwait demonstrating the injection of an ASP slug through a single well. The single well chemical tracer (SWCT) test revealed a 67% reduction in residual oil saturation (Al-Murayri and others, 2019).

3.3.4 Engineered Water Injection

Engineered water injection (EWI) or low-salinity waterflooding (LSWF) refers to the injection of brine with modified salinity into the reservoir to perform the functions of waterflooding, displacement, and pressure support, in addition to wettability alteration as a result of the salinity equilibrium disturbance inside the reservoir. As discussed above, a carbonate rock normally possesses a positive charge on its surface that attracts the oil that possesses negatively charged (-COO-) groups, and therefore, carbonates are usually oil-wet (Tetteh and others, 2020). Carbonate reservoirs are usually associated with high salinity in situ brines, which support the positive charges present on the carbonate surface. EWI is designed to reduce the injection brine salinity, leading to a reduction in the ionic strength of the brine and reducing the positive charges on the rock surface (Saeed and others, 2023). Moreover, the addition of specific ions such as

SO_4^{2-}, Mg^{2+}, and Ca^{2+} can also assist in favorably altering the rock wettability (Zhang and others, 2007). The application of EWI requires an oil-wet or mixed-wet reservoir with a high-salinity brine and good water conformance reservoir properties such that early water breakthrough is not encountered. Moreover, it was anticipated that the presence of crude oil with a high base number, which describes the ability to neutralize acids, gives rise to positive charges on the oil surface and would make the reservoir a better candidate for EWI (Saeed and others, 2022). It was also observed that fines migration was associated with some EWI core flooding experiments, which gives risk of pore plugging in the case of tight reservoirs, reducing the reservoir flow properties (Tang and Morrow, 1999). However, mineral dissolution was also observed in some experiments (Den Ouden, 2014), which improves reservoir permeability. Therefore, these two effects may cancel one another if both occur at the same time.

Numerous experimental studies investigated the use of EWI in carbonate samples at varying conditions. Seccombe and others (2008) conducted low-salinity core-flooding experiments in carbonate core samples where the in situ brine salinity was 54,000 ppm and the injected brine salinity was less than 4000 ppm. Their results indicated that 40% incremental recovery was observed due to the low salinity injection. RezaiDoust and others (2009) observed wettability alteration in a carbonate sample as a result of injecting low-salinity brine and indicated that the wettability alteration was dependent on the presence of SO_4^{2-}, Mg^{2+}, and Ca^{2+} in the injected brine. In another set of experiments, Yousef and others (2011) conducted a series of core-flooding experiments in carbonate chalk core samples where the injected brine was diluted between 2 and 100 times compared to the in situ brine salinity of 213,000 ppm. Their results showed that an incremental oil recovery of up to 8.5% was achievable as a result of the LSWF and attributed that to an underlying wettability alteration. They also increased pressure drop, which was explained by fines migration as a result of disturbing the initial equilibrium within the crude oil-brine-rock system because of the introduction of the low-salinity brine.

This summary shows that a variety of EOR methods have been used to improve oil production performance in carbonate reservoirs across the world. A few EOR technologies have also been applied to the Williston Basin. Results showed that a considerable improvement in oil recovery could be achieved when a suitable EOR method was selected for the target reservoir. Because of the complicated nature of carbonate reservoirs and the HTHS conditions in many North Dakota conventional reservoirs, the EOR method and procedure need to be carefully selected and designed for each field.

4.0 FOREMAN BUTTE FIELD DESCRIPTION, DATA ACQUISITION, AND LABORATORY EVALUATIONS

4.1 Foreman Butte Field Description

The Foreman Butte oil field is located in the North Dakota portion of the Williston Basin (Figure 4-1). Field production occurs from the Ratcliffe interval of the Charles Formation within the Mississippian Madison Group (Figure 4-2). The field produces from the Flat Lake and Alexander units, with a combined gross thickness of 20–25 feet at an average depth of 9330 feet below the surface. The reservoir is capped by the Charles Formation halite and anhydrite that is laterally continuous for this part of the Williston Basin, which can be readily mapped using well logs and seismic data.

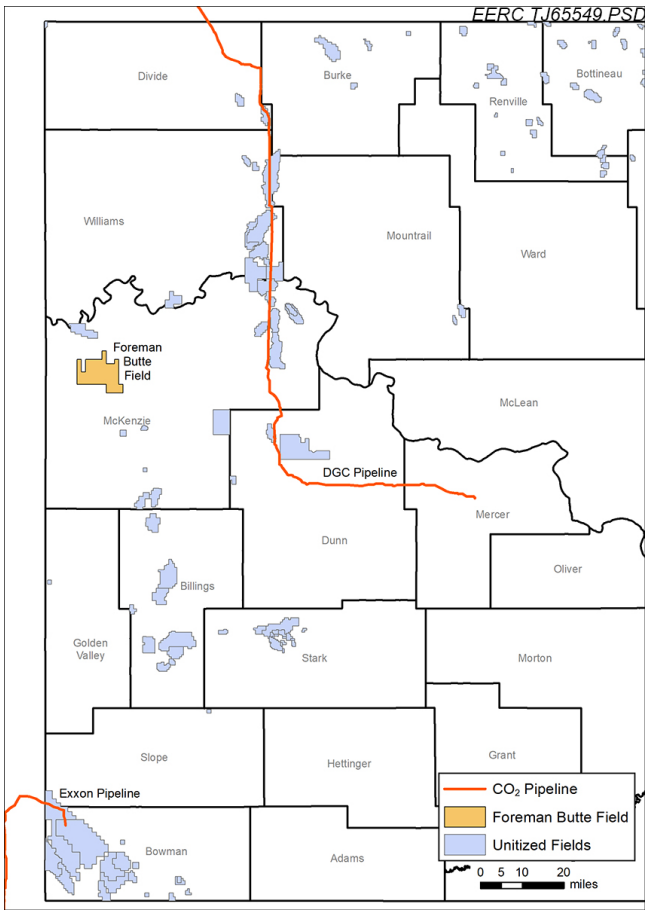

Figure 4-1. Foreman Butte oil field location and unitized legacy oil fields identified as near-term candidates to investigate CO_2 EOR.

The Flat Lake and Alexander units are predominantly limestone, with interbeds of anhydrite within. Effective porosity for both units ranges from 3.6% to 18%, with an average matrix permeability of 1 mD. Production analyses and whole core observations indicated that the field is naturally fractured, likely from associated tectonic events, stratigraphic drape, and post depositional faulting, which impact system permeability. These analyses provide additional information that aids in characterizing the fractured reservoir through drainage rather than relying only on the matrix properties.

Deposition of the Ratcliffe interval occurred in an open to progressively restricted marine environment along the eastern margin of the basin. Based on available whole core, five rock textures were identified including brachiopod-bryozoan-echinoderm packstone/wackestone, peloid-ooid packstone/wackestone, ostracod-foraminifera, laminated mudstone/wackestone, and anhydrite-dolomite mudstone (Dunham, 1962). Additionally, minor organic quartz siltstones were encountered in the Ratcliffe interval, suggesting an element of a clastic mixed system, but the texture is not considered to be volumetrically dominant. The peloid-ooid packstone/wackestone is the main oil-bearing facies, with associated higher porosities compared to the other textures.

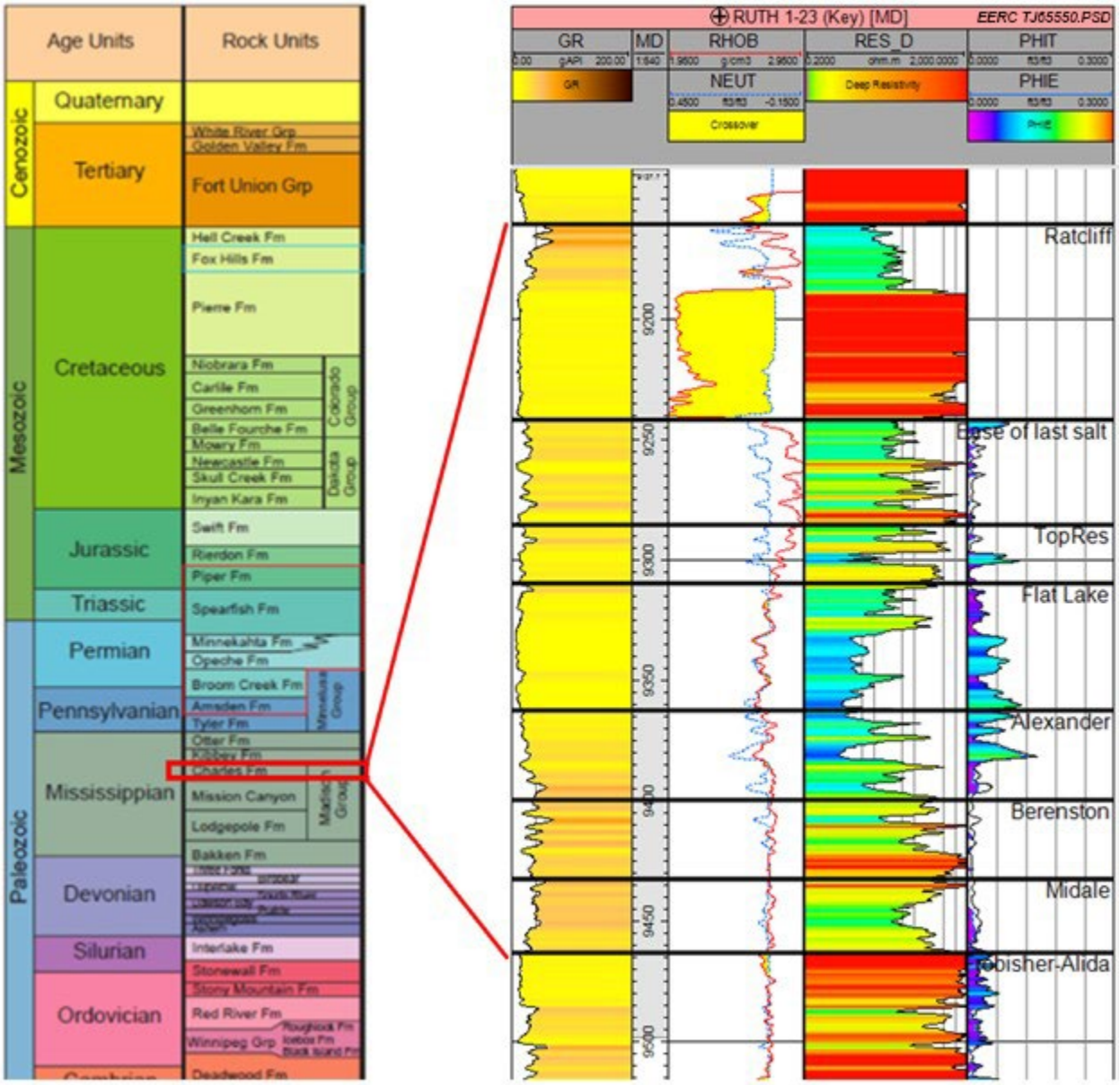

Figure 4-2. Foreman Butte oil field representative stratigraphic section.

Figure 4-3 shows various well logs collected from a new well, the Willy Miranda State 16-4 (API No. 33053097780000, NDIC No. 38630), that was cored through the Ratcliffe pay zone. Figure 4-4 shows permeability from core sample measurements for the another well nearby. The porosity of the pay zone is generally lower than 10%, with the exception of a few thin layers. The permeability is in the range of 0.001–20 mD, with most of the pay zone showing a permeability of less than 0.1 mD. These indicate that this deep reservoir is not only tight but also strongly heterogeneous.

Natural fractures were observed in the core samples obtained from the reservoir, as illustrated in Figure 4-5. The left three core samples show that the natural fractures are randomly distributed in different geometries and orientations—both vertical and horizontal fractures with different lengths appear in these samples. For comparison, the fourth core sample on the right-hand side shows an intact rock without the presence of natural fractures. Drilling and production activities showed that natural fractures are distributed across the reservoir in the Ratcliffe interval (Hirsch and others, 1981; Woo and Cramer, 1984; Begnaud and Claiborne, 1985).

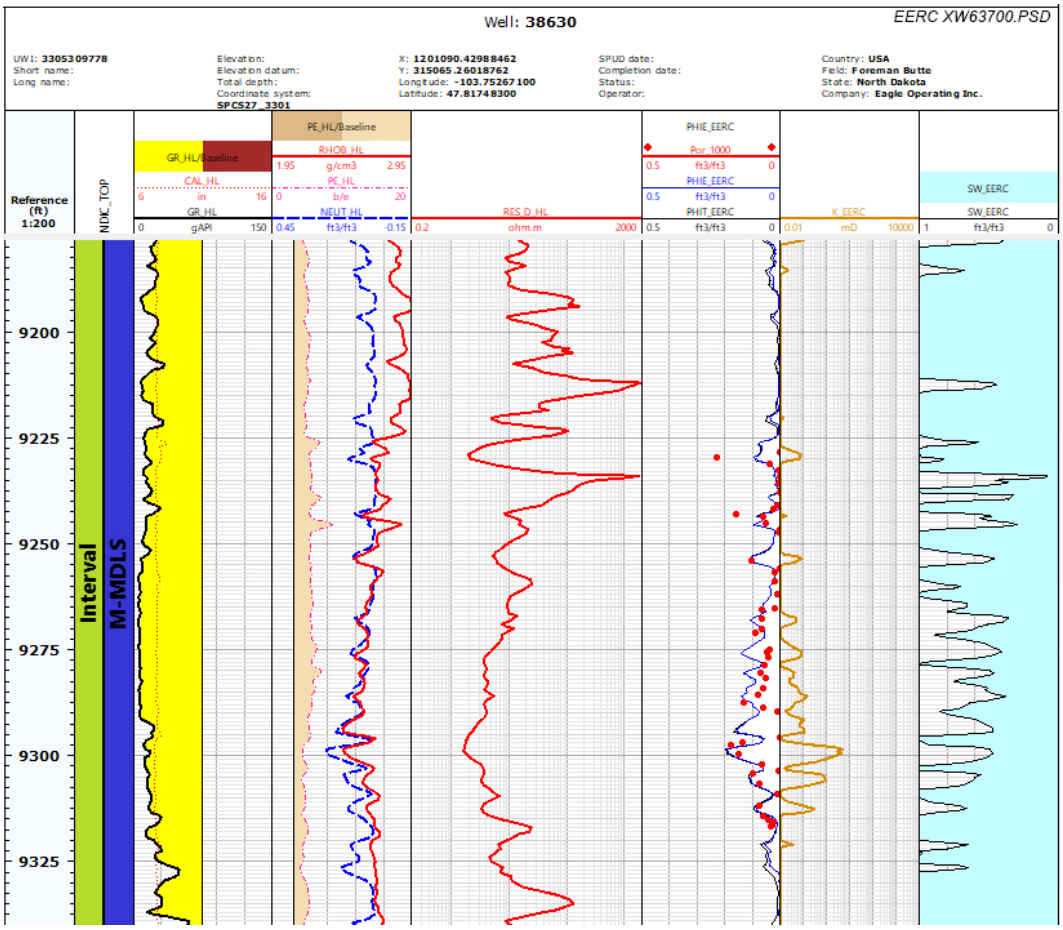

Figure 4-3. Well logs collected from the Willy Miranda State 16-4 well drilled in Foreman Butte Field with porosity log-matched to core data.

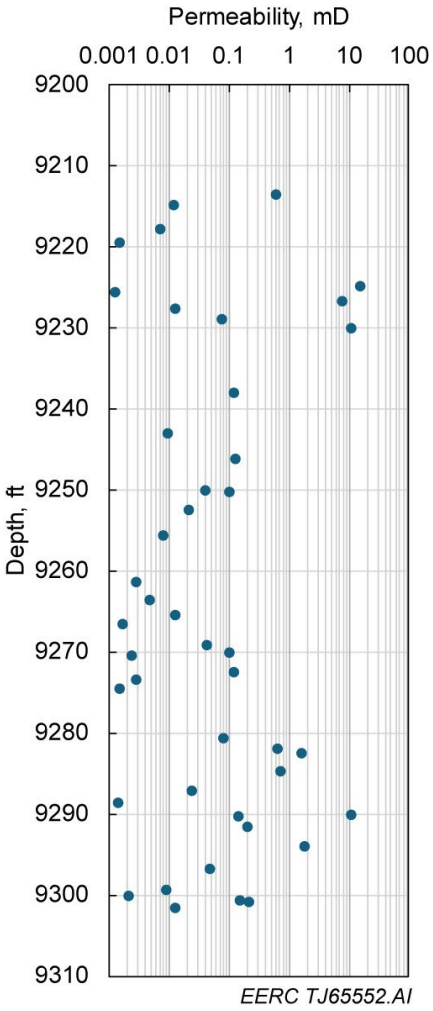

Figure 4-4. Distribution of permeability with depth based on core measurements.

Shell recovered over 1500 feet of core samples from three wells at the Mondak Field to analyze the natural open fractures in the interval (Hirsch and others, 1981). To delineate these fractures using wireline logs, the company ran the commercially available logging tools as well as the prototype devices designed to respond to open fractures. The results showed that most of the open natural fractures observed in the core samples are vertical, with a length ranging from several inches to several feet and a width typically less than a fraction of a millimeter. Begnaud and Claiborne (1983) observed that natural fractures played varying roles in oil production from reservoirs in the Mission Canyon and Ratcliffe units and that fracture properties might change with time as production went on.

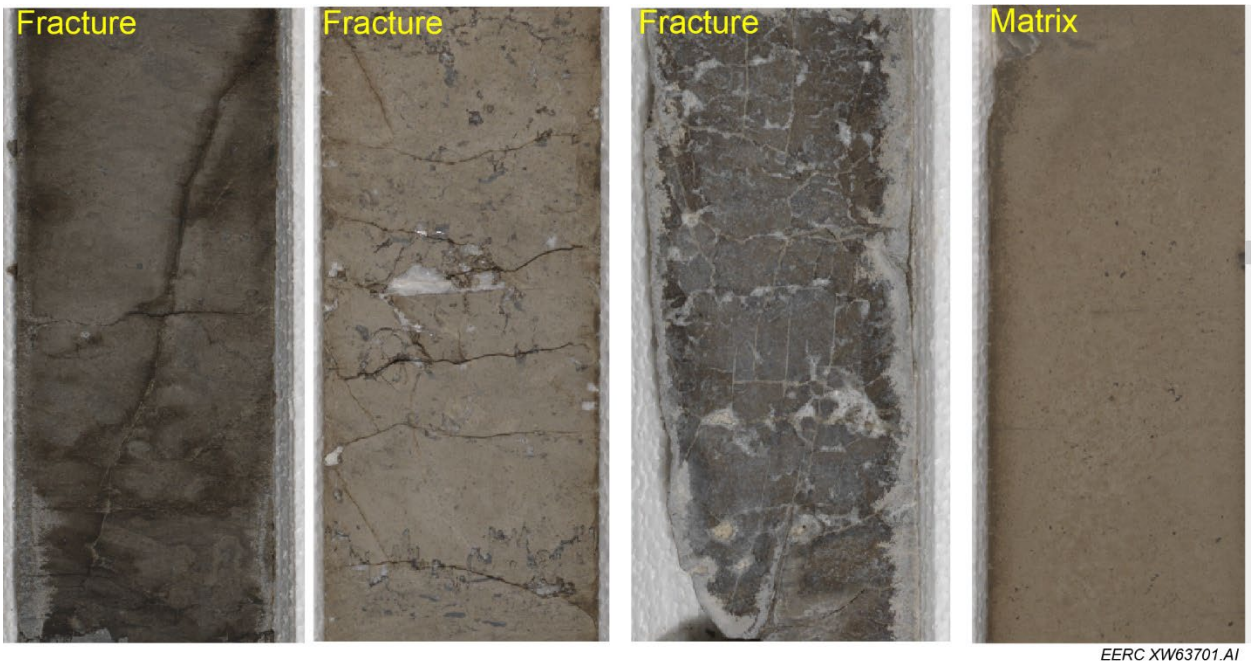

Figure 4-5. Illustration of natural fractures observed on the core samples collected from the reservoir.

4.2 Data Reconnaissance, Management, Needs, and Acquisition

4.2.1 Data Reconnaissance and Management

For maximum efficiency, determining the lateral and vertical/geological areas of interest should be done before collection of available public data begins. Preference was given to data sources from state oil and gas commissions, such as North Dakota Industrial Commission (NDIC) Oil and Gas Division. Secondary priority was given to subscription or licensed data (e.g., IHS Markit from S&P Global or Enverus). If subscription or licensed data are to be used for a project, rules and requirements for that data must be discussed with any client and project team to ensure data and interpretation delivery of final products comply. The publicly available data can be downloaded and conditioned quickly for an evaluation of oil-productive properties and have limited overhead on the use of the data.

A project-level primary database was created to track and hold all unique well-level data, such as American Petroleum Institute (API) number, NDIC ID number, legal well name, legal location, spud date, completion data, casing program, and any other permanent data specific to that well. Additional databases for data files and locations (e.g., geophysical well log data, production data) can be created separately and linked to the primary database by using either the well identifier such as API or NDIC ID. The databases generated clear and concise datasets for all project team members to ensure data-loading into applicable software packages for future evaluations. A final data audit in report or map format was suggested to ensure all team members were aware of data distribution for the area of interest (AOI). This data audit can be used to make final adjustments with decision-makers on the project boundaries and may identify knowledge gaps or data that have

yet to be available to the project team. Data organization and maintenance includes cleaning cycles to remove unneeded data or synchronizing fixed data within the AOI. In cases where public and private sources indicate conflicting data, the data must be reconciled.

4.2.2 Data Needs and Acquisition

Various data types provide valuable information to undertake a revitalization project involving EOR. This section discusses the most commonly used data and the datasets that were used in the case of the Foreman Butte Field.

Pressure data measurements assist in providing reservoir history and insights regarding production drive mechanisms during primary production. Pressure buildup tests, falloff tests, downhole static pressure measurements, and fluid levels (e.g., producing or static) provide calibration points for numerical simulations. The available pressure points were collected and used to perform rate-time analysis (RTA) and estimate the reservoir properties.

Fluid properties relative to pressure, volume, temperature (PVT) data should be obtained from testing an oil sample, providing input for compositional simulations. Available PVT data can save time in starting the compositional simulations of the reservoir. Oil composition data should also be saved and catalogued. Analogous PVT data from nearby Little Knife Field were used for the Foreman Butte Field PVT model because of the low quality of fluid sample collected from the Foreman Butte Field during this project.

Water analyses provided dissolved concentrations and water resistivity for water saturation calculations. Moreover, conducting water analyses over time can also track the changes in water composition after waterfloods to help determine scaling and corrosion risks.

Previous structure, thickness, and other seismic attribute interpretations can provide needed context of a field or AOI decision history. Bubble maps of production and injection data were helpful in making a preliminary determination of an AOI.

2D and 3D seismic interpretations, integrated with previously discussed data types, can be useful during initial evaluations of a field study. Additionally, seismic data and interpretations can be beneficial in later project stages for structure and isopach mapping, fault identification, and property modeling of the zone of interest (ZOI).

Geophysical well log data, available in DLIS and LAS formats, are loadable in log analysis software such as Techlog or geological interpretation and modeling software (e.g., Kingdom, Petrel, Petra). Raster image files may also be used and formatted for well correlations or digitized, whenever necessary. The use of raster images requires more effort, and use should be balanced against project needs. Later petrophysical interpretation goals should be considered in dictating the possible interpretations from the available datasets. The following well logs are useful if available:

- Gamma ray
- Spectral gamma ray

- Compensated neutron/density
- Sonic (compressional and shear)
- Resistivity/saturation (resistivity, microresistivity, induction)
- Borehole image
- Dipmeter
- Nuclear magnetic resonance (NMR)
- Lithology
- Cement bond log (CBL)/ultrasonic inspection (USI) tool

Available CBL data can assist with mechanical integrity assessment for possible risks and determine if remedial work is needed to prevent CO_2 migration outside the target reservoir.

Core slab and thin-section photographs from previously drilled wells involving the zones of interest are available from some state sources like NDIC. These data, coupled with lithology logs generated by wellsite geologists and/or core descriptions, should be made available for rock type and facies determinations within the reservoir.

Production and injection data for each well were also available within the database or downloadable. These data required review and manipulation to focus on the ZOI. It is recommended to map the cumulative volumes and production performance indicators to identify productive areas to determine potential sweet spots.

Published literature was reviewed to find relevant technical articles for Foreman Butte Field, target reservoirs, and analogous reservoirs. This provided insight into previous findings and helped reduce rework. A special focus was given to descriptions of regional geology, depositional setting, structural setting and history, orientation and density of natural fracturing, effect of fracturing on reservoir performance, waterflood performance, testing that will provide guidance as to ranges and averages of rock and fluid properties, and methodologies that can provide guidance to define fluid contacts.

Some operating partners make proprietary data available for projects. Care must be taken to keep these data confidential and the use of the data within the terms of our contract with the partner. Any data provided by a partner needs to be reviewed, collected, and integrated with data from other sources.

Routine core analyses (RCAL) should be in field or well files and, if in hard copy form only, should be digitized and compiled into a spreadsheet database to enable further petrophysical analyses and correlation to log data. Special core analyses (SCAL) allowed a thorough assessment of CO_2 potential. If possible, locate all physical core samples for additional tests that may not have been run originally for later correlations to well logs and field tests.

4.3 Analysis of Production and Injection Data

Seventeen horizontal wells from Foreman Butte Field were selected for review to develop a better understanding of individual well behavior and group performance in this low matrix

permeability, naturally fractured reservoir, as shown in Figure 4-6. The wells were drilled from 2004 to 2006 and then started oil production with open hole completions. The horizontal laterals were completed at an average depth of 9330 feet and an average length of 5300 feet. A large variation in initial oil production rate and cumulative oil production was observed in these wells: initial oil production rates ranged 52 to 515 bpd and cumulative oil production ranged 17 to 200 Mbbl, as shown in Figure 4-7. All of the wells had high initial water cuts ranging from 25% to 85%, as shown in Figure 4-8. A clear correlation could be observed between the initial water cut and cumulative oil production for these wells, as demonstrated in Figure 4-9. These observations indicated that the oil saturation distribution in the reservoir is highly uneven and the main pay zone might be in a capillary pressure transition zone with high water saturation. Additional discussion of capillary pressure data is found in Appendix A.

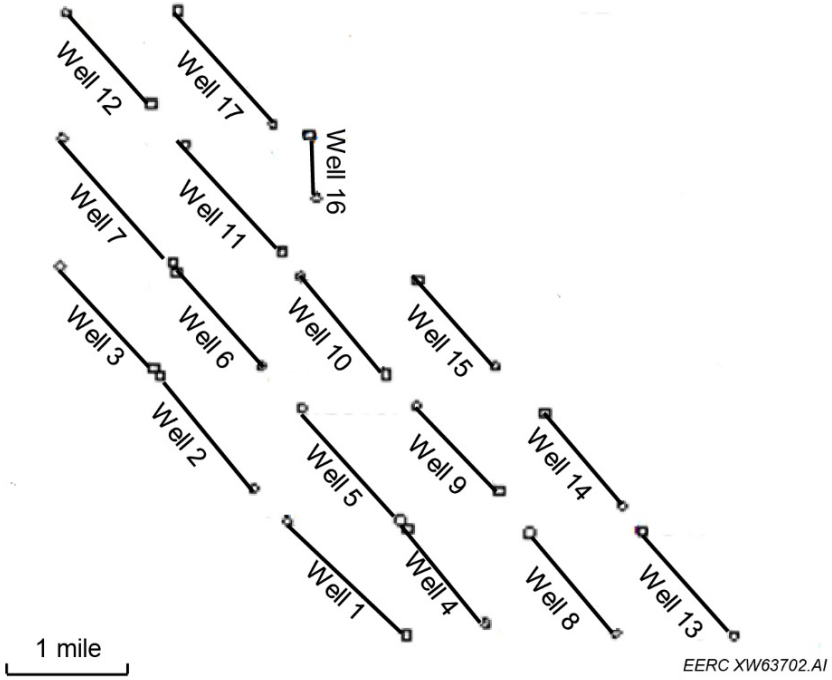

Figure 4-6. The 17 horizontal wells selected from Field A where the main pay zone is in the Ratcliffe interval.

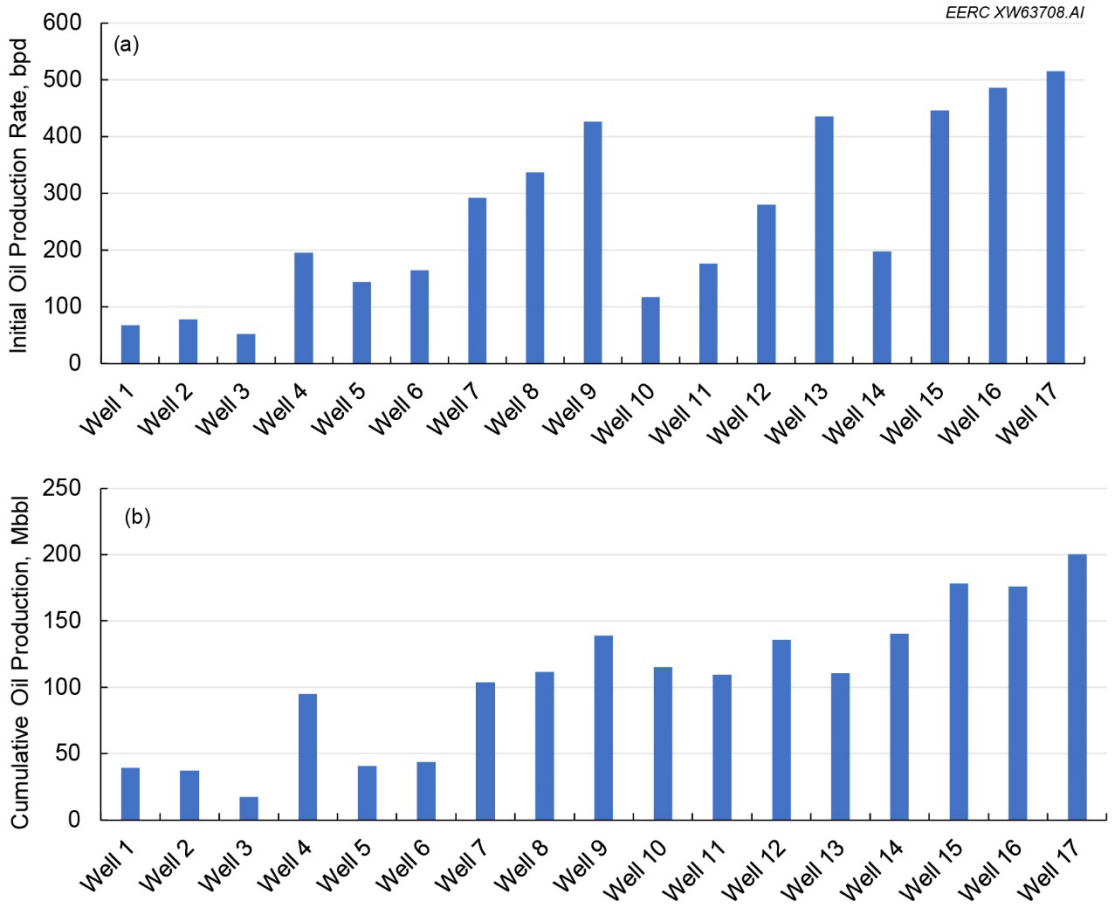

Figure 4-7. Oil production performance of the selected wells in Field A: a) initial oil production rate and b) cumulative oil production.

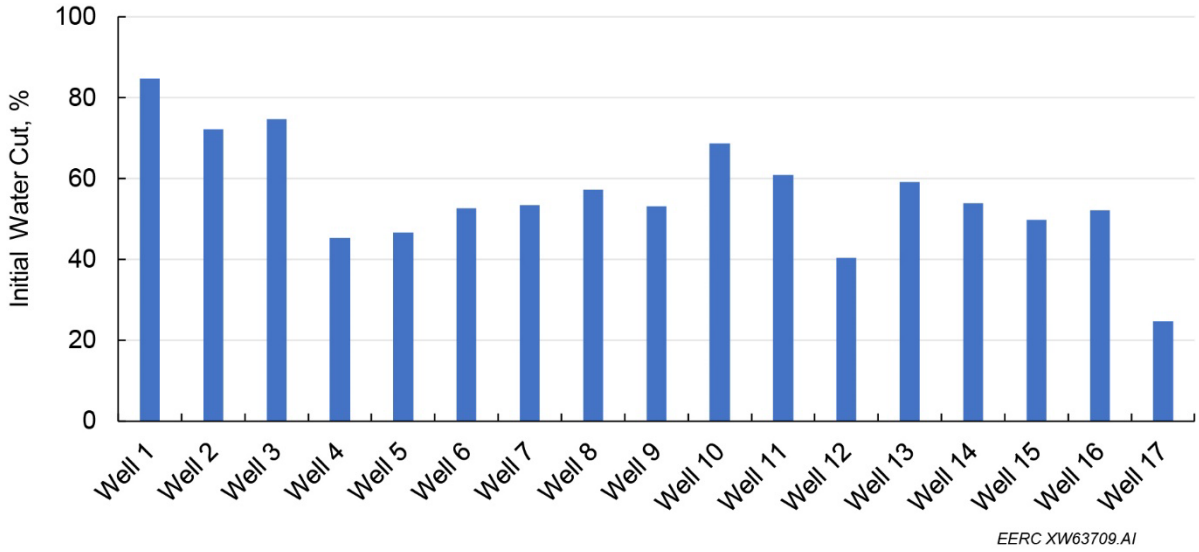

Figure 4-8. Initial water cut of the 17 wells in Field A.

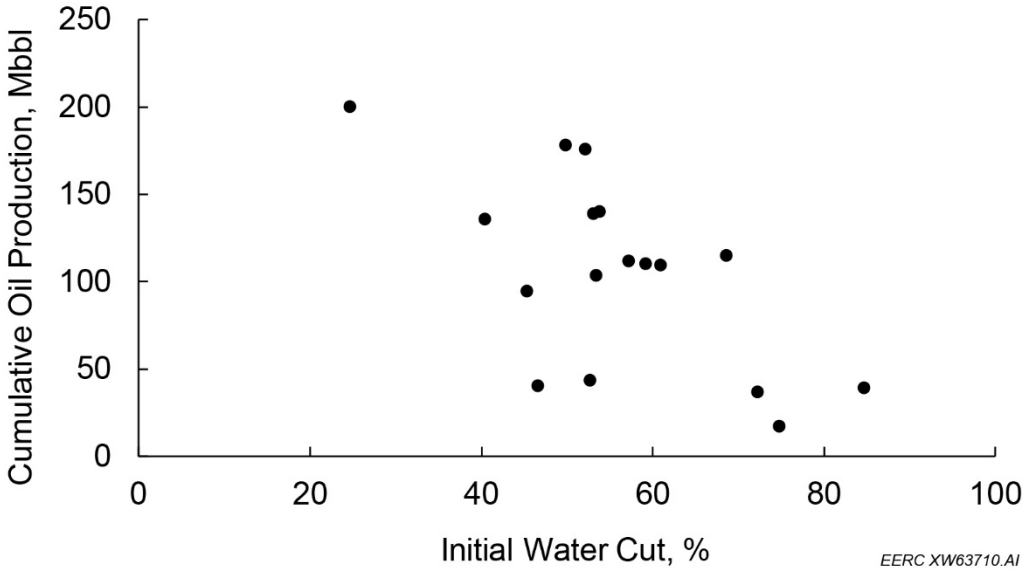

Figure 4-9. Correlation between initial water cut and cumulative oil production for the 17 wells in Field A.

Water injection at the field started in Well 5 in October 2017, as shown in Figure 4-10. Data indicated that the maximum injection rate was limited to around 1650 bpd because of the low-permeability rock matrix surrounding the well. Wells 1, 2, and 6 have been shut in since 2013 because of their low oil production rates. Oil and water production responses have been monitored in offset Wells 4, 8, 9, and 10. Little change in water cut was observed in Wells 4 and 8, indicating that the communication between the injection well and these two production wells was weak. Conversely, increasing water cut was observed in Wells 9 and 10 after water injection started, as shown in Figure 4-11, implying that high-conductivity channels probably existed between Well 5 and Wells 9 and 10. The production and injection data further confirmed that the reservoir is highly heterogeneous. Accurately predicting the behavior of fluid flow in the reservoir was challenging because of the uncertainties in the distribution of permeability, porosity, initial oil saturation, and natural fractures across the reservoir. To address this challenge, a simulation workflow was developed to tune the matrix and fracture properties through detailed history matching.

Additional production data analysis is presented in Section 6.0 and Appendix B.

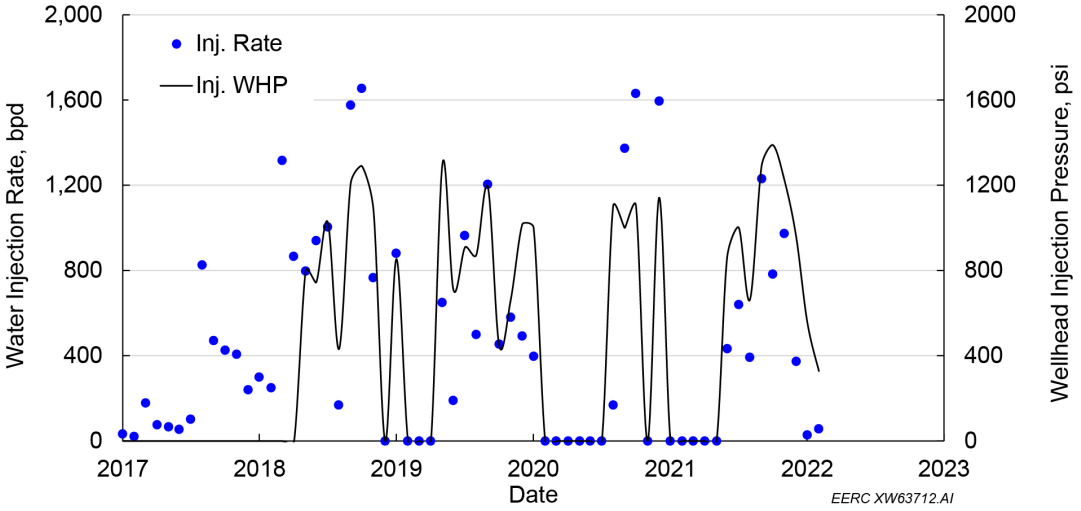

Figure 4-10. Water injection performance in Well 5.

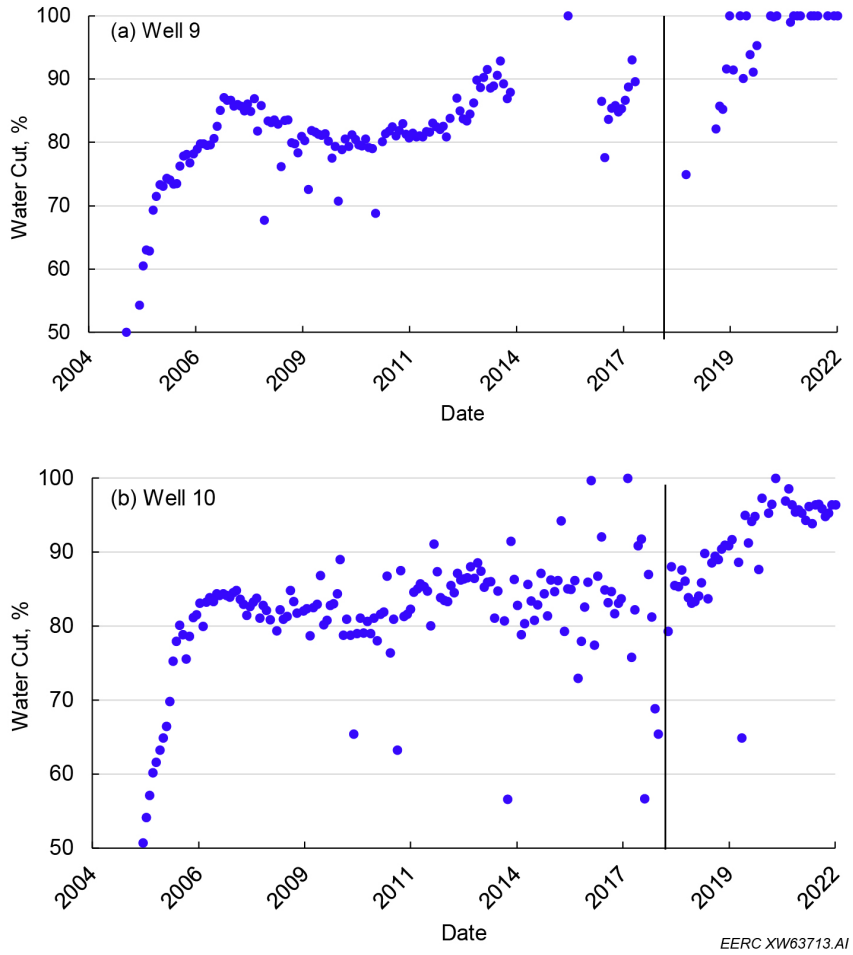

Figure 4-11. Change of water cut in offset wells after water injection started: a) Well 9, b) Well 10. The black line indicates water injection started in Well 5.

4.4 Laboratory Evaluations

Several different laboratory tests were performed to investigate different rock and fluid interactions. In the case of Foreman Butte, a new well, Willy Miranda State 16-4, was drilled and whole core was acquired through the Ratcliffe interval. A comprehensive RCAL, SCAL, and core description sampling program that was recommended were completed (Table 4-1). These tests were recommended because of the lack of analogous field data available and represented a testing program for critical data needed for modeling a miscible CO_2 flooding process. In the absence of physical core samples within the AOI or ZOI, the best possible analogue field data or literature search can be used as a substitute, but that will increase uncertainty. Figure 4-3 (in Section 4.1) showed the measured values for the petrophysical parameters calculated from log and core data obtained from the Willy Miranda well. Core plugs were carefully selected from the available core with the intent of providing a representative cross-section of reservoir rock types.

Table 4-1. Special Core Analyses for CO_2 EOR Evaluation

Evaluation	Purpose	Sample Description
Core Natural Light and Ultraviolet (UV) Photography	Initial lithological assessment, augment petrographical and petrophysical analyses	89' of core slabbed and photographed
Standard Core Analysis (porosity/permeability/grain density)	Foundation for numerous petrophysical and reservoir engineering analyses	49 core plugs measured
Thin Sections	Determine mineral components, identify lithofacies, ichnofacies, and diagenetic phases	12 thin sections prepared
X-Ray Diffraction and Fluorescence	Assess mineralogy and help in calibrating lithological model	12 samples tested
IFT/Contact Angle	Determine mobility of the reservoir oil and wetting preference of the rock	8 samples measured
High-Pressure Mercury Injection	Characterize pore geometry, entry pressure, and relative permeability	8 samples tested
CO_2 Core Flooding	Characterize flow of CO_2 in reservoir	2 samples tested
CO_2–Oil Relative Permeability	Characterize flow of CO_2 in reservoir	1 sample tested
Brine–Oil Capillary Pressure Testing	Oil–water relative permeability	4 samples tested
Core Resistivity Testing	Calculate resistivity index and Archie exponents	4 samples tested
Rock Evaluation Analysis	Determine free oil and residual oil saturation	4 samples tested

To replicate the high salinity conditions prevalent in the formation, a synthetic brine was prepared with a total dissolved solids concentration of 266 g/l. However, such high salinity, combined with elevated reservoir temperature, presents challenges in selecting suitable surfactants for EOR performance evaluation. To assess surfactant EOR performance, a service provider provided three different surfactants samples, and three surfactant solutions were prepared by mixing 1 ppm of each surfactant with formation brine. The core plugs were then subjected to multiple EOR injection schemes to compare the performance of water, gas, and surfactant injection. Table 4-2 lists the properties of the rock samples selected for these experiments.

Table 4-2. Selected Rock Sample Properties with Corresponding Surfactant

Sample ID	Porosity, %	Permeability, mD	Pore Volume, ml	Tested Surfactant
Sample 1	16.83	2.48	9.37	A
Sample 2	8.73	0.15	4.82	B
Sample 3	14.09	0.67	8.02	C

The additional technical details of the execution and results of these tests are presented in Appendix A. Results are highlighted below.

4.4.1 Miscibility Pressure Tests

CO_2 MMP is one of the most important parameters for designing an effective EOR project. When the reservoir pressure is maintained above MMP, miscible flooding can be achieved to promote displacement efficiency and facilitate better oil extraction since the IFT between oil and CO_2 becomes minimal or even zero. Injecting CO_2 below the MMP (immiscible flooding) may result in poor sweep efficiency since CO_2 could not be fully miscible with the oil in pore space, thus reducing the effectiveness of the EOR operation. Therefore, it is usually desirable to have miscible CO_2 flooding in actual field operations to maximize the EOR performance.

The Foreman Butte oil MMP measured at a reservoir temperature of 230°F. Results show that the tested oil had an MMP of 3418 psi with CO_2 and 1669 psi with ethane.

4.4.2 Capillary Pressure Tests

A capillary pressure transition zone is a region where water saturation changes gradually with decreasing depth from 100% water to connate water saturation as the oil saturation increases. Capillary pressure is defined as the difference in fluid pressure across an interface between two fluids in a confined volume. In an oil reservoir, it is the pressure difference across the oil–water interface, which is a function of the fluid and rock properties. Capillary pressure plays a crucial role in determining the thickness of a transition zone. Studies showed that the thickness of a transition zone may vary from a few feet in high-permeability reservoirs to more than 300 feet in low-permeability reservoirs such as carbonate reservoirs because of extreme heterogeneity (Masalmeh and others, 2007; Bera and Belhaj, 2016; Shi and others, 2018; Dakhelpour-Ghoveifel and others, 2019). Foreman Butte Field appears to exist within the range of a long capillary pressure transition zone.

Capillary pressure was measured both using high-pressure mercury injection (HPMI) and a brine–synthetic oil system. Pore throat distributions were calculated from HPMI results, and the oil brine capillary pressure measurements were used to guide creation of relative permeability curves. A summary of calculated pore throat sizes is shown in Table 4-3.

Table 4-3. Calculation of Pore Throat Radii from HPMI Measurements for Selected Core Plugs

Samples	Depth, ft	Porosity, %	Swanson Permeability, mD	Median Throat radius, µm	Pore radius, µm
131811m	9226.6	17.2	8.43	1.28	4.49
131818m	9237.9	11.3	0.453	0.297	0.568
131829m	9260.6	6.7	0.0153	0.0694	0.237
131834m	9269	6.1	0.0164	0.0815	0.582
131836m	9272.4	15	1.12	0.389	0.707
131841m	9281.9	14.5	1.07	0.45	1.38
131842m	9282.5	19.6	3.77	0.692	4.29
131846m	9289.2	10	0.403	0.346	1.05

4.4.3 IFT and Contact Angle Tests

The pendant drop technique was used to measure IFT between the oil and several different mixtures of brine and surfactants. The measurements were made at reservoir conditions of 230°F and 4500 psi. Rock–fluid wettability interactions were also investigated using the sessile drop contact angle method.

Three surfactant solutions were prepared using the three surfactants, A, B, and C, denoted as SS-A, SS-B, and SS-C. To understand reservoir fluid interactions, measurements were conducted by introducing an oil drop into a chamber filled with fresh water, formation brine, SS-A, SS-B, and SS-C at 230°F and 4500 psi. Crude oil and formation brine exhibited an IFT of 31.42 mN/m under reservoir conditions, which is nearly 10 mN/m higher than the IFT of the crude oil and freshwater system. This difference suggests that the complexity of the brine and the presence of cations and anions further contribute to the increased IFT. The results show that adding 1 ppm of surfactant to the brine led to a significant reduction in IFT, resulting in values of 1.06, 0.73, and 0.55 mN/m for SS-A, SS-B, and SS-C, respectively.

The contact angle technique was employed to assess reservoir wettability and investigate the impact of surfactant injection on altering the wettability state. The results suggest that the reservoir exhibits mixed-wettability characteristics when in contact with fresh water and oil but tends to be strongly oil-wet when interacting with brine and oil. Upon the addition of 1 ppm of SS-A, there was a slight decrease in the contact angle from 138° to 124°, maintaining the wettability state as oil-wet. In contrast, SS-B and SS-C significantly reduced the contact angle, effectively shifting the wettability state toward water-wet. Specifically, the contact angle decreased from 138° for the oil–brine system to 58° and 18° for SS-B and SS-C, respectively.

4.4.4 Emulsion Tests

Tests were conducted to assess the emulsion properties of surfactant and crude oil. The results indicate that all emulsions exhibited spontaneous breakdown after a period of time, which is desirable for effective surfactant EOR processes. SS-A formed the highest emulsion volume; however, it experienced the quickest breakdown. While the emulsion formed using SS-B performed slightly better, SS-C's emulsion exhibited the most consistent breakdown over time, indicating higher stability and performance compared to SS-A and SS-B.

4.4.5 Oil Recovery Tests

Injection tests were conducted at a reservoir temperature of 230°F and an injection pressure of 4000 psi. After brine injection, 45.9% of the oil was displaced from Sample 1. However, subsequent injection of SS-A with 25 days of soak time resulted in an ultimate recovery factor of 49%. Displacement of almost 6% of additional oil was achieved after subsequent injections while also using additional surfactant additives. Once surfactant injection ceased to yield further oil displacement, CO_2 was introduced, leading to an additional 4% increase in oil production for a total recovery of 59%.

Similar EOR schemes were tested to measure the oil recovery following the injection of SS-B and SS-C using Rock Samples 2 and 3, respectively. Brine injection tests conducted on Cores 2 and 3 resulted in oil recovery factors of 25% and 40%, respectively. Following a 47-day soaking period, oil recovery using SS-B injection reached its peak at 56% recovery. Subsequently, ethane injection was initiated, leading to the displacement of an additional 14.5% of oil and resulting in a final recovery factor of 70.5%. For Core 3 after 18 days of soaking, SS-C injection reached its peak at 55.6% recovery. Subsequent ethane injection helped displace 27.5% more oil, resulting in an ultimate recovery factor of 83.13%.

4.4.6 Formation Resistivity Tests

Formation resistivity testing was performed to increase the confidence level of water saturation calculations. Default values of 2.0 for both cementation and saturation exponents are commonly used in the Archie equation to calculate water saturation from log resistivity. Actual values were determined by core testing to provide higher precision in saturation calculations. The results of this testing are shown in Table 4-4.

Table 4-4. Results of Formation Resistivity Determination Using Core Plugs

					Archie Equation Variables		
Sample	Depth, ft	Permeability, mD	Porosity, %	Grain Density, g/cc	Formation Resistivity Factor, F	Cementation Exponent, M	Saturation Exponent, N
131811	9226.6	7.694	17.08	2.77	42.4	2.120	2.104
131834	9269.0	0.075	7.33	2.73	217.0	2.058	2.201
131841	9281.9	0.676	14.42	2.76	52.2	2.043	2.101
131846	9289.2	0.162	10.79	2.81	116.1	2.136	2.178

5.0 GEOLOGIC MODELING AND SIMULATION

To mimic the fluid flow behavior in the reservoir, a detailed geologic model was created using SLB's Petrel®, and then a compositional reservoir simulation model was built using Computer Modelling Group Ltd.'s (CMG's) GEM®. The 17 wells shown in Figure 4-6 (in Section 4.3) were included in the model. The length, width, and height of the original reservoir model is approximately 40,350 × 16,350 × 100 feet, with 135, 55, and 45 grid cells in the X, Y, and Z directions, respectively. The total bulk volume of the reservoir model is 7.29×10^7 feet^3. The geologic model was constructed using corner grids in Petrel® based on available well log and core data to distribute the tight and heterogeneous initial values for porosity, permeability, and oil saturation, as shown in Figure 5-1. Most of the reservoir matrix exhibited low porosity (less than 10%) and permeability (less than 0.1 mD), with a few thin layers showing higher porosity (≥10%) and permeability (≥0.1 mD).

Steps of the recommended evaluation and characterization workflow for geologic model are presented in detail in Appendix B.

The oil saturation distribution is irregular and comparatively low and was represented in the reservoir as in a capillary transition zone with high water saturation. Capillary pressure transition zones may hold a substantial portion of the total oil in place in a reservoir, where the oil production performance and recovery depend heavily on several geological and petrophysical properties that can be measured by SCAL such as pore size distribution, capillary pressure, and relative permeability (Spearing and others, 2014; Mohamed and others, 2017; Shi and others, 2018). Capillary pressure is one of the most important factors needed to understand the fluid flow behavior in a transition zone. Capillary pressure data can provide valuable information on the size and sorting of pore throats and the pressure difference required to move fluids through the pores (Jin and Wojtanowicz, 2014; Bera and Belhaj, 2016; Zhang and others, 2019, 2020). Therefore, high-pressure mercury injection capillary pressure (MICP) tests were performed to measure the capillary pressure in this reservoir. Figure 5-2 illustrates a capillary pressure curve that was measured by MICP using a representative core sample from the reservoir with a porosity of 0.11 and a permeability of 0.45 mD. The curve indicates that a high differential pressure is required to displace oil through a large portion of pore throats in this reservoir. The steep change of the slope implies that oil is difficult to produce in the deeper transition zone since an extremely high differential pressure is required to overcome the capillary force between oil and water in the pore throats.

Figure 5-1(c) shows that most of the reservoir had an initial oil saturation lower than 0.5. Additionally, the figure depicts a decreasing trend in oil saturation with increasing depth, where the effect of gravity on oil migration is clear. The distribution of reservoir properties correlated well with the oil production and water cut behaviors that were shown in Figures 4-7–4-9 in Section 4.3.

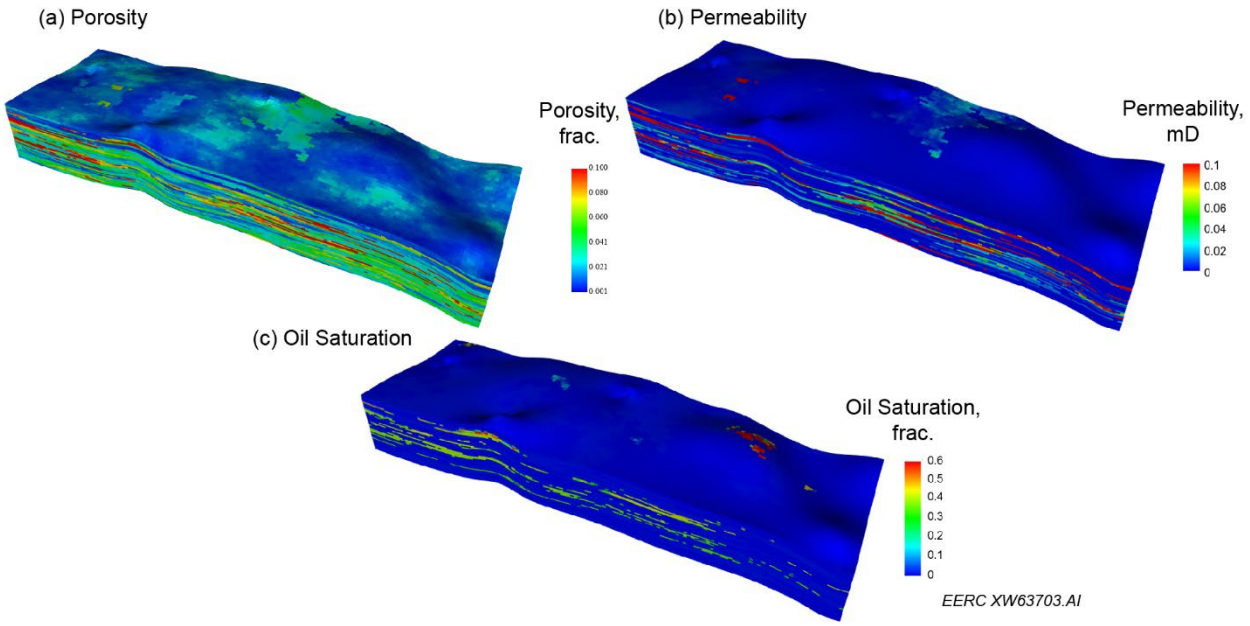

Figure 5-1. Distribution of different reservoir properties in the geologic model: a) porosity, b) permeability, and c) water saturation. The height of the reservoir model was amplified 50 times to better display the vertical distribution of the reservoir properties.

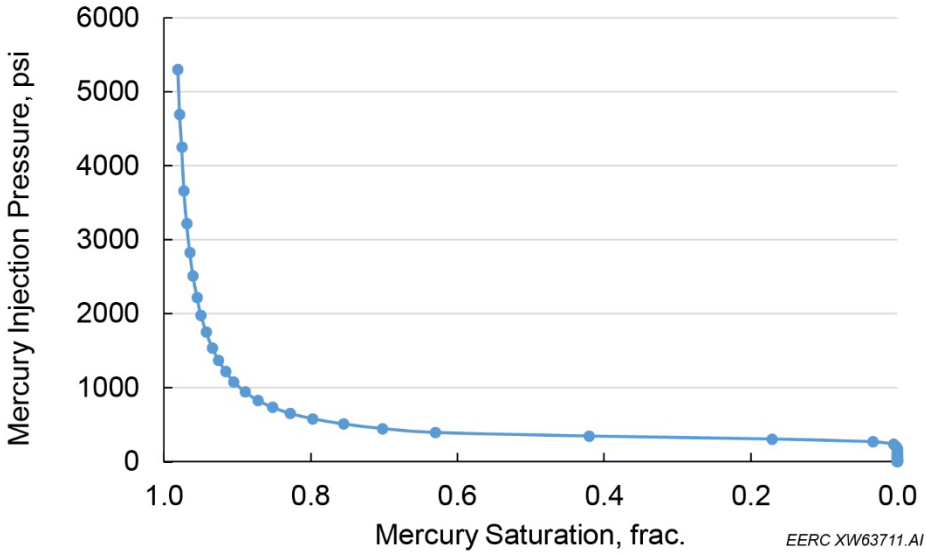

Figure 5-2. Capillary pressure curve measured by MICP using a core sample with a porosity of 0.11 and a permeability of 0.45 mD.

In addition to the many wells in the field, natural fractures were also involved in the model. Selecting a high-efficiency fracture simulation method became a precondition for history matching. The embedded discreet fracture model (EDFM) approach was effective to integrate natural fractures into a reservoir simulation model. Different from most fracture simulation

methods, EDFM constructed all fractures explicitly by separating and describing the fracture and matrix grids independently. The fractures were divided into segments and then connected using nonneighboring connections (NNCs) to make sure the fluid can flow through the fractures. This treatment greatly improved flow calculation efficiency in the simulation process (Xu, 2015; Lie and Møyner, 2021; Zhao and others, 2022). Fracture and matrix grids were then coupled to each other via source–sink relations when the simulation model was finalized. EDFM homogenized small natural fractures by adjusting the length, width, porosity, permeability, and transmissibility when tuning the model to make the simulation model run smoothly (Ma and others, 2022). This hierarchical modeling approach made EDFM versatile and convenient to handle complex fracture networks. Employing the EDGS® Suite software, Figure 5-3 shows the simulation model of the studied reservoir with wells and natural fractures integrated (shown in the figure as scattered dots).

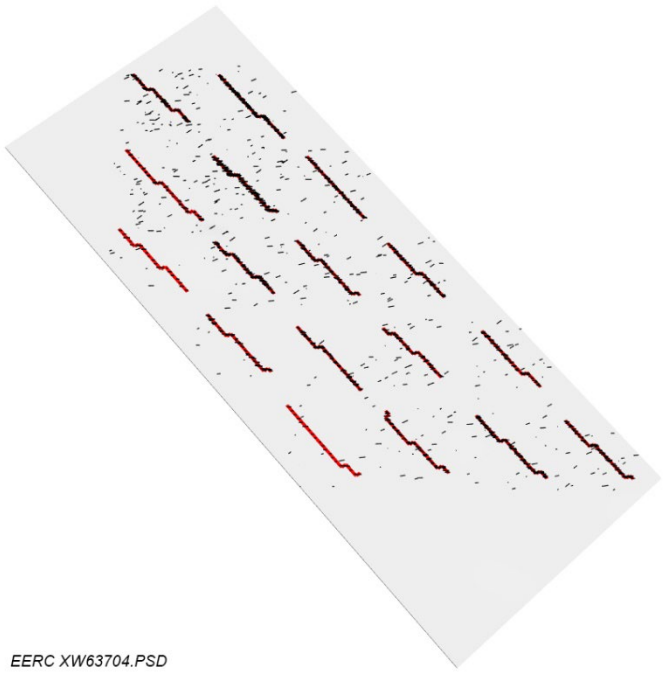

Figure 5-3. Distribution of wells and natural fractures in the simulation model.

5.1 Simulation Workflow Development

Because of the uncertainties in rock and natural fracture properties, initial simulation results deviated from historical data, which is a normal circumstance at the start of the history-matching process. Adjusting only the matrix properties could not make the model match the historical data satisfactorily; however, the initial simulation runs showed that the results were sensitive to the cells in the near-wellbore region. Tuning the natural fracture properties in these areas showed that simulation results were close to historical data, especially in the early stage of production. Later, the matrix properties within the drained reservoir volume (DRV) became more influential on fluid flow behavior. These observations indicated that 1) the properties of natural fractures in the near-wellbore areas should be mainly adjusted for early-stage history matching, 2) the main DRV of each well might be limited around the wellbore because of the tightness of the rock matrix in the

reservoir, and 3) the rock matrix properties in the DRV were mainly responsible for late-stage history matching. Therefore, a fracture and DRV optimization (FDO) workflow (Figure 5-4) was proposed to optimize the history-matching quality for this tight and naturally fractured reservoir.

The workflow began with an initialization of the simulation model to make sure the model could run through the available production history in a reasonable time. The essential matrix and fracture parameters such as porosity, permeability, and fluid saturations were tuned based on available well logs, core measurements, etc. When the model was able to run smoothly, the results were compared with historical data and this case was kept as a baseline model. If the results were satisfied, i.e., met accuracy requirements, history matching was completed. If the simulation results deviated from historical data, then the properties of the near-wellbore grids mainly focused on natural fractures were tuned to match the production data for the early production period.

When the data of the early production period were matched, the properties of grids beyond the near-wellbore region were tuned to match the remaining historical data. The impact of matrix properties became more important for late-stage production. Figure 5-5 schematically illustrates a DRV near a natural fracture. Based on the fracture grids that were generated in EDFM, all matrix cells that are connected to the fractures were identified and grouped based on their connected fractures. Properties such as permeability, relative permeability curves, and transmissibility were tuned in these cells to match historical data. Some natural fracture properties such as length, width, and permeability might also be tuned in this stage. The matrix cells were also updated when the length or width of their connected fracture was tuned; as a result, the DRV was updated. The updated reservoir model was then rerun and compared to historical data until a satisfactory history match was achieved.

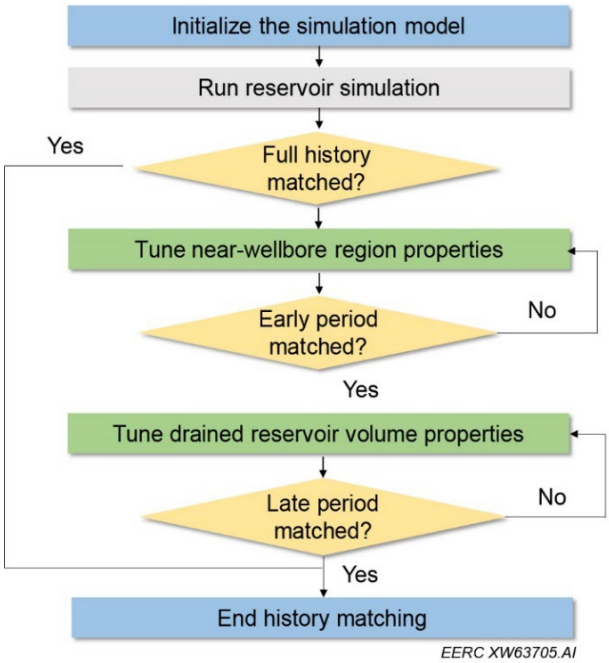

Figure 5-4. Simulation workflow for tight and naturally fractured reservoir history matching.

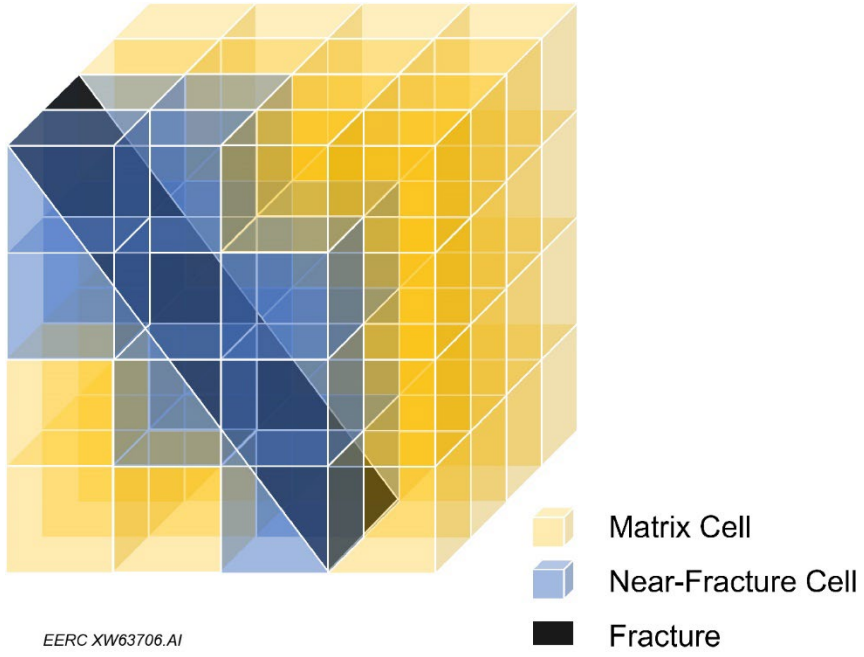

Figure 5-5. Illustration of a DRV near a natural fracture. The black piece represents a natural fracture embedded in the reservoir matrix, the blue blocks represent the cells that are directly connected to the fracture, and the yellow blocks represent the matrix cells that are not directly connected to the fracture.

5.2 History-Matching Results

Detailed history matching was performed for the 17 wells based on the workflow proposed in this study. Reasonable production history-matching results, including liquid rate, oil rate, and water rate, were achieved for both field and individual wells, as shown in Figures 5-6, 5-7, and 5-8. Because of a lack of gas compositional data, the gas production rate was not set as an objective for history matching. However, this did not impact the verification of the proposed method in this study. The liquid production rate was set as the primary production constraint. Therefore, the liquid rate was matched very well for all the wells. This indicated that the grids in the model had adequate conductivity to deliver the fluid volume. The plots on oil and water production rates showed only slight variations between the simulation results and production history. The matching results indicated that the simulation model could effectively mimic liquid flow in this reservoir. The variations between the simulation and production also implied there were still uncertainties in the fracture and matrix properties and the simulation results could be further improved when more data are available to reduce the uncertainties.

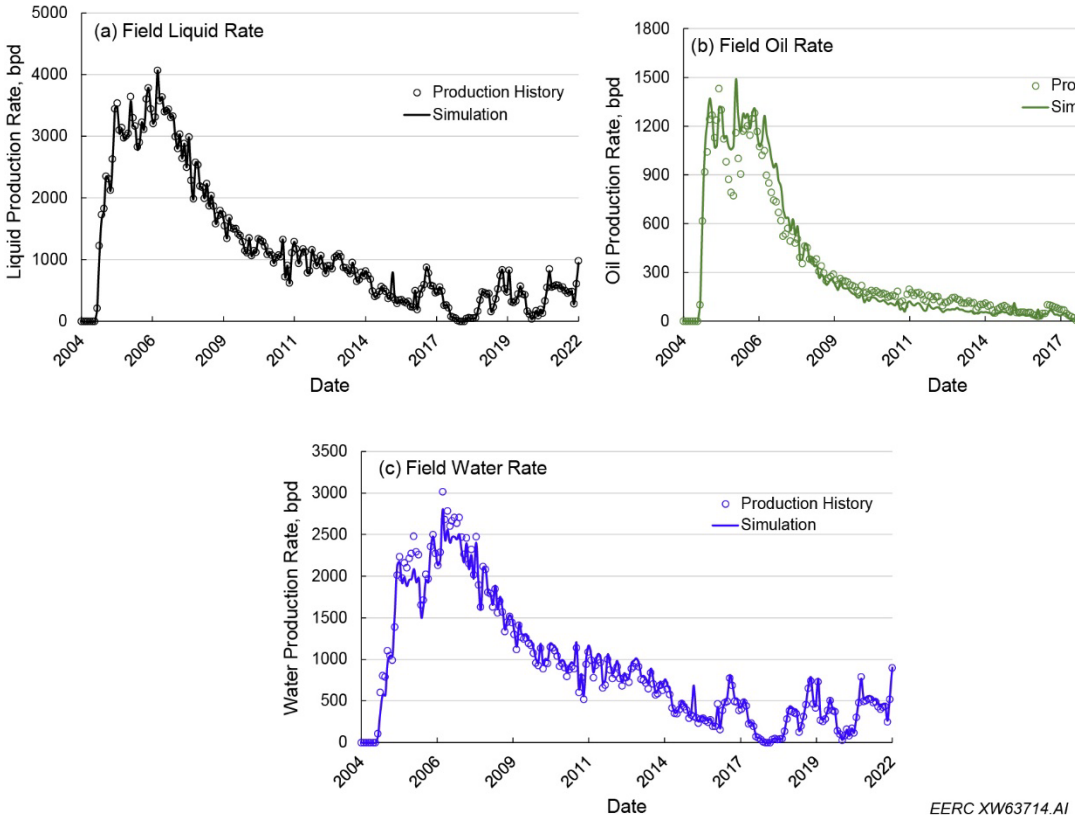

Figure 5-6. History-matching results for production rates in Field A: a) liquid rate, b) oil rate, and c) water rate.

5.3 Water-Flooding Simulations

Compared to other methods that are feasible to be applied in carbonate reservoirs to increase oil recovery, water injection is generally considered easy to perform, inexpensive, and efficient in displacing oil with low to medium gravity (Yousef and others, 2011; Xu and others, 2020). Since October 2017, water injection has been applied in this tight carbonate reservoir to maintain reservoir pressure and drive oil toward the nearby production wells. However, significant incremental oil production was not observed in the nearby production wells. To improve the performance of production by optimizing water injection, the water injection history was analyzed and different water injection optimization strategies were simulated and evaluated.

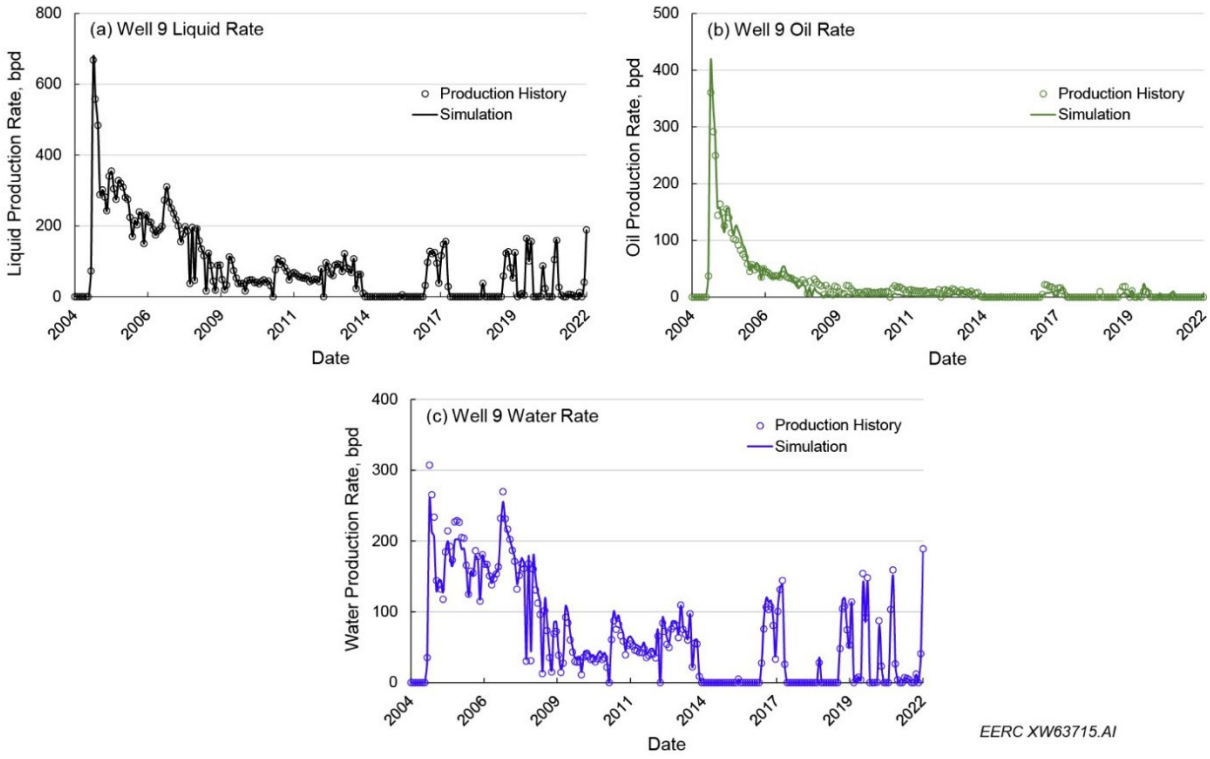

Figure 5-7. History-matching results for production rates in Well 9: a) liquid rate, b) oil rate, and c) water rate.

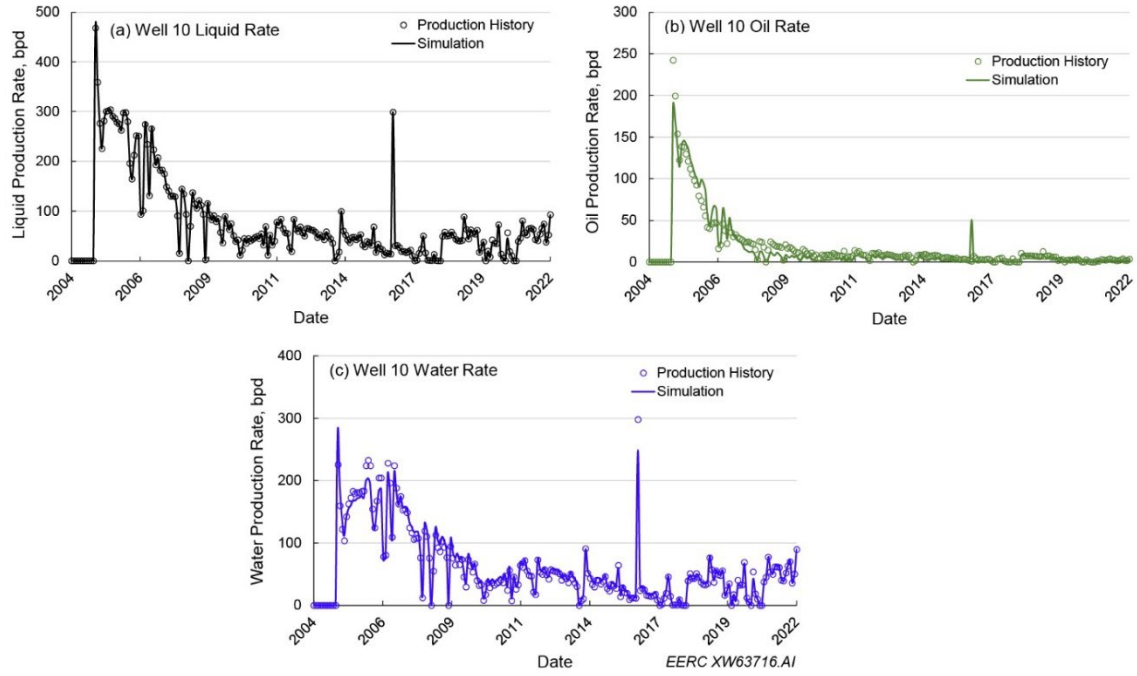

Figure 5-8. History-matching results for production rates in Well 10: a) liquid rate, b) oil rate, and c) water rate.

Water injection has been performed in Well 5 to improve oil production in the nearby wells. To evaluate the connectivity between the injection well and the nearby production wells, the responses of oil and water production have been monitored in the offset Wells 4, 8, 9, and 10, as illustrated in Figure 5-9. Other offset Wells 1, 2, and 6 have been shut in since October 2017.

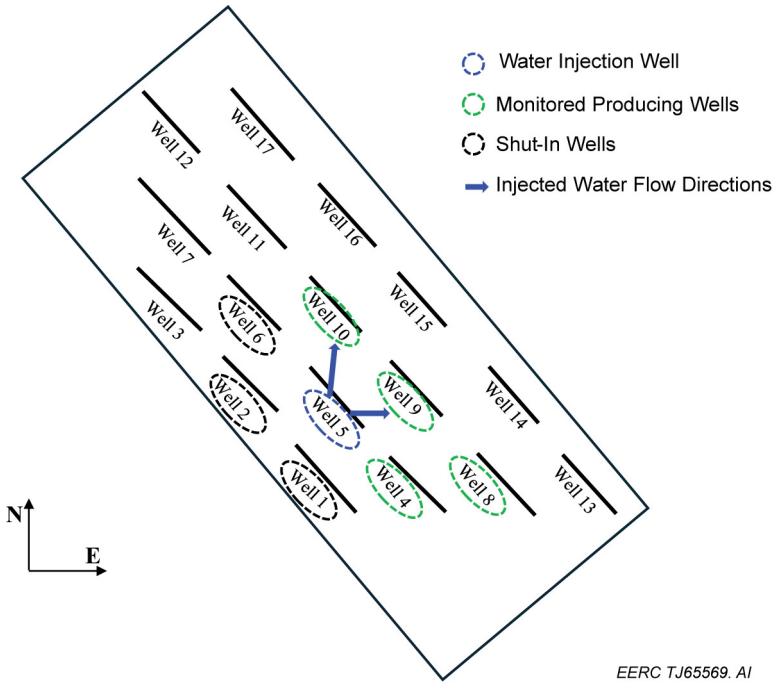

Figure 5-9. Schematic illustrating water injection and production monitoring since October 2017.

The reservoir model could generally reproduce the injection history for Well 5, as shown in Figure 5-10. An increasing water cut was observed in Wells 9 and 10 since the start of water injection, indicating that relatively high-permeability paths probably existed between the injection well and the two production wells. For Wells 4 and 8, the change in water cut was little, indicating no significant communication between the injection well and the two production wells, 4 and 8. The modeling results of water cut for Wells 9 and 10 since October 2017 captured the trends of the historical production data, as shown in Figure 5-11.

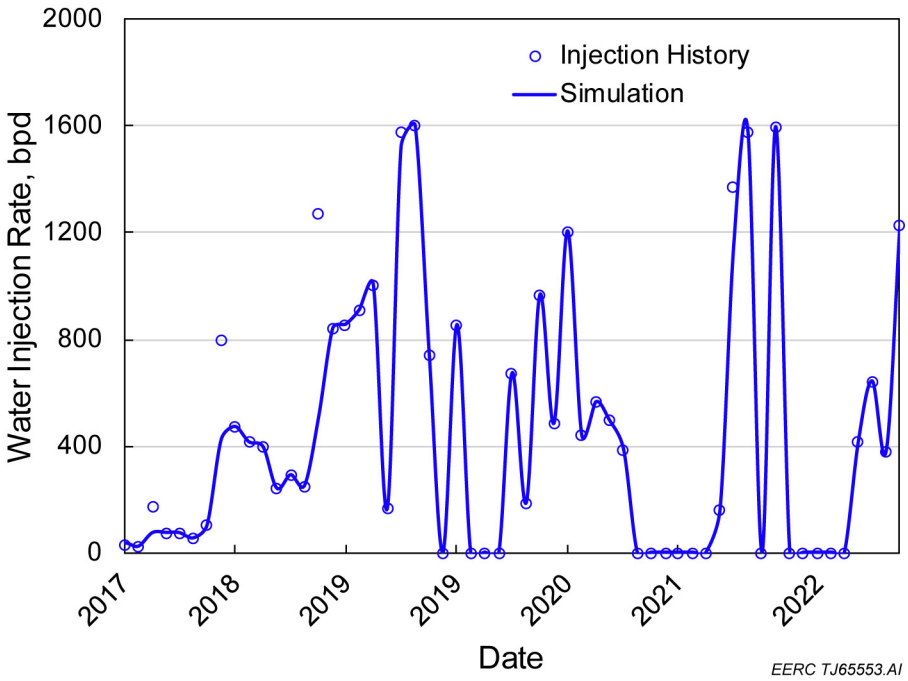

Figure 5-10. History-matching results for injection rates in Well 5.

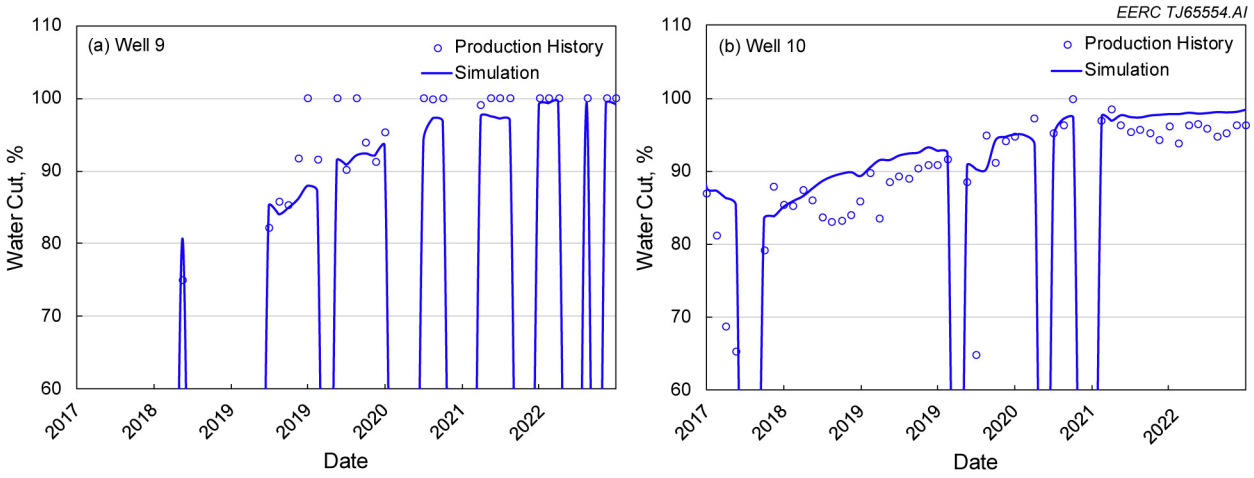

Figure 5-11. History-matching results for water cuts in Wells 9 and 10.

Once the simulation was history matched, including the water injection at Well 5, several different scenarios were evaluated to consider the effectiveness of the water injection and estimate if waterflood performance could be improved. Sections 5.3.1–5.3.3 briefly summarize the results of that work. Section 5.4 discusses the potential for CO_2 injection. Section 5.5 discusses surfactant EOR, and Section 5.6 discusses infill drilling potential. More detailed discussions and figures should be reviewed in Appendix C.

5.3.1 Scenario 1 – Skin Factor Effect on Offset Well Production

The production wells had apparent skin damage near the wellbore after years of production due to scale deposition, salt precipitation, etc., leading to minimal oil production in many wells. The reservoir model took skin damage into account by assigning different skin factor values to each well to achieve a satisfactory history-matching result. The estimated skin factor values for Wells 9 and 10 were +3 and +10, respectively, at the end of the production history.

Five predictive cases were designed to assess the skin effects on the liquid, oil, and water production in Wells 9 and 10. Water was injected through Well 5 with a constant injection rate of 500 bpd for 10 years. The setup for the injection and production constraints of injection Well 5 and production of Wells 9 and 10 is summarized in Table 5-1. Case 1 served as a baseline case with Wells 9 and 10 having skin factors of 3 and 10, respectively. Simulation results showed that 1957 and 4105 bbl of oil could be produced from Wells 9 and 10, respectively, in 10 years. In the meantime, the water production could reach 573,043 and 399,525 bbl in Wells 9 and 10, respectively, as shown in Figure 5-12.

Table 5-1. Constraints Setup of the Injection and Production Wells for Scenario 1

	Well 5	Well 9			Well 10		
Case No.	Injection Rate, bpd	Skin	Max. Production Rate, bpd	Min. Pressure, psi	Skin	Max. Production Rate, bpd	Min. Pressure, psi
1		3			10		
2		1.5			5		
3	500	0	700	500	0	700	500
4		−1			−1		
5		−2			−2		

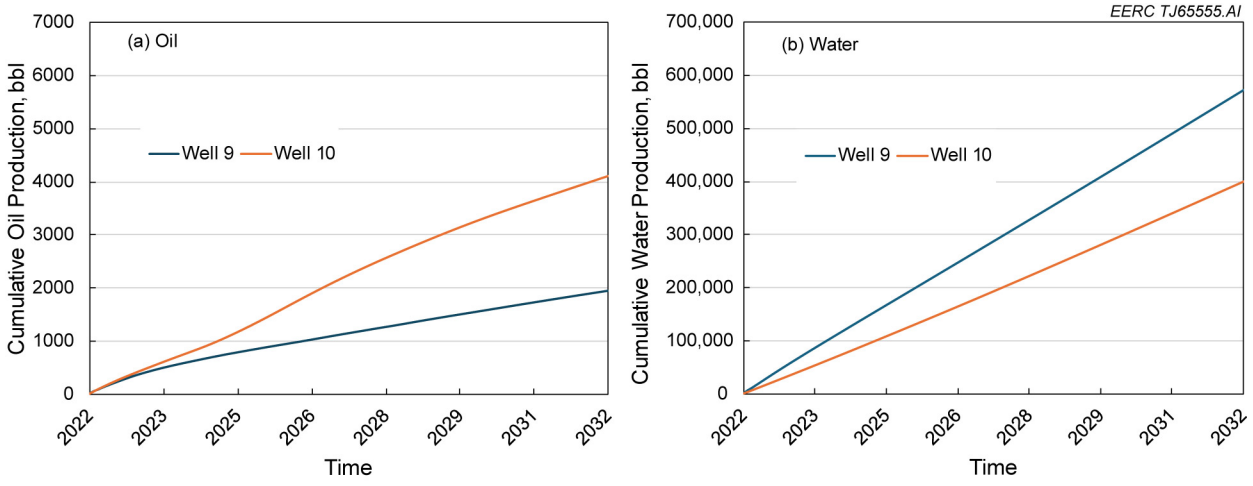

Figure 5-12. Simulation results of Case 1: a) cumulative oil production and b) cumulative water production during 10 years of predictive period.

Smaller skin factors were applied to Cases 2–5, as shown in Table 5-1, to analyze the effect of reduced skin factors on oil and water production. The results showed that reducing skin factors contributed to greater liquid production for both wells during the predictive period. Reducing skin to −2 yielded incremental liquid production of 89,936 bbl and 234,217 bbl for Wells 9 and 10, respectively, as shown in Figure 5-13a. An increase in oil production of up to 5995 bbl was observed in Well 10, whereas a decrease in oil production was observed in Well 9 with reduced skin factors, as shown in Figure 5-13b. Since it became easier for fluids to flow into the wells with smaller skin factors, a significant increase in water production was observed in both wells, as shown in Figure 5-13c. The water cut reached approximately 99.7% and 99% for Wells 9 and 10, respectively, after 10 years of water injection treatment regardless of changing skin factor values. The modeling results suggested that removing skin damage could allow more liquid to be produced from the reservoir. However, removing skin may not solve the issue of high water cut since there is less mobile oil in the reservoir with production going on.

5.3.2 Scenario 2 – Water Injection Rate Effect on Offset Wells Production

To investigate the effect of water injection rate on production of offset wells, five cases (Cases 6–10) with different water injection rates were designed to compare the production performance. The tracer function was used in the simulation to track the dynamic distribution of injection water. The injection and production constraints setup for Wells 5, 9, and 10 is summarized in Table 5-2.

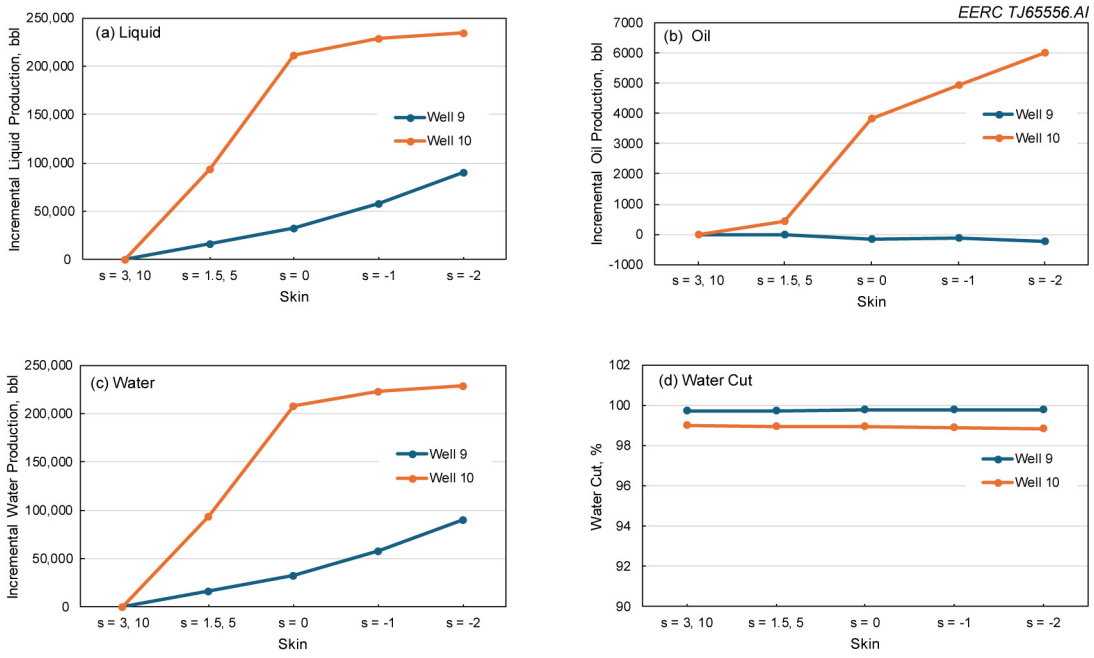

Figure 5-13. Effects of reduced skin factor on Wells 9 and 10 during the predictive period: a) cumulative liquid production, b) cumulative oil production, c) cumulative water production, and d) water cut.

Table 5-2. Constraints Setup of the Injection and Production Wells for Scenario 2

	Well 5	Well 9			Well 10		
Case No.	Injection Rate, bpd	Skin	Max. Production Rate, bpd	Min. Pressure, psi	Skin	Max. Production Rate, bpd	Min. Pressure, psi
1	500	3	700	500	10	700	500
6	0						
7	800						
8	1000						
9	1230						
10	1500						

The results suggest that increasing water injection rate contributed to higher liquid, oil, and water production in both Wells 9 and 10. With a water injection rate of 1500 bpd, cumulative oil production increased to 5908 and 4770 bpds for Wells 9 and 10, respectively. However, compared to the insignificant increase in oil production, the increase in water production was as high as 1,488,111 bbl and 628,867 bbl, respectively for Wells 9 and 10, as shown in Figure 5-14.

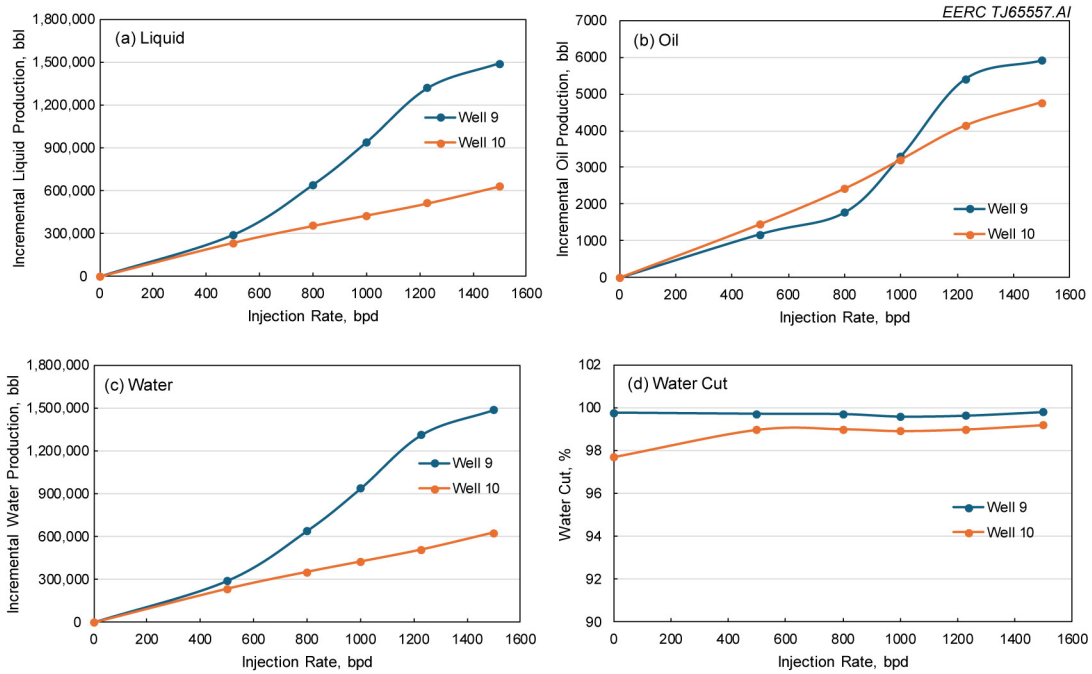

Figure 5-14. a) Incremental liquid production, b) incremental oil production, c) incremental water production, and d) water cut of production for Wells 9 and 10 after 10 years of prediction for Case 1 and Cases 6–10 of Scenario 2. The incremental production represents the cumulative production of each case at the end of prediction subtracted by that of Case 6 (no water injection).

5.3.3 Scenario 3 – Minimum Bottomhole Pressure (BHP) Effect on Offset Wells Production

The production performance of Wells 9 and 10 was also affected by their operational status. Three additional prediction models were built with different minimum BHP in Wells 9 and 10. The injection and production constraints setup of Wells 5, 9, and 10 for Scenario 3 is summarized in Table 5-3.

Table 5-3. Constraints Setup of the Injection and Production Wells for Scenario 3

	Well 5	Well 9			Well 10		
Case No.	Injection Rate, bpd	Skin	Max. Production Rate, bpd	Min. Pressure, psi	Skin	Max. Production Rate, bpd	Min. Pressure, psi
1	500	3	700	500	10	700	500
11				1000			1000
12				1500			1500
13				2000			2000

The simulation results of Cases 11, 12, and 13 were compared with that of Case 1. When minimum BHP reduced from 2000 psi to 500 psi, the incremental oil production in Wells 9 and 10 was up to 1042 and 2174 bbl, respectively, while the incremental water production was up to 255,715 and 159,265 bbl, respectively, as shown in Figure 5-15.

Simulations of different strategies to optimize water injection treatment suggested that reducing skin, increasing water injection rate, and reducing well BHP are approaches to ensure incremental oil production in the production wells. However, the increase in oil production was not significant and at the expense of increasing water production. These results imply that the operators need to improve the ability of the equipment to process large amounts of water to achieve incremental oil production during water injection treatments. Alternative strategies should be analyzed and applied to achieve greater increase in oil production and minimize water cut in offset production wells.

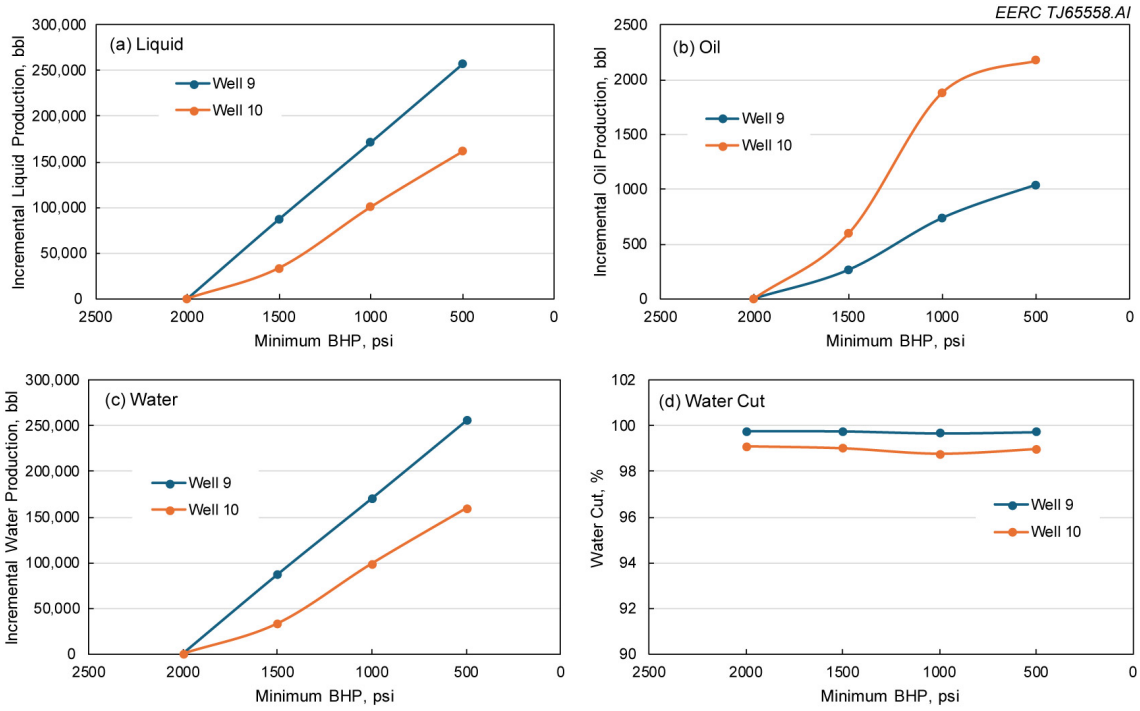

Figure 5-15. a) Incremental liquid production, b) incremental oil production, c) incremental water production, and d) water cut of production for Wells 9 and 10 after 10 years of prediction for Cases 1, 11, 12, and 13 of Scenario 3. The incremental production represents the cumulative production of each case at the end of prediction subtracted by that of Case 13 (minimum BHP of 2000 psi).

5.4 CO_2 EOR

Compared to water, CO_2 has more advantages as an injectant in enhancing oil recovery because of higher solubility in oil, lower IT, and higher mobility than water; in addition, CO_2 can dissolve in oil, reduce oil viscosity, and swell the oil, thus contributing to more oil production in the production wells (Dellinger and others, 1984; Grigg and Schechter, 1997; Davarpanah and others, 2019).

Five cases were designed and compared with Case 6 (no water or CO_2 injection case) to investigate the effect of increasing the CO_2 injection rate on the improvement of oil production. Well 5 was converted into a gas injection well to inject CO_2 for 10 years. Wells 9 and 10 were produced and monitored. The injection and production well constraint setup is summarized in Table 5-4.

Table 5-4. Constraint Setup of the Injection and Production Wells for the CO_2 EOR Scenario

	Well 5	Well 9			Well 10		
Case No.	Injection Rate, MMscf/d	Skin	Max. Production Rate, bpd	Min. Pressure, psi	Skin	Max. Production Rate, bpd	Min. Pressure, psi
6	0	3	700	500	10	700	500
14	1						
15	2						
16	3						
17	4						
18	5						

Compared to all the water injection strategies, the performance of CO_2 flooding is better for improving oil production, exhibiting much higher incremental oil production and significant reduction in water cut for Wells 9 and 10 through the application of CO_2 EOR. Comparison of the CO_2 EOR performance between Wells 9 and 10 suggests that Well 9 could achieve higher incremental oil production and greater reduction in water cut than Well 10, as shown in Figure 5-16.

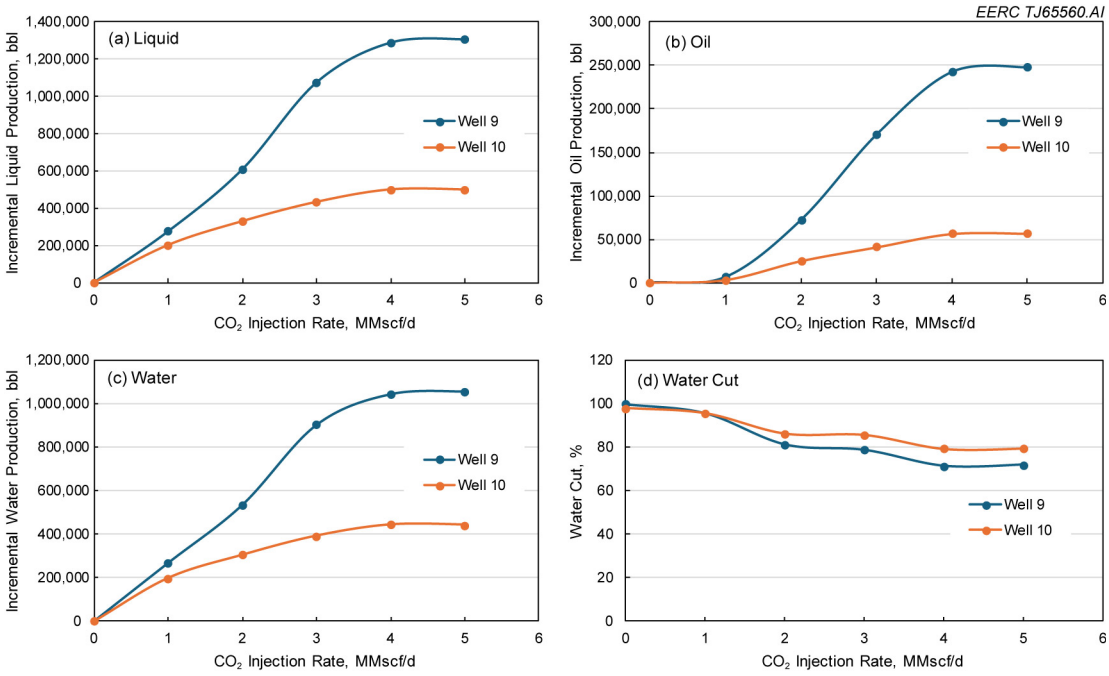

Figure 5-16. a) Incremental liquid production, b) incremental oil production, c) incremental water production, and d) water cut of production for Wells 9 and 10 after 10 years of prediction for Case 6 and Cases 14–18 of the CO_2 EOR scenario. The incremental production represents the cumulative production of each case at the end of prediction subtracted by that of Case 6 (no water injection).

5.5 Surfactant EOR

Based on the formation integrity test (FIT) and contact angle test results, surfactant injection was also evaluated as a potential method for improving field performance. Surfactants improve oil recovery by various mechanisms including the creation of microemulsion due to a decrease in the IT between the oil and water phases and reservoir rock wettability alteration toward more favorable water-wet conditions (Sheng, 2010). In this work, the research focus was placed on wettability alteration, as it was observed to be the prevailing mechanism based upon experimental results. Four cases were designed to investigate the surfactant effects. The wettability alteration process was adopted in numerical simulations by adjusting the relative permeability curves based on the surfactant strength, as observed from the results of the core-flooding experiments (no surfactant, weak surfactant, normal surfactant, and strong surfactant). The setup of the injection and production constraints was the same as Case 1 (Table 5-1).

The results of the four simulated surfactant cases in terms of cumulative liquid, oil, and water production from Wells 9 and 10 are shown in Figures 5-17 and 5-18, respectively. Results distinctly show that the liquid and water production remained almost unchanged between the four cases. However, the cumulative oil production from Wells 9 and 10 showed an increase directly dependent upon surfactant utilization. Similar increases in oil production and decrease in water have been noted in the literature from field application observations. For example, in Semoga Field in Indonesia, the average oil production increased from 425 bpd to 928 bpd and the water cut dropped from 96% to 88% as a result of surfactant flooding (Rilian and others, 2010). Cheng and Kwan (2012) reported an incremental oil production between 29% and 71% from the application of an anionic surfactant in a dolostone reservoir of Yates Field. Therefore, the results of the simulation work conducted in this study suggest a possible successful field-scale application in Foreman Butte Field through proper design and the operation could continue utilizing the existing water injection infrastructure and facilities.

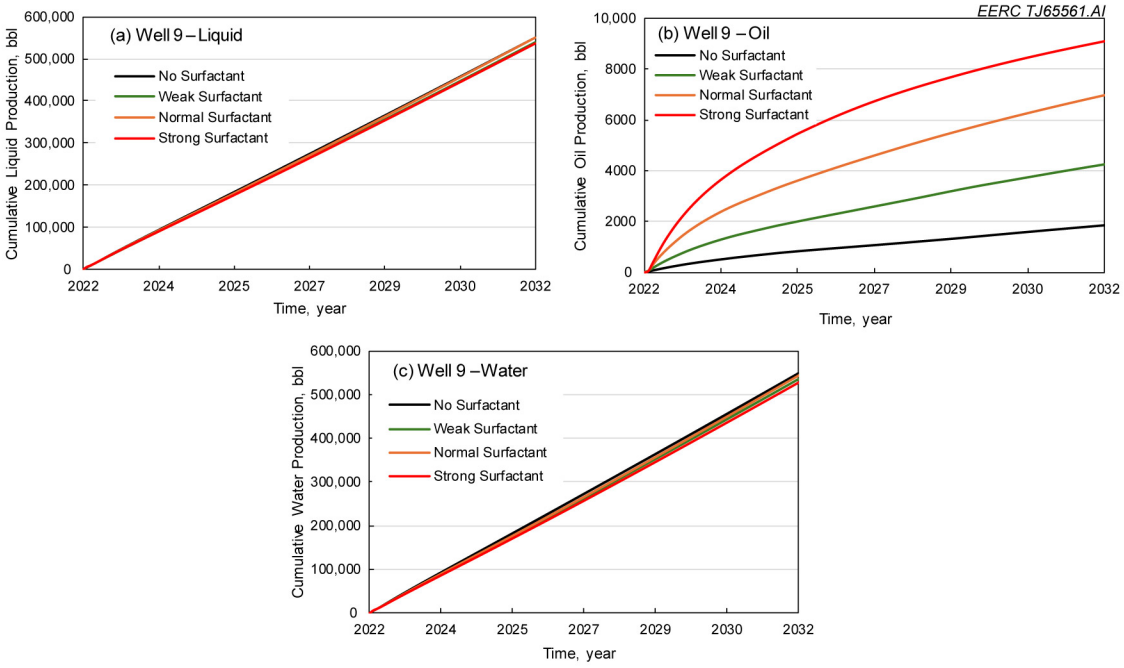

Figure 5-17. a) Incremental liquid production, b) incremental oil production, and c) incremental water production of Well 9 for the various surfactant EOR cases.

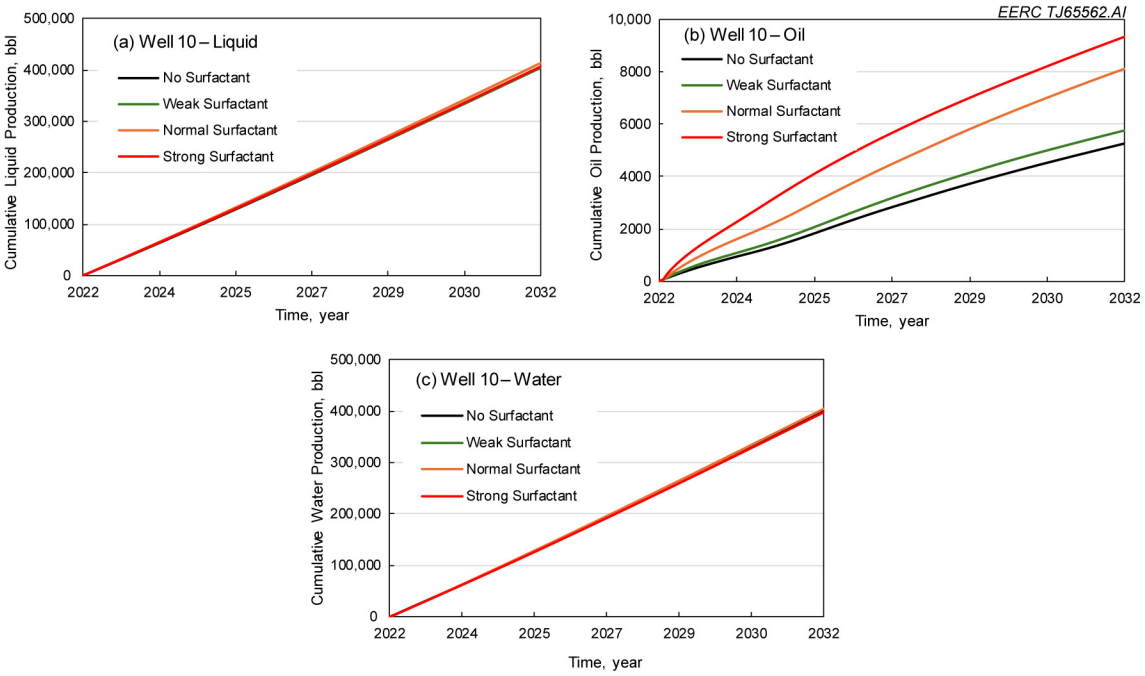

Figure 5-18. a) Incremental liquid production, b) incremental oil production, and c) incremental water production of Well 10 for the various surfactant EOR cases.

5.6 Infill Well Drilling

Infill well drilling is a commonly adopted industrial practice to improve oil recovery in heterogeneous reservoirs. This technique could be applied to any stage of reservoir development, especially in legacy fields with years of waterflood treatment (Fuller and others, 1992; Syed and others, 2021). Incremental oil production could be accomplished by infill well drilling, which may improve sweep efficiency, lateral formation connectivity, and enable recovery of "wedge-edge" oil (Driscoll, 1974; Gould and Munoz, 1982; Syed and others, 2021).

A prediction model was built to evaluate the oil production performance of infill wells. Four infill wells—Infill1, Infill2, Infill3, and Infill4—were added to the model at different locations. The locations of added infill wells are shown in Figure 5-19. All the infill wells were produced with the maximum liquid rate constraint of 300 bpd and minimum BHP of 500 psi for 10 years. The cumulative oil production of each infill well during the 10-year prediction period is shown in Figure 5-20a and is compared with the average cumulative oil production of their nearby two wells' production history, as shown in Figure 5-20b. The results suggest that the infill wells with higher average cumulative oil production in the nearby two existing wells produce more oil during the prediction period. This can be observed from comparing the expected cumulative oil production from Infill1 and Infill2 to Infill3 and Infill4. The predicted cumulative oil produced from Infill1 and Infill2 were 15,591 bbl and 9647 bbl, respectively, and they correspond to the existing nearby well pairs with highest production, which are Wells 11 and 16 for Infill1 and Wells 8 and 13 for Infill2. Infill3 and Infill4 resulted in lower expected cumulative oil production similar to the relatively lower cumulative oil produced by the nearest well pairs, Wells 1 and 7 for Infill3 and Wells 3 and 5 for Infill4. The results imply that drilling infill wells could be an effective approach to improve oil recovery for the tight legacy oil field. The locations of infill wells should be selected close to the existing wells with high cumulative oil production to potentially achieve meaningful oil production in the infill wells.

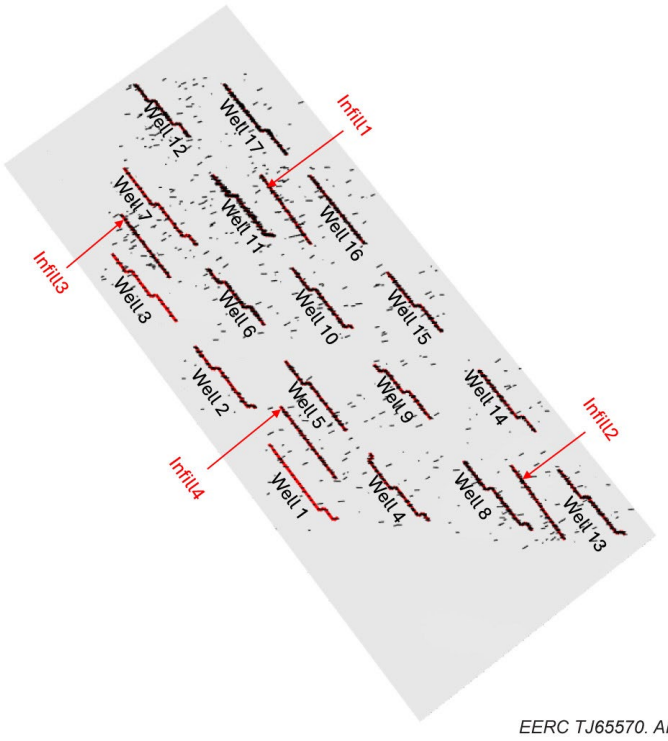

Figure 5-19. Distribution of wells and natural fractures for the model with four infill wells.

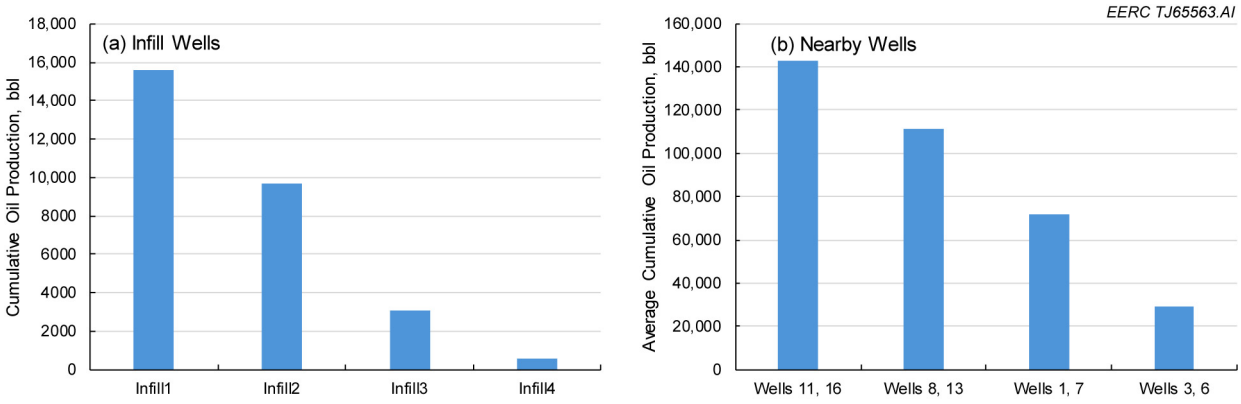

Figure 5-20. Cumulative oil production of the infill wells a) during the 10-year prediction period and average oil production of their nearby two existing wells b) before adding infill wells.

5.7 Application for Another Conventional Oil Field in North Dakota

The success of implementing the detailed modeling and high-efficiency field-scale simulation tools and their workflow for Foreman Butte Field evaluation led to an additional evaluation to test their applicability to another oil field located in southwest North Dakota, as

described in Appendix D. The main pay zone is also a carbonate reservoir but is produced from the Ordovician Red River Formation, which consists of dolomitized laminated carbonate with permeable intervals. The simulation model was created with five wells (Wells A, B, C, D, and E) that have a production history dating back to the 1960s. All the wells were drilled vertically during the initial completion and were stimulated by matrix acidizing or acid frac treatments to improve production. Wells A, D, and E were recompleted with lateral sections. Well B was treated with water injection from 1970 to 1985. Wells A and E have been treated with water injection and HPAI to improve oil production in this section.

The simulation model was successfully history matched to build the baseline model; investigations were continued, including water flooding, continuous CO_2 injection, CO_2 WAG EOR; and different oil production strategies were compared. The findings from this investigation include the following:

- Injecting water or CO_2 while suspending production ensured that the reservoir pressure was restored so the target liquid production rate could be achieved when production was resumed.

- The improved cases of water injection, continuous CO_2 injection, and CO_2 WAG showed better oil production and reservoir pressure responses than the no-injection case.

- Increasing the water injection rate contributed to improvement in oil production at the expense of treating significant amounts of produced water from the reservoir.

- Increasing the CO_2 injection rate resulted in an increase in oil production from the reservoir under miscible or near-miscible conditions.

- CO_2 WAG had benefits of both water injection and CO_2 injection to achieve better EOR performance.

- Drilling new infill wells could contribute to additional oil production.

The investigation demonstrated that water flooding, CO_2 flooding, or the CO_2 WAG process could result in significant oil production improvement for a conventional field in North Dakota. This case validates the effectiveness of the investigation methodology and workflow, showcasing the potential for additional resource extraction from conventional oil fields in the region. In addition, the investigation into different operational strategies offers valuable insights for both operators and the state, aiding in field development prioritization when various economic factors are considered. By understanding the relative advantages and limitations of each EOR technique under specific reservoir conditions, stakeholders can make more informed decisions about where to allocate resources and which methods to implement. Through the investigations, it is also worth noting the importance of tailoring EOR approaches to the unique characteristics of each reservoir, considering factors such as reservoir heterogeneity, fluid properties, and existing infrastructure. This approach not only enhances oil recovery but also ensures cost-effectiveness and maximizes the economic return on investment.

Appendix D contains a complete workflow and technical details of the evaluation for another North Dakota carbonate reservoir revitalization feasibility study using water flooding and CO_2 EOR.

6.0 FACILITY AND OPERABILITY ASSESSMENT

6.1 Facility Assessment

The wells within Foreman Butte Field are single producing wells that operate to individual tank batteries typically requiring a low-pressure heater treater (less than 150 psig) and atmospheric oil and water stock tanks. Each battery maintains a flare on-site to combust produced gas that cannot be sold. However, the gas volumes that are flared remain very limited. Some of the wells have the capability to move the produced water through a saltwater disposal (SWD) system, which requires a low-pressure pump to move the water from the tank batteries to the disposal well. No additional equipment is installed in the tank batteries.

The wells are operated with beam pumping units powered by electrical motors, many with pump-off controllers to monitor the producing fluid levels and minimize pump-off conditions. The overall average production within the field is 20 bpd oil, 162 bpd water, and 7 Mscf/d. Recent tests that upsized the pumping equipment to larger beam pumping units or Rotoflex units have resulted in increases in oil, water, and gas production volumes. Stabilized production after the installation of high-volume pumping equipment has shown production increases of approximately 30 bpd oil, 200 bpd water, and 20 Mscf/d, with the production levels remaining flat for months after the installation of the larger pumping equipment.

Based on the results from upsizing the pumping equipment, EEPT is planning to install an electric submersible pump (ESP) in one well. The range of the ESP will be roughly double the current fluid production from the selected well and provide much needed bottomhole condition data (pressure, temperature). With the well producing to a single well battery, daily production rates will be provided by direct measurements. To accomplish this work, some upgrades to the facility were required, that being an upsize in the electrical system to handle the demands of the ESP.

As for the opportunity and challenges of the facility and operability for a general operation involving water flooding, CO_2, and/or other EOR operation, many advanced and increasingly complex technologies are required and must be employed in order to extract as much of the original oil in place (OOIP) economically. Typically, primary production based on the pressure depletion of the reservoir to produce the fluids is the initial phase undertaken after a well is drilled and completed. As primary oil production declines, additional processes such as waterflooding and CO_2 enhanced recovery are investigated through detailed geologic and reservoir studies to determine their applicability for the field being investigated.

Normally, a waterflood will precede a CO_2 project because of lower investments and wide availability of water. Detailed geologic and reservoir studies will be conducted to provide an estimate of the production and injection streams associated with the project. With the development

of a waterflood project, investments for new facilities for the increase production volumes; sourcing of water; and the drilling of new water supply wells, field infrastructure and utilities, and water disposal capacity will be required.

Once the waterflood has matured, a second and more complex project is investigated: CO_2 enhanced recovery. This project entails injecting CO_2 into the producing formation at or near the MMP to move more of the remaining oil left in the formation after the primary and waterflooding phases. A CO_2 project will require a source for the CO_2, which is normally piped into the project from a pipeline or captured source near the project.

For the development of a CO_2 project, many changes or upgrades to the field will be required. These will include field utilities (power, water supply and disposal, and fuel gas) and expansion of the separation facilities to capture the produced CO_2 at various pressures to limit the power consumption by the compressors to reinject the CO_2. A new injection system to deliver the CO_2 to the injection will need to be installed, while the production lines may need to be upgraded if they are unable to handle the production of CO_2 with the produced fluids or if they need to be rerouted to a central facility.

Overall, each phase of enhancing the recovery of oil and gas from a particular field will require higher levels of investment to implement the project. As long as the recovered oil and gas are sufficient to provide the necessary economics, a project can be implemented to recover additional oil.

Additional detailed discussion is included in Deliverable 3 – Facilities Assessment: Opportunities and Challenges for Revitalization.

6.2 Productivity Assessment

EEPT owns a total of 32 wells that produce from the Ratcliffe Formation in Foreman Butte Field, as shown in Figure 6-1. The wells were drilled on a nominal 640-acre spacing, each well was drilled with a single horizontal lateral, and 12 of the wells are active producers. One well has been converted to water injection for a waterflood pilot. Nine of the wells are classified as inactive but produced within the last year. One well is listed as temporarily abandoned, and six of the wells are classified as temporarily abandoned-observation in connection with the waterflood pilot. Three wells have been plugged and abandoned.

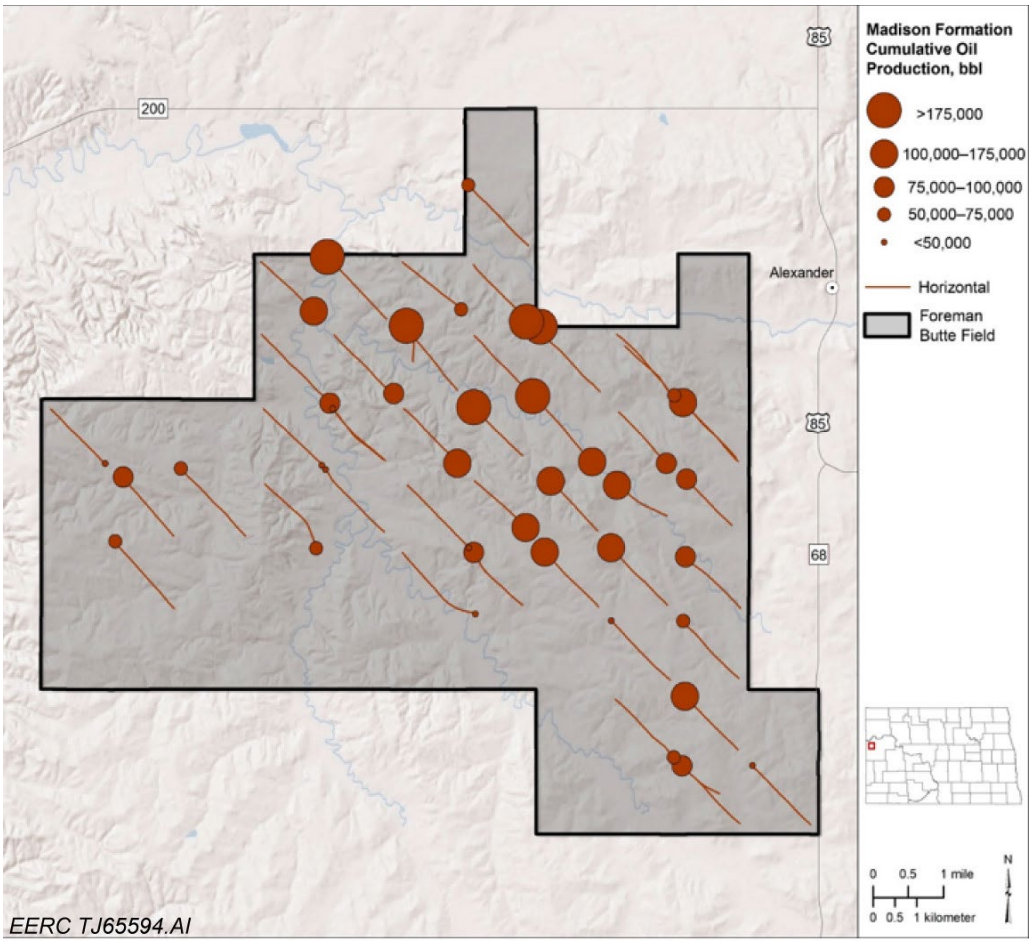

Figure 6-1. Map showing Foreman Butte wells owned by EEPT, with bubbles posted to represent cumulative oil recovery.

6.2.1 Analysis of Production Data

Decline curve analysis (DCA) is performed using production data from legacy wells to group wells by similar performance characteristics. Plotting of decline rate, followed by calculations of hyperbolic decline coefficients and terminal decline rates, is used to determine per-well estimated ultimate recoveries (EURs). This provides a starting point for production data analysis and RTA, which is an additional method that uses production data to further analyze reservoir behavior.

DCA only accounts for the variation of production with time assuming boundary-dominated flow. Blasingame and others (1989) suggested the RTA method, which accounts for changes in pressure versus time. The normalized rate and material balance time are plotted, with material balance time being defined as cumulative production divided by current producing rate for a given point in time. This approach allows the estimation of permeability, skin, drainage area, and OOIP.

The use of the RTA approach requires the availability of pressure and rate data versus time; however, in Foreman Butte, only initial reservoir pressure and current BHP data were available. The saturation (bubble-point) pressure of the reservoir fluid was known from lab tests, and GOR behavior was used to estimate the point at which the reservoir reached the bubble point. Cumulative gas production was plotted against cumulative oil production on log-log scales (Figure 6-2). For early production above the bubble-point pressure, the data points plot on a straight line, with initial deviation from that straight line indicating that point at which the pressure has dropped below the bubble point. Using this approach, the time when each well drops below bubble-point pressure is identified and used in the next steps.

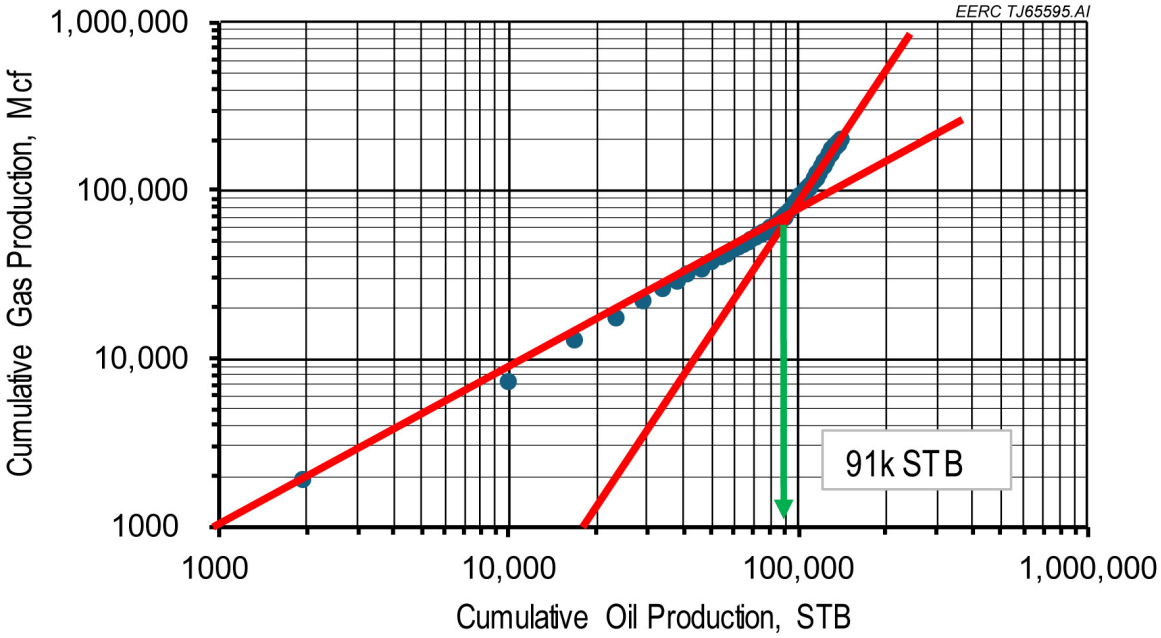

Figure 6-2. Log-log plot of cumulative oil production vs. cumulative gas production. The diversion from the straight line illustrates the time where the pressure dropped below bubble point.

At this stage in the field's production life, three pressure data points are available (initial reservoir pressure, bubble-point pressure, and current BHP). Four different hypothetical lines were used to fit the three points; then the pressure profile was used to perform RTA and estimate the reservoir properties. Suggested fits are illustrated in Figure 6-3.

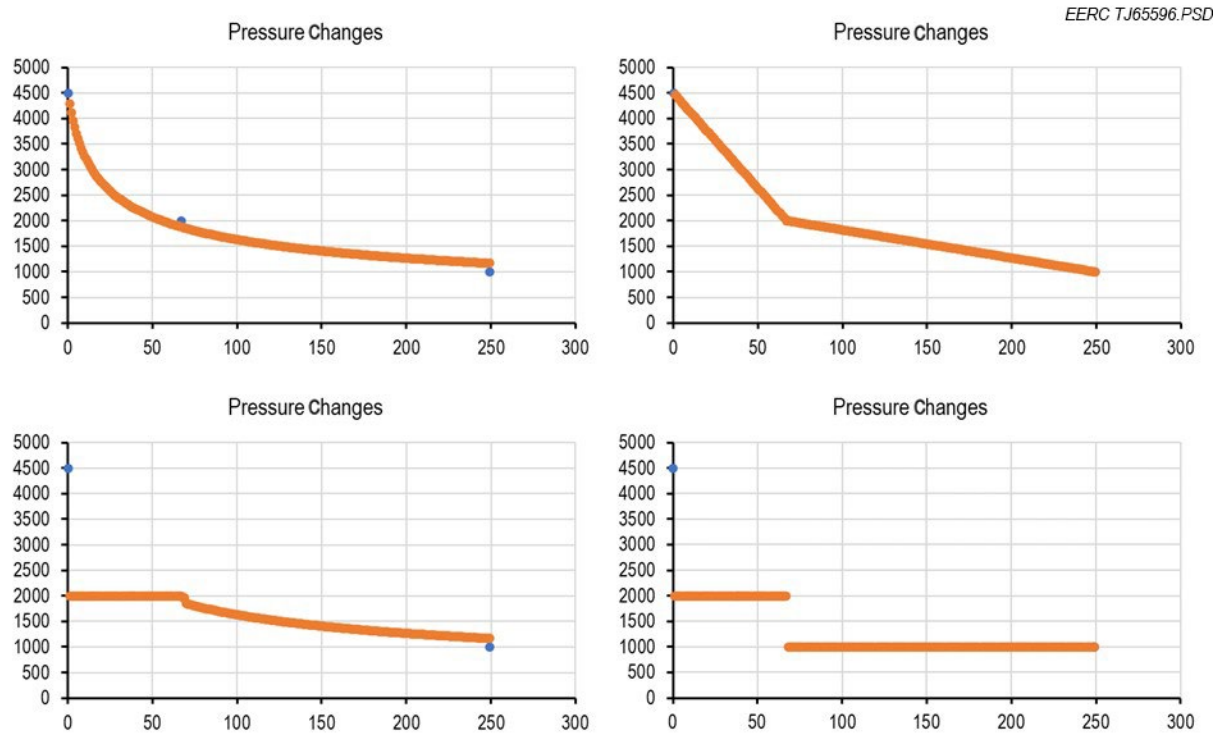

Figure 6-3. Assumed pressure vs. time decline curves for a well to perform RTA. Y-axis units are psia; X-axis units are months on production.

The plots were challenging to match using Blasingame type curve (Blasingame and others, 1989) since all pressure data are synthetic. The boundary-dominated flow was easier to match because the pressure drop at a late stage of the well life is small and can be predictable. The results of this analysis can be used to support geologic modeling efforts. For instance, the large drainage area and low-permeability estimate imply the existence of natural fractures throughout the drainage area.

6.2.2 Simplified Material Balance

The following assumptions were made to calculate the drainage area using material balance:

- Solution gas drive is the primary recovery mechanism.
- Porosity is 0.12, constant for the reservoir.
- Water saturation is 0.45, constant for the reservoir.
- Initial reservoir pressure of 4430 psi.
- Temperature of 230ºF.
- Water compressibility of $3 \cdot 10^{-6}$ psi^{-1}.
- Gross pay height is 22 feet with ratio of net-to-gross pay of 0.6.

The following steps are then executed:

1. The recovery factor was calculated at bubble-point pressure using Equation 6-1:

$$RF_{P_b} = \frac{N_{p@P_b}}{N} = \frac{B_{oi}}{Bob}\frac{C_t(P_i - P_b)}{1 - S_{wi}} \quad \text{[Eq. 6-1]}$$

   $N_{p@P_b}$ was estimated from the log-log plot of cumulative oil production and cumulative gas production, as illustrated in Figure 6-2.

2. Once the recovery factor and the cumulative production at bubble point were determined, the OOIP for the drainage area of the well was calculated, as follows in Equation 6-2:

$$\text{OOIP} = \frac{N_{p@P_b}}{RF_{P_b}} \quad \text{[Eq. 6-2]}$$

3. The OOIP per acre was also estimated using the volumetric method, Equation 6-3:

$$\frac{\text{OOIP}}{Acre} = \frac{7758(1 - S_{wi})\varphi}{B_{oi}} \quad \text{[Eq. 6-3]}$$

4. The drainage area was then calculated using the following, Equation 6-4:

$$\text{Drainage Area} = \frac{OOIP\ (Material\ Balance)}{OOIP\ (\frac{Volumetric}{acre})} \quad \text{[Eq.6-4]}$$

Based on the simplified method, the recovery factors and drainage areas were estimated for all Foreman Butte wells. Results are illustrated in Figures 6-4 and 6-5.

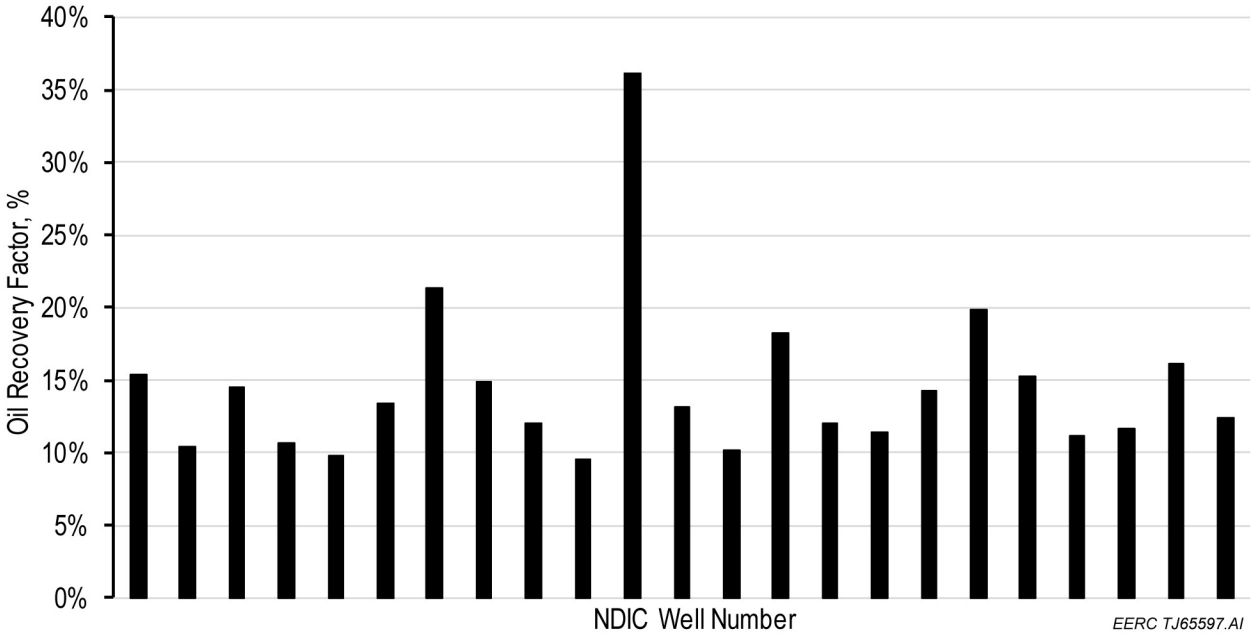

Figure 6-4. Recovery factor calculated from material balance.

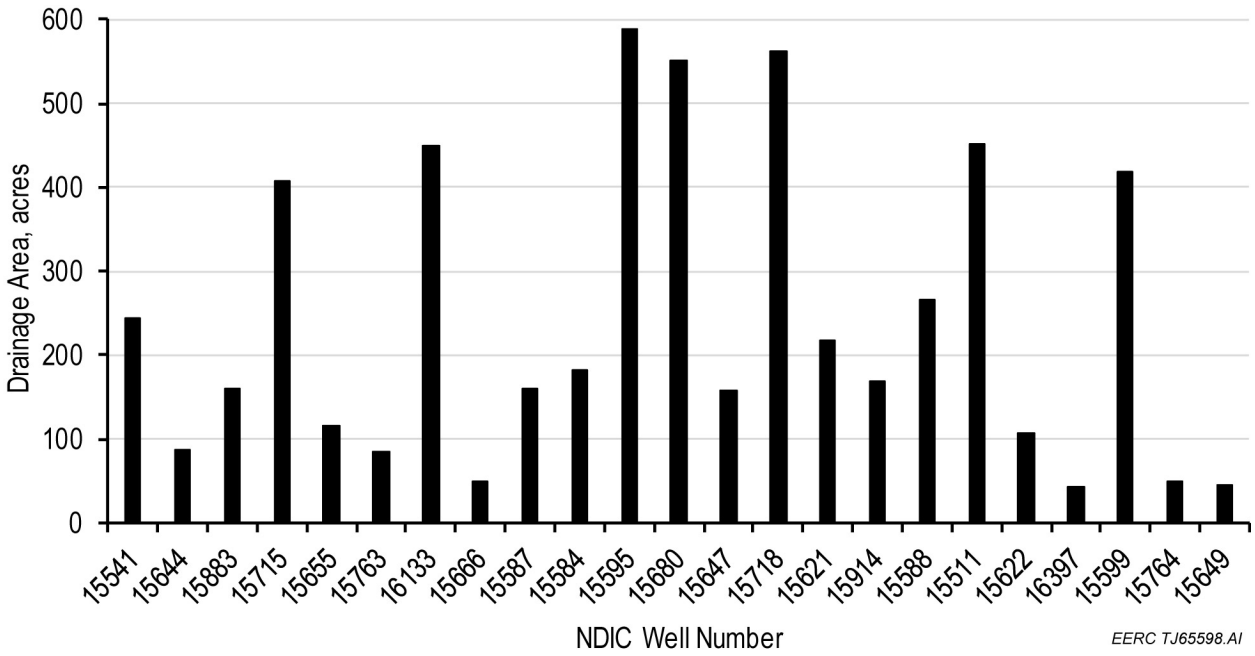

Figure 6-5. Drainage area calculated from material balance.

Several questions can be asked about the different performance of these wells. For instance, can wells attain 20% recovery? The drainage areas of wells are different, which can support the efforts of geomodeling in incorporating natural fractures and higher permeability and porosity zones. The difference in drainage areas could be interpreted as indicating potential for well simulations or infill drilling if natural fractures are not as prevalent in those well locations.

These calculated drainage areas were used to create the drainage map shown in Figure 6-6. Depiction of the calculated drainage area assumes drainage extends outward from the NW–SE diagonal of each section along which the horizontal lateral was drilled. This is useful to see where some unswept acreage may exist that could be a target for future drilling or well stimulation.

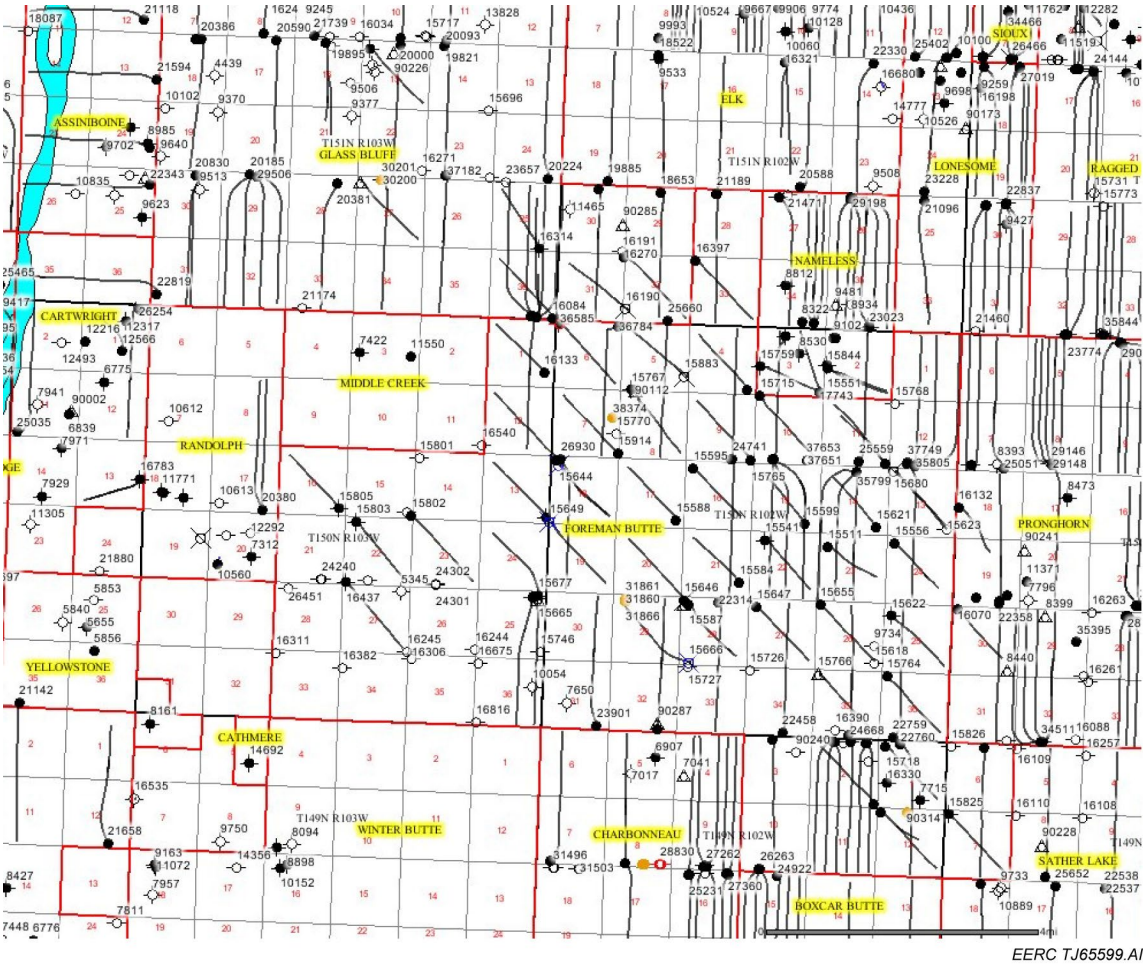

Figure 6-6. Map depicting drainage areas of Foreman Butte horizontal wells.

6.3 Assessment of Production Enhancement Opportunities

Plots of oil cut versus cumulative oil production were used to determine the remaining reservoir potential for oil recovery of each well, as shown in Figure 6-7. These graphs were used as a tool to evaluate the potential production for economic return associated with acceleration of what could be considered additional recovery. This approach will be discussed before exploring the potential to increase recovery beyond what is achievable by the reservoir's natural drive mechanisms. It will be shown that there is significant potential for excellent economic return simply by accelerating oil recovery in this tight reservoir

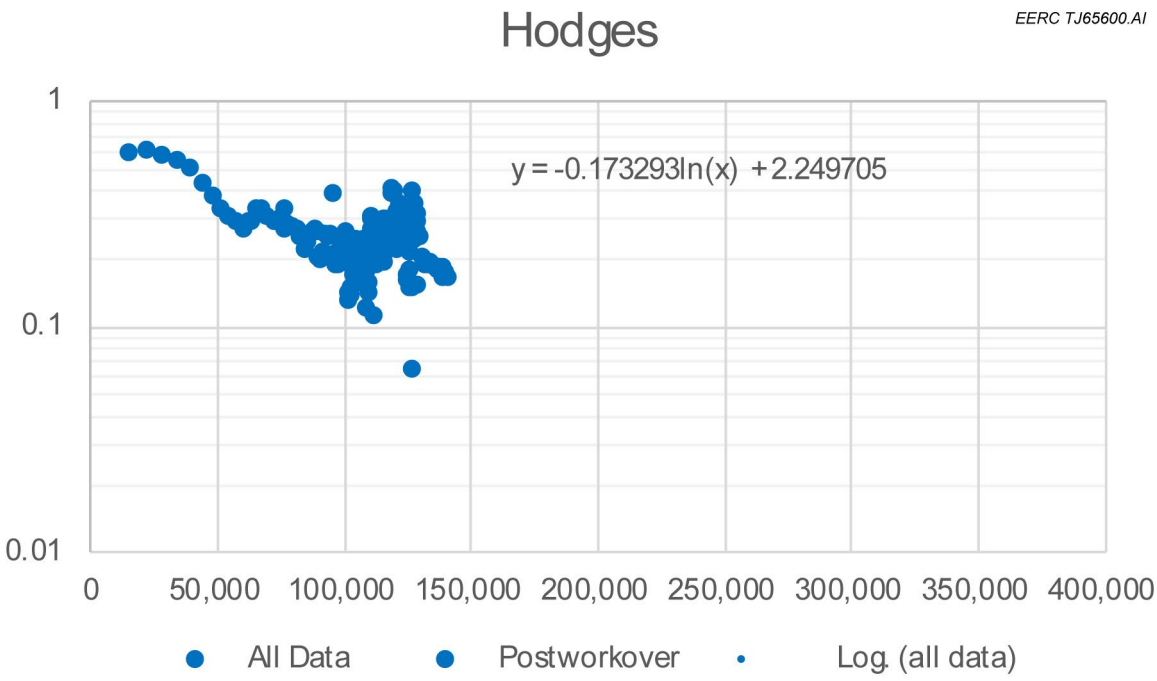

Figure 6-7. Oil cut versus cumulative oil plot for selected well to demonstrate methodology of estimating the reservoir potential.

Based on data supplied by the operator, an estimated 7% oil cut was considered to be the economic limit for wells in this field. The oil cut versus cumulative oil trendline was extrapolated to the 7% oil cut to determine ultimate oil recovery from this well. In this case, the projected ultimate oil recovery from this well is 290,000 barrels, and since it has produced 145,000 barrels to date, it has 145,000 barrels remaining to be recovered. These graphs were created for all active wells and selected inactive wells that may be candidates for reactivation. Graphs for additional wells are shown in Figure 6-8.

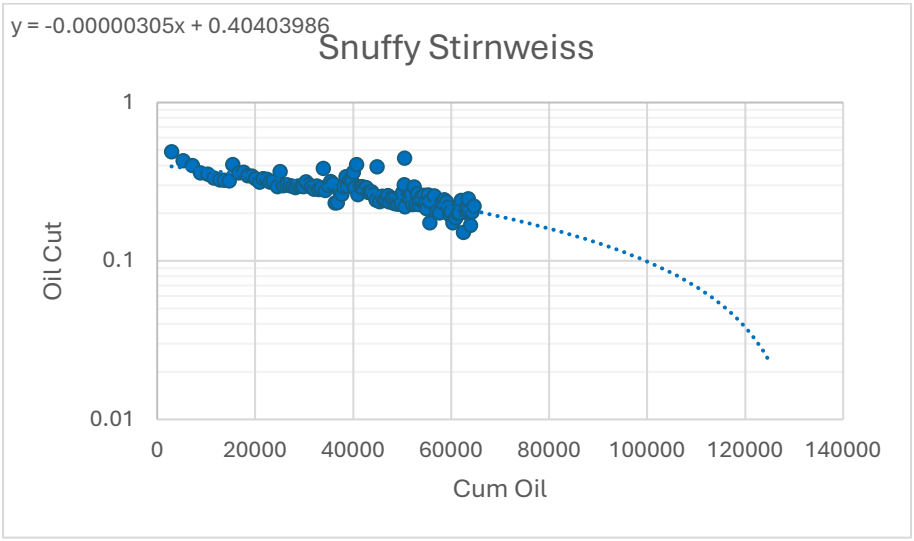

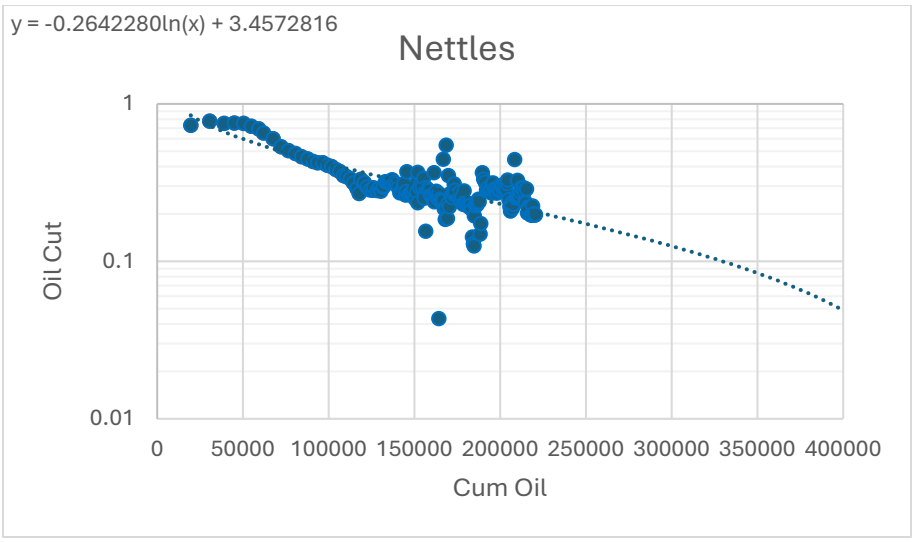

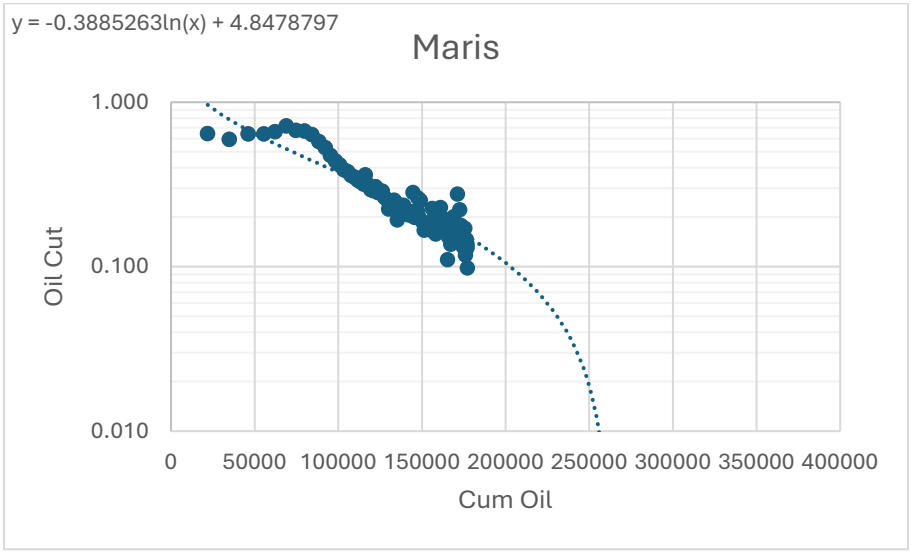

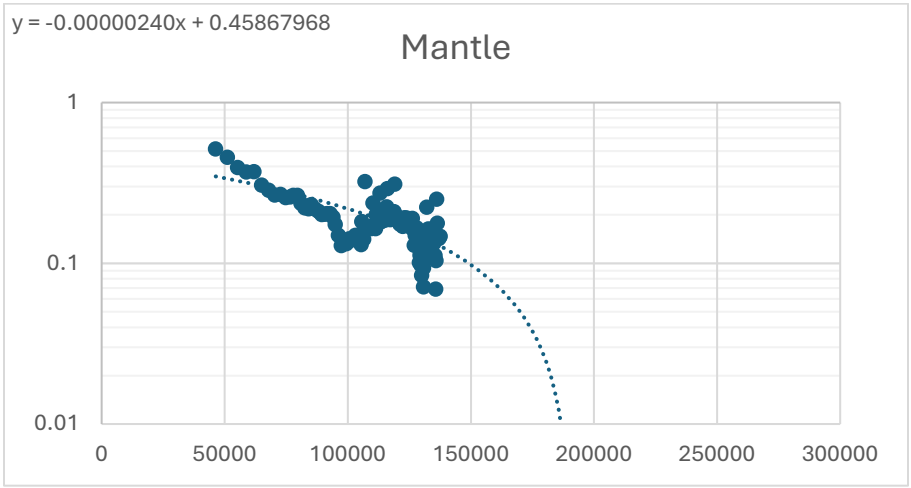

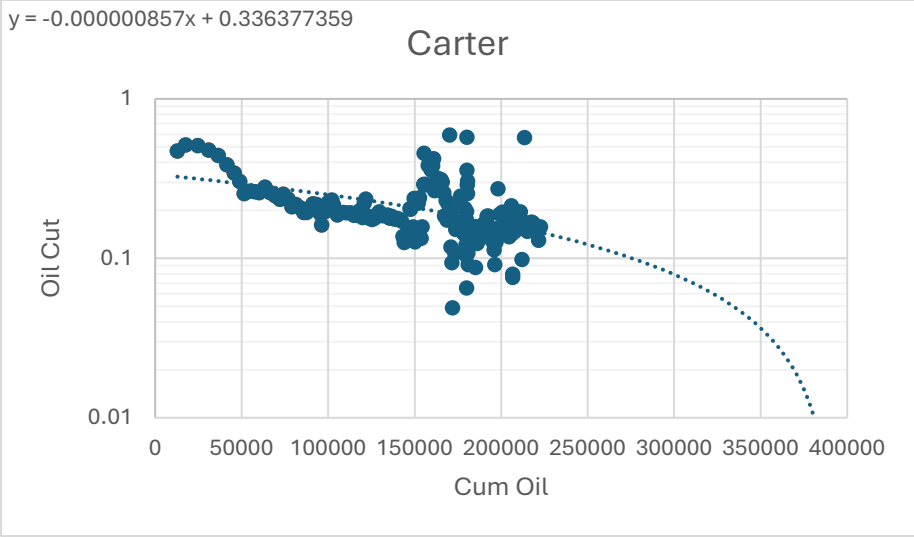

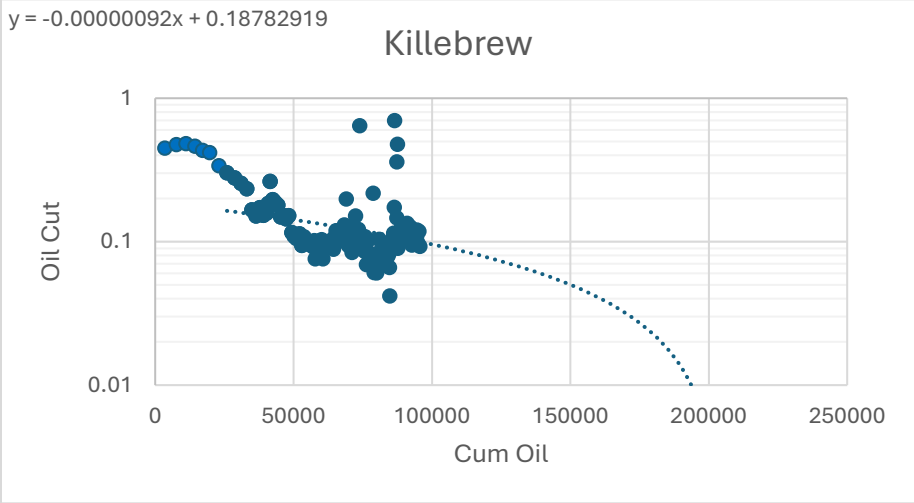

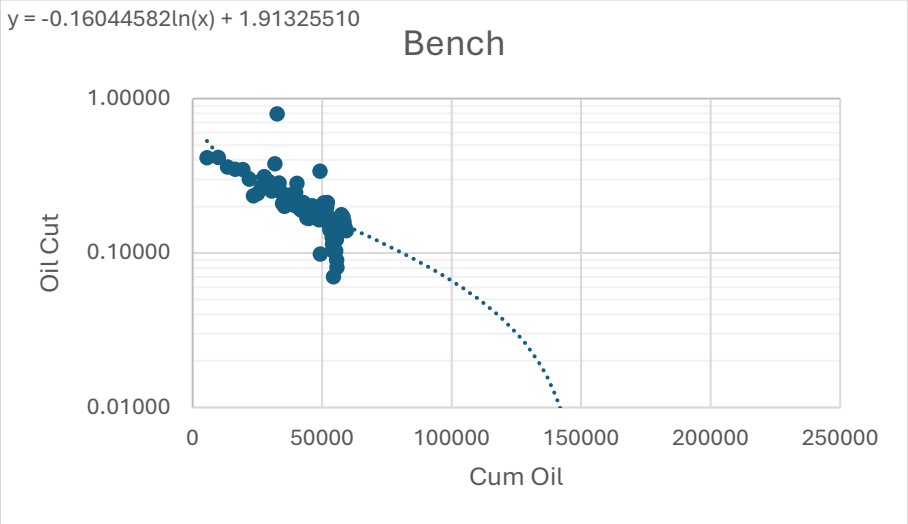

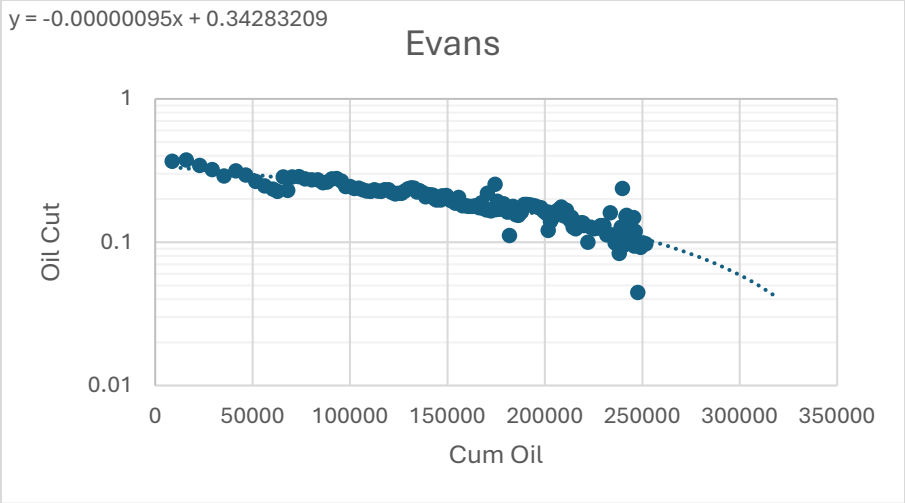

Figure 6-8. Oil cut versus cumulative oil production plot for different wells in the field.

Table 6-1 provides an example of general data for and summarizes the assessment of potential for economic upside of the wells in Foreman Butte Field, including a range of most likely and optimistic estimates of remaining reserves (most likely and high recovery cases). The table also includes the cumulative oil recovery, the current producing oil cut, and the calculated drainage area of each well, as a guide to indicate potential to drain new acreage through well cleanouts or stimulation. A similar approach can be applied to other fields in North Dakota.

Table 6-1. Foreman Butte Well Summary with Pertinent Statistics for Production Evaluation

Well	Cumulative Oil Production, Mbbl	Latest Oil Cut	P50 Potential by Oil Cut – Cum. Oil	P10 Potential by Oil Cut – Cum. Oil	Drainage Area, Acres	Enhancement Potential
Snuffy Stirnweiss	68	0.149	41	45	43	High
Bonds	87	0.062	Minimal	–	87	Low
Sosa	182	0.087	Minimal	–	43	Low
Nettles	221	0.241	148	189	418	High
Ruth	160	0.071	Minimal	–	452	Low
Maris	178	0.122	41	47	588	Fair
Hodges	144	0.175	145	210	448	High
Robinson	115	0.136	24	38	266	Fair
Mantle	139	0.156	23	47	182	Fair
Carter	223	0.146	88	122	1039	High
McGwire	113	0.092	Minimal	–	157	Low
Killebrew	96	0.096	32	44	160	Fair
Palmeiro	94	0.079	Minimal	–	218	Low
Ripken Jr	111	0.059	Minimal	–	169	Low
Foxx	111	0.079	Minimal	–	115	Low
Bench	59	0.132	97	104	161	High
Snider	66	0.095	17	53	106	Fair
Kingman	106	0.09	Minimal	–	–	Low
Murphy	184	0.127	22	53	562	Fair
Banks	44	0.16	Minimal	–	87	Low
Evans	252	0.096	38	85	408	Fair
Belle	130	0.09	Minimal	–	–	Low
Galarraga	68	0.063	Minimal	–	84	Low
Thomas	62	0.07	Minimal	–	50	Low
Matthews	171	0.062	Minimal	–	551	Low
Jackson	39	0.137	Minimal	–	49	Low
Williams	37	0.145	Minimal	–	45	Low
Schmidt	91	–	None	None	107	None
Bagwell	4	–	None	None	20	None
Aaron	140	–	None	None	245	None
Gonzalez	176	–	None	None	416	None
Mays	41	–	None	None	–	None
Total Potential Mbbl			**716**	**1037**		

The estimated reservoir potential to production (R/P) metric was also calculated for the wells with potentially remaining recovery, which is the remaining recovery divided by the current production. Three wells had sufficient recovery and a sufficiently low oil production rate that they would take over 20 years to produce the remaining potential: Nettles, Hodges, and Bench. In addition, the currently inactive Snuffy Stirnweiss well had a good oil cut but produced at a very low rate; if it could be returned to production at its last recorded oil production rate, its R/P ratio would be 14 years.

These four wells were categorized as having high economic potential, along with the Carter, based on its sheer volume of remaining potential, although its R/P ratio was only 8 years. Possible future activities include inflow performance enhancement by upgrading artificial lift capacity,

cleaning fill out of laterals, and some kind of stimulation. The laterals of the Hodges and Bench wells have already been partially cleaned out, with about one-third of the lateral having been cleaned with the drill bit in both cases. These wells experienced sustained production increases of 27 bpd oil and 19 bpd oil, respectively. However, given their remaining potential and projected long production lives, additional work can still be easily justified. As of 2023, the Bench well was pumped off and the Hodges had 2500 feet of gas-free fluid above pump depth. Therefore, any productivity enhancement of the Bench well going forward would have to be done through cleaning out the rest of the lateral or through stimulation, while the Hodges presents an opportunity to increase productivity through upgrading artificial lift capacity.

To illustrate the economic potential associated with increasing fluid production, the Hodges is offered as an example. Two scenarios are presented: one, where artificial lift is upgraded and the total fluid production is increased by 50%, at a cost of $450,000; a second where additional work is done that would double fluid production. This could include some combination of cleanout, stimulation, and artificial lift upgrade, but for the purposes of this illustration, it is assumed that $900,000 would be spent in a manner that would accomplish the goal of doubling well productivity. Assumptions inherent in these scenarios include a water disposal cost of $2.00 per barrel, that the well will follow its same historical water cut trend after the workover (except as noted above in the last scenario), and a WTI oil price of $75. Economic calculations show that each case has a net present value (NPV) of approximately $700,000. This analysis supports continuing to do the cleanout and lift upgrade work while looking for more aggressive measures to increase productivity. Each well will provide its own unique opportunity based on its history and current operating parameters, but further consideration of the Snuffy Stirnweiss, Bench, Hodges, and Nettles wells for productivity enhancement is highly recommended.

Recommending a specific stimulation program is beyond the scope of this report, but it is recommended that acid stimulation be considered first before doing any fracking with proppant. These wells were not stimulated on initial completion and very little acid has ever been pumped into any of the wells. Fracturing with proppant runs a high risk of communicating with zones above and below that would present risks of loss of containment or production of extraneous water. It may be wise to start with acidizing alone and evaluate results before proceeding with more expensive sand fracs.

A further consideration in aggressively seeking productivity improvements is the possible status of Foreman Butte Field as a residual oil zone, or “ROZ” type of reservoir. The Madison Formation in the Williston Basin has been identified by Advanced Resources International (2006b) and Burton-Kelly (2017) as having an extensive ROZ component. The high water saturations known to exist and the initial average producing water cut of 50% at Foreman Butte are indicators that this field may have characteristics of a ROZ.

The ROZ fields have been exploited primarily using two methods: CO_2 flooding and dewatering. Dewatering significantly lowers reservoir pressure, which in turn causes gas in small pores to be liberated, which causes oil to flow out of the tight pores. In order to produce this effect at Foreman Butte, much larger volumes of fluid must be produced so that reduced pressure can be achieved over a sufficiently large reservoir volume to cause incremental production.

6.4 Economic Considerations of CO_2 EOR

As one of the prominent EOR processes that can be widely applied to the carbonate reservoirs of Madison Group, it presents significant potential of incremental oil recovery. Average ultimate oil recovery from Williston Basin conventional oil fields after primary production and water injection is less than 30% of oil in place. Table 6-2 summarizes estimated oil recovery from a group of oil fields in the Williston Basin. The data indicate a substantial amount of oil remains in fields producing from the Madison Group; however, CO_2 EOR is an expensive venture that will yield a positive economic return only under certain favorable conditions.

Table 6-2. Summary of Estimated Oil Recovery Factors from Select Williston Basin Oil Fields

Field Unit	Reservoir	Estimated Oil in Place, MMbbl	Cumulative Oil Production, MMbbl	Recovery Factor
Charlson	Silurian	106	19	0.179
Antelope Madison Unit	Madison	100	17.5	0.175
Blue Buttes Madison Unit	Madison	93	35	0.376
Charlson N. Madison Unit	Madison	80	24	0.3
Blue Buttes	Silurian	74	13	0.176
Hawkeye Madison Unit	Madison	44	15	0.341
Charlson S. Madison Unit	Madison	9.6	4.5	0.469
Antelope Devonian Unit	Devonian	16.3	6.4	0.39
Clear Creek Madison Unit	Madison	27	9.9	0.367
Antelope	Silurian	23.4	4.6	0.197
Stoneview	Stonewall	30	5.6	0.187
Tioga	Madison	216	59.9	0.277
Beaver Lodge	Madison	172	56.7	0.33
Beaver Lodge	Devonian	172	74.8	0.435
Little Knife	Madison	294	95	0.323
T.R. Big Stick, Whiskey Joe, Tree Top	Madison	333.9	98.5	0.295
Cedar Hills South Unit	Ordovician	456.5	131.3	0.288

A process of reviewing CO_2 EOR economic potential is presented using the Foreman Butte simulation results as an example. Simulation results were upscaled to forecast CO_2 injection, incremental oil production, and CO_2 production that would require reinjection. From simulations, dimensionless curves were generated that show the cumulative production of oil and CO_2 as a function of cumulative CO_2 injection, with the dimensionless character resulting from all of these values being defined as a fraction of reservoir hydrocarbon pore volume. The dimensionless oil recovery curve used is depicted in Figure 6-9, and the dimensionless CO_2 production curve is depicted in Figure 6-10.

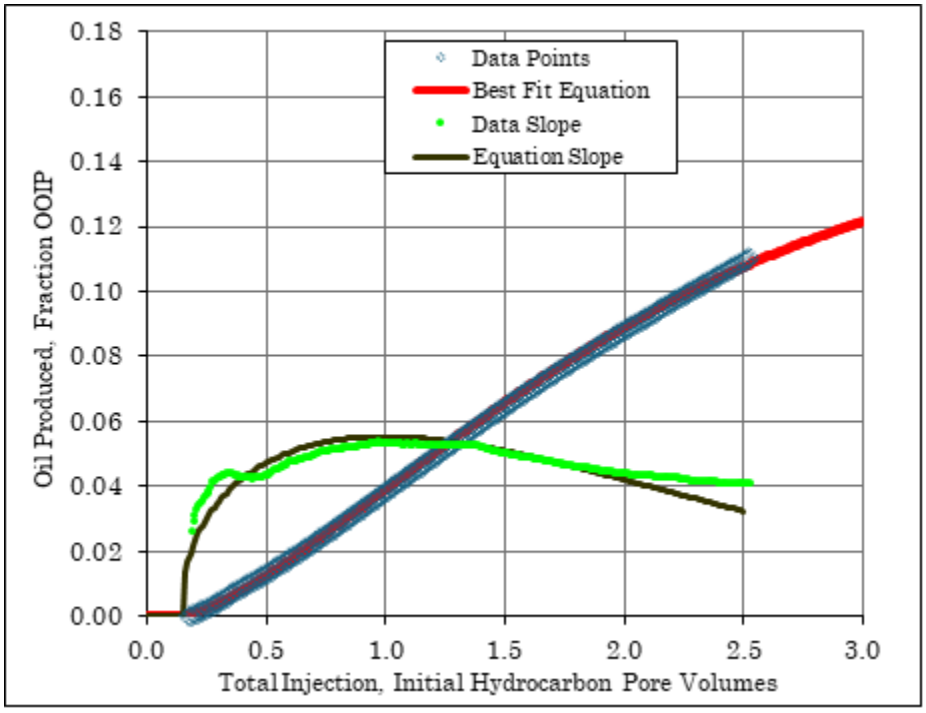

Figure 6-9. Dimensionless oil recovery curve.

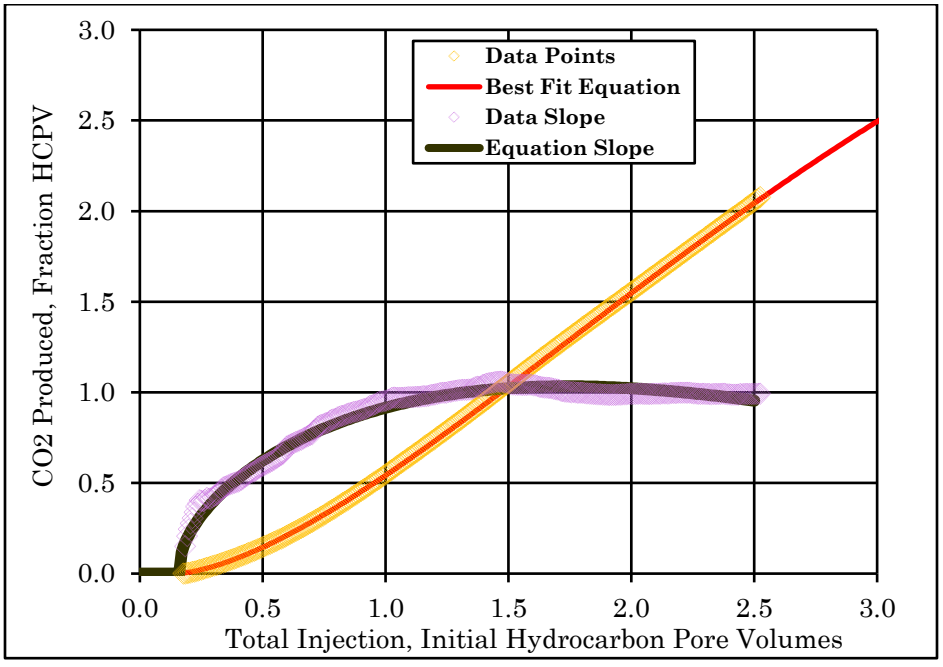

Figure 6-10. Dimensionless CO_2 recovery curve.

The graphs show the raw data points, a curve that fits best to those data points, and the instantaneous slopes of the raw data and the best fit lines. The calculated slopes are proportional to the instantaneous oil production rate at the specified cumulative CO_2 injection volume. The best fit curve is matched to the data using Equation 6-5:

$$y=a(1-e^{-b(x-c)^{\wedge}d}) \quad \text{[Eq. 6-5]}$$

Where:

a = the horizontal asymptote representing the maximum theoretical oil recovery.
b = shape coefficient that controls the initial upward slope.
c = initial time lag/x-intercept of the curve.
d = shape coefficient controlling character of the curve where a value greater than one produces an s-shaped curve as observed in conventional EOR projects, a value of one indicates an immediate exponential decline, and a value less than one produces an early-peak, immediately hyperbolic decline as observed in an unconventional well.
x = independent variable: pore volume injected for an EOR dimensionless curve or time in this application to unconventional wells.
y = oil recovery in terms of pore volume or actual barrels.

This equation is then entered into a time-series spreadsheet to calculate oil and CO_2 production at any point in time, given a specified injection rate. This technique allows for a simplified sensitivity analysis in which oil production over time can be predicted for various injection rates.

The area targeted by CO_2 injection is outlined in green (Figure 6-11). The solid red arrows represent existing wells that were assumed to be converted to CO_2 injectors, and dashed magenta arrows indicate new assumed injection wells that would have to be drilled. The new injector located furthest to the northwest would have an extended lateral length. The criteria used to choose this area were 1) a continuous area (as much as possible) of wells that cumulatively produced over 90,000 bbls of oil; 2) an area of continuous reservoir quality bounded by areas of poorer quality, based on the geological map interpretation; and 3) inclusion of continuous acreage leased by the operator in the field with the strongest acreage position. This area includes seven sections of acreage (and five associated wells) just outside of the legal boundary of Foreman Butte Field, as subsurface geological boundaries do not coincide with regulatory field limits. The target area or hypothetical EOR unit, as is currently being produced, is predicted to have an estimated primary oil recovery of 5.3 MMbbls, 4.6 MMbbls of which have been produced to date. This amounts to 90% of the expected ultimate primary oil recovery from the geological reservoir body, with the remaining 10% being dispersed among scattered wells with lower productivity.

The original oil in place estimation for this area is 26.6 million barrels, and this was used to generate the dimensionless curve forecast. Water injection rate is based on the sustained injection rate of the Mays well over the last year; it has injected an average of 1460 barrels of water per day. On a reservoir volume basis, this equates to approximate 2.8 MMscf/d of CO_2 injection. A higher injection rate could be expected due to the higher mobility of CO_2 and the fact that water

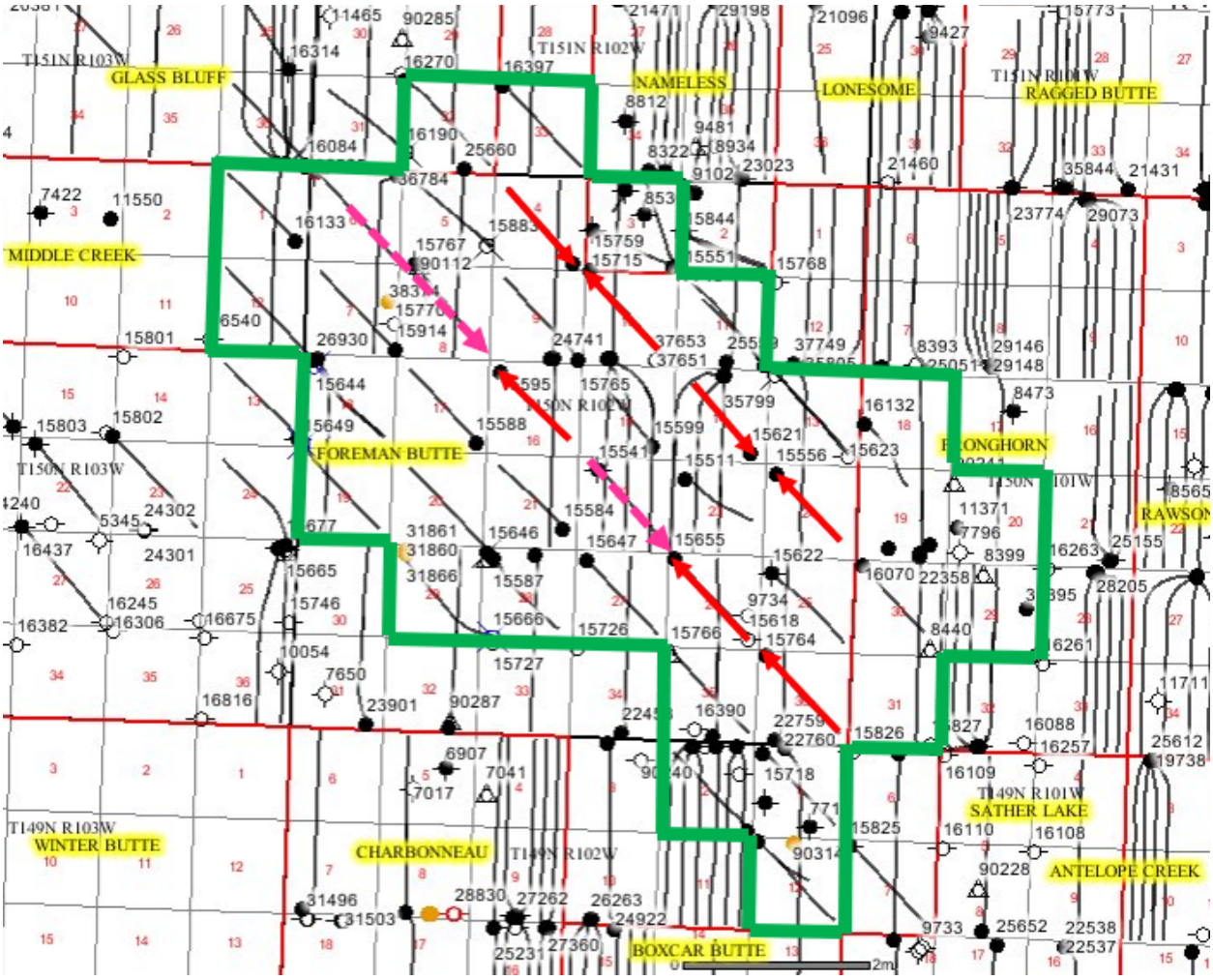

Figure 6-11. Map showing boundary of hypothetical unitized area/target CO_2 flood area, assumed new injection wells, and assumed conversions of existing wells for injection.

injection pressure is not at the current maximum allowable pressure nor likely at or exceeding any expected CO_2 injection pressure limits. Conversely, it has not been proven whether this injection rate could be sustained over time in a scenario where there are nine injection wells instead of only one in the field, and reservoir pressure increases because of water injection. Based on these considerations, it was assumed that injection could be maintained at 20% higher than the established water injection rate, or 3.4 MMscf/d per well, with the lone extended reach injector at a rate of 5.5 MMscf/d, for a total of 32.7 MMscf/d. A sensitivity analysis was done using a rate of 5 MMscf/d for each of the group of eight injectors and 8 MMscf/d for the extended reach injector, for a total of 48 MMscf/d.

Using these two injection rate scenarios and the dimensionless curve methodology, incremental produced volumes of oil and CO_2 were forecast for the field. These forecasts, along with the resulting forecast of CO_2 purchases, are shown in Figures 6-12–6-14.

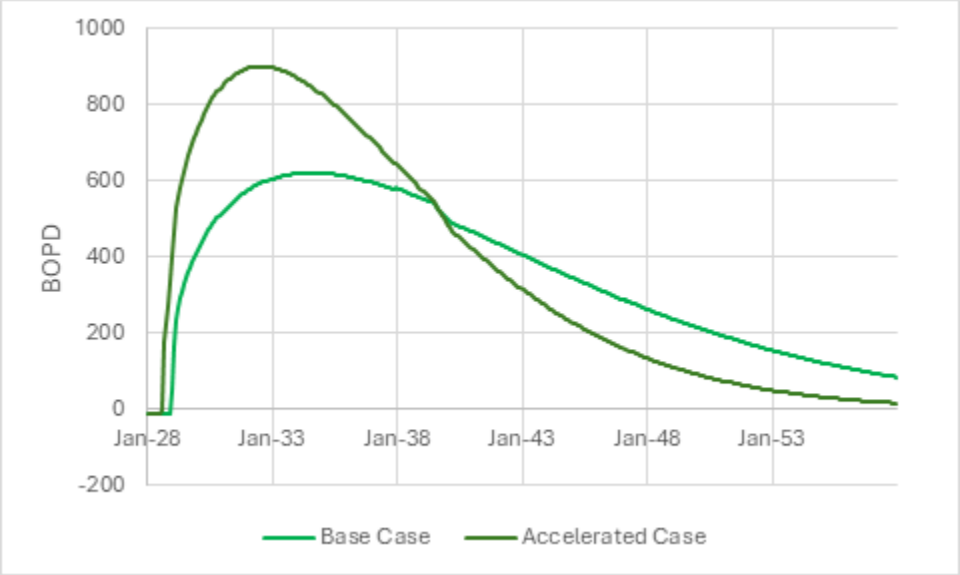

Figure 6-12. Incremental oil production forecasts for base case and accelerated injection case.

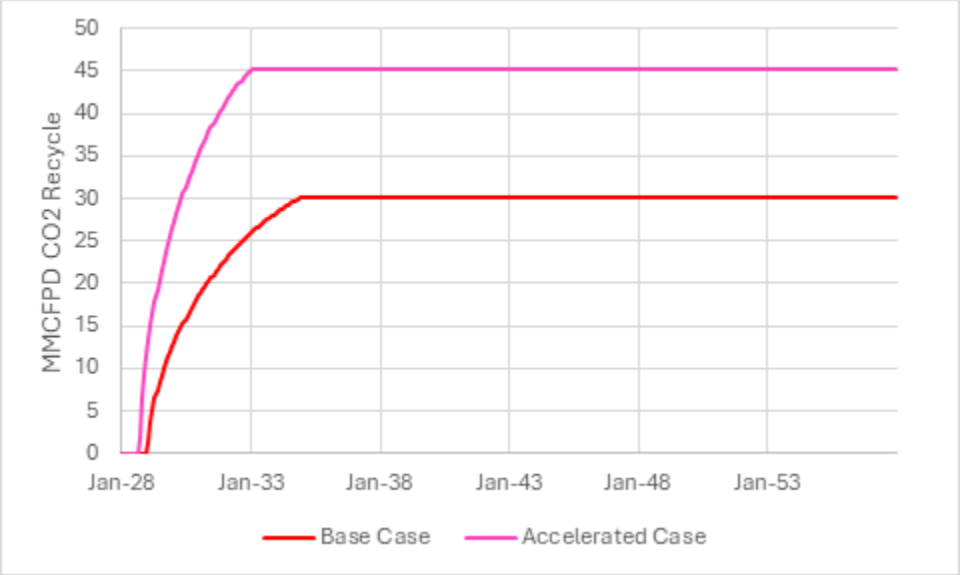

Figure 6-13. CO_2 production forecasts for base case and accelerated injection case.

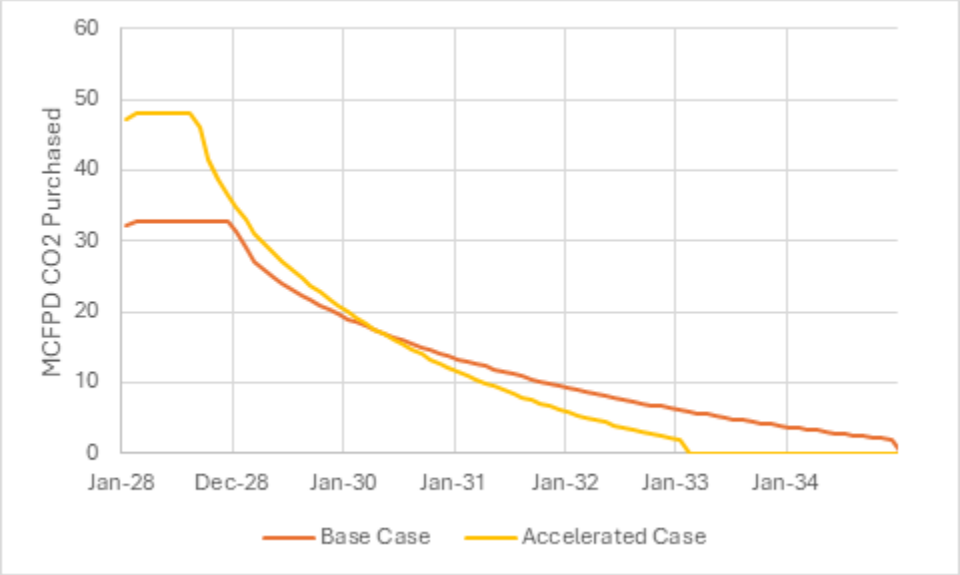

Figure 6-14. CO_2 purchase (storage) forecasts for base case and accelerated injection case.

Estimated capital expenditures are summarized in Table 6-3. These include costs for well work necessary to properly equip wells for CO_2 flooding operations, surface facilities to aggregate fluids, test producing wells, piping to take CO_2 to individual injection wells, and construction of a CO_2 recycle facility that will treat and recompress CO_2 so it can be reinjected into the reservoir. For this analysis, CO_2 supply is assumed to be readily available and no costs are assumed for the construction of a pipeline to supply CO_2 to the field. Capital costs are summarized in Table 6-3.

Table 6-3. Estimated Capital Expense Projections for Base Case and Accelerated Case

	Base Case Estimation	Accelerated Case Estimation
Recycle Facility	$34,176,680	$45,020,680
Produced Fluid Gathering and Handling	$24,493,998	$24,493,998
CO_2 Injection System	$9,441,553	$9,441,553
Testing and Separation	$14,417,931	$14,417,931
Engineering, Automation, Misc.	$22,283,143	$22,283,143
Well Work (producers)	$8,418,000	$8,418,000
Well Work (injectors)	$5,404,000	$5,404,000
Drilling (injectors)	$8,600,000	$8,600,000
Drilling (injectors)	$9,100,000	$9,100,000
Total	**$136,335,304**	**$147,179,304**

Operating expenses were assumed to be roughly equal to current operating costs, except for costs to recycle produced CO_2 and costs to treat additional produced oil. Recycle cost of 27 cents per Mscf of CO_2 was calculated using an assumed electric power acquisition cost of 7 cents per kWh, compressor inlet pressure of 400 psi, and discharge pressure of 2000 psi. An oil-treating cost of 30 cents per barrel was included. The profile of other well-related operating expenses will change, but increased operating costs due to having more active wells will be offset by lower costs due to not requiring artificial lift, as wells will flow naturally once they produce a significant volume of CO_2. Water disposal is assumed, for simplification, to not change appreciably over the project life; although there may be more water disposed in the early days of CO_2 injection. It was decided to not pursue an in-depth evaluation of well-level operating costs, as any resulting improvement in precision of the economic evaluation would not be expected to significantly lower the uncertainty inherent in the economic analysis and therefore would not justify the required effort.

Other fixed-value assumptions used in the economic evaluation are as follows: a net royalty interest of 0.785 (actual owned interest in the field), total mineral taxes of 10% with a 5% EOR exemption during the first 10 years of oil production, and a natural gas severance tax of 14%. Oil prices and CO_2 prices were varied, as shown in Table 6-4, which summarizes the incremental economic sensitivities to those prices. Two CO_2 price cases were used: the first where the cost of CO_2 was $25 per tonne (the difference in the 45Q credit values for geologic storage and utilization) and the second case assumed that CO_2 had zero associated cost. Both scenarios were run at $80, $100, and $120 per barrel WTI pricing assumption for oil. In order to achieve a 10% internal rate of return (IRR) in the accelerated case, a WTI oil price would need to be higher than $120, in the accelerated case where CO_2 is free, and even higher in the case where CO_2 is purchased at $25 per tonne (approximate $1.28 per Mscf). Breakeven prices are even higher for the base case.

Table 6-4. Economic Indicators (internal rate of return, net present value, and present value ratio) for a CO_2 Project at Foreman Butte Field

Development Case Assumption	**Base**					
CO_2, $/tonne	**25**			**0**		
Oil Price, $/bbl	**80**	**100**	**120**	**80**	**100**	**120**
IRR	−2.1%	1.2%	3.9%	0.9%	4.3%	7.1%
NPV, MM$	(99.6)	(79.1)	(58.7)	(64.4)	(44.0)	(23.6)
NPV/I	−0.70	−0.56	-0.42	−0.53	−0.36	−0.19
Development Case Assumption	**Accelerated**					
CO_2, $/tonne	**25**			**0**		
Oil Price, $/bbl	**80**	**100**	**120**	**80**	**100**	**120**
IRR	−3.5%	1.1%	4.8%	4.0%	5.2%	9.1%
NPV, MM$	(95.0)	(71.0)	(44.0)	(60.0)	(33.0)	(7.0)
NPV/I	−0.62	−0.47	−0.30	−0.47	−0.26	−0.05

As can be seen, CO_2 flooding is not economically attractive at Foreman Butte. Since this field is not typical of Williston Basin conventional fields, this evaluation should not be interpreted as a blanket indictment of CO_2 flooding for conventional reservoirs in North Dakota. It is intended to point out the challenges that must be addressed and the need for careful upfront detailed screening of fields to find those candidates that have the highest economic potential.

The specific characteristics of Foreman Butte make CO_2 EOR economically challenging. The reservoir has extremely low permeability, and flow is dominated by natural fractures. While CO_2 injection can recover incremental oil, the process requires recycling excess CO_2 volumes because of inevitable channeling caused by these fractures. The oil target reservoir is dispersed over a large acreage tract. The estimated target oil in place of 26 million barrels is located underneath 40 sections, or 25,600 acres. For comparison, the Beaver Lodge (Devonian) Unit has estimated 172 million barrels of oil in place located under approximately 16,000 acres. The dispersed nature of the oil target translates to higher capital for production and injection lines and higher operating costs because of higher pressure drops and increased maintenance in the longer lines. The net royalty interest of 0.785 is low and hampers profitability in a process that is relatively high volume but low margin. Horizontal wells present an uncertain, and likely higher, cost structure because of their unique operational parameters and higher costs related to well intervention, as experience with their use in a CO_2 project is limited.

Future work to more accurately quantify CO_2 potential in North Dakota should include a CO_2 injection pilot in a conventional field that has favorable reservoir quality and/or a study of a group of the larger conventional oil fields that would include a comprehensive capital expense estimation for multiple development scenarios and probabilistic analyses using a range of possible tertiary response profiles, used for economic analyses showing sensitivities to oil prices and CO_2 acquisition costs.

6.5 Surveillance and Data Integration

As projects are developed from primary production to IOR or EOR, the level of surveillance and data capture increases. Detailed reviews of available information from well files, public data from the NDIC, published reports on the project area, etc., form much of the preliminary data required for the evaluation of the project. Additional surveillance such as seismic surveys, through the purchase of existing data or new surveys, supplement the preliminary data of the project evaluation.

The surveillance and data capture may include seismic surveys, geologic and reservoir studies, and production and operational data associated with the projects. This information will be used throughout the life of the project in assessing the effectiveness of the project as well as providing the basis for the reporting to regulating industries. Surveillance requires a robust data storage and retention system that allows for easy access throughout the life of the project as well as being adaptable to updated and new programs used as evaluation tools. With the need of multiple sites requiring the information, from field or home office environments, data accessibility at all sites is necessary.

In addition, live monitoring of various process systems through supervisory control and data acquisition (SCADA) and automated systems provides a method to limit the intervention of operators. In addition, SCADA and automated systems offer constant monitoring of the system such that events that are outside the design parameters can be automatically adjusted up to and including shutting down of the system or facility. This can be an effective method of limiting the effects of an event. Surveillance and data integration incorporate data from many aspects that provide the basis for project development. By using and expanding the datasets, the project can be evaluated for effectiveness on the recovery of oil and gas assets.

Additional detailed discussion is included in Deliverable 4 – Surveillance and Data Integration – Priorities for Revitalization.

6.6 CO_2 EOR Screening for Conventional Reservoirs

Determining the feasibility of CO_2 EOR for a specific field is a complex process, and traditional screening criteria can be overly arbitrary, often resulting in an inaccurate assessment if a single criterion is not met. In this study, a new machine learning-based CO_2 EOR screening approach was developed, particularly for deep-depth reservoirs. An extensive EOR database encompassing 464 EOR projects from 18 countries was compiled. Based on the analysis of this database using boxplot techniques, new screening criteria were established, and parameter weight factors were determined through importance permutation techniques. An innovative CO_2 EOR scoring approach was introduced, employing membership functions, composite screening scores, and six different machine learning algorithms. This method demonstrated high prediction accuracy across the global EOR projects database and shows promise for providing recommendations on the feasibility of CO_2 EOR in deep-depth reservoirs in North Dakota. Using the newly developed methods, several oil fields in North Dakota were analyzed with the estimated reservoir and fluids properties, based on the literature data. The example of the analysis is shown in Table 6-5.

The detail of the work has resulted in a peer-reviewed journal article, published in Geoenergy Science and Engineering, shown in Appendix E.

Table 6-5. Example of Prediction Score Table for a Few Selected Oil Fields in North Dakota

Reservoirs	Average Formation Depth, ft	Average Porosity, %	Average Oil Viscosity, cp	Average Oil Density, API	Average Reservoir Temperature, F	Prediction Score							
						CO_2 EOR Scoring System (CESS)	Random Forest	Adaptive Boosting	Gradient Boosting	XGBoost	Stacking	Artificial Neural Network (ANN)	Ensemble Voting
Hawkeye Madison	9230	9	1	41	240	81	94	92	93	90	91	94	94
Tioga Madison	8350	8	2	41	212	95	96	96	97	96	97	96	95
Beaver Lodge Madison	8590	8	2	43	224	90	96	95	94	95	96	96	94
Antelope Madison	9088	5	2	40	240	78	93	92	93	88	89	93	90
Beaver Lodge Devonian	10,490	12	4	41	249	72	80	82	90	84	84	80	85
Blue Buttes Madison	9400	10	0	42	240	82	93	90	88	83	89	93	90
Red Wing Creek Madison	9454	10	0	40	217	93	97	95	88	96	96	97	94
Plaza Madison	7441	5	3	36	163	96	93	95	98	93	94	93	93
Stoneview Stonewall	11,667	4	3	42	238	72	87	88	93	79	80	87	86
Charlson North Madison	8998	9	2	42	236	84	94	92	92	89	90	94	91
Big Stick Madison	9238	9	3	37	240	81	93	92	94	89	90	93	90
T. R. Madison	9255	7	3	37	237	81	92	91	94	87	87	92	89

Note: Reservoir porosity, oil viscosity, and density are estimated based on the public available data and subject to further investigation and verification.

7.0 CONCLUSIONS AND RECOMMENDATIONS FOR FUTURE WORK

Through close collaboration with EEPT, the EERC conducted a thorough technical evaluation on Foreman Butte Field, a legacy conventional oil field producing from the Madison Group, that includes new strategic data acquisition, laboratory evaluations to assess EOR performance and characterize rock-fluid interactions, core-flooding experiments, detailed geologic characterizations, static geologic model construction, and field-scale simulation using high-efficiency workflow and model. The investigation results in the following conclusions and recommendations.

The study showed that for Foreman Butte Field, natural fractures, a tight rock matrix, and residual oils were observed from cores from a newly drilled stratigraphic well that drilled through the Ratcliffe interval of the Charles Formation of Madison Group. The recovery factors remain low and decline fast during primary production. Core-flooding experiments demonstrated the effectiveness of various EOR methods, including water flooding and CO_2 flooding, in improving oil recovery. However, because of the reservoir's natural fracture network and high water saturation and the rock's oil-wet and mixed-wet characteristics and heterogeneity, CO_2 flooding is more effective in extracting oil compared to water flooding.

Carbonate reservoirs are widely distributed among the main oil-producing formations, such as Charles, Mission Canyon, Lodgepole, Red River, etc. These reservoirs exhibit a broad spectrum of pore types and sizes, ranging from micropores in mudstones to large vugs and caves. This heterogeneity in pore structure significantly influences the flow of hydrocarbons. Because of this complexity, developing alternative approaches and EOR techniques is crucial to reviving different types of legacy oil field reservoirs. A thorough review of various EOR techniques for carbonate reservoirs has been conducted to provide a deeper understanding of the methods available for improving oil production. This review highlights the importance of selecting the appropriate EOR method based on the specific characteristics of each reservoir. Understanding critical reservoir characteristics, such as porosity, permeability, fluid saturation, and rock wettability, is key to successfully implementing cost-effective techniques for enhancing oil recovery and prolonging production.

Detailed geologic modeling and high-efficiency field-scale simulation workflows have been developed to effectively assess the performance of different EOR methods in various types of reservoirs, including carbonate reservoirs. These tools allow for a better characterization of the reservoir, facilitating the selection and optimization of EOR techniques at the various operation conditions. Those can be evaluated and tailored to the specific reservoir and fluid properties of the reservoirs.

In addition, the facility and operability assessment suggests careful evaluation of the operational conditions and challenges for implementing the different EOR techniques. These evaluations include assessing facility upgrades needs, integrity existing and new infrastructure, and facilities' compatibility of different injection fluids with a reservoir and capability of managing the reservoir pressure and fluids dynamics changes and differences compared to the primary production. Upgrading the equipment and employing completion techniques can enhance oil production, prior to effectively implementing the new IOR and/or EOR strategies.

8.0 REFERENCES

Advanced Resources International, Inc., 2006a, Basin oriented strategies for CO_2 enhanced oil recovery—Williston Basin: Technical report for U.S. Department of Energy, February.

Advanced Resources International, 2006b, Technical oil recovery potential from residual oil zones—Williston Basin: Report for the U.S. Department of Energy, Office of Fossil Energy, February. https://www.adv-res.com/pdf/Basin%20Oriented%20Strategies%20-%20Williston_Basin.pdf.

Al Basry, A., Al Hajeri, S., Saadawi, H., Al Aryani, F., Obeidi, A., Negahban, S., and Al Yafei, G., 2011, Lessons learned from the first miscible CO_2-EOR pilot project in heterogeneous carbonate oil reservoir in Abu Dhabi, UAE: Paper presented at the SPE Middle East Oil and Gas Show and Conference, Manama, Bahrain, September 2011. https://doi.org/10.2118/142665-MS.

Al-Amrie, O., Peltier, S., Pearce, A., Abu-Dhabi, T., Al-Yafei, A., Morel, D., Bourrel, M., Bursaux, R., Cordelier, P., Jouenne, S., and Juilla, H., 2015, The first successful chemical EOR pilot in the UAE—one spot pilot in high temperature, high salinity carbonate reservoir, *in* Abu Dhabi International Petroleum Exhibition and Conference: Abu Dhabi, UAE, November 2015. https://doi.org/10.2118/177514-MS.

Al-Murayri, M.T., Kamal, D.S., Suniga, P., Fortenberry, R., Britton, C., Pope, G.A., Liyanage, P.J., Jang, S.H., and Upamali, K.A., 2017, Improving ASP performance in carbonate reservoir rocks using hybrid-alkali: Paper presented at the SPE Annual Technical Conference and Exhibition, San Antonio, Texas, USA, October 2017. https://doi.org/10.2118/187213-MS.

Al-Sinani, I.S., Al-Jabri, S.H., Al-Rawahy, N.A., Al-Rawahy, I., Al-Hinai, K., and Leksono, M., 2016, Modified surfactant injection to enhance oil production and recovery, case study—Omani carbonate reservoir: Paper presented at the SPE EOR Conference at Oil and Gas West Asia, Muscat, Oman, March 2016. https://doi.org/10.2118/179851-MS.

Begnaud, W.J., and Claiborne, E.B., 1985, Vertical fracture growth considerations in the Mission Canyon/Ratcliffe Formations of the North Alexander Area: Presented at the SPE Annual Technical Conference and Exhibition, Las Vegas, Nevada, September. SPE-14375-MS. https://doi.org/10.2118/14375-MS.

Bera, A., and Belhaj, H., 2016, A comprehensive review on characterization and modeling of thick capillary transition zones in carbonate reservoirs: Journal of Unconventional Oil and Gas Resources, v. 16, p. 76–89.

Bethel, F.T., and Welbourn, M.E., 1959, Applications of recent reservoir and petrophysical developments to a field study: Paper presented at the SPE Rocky Mountain Petroleum Technology Conference/Low-Permeability Reservoirs Symposium, Casper, Wyoming, USA, April 1959. https://doi.org/10.2118/1218-G.

Blasingame, T.A., Johnston, J.L., and Lee, W.J., 1989, Type-curve analysis using the pressure integral method: Paper presented at the SPE California Regional Meeting, Bakersfield, California, April 1989. https://doi.org/10.2118/18799-MS.

Brannan, G., and Whitington Jr, H.M., 1977, Enriched-gas miscible flooding—a case history of the levelland unit secondary miscible project: Journal of Petroleum Technology, v. 29, no. 8, p. 919–924.

Burke, R.B., and Lasemi, Z., 1995, A preliminary comparison of Waulsortian mound facies in the Williston and Illinois Basins. Williston Basin Symposium.

Burton-Kelly, M., 2017, Residual oil zone screening with basin evolution modeling: Presented at the Midland CO_2 Conference, Midland, Texas, December. https://www.co2conference.net/wp-content/uploads/2017/12/8-Peck-EERC-Williston-Basin-ROZ-12-06-17.pdf

Cheng, A.M., and Kwan, J.T., 2012, Optimal injection design utilizing tracer and simulation in a surfactant pilot for a fractured carbonate yates field: Paper presented at the SPE Improved Oil Recovery Conference, Tulsa, Oklahoma, USA, April 2012. https://doi.org/10.2118/154270-MS.

Christman, P.G., and Gorell, S.B., 1990, Comparison of laboratory- and field-observed CO_2 tertiary injectivity: Journal of Petroleum Technology, v. 42, no. 2, p. 226–233.

Dakhelpour-Ghoveifel, J., Shegeftfard, M., and Dejam, M., 2019, Capillary-based method for rock typing in transition zone of carbonate reservoirs. Journal of Petroleum Exploration and Production Technology, v. 9, p. 2009–2018.

Davarpanah, A., Mirshekari, B., and Razmjoo, A.A., 2019, A simulation study of water injection and gas injectivity scenarios in a fractured carbonate reservoir—a comparative study: Petroleum Research, v. 4, no. 3, p. 250–256.

Dawoud, A., El Mahdi, A., Bidinger, C., Basioni, M., Ayoub, M., Al Shehhi, A.S., and Khoori, S.A., 2010, Early miscible hydrocarbon gas injection in Abu Dhabi heterogeneous carbonate reservoir: Paper presented at the SPE EOR Conference at Oil and Gas West Asia, Muscat, Oman, April 2010. https://doi.org/10.2118/129238-MS.

DeHekker, T.G., Bowzer, J.L., Coleman, R.V., and Bartos, W.B., 1986, A progress report on polymer-augmented waterflooding in Wyoming's North Oregon Basin and Byron fields: Paper presented at the SPE Improved Oil Recovery Conference, Tulsa, Oklahoma, USA, April 1986. https://doi.org/10.2118/14953-MS.

Dellinger, S.E., Patton, J.T., and Holbrook, S.T., 1984, CO_2 mobility control: Society of Petroleum Engineers Journal, v. 24, no. 2, p. 191–196.

Den Ouden, L., 2014, Calcite dissolution behaviour during low salinity water flooding in carbonate rock [Master's thesis]: Delft University of Technology.

Denney, D., 2011. 30 years of successful high-pressure air injection—performance evaluation of Buffalo Field, South Dakota: Journal of Petroleum Technology, v. 63, no. 1, p. 50–53.

Driscoll, V.J., 1974, Recovery optimization through infill drilling concepts, analysis, and field results: Paper presented at the fall meeting of the Society of Petroleum Engineers of AIME, Houston, Texas, October 1974. doi: https://doi.org/10.2118/4977-MS.

Dunham, R.J., 1962, Classification of carbonate rocks according to depositional texture, *in* Ham, W.E., ed., Classification of carbonate rocks: American Association of Petroleum, Geologists Memoir, p. 108–121.

Fuller, S.M., Sarem, A.M., and Gould, T.L., 1992, Screening waterfloods for infill drilling opportunities: Paper presented at the SPE International Oil and Gas Conference and Exhibition in China, Beijing, China, March 1992. https://doi.org/10.2118/22333-MS.

Gaswirth, S.B., Lillis, P.G., Pollastro, R.M., and Anna, L.O., 2010, Geology and undiscovered oil and gas resources in the Madison Group, Williston Basin, North Dakota and Montana: Mountain Geologist, v. 47, no. 1, p. 71–90.

Gdanski, R.D., 2005, Recent advances in carbonate stimulation: Paper presented at the International Petroleum Technology Conference, Doha, Qatar, November 2005. https://doi.org/10.2523/IPTC-10693-MS.

Gerhard, L.C., and S.B. Anderson, 1988, Geology of the Williston Basin (United States portion), *in* Sloss, L.L., ed., Sedimentary cover- North American craton, U.S.: GSA, Boulder, Colorado, The Geology of North America, v. D-2, p. 221–241.

Good, P.A., and Downer, D.G., 1988, Cedar Creek Anticline carbon dioxide injectivity test—design, implementation, and analysis: Paper presented at the SPE Improved Oil Recovery Conference, Tulsa, Oklahoma, April 1988. https://doi.org/10.2118/17326-MS.

Gould, T.L., and Mupoz, M.A., 1982, An analysis of infill drilling *in* Proceedings of the SPE Annual Technical Conference and Exhibition: New Orleans, Louisiana, 1982, p. 26–29, SPE 11021

Grigg, R.B., and Schechter, D.S., 1997, State of the industry in CO_2 floods: Paper presented at the SPE Annual Technical Conference and Exhibition, San Antonio, Texas, October 1997. https://doi.org/10.2118/38849-MS.

Gulf Oil, 1983, Little Knife Field CO_2 minitest, Billings County, North Dakota: Final report, volume I, technical report for the U.S. Department of Energy Contract No. DE-AC21-79MC08383, Gulf Oil Exploration and Production Company, July.

Hirsch, J.M., Cisar, M.T., Glass, S.W., and Romanowski, D. A., 1981, Recent experience with wireline fracture detection logs: Paper presented at the SPE Annual Technical Conference and Exhibition, San Antonio, Texas, October. SPE-10333-MS. https://doi.org/10.2118/10333-MS.

Holubnyak, Y., Watney, W., Hollenbach, J., Rush, J., Fazelalavi, M., Bidgoli, T., and Wreath, D., 2018, Pilot scale CO_2 EOR at Wellington Filed in south central Kansas: Paper presented at the SPE Improved Oil Recovery Conference, Tulsa, Oklahoma, April 2018. https://doi.org/10.2118/190308-MS.

Jarvie, D.M., 2001, Williston Basin petroleum systems—inferences from oil geochemistry and geology: Mountain Geologist, v. 38, no. 1, p. 19–42.

Jin, L., and Wojtanowicz, A.K., 2014, Progression of injectivity damage with oily waste water in linear flow: Petroleum Science, v. 11, p. 550–562.

Johnson, M.S., 1995, Dickinson field lodgepole reservoir—significance of this waulsortian-type mound to exploration in the Williston Basin: Mountain Geologist, v. 32, no. 3.

Kerr, S.D., 1988, Overview—Williston Basin carbonate reservoirs, *in* Goolsby, S.M., and Longman, M.W., eds., Occurrence and petrophysical properties of carbonate reservoirs in the Rocky Mountain region: RMAG, p. 251–274.

Kumar, V.K., Fassihi, M.R., and Yannimaras, D.V., 1995, Case history and appraisal of the Medicine Pole Hills unit air-injection project: SPE Reservoir Engineering, v. 10, no. 3, p.198–202.

Lie, K.A., and Møyner, O., eds., 2021, Advanced modelling with the MATLAB Reservoir Simulation Toolbox: Cambridge University Press, 500 p.

Ling, K., Shen, Z., Han, G., He, J., and Peng, P., 2014, A review of enhanced oil recovery methods applied in Williston Basin, *in* SPE/AAPG/SEG Unconventional Resources Technology Conference: Denver, Colorado, USA, August 2014. https://doi.org/10.15530/URTEC-2014-1891560.

Mabkhout AlSeiari, R.A., Bhushan, Y., Igogo, A., Singh, M.K., Marzooqi, S.A., Al Hammadi, S.A., Khan, S.H., Mohamed, M.A., Brodie, J., Tenaiji, A.A., and Al Ali, M.Y., 2022, A success story of the first miscible CO_2 WAG miscible WAG pilots in a giant carbonate reservoir in Abu Dhabi: Paper presented at the Abu Dhabi International Petroleum Exhibition and Conference, Abu Dhabi, UAE, October 2022. https://doi.org/10.2118/211456-MS.

Manrique, E.J., Muci, V.E., and Gurfinkel, M.E., 2007, EOR field experiences in carbonate reservoirs in the United States: SPE Reservoir Evaluation & Engineering, v. 10, no. 6, p. 667–686.

Masalmeh, S.K., Shiekah, I.A., and Jing, X.D., 2007, Improved characterization and modeling of capillary transition zones in carbonate reservoirs: SPE Reservoir Evaluation and Engineering, v. 10, no. 2, p. 191–204.

Mohamed, A.A.I., Belhaj, H., Gomes, J.S., and Bera, A., 2017, Petrographic and diagenetic studies of thick transition zone of a middle-east carbonate reservoir: Journal of Petroleum and Gas Engineering, v. 8, no. 1, p. 1–10.

Montgomery, S.L., 1996, Mississippian lodgepole play, Williston Basin—a review: AAPG Bulletin, v. 80, no. 6, p. 795–810.

Moore, R.G., Mehta, S.A. and Ursenbach, M.G., 2002, A guide to high pressure air injection (HPAI) based oil recovery, *in* SPE/DOE Improved Oil Recovery Symposium: Tulsa, Oklahoma, April 2002. https://doi.org/10.2118/75207-MS.

North Dakota Legislative Management, 2024, North Dakota oil and gas industry impacts study 2014-2019: North Dakota Legislative Management. Prepared by KLJ, Inc., 215 p.

North Dakota Industrial Commission, 2024. Department of Mineral Resources, Oil and Gas Division: https://www.dmr.nd.gov/oilgas/ (accessed March 26, 2024).

Pickard, C.F., 1994, Twenty years of production from an impact structure, Red Wing Creek Field, McKenzie County, North Dakota: Paper presented at the Annual AAPG-SEPM-EMD-DPA-DEG Convention, Denver, June 12–15, p. 234.

RezaeiDoust, A., Puntervold, T., Strand, S., and Austad, T., 2009, Smart water as wettability modifier in carbonate and sandstone—a discussion of similarities/differences in the chemical mechanisms: Energy and Fuels, v. 23, no. 9, p. 4479–4485.

Rilian, N.A., Sumestry, M., and Wahyuningsih, _, 2010, Surfactant stimulation to increase reserves in carbonate reservoir: a case study in Semoga Field: Paper presented at the SPE EUROPEC/EAGE Conference and Exhibition, Barcelona, Spain, June 2010. https://doi.org/10.2118/130060-MS.

Ruzyla, K., and Friedman, G.M., 1982, Geological heterogeneities important to future enhanced recovery in carbonate reservoirs of Upper Ordovician Red River Formation at Cabin Creek Field, Montana: SPE Journal, v. 22, no. 3, p. 429–444.

Saeed, M., and Jadhawar, P., 2023, Surface complexation modeling of HPAM polymer–brine–sandstone interfaces for application in low-salinity polymer flooding: Energy and Fuels, v. 37, no. 9, p. 6585–6600.

Saeed, M., Jadhawar, P., Ayirala, S.C., Abhishek, R., and Zhou, Y., 2023, Modelling the effects of reservoir parameters and rock mineralogy on wettability during low salinity waterflooding in sandstone reservoirs: Journal of Petroleum Science and Engineering, v. 215, p. 110676.

Saeed, M., Jadhawar, P., Ayirala, S.C., Abhishek, R., and Zhou, Y., 2023, Modelling the effects of reservoir parameters and rock mineralogy on wettability during low salinity waterflooding in sandstone reservoirs: Journal of Petroleum Science and Engineering, v. 215, p.110676.

Saeed, M., Jadhawar, P., Zhou, Y., and Abhishek, R., 2022, Triple-layer surface complexation modelling—characterization of oil-brine interfacial zeta potential under varying conditions of temperature, pH, oil properties and potential determining ions: Colloids and Surfaces A: Physicochemical and Engineering Aspects, v. 633, p.127903.

Seccombe, J.C., Lager, A., Webb, K., Jerauld, G., and Fueg, E., 2008, Improving wateflood recovery—LoSal™ EOR field evaluation: Paper presented at the SPE Improved Oil Recovery Conference, Tulsa, Oklahoma, USA, April 2008. https://doi.org/10.2118/113480-MS.

Sharma, M., Alcorn, Z.P., Fredriksen, S.B., Rognmo, A.U., Fernø, M.A., Skjæveland, S.M., and Graue, A., 2020, Model calibration for forecasting CO_2-foam enhanced oil recovery field pilot performance in a carbonate reservoir: Petroleum Geoscience, v. 26, no. 1, p. 141–149.

Sheng, J.J., 2010. Modern chemical enhanced oil recovery: theory and practice. Gulf Professional Publishing, 648 p.

Shi, S., Belhaj, H., and Bera, A., 2018, Capillary pressure and relative permeability correlations for transition zones of carbonate reservoirs: Journal of Petroleum Exploration and Production Technology, v. 8, p. 767–784.

Shuler, P.J., Lu, Z., Ma, Q., and Tang, Y., 2016, Surfactant huff-n-puff application potentials for unconventional reservoirs, *in* SPE Improved Oil Recovery Conference Tulsa, Oklahoma, April 2016, p. SPE-179667. https://doi.org/10.2118/179667-MS.

Sorensen, J.A., and Hamling, J.A., 2016, Historical Bakken test data provide critical insights on EOR in tight oil plays: The American Oil & Gas Reporter, v. 59, no. 2, p. 55–61.

Spearing, M.C., Abdou, M., Azagbaesuweli, G., and Kalam, M.Z., 2014, Transition zone behaviour: the measurement of bounding and scanning relative permeability and capillary pressure curves at reservoir conditions for a giant carbonate reservoir: Paper presented at the Abu Dhabi International Petroleum Exhibition and Conference, Abu Dhabi, UAE, November. SPE-171892-MS. https://doi.org/10.2118/171892-MS.

Straight, D.H. Jr., and Fallin W.S., 1992, Dolphin Field—a successful miscible gas flood in a small volatile oil reservoir: Paper presented at the SPE Rocky Mountain Regional Meeting, Casper, Wyoming, May 1992. https://doi.org/10.2118/24333-MS.

Syed, F.I., Negahban, S., and Dahaghi, A.K., 2021, Infill drilling and well placement assessment for a multi-layered heterogeneous reservoir: Journal of Petroleum Exploration and Production, v.11, no. 1, p. 901–910.

Tang, G.Q., and Morrow, N.R., 1999, Influence of brine composition and fines migration on crude oil/brine/rock interactions and oil recovery: Journal of Petroleum Science and Engineering, v. 24, nos. 2–4, p. 99–111.

Tetteh, J.T., Brady, P.V., and Ghahfarokhi, R.B., 2020, Review of low salinity waterflooding in carbonate rocks—mechanisms, investigation techniques, and future directions: Advances in Colloid and Interface Science, v. 284, p. 102253.

Thakur, G.C., Lin, C. J., and Patel, Y.R., 1984, CO_2 minitest Little Knife Field ND—a case history: Paper presented at the SPE Enhanced Oil Recovery Symposium, Tulsa, Oklahoma, April 1984. https://doi.org/10.2118/12704-MS.

Varfolomeev, M.A., Ziniukov, R.A., Yuan, C., Khairtdinov, R.K., Sitnov, S.A., Sudakov, V.A., Zhdanov, M.V., Mustafin, A.Z., Usmanov, S.A., Sattarov, A.I., and Glukhov, M.S., 2020, Optimization of carbonate heavy oil reservoir development using surfactant flooding—from laboratory screening to pilot test, *in* SPE Russian Petroleum Technology Conference, Virtual, October 2020, p. D033S013R006. https://doi.org/10.2118/201905-MS.

Watts, B.C., Hall, T.F., and Petri, D.J., 1997, The horse creek air injection project—an overview, *in* SPE Rocky Mountain Petroleum Technology Conference/Low-Permeability Reservoirs Symposium: Casper, Wyoming, p. SPE-38359. https://doi.org/10.2118/38359-MS.

Watts, R.J., Gehr, J.B., Wasson, J.A., Evans, D.M., and Locke, C.D., 1982, A single CO_2 injection well minitest in a low-permeability carbonate reservoir: Journal of Petroleum Technology, v. 34, no. 08, p. 1781–1788.

Weiss, W.W., 1992, Performance review of a large-scale polymer flood: Paper presented at the SPE Improved Oil Recovery Conference, Tulsa, Oklahoma, USA, April 1992. https://doi.org/10.2118/24145-MS.

Woo, G.T., and Cramer, D.D., 1984, Laboratory and field evaluation of fluid-loss additive systems used in the Williston Basin: Paper presented at the SPE Rocky Mountain Regional Meeting, Casper, Wyoming, May. SPE-12899-MS. https://doi.org/10.2118/12899-MS.

Xu, Y., 2015, Implementation and application of the embedded discrete fracture model (EDFM) for reservoir simulation in fractured reservoirs [Master Thesis]: The University of Texas, Austin.

Xu, Z.X., Li, S.Y., Li, B.F., Chen, D.Q., Liu, Z.Y., and Li, Z.M., 2020, A review of development methods and EOR technologies for carbonate reservoirs: Petroleum Science, v. 17, p. 990–1013.

Yang, H.D., and Wadleigh, E.E., 2000, Dilute surfactant IOR-design improvement for massive, fractured carbonate applications: Paper presented at the SPE International Oil Conference and Exhibition in Mexico, Villahermosa, Mexico, February 2000. https://doi.org/10.2118/59009-MS.

Yousef, A.A., Al-Saleh, S., Al-Kaabi, A., and Al-Jawfi, M., 2011, Laboratory investigation of the impact of injection-water salinity and ionic content on oil recovery from carbonate reservoirs: SPE Reservoir Evaluation & Engineering, v. 14, no. 5, p. 578–593. October 2011. https://doi.org/10.2118/137634-PA.

Zhang, P., Tweheyo, M.T., and Austad, T., 2007, Wettability alteration and improved oil recovery by spontaneous imbibition of seawater into chalk—impact of the potential determining ions Ca2+, Mg2+, and SO42−: Colloids and Surfaces A—Physicochemical and Engineering Aspects, v. 301, nos. 1–3, p.199–208.

Zhang, S., Li, Y., and Pu, H., 2020, Studies of the storage and transport of water and oil in organic-rich shale using vacuum imbibition method: Fuel, v. 266, p. 117096.

Zhang, S., Pu, H., and Zhao, J.X., 2019, Experimental and numerical studies of spontaneous imbibition with different boundary conditions—case studies of Middle Bakken and Berea cores: Energy & Fuels, v. 33, no. 6, p. 5135–5146.

Zhao, J., Jin, L., Azzolina, N.A., Wan, X., Yu, X., Sorensen, J.A., Kurz, B.A., Bosshart, N.W., Smith, S.A., Wu, C., Vrtis, J.L., Gorecki, C.D., and Ling, K., 2022, Investigating enhanced oil recovery in unconventional reservoirs based on field cases review, laboratory and simulation studies: Energy & Fuels, v. 36, no. 24, p. 14771–14788.

APPENDIX A

LABORATORY EVALUATIONS

LABORATORY EVALUATIONS

Section 4.4 of the report presents a summary of laboratory results. This Appendix provides a more complete discussion of the work performed.

Miscibility Pressure Tests

In addition to the core analysis program, minimum miscibility pressure (MMP) experiments were performed between CO_2 with Foreman Butte oil and ethane (C2) with Foreman Butte oil. These experiments provide critical information for enhanced oil recovery (EOR) evaluations, for both numerical simulation and field operation criteria.

CO_2 MMP is one of the most important parameters for designing an effective EOR project. When the reservoir pressure is maintained above MMP, miscible flooding can be achieved to promote displacement efficiency and facilitate better oil extraction since the interfacial tension between oil and CO_2 becomes minimal or even zero. Injecting CO_2 below the MMP (immiscible flooding) may result in poor sweep efficiency since CO_2 could not be fully miscible with the oil in pore space, thus reducing the effectiveness of the EOR operation. Therefore, it is usually desirable to have miscible CO_2 flooding in actual field operations to maximize the EOR performance (Taber and others, 1997a,b; Kamari and others, 2015; Dindoruk and others, 2021). A variety of experimental methods, such as slim tube (ST) experiments, the rising bubble apparatus (RBA), and the vanishing interfacial tension (VIT) technique, have been developed to measure CO_2 MMP in laboratories (Ahmad and others, 2016; Zhao and others, 2021).

The VIT method was employed to measure MMP for the oil sample collected from the field. The method can determine the MMP efficiently as the interfacial tension (or capillary pressure) between oil and gas approaches zero when the pressure reaches MMP. The detailed gas preparation and MMP measurement processes are described in Hawthorne and others (2016). Figure A-1 shows an example of measuring MMP for a light oil sample with rich gas under reservoir conditions (Jin and others, 2022). The MMP between Foreman Butte oil and different gases was measured at a reservoir temperature of 230°F. Results show that the tested oil had an MMP of 3418 psi with CO_2 and 1669 psi with ethane.

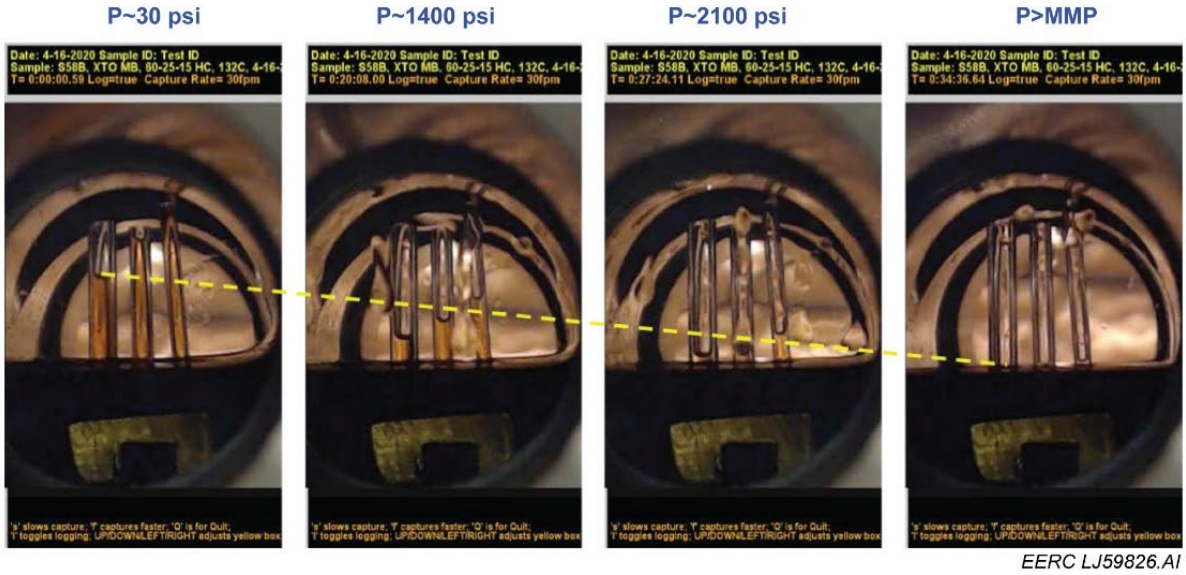

Figure A-1. Illustration of CO_2 MMP measurement using the VIT technique under reservoir temperature.

Capillary Pressure Tests

A capillary pressure transition zone is a region where oil and water saturations change gradually with decreasing depth from 100% water to connate saturation as the oil saturation increases. Capillary pressure is defined as the difference in fluid pressure across an interface between two fluids in a confined volume. In an oil reservoir, it is the pressure difference across the oil–water interface, which is a function of the fluid and rock properties. Capillary pressure plays a crucial role in determining the thickness of a transition zone. Studies showed that the thickness of a transition zone may vary from a few feet in high-permeability reservoirs to more than 300 feet in low-permeability reservoirs such as carbonate reservoirs because of extreme heterogeneity (Masalmeh and others, 2007; Bera and Belhaj, 2016; Shi and others, 2018; Dakhelpour-Ghoveifel and others, 2019). Foreman Butte Field appears to exist within the range of a long capillary pressure transition zone.

Capillary pressure was measured using both high-pressure mercury injection (HPMI) and a brine–synthetic oil system. The results of these tests are presented in Figures A-2 and A-3. Pore throat distributions were calculated from HPMI results, and the oil brine capillary pressure measurements were used to guide creation of relative permeability curves. A summary of calculated pore throat sizes is shown in Table A-1.

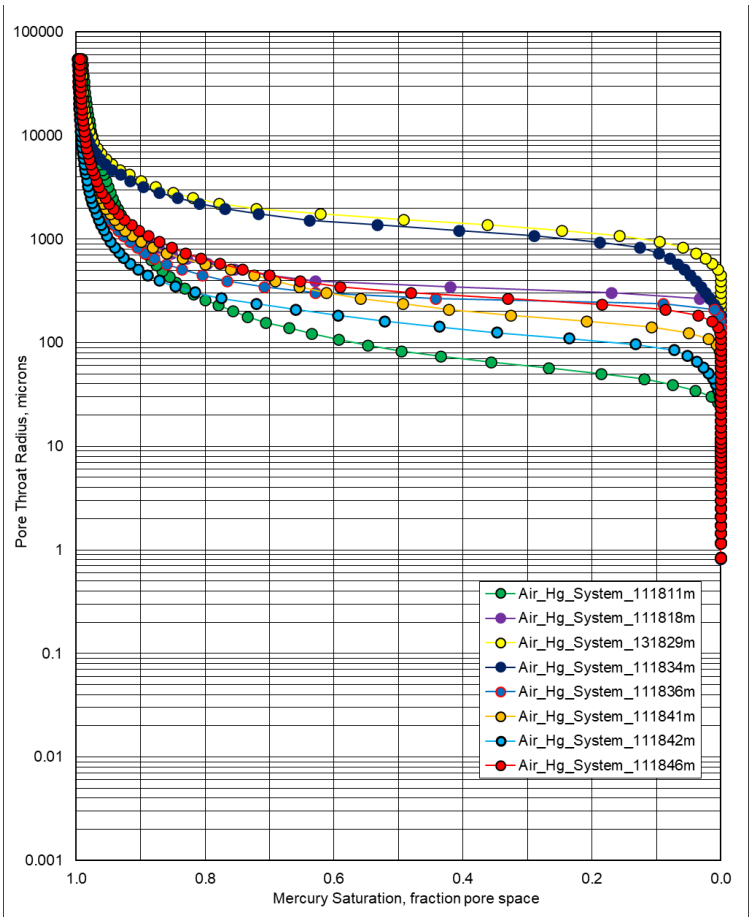

Figure A-2. Capillary pressure measurements using HPMI.

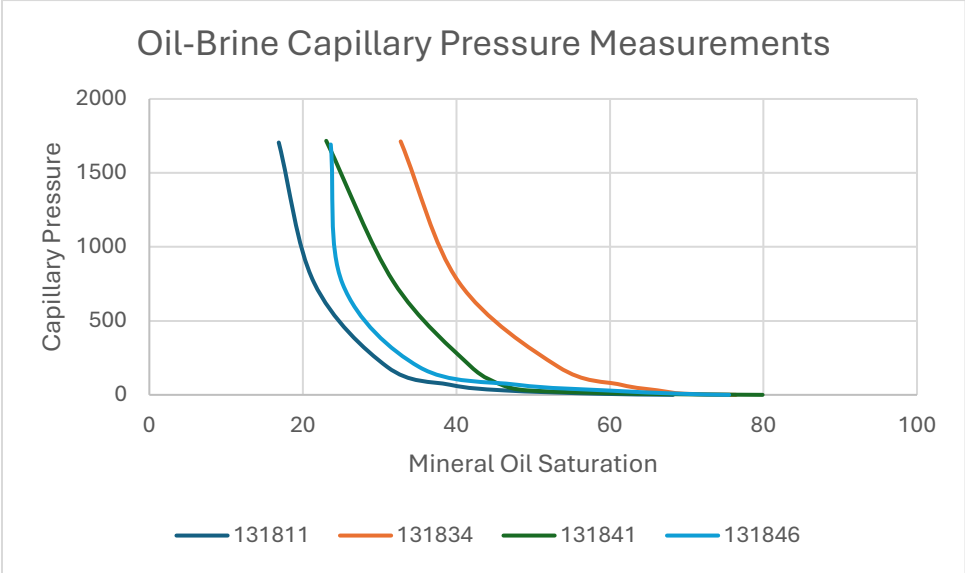

Figure A-3. Oil–brine capillary pressure measurements.

Table A-1. Calculation of Pore Throat Radii from HPMI Measurements for Selected Core Plugs

Samples	Depth, ft	Porosity, %	Swanson Permeability, mD	Median Throat radius, µm	Pore radius, µm
131811m	9226.6	17.2	8.43	1.28	4.49
131818m	9237.9	11.3	0.453	0.297	0.568
131829m	9260.6	6.7	0.0153	0.0694	0.237
131834m	9269	6.1	0.0164	0.0815	0.582
131836m	9272.4	15	1.12	0.389	0.707
131841m	9281.9	14.5	1.07	0.45	1.38
131842m	9282.5	19.6	3.77	0.692	4.29
131846m	9289.2	10	0.403	0.346	1.05

IFT and Contact Angle Tests

The pendant drop technique was utilized to measure interfacial tension (IFT) between the oil and several different mixtures of brine and surfactants. The measurements were made at reservoir conditions of 230°F and 4500 psi. Also, rock–fluid wettability interactions were investigated using the sessile drop contact angle method, following the experimental setup illustrated in Figure A-4.

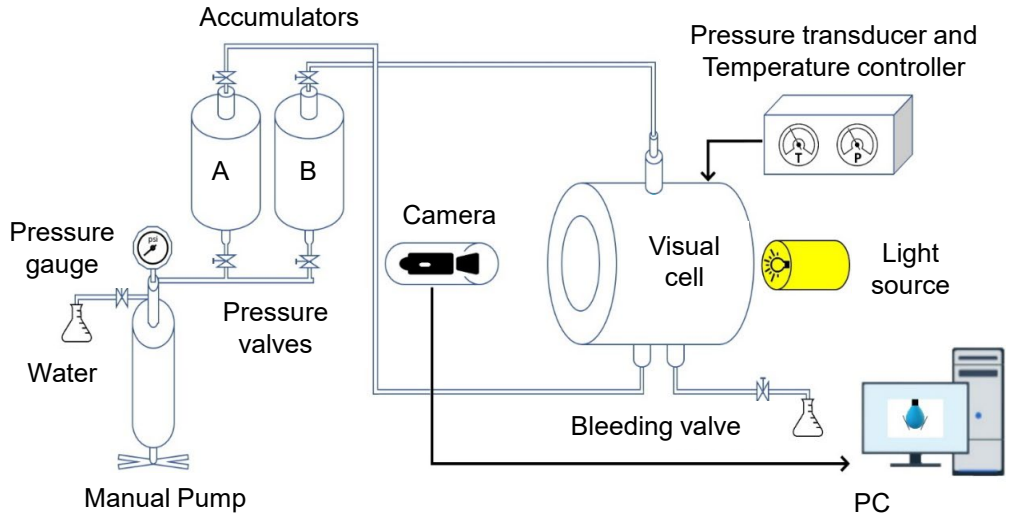

Figure A-4. Schematic of pendant/sessile drop setup for IFT and contact angle measurements.

Three surfactant solutions samples were prepared using three surfactants, A, B, and C, denoted as SS-A, SS-B, and SS-C. To understand reservoir fluid interactions, measurements were conducted by introducing an oil drop into a chamber filled with fresh water, formation brine, SS-A, SS-B, and SS-C at 230°F and 4500 psi. As illustrated in Figure A-5, crude oil and formation brine exhibited an IFT of 31.42 mN/m under reservoir conditions, which is nearly 10 mN/m higher than the IFT of the crude oil and freshwater system. This difference suggests that the complexity of the brine and the presence of cations and anions further contribute to the increased IFT. The results show that adding 1 ppm of surfactant to the brine led to a significant reduction in IFT, resulting in values of 1.06, 0.73, and 0.55 mN/m for SS-A, SS-B, and SS-C, respectively.

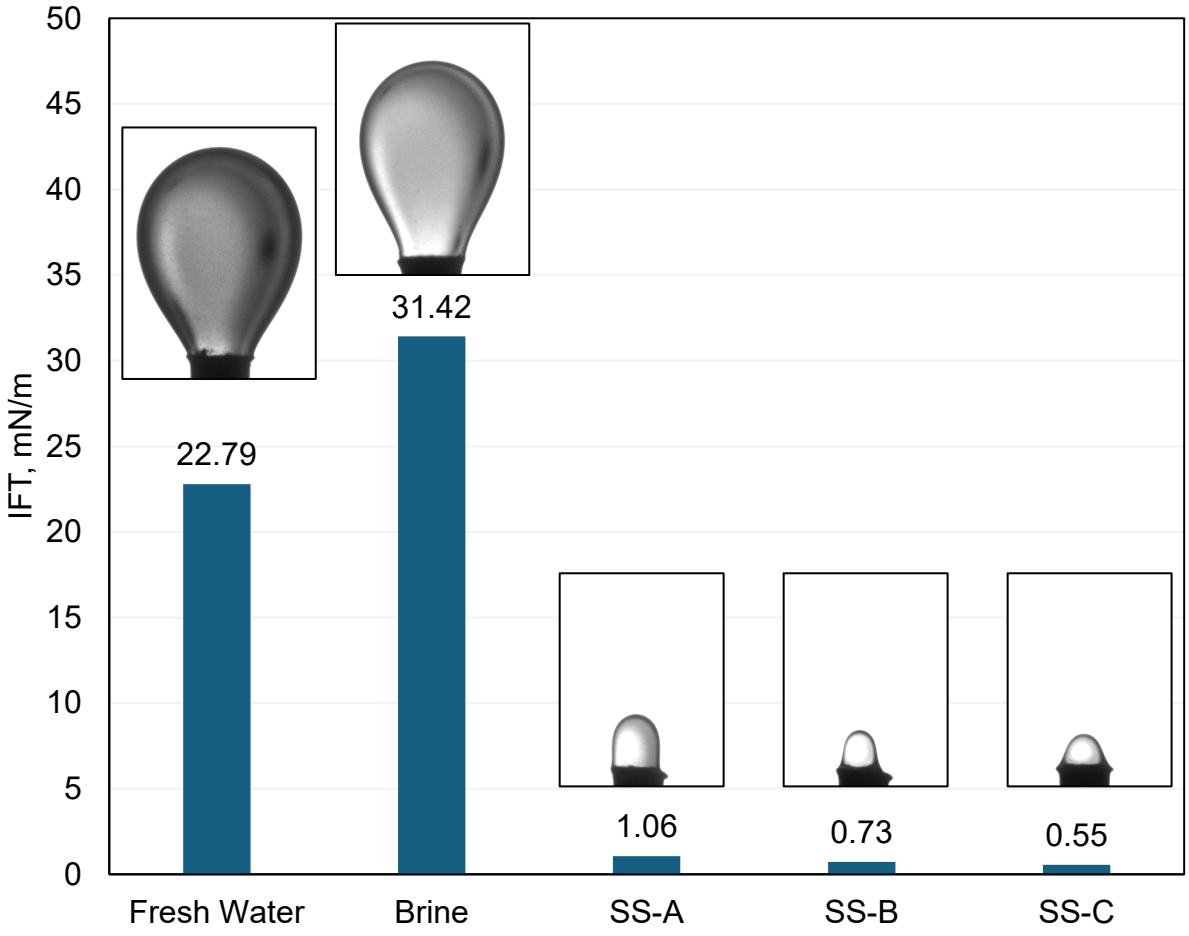

Figure A-5. IFT measurement results of a crude oil droplet surrounded by fresh water, formation brine, and surfactant solutions A, B, and C.

As mentioned earlier, the contact angle technique was employed to assess reservoir wettability and investigate the impact of surfactant injection on altering the wettability state. A droplet of fresh water, brine, SS-A, SS-B, and SS-C was introduced onto a rock surface surrounded by crude oil. The contact angle, measured from the interface between the rock and introduced droplet to the interface between the introduced droplet and oil, was determined. Figure A-6 illustrates the different wettability states based on the measured contact angle. According to Chilingar and Yen (1983), the rock is considered water-wet if the contact angle measured through the water droplet is between 0° and 80°, mixed-wet for values between 80° and 100°, and oil-wet when the contact angle measured through the water droplet is higher than 100°.

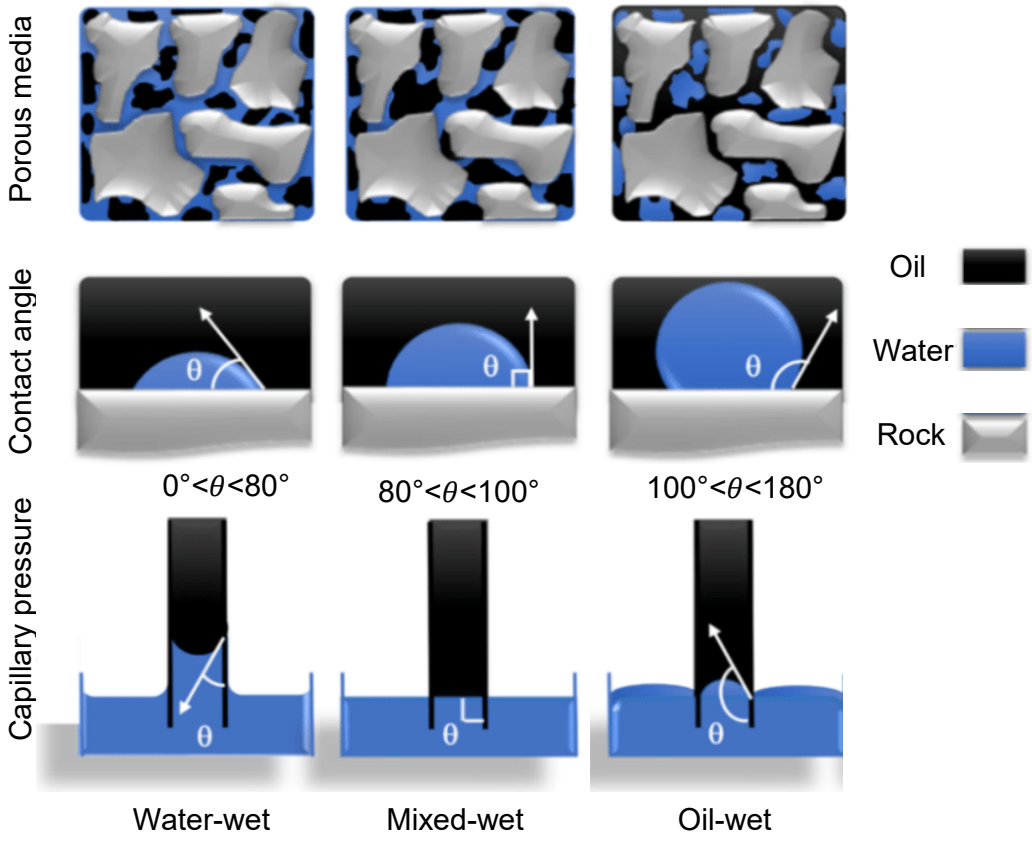

Figure A-6. Display of the different wettability states based on the contact angle of a water droplet introduced on a rock surface surrounded by oil.

The results presented in Figure A-7 suggest that the reservoir exhibits mixed-wettability characteristics when in contact with fresh water and oil but tends to be strongly oil-wet when interacting with brine and oil. Upon the addition of 1 ppm of SS-A, there was a slight decrease in the contact angle from 138° to 124°, maintaining the wettability state as oil-wet. In contrast, SS-B and SS-C significantly reduced the contact angle, effectively shifting the wettability state toward water-wet. Specifically, the contact angle decreased from 138° for the oil–brine system to 58° and 18° for SS-B and SS-C, respectively.

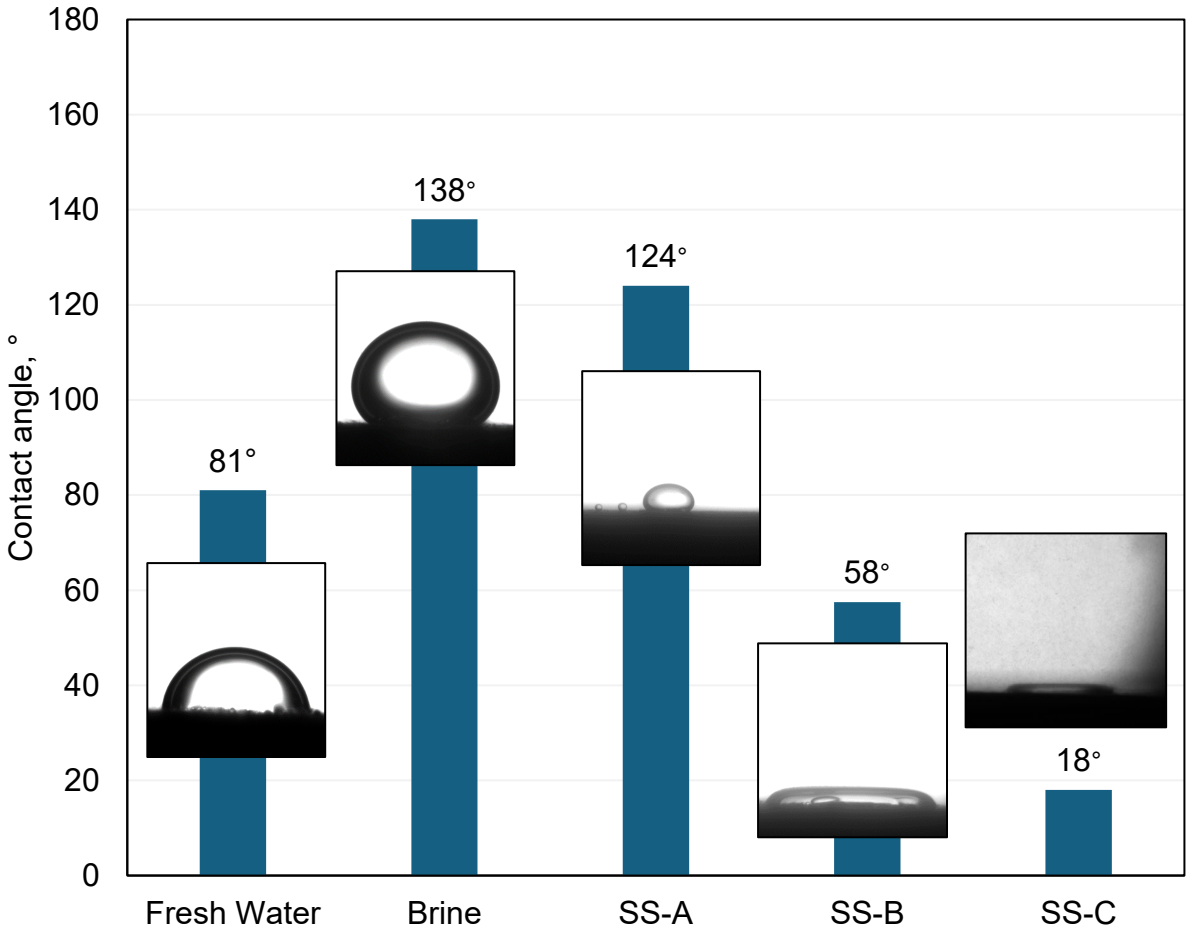

Figure A-7. Contact angle measurement results of fresh water, formation brine, SS-A, SS-B, SS-C droplet introduced on reservoir rock sample and surrounded by oil.

Emulsion Tests

As part of the comprehensive evaluation of fluid interactions and to better understand the performance of surfactants, further tests were conducted to assess the emulsion properties of surfactant and crude oil. Emulsion tests were conducted by combining equal volumes of oil and each surfactant solution in a graduated pipette. These mixtures were then allowed to stabilize at reservoir temperature before being vigorously shaken for 60 seconds. The resulting emulsions were monitored over time to assess their stability and characteristics. Emulsions can be advantageous in surfactant EOR because they help in reducing IFT between the injected surfactant solution and the oil in the reservoir (Yuan and others, 2015). This reduction in IFT allows for better mobility of the oil, facilitating its displacement and recovery from the reservoir (Yuan and others, 2015). Additionally, emulsions can also help in improving sweep efficiency and reducing channeling effects during the injection process. However, very stable emulsions can cause problems of decreased injectivity, reservoir plugging, and difficulties in separation.

The results depicted in Figure A-8 indicate that all emulsions exhibited significant breakdown after a period of time, which is desirable for effective surfactant EOR processes. SS-A formed the highest emulsion volume; however, it experienced the quickest breakdown. While the emulsion formed using SS-B performed slightly better, SS-C's emulsion exhibited the most consistent breakdown over time, indicating higher stability and performance compared to SS-A and SS-B.

Oil Recovery Tests

All the rock samples were initially cleaned and saturated with oil, and the core weight differences were used to determine the original oil volume in place. Injection tests were conducted at a reservoir temperature of 230°F and an injection pressure of 4000 psi. Results of all the injection tests are presented in Figures A-9 and A-10. After brine injection, 45.9% of the oil was displaced from Sample 1. However, subsequent injection of SS-A without any preinjection soaking did not yield any oil production. Following a 5-day soaking period, further injection led to an incremental

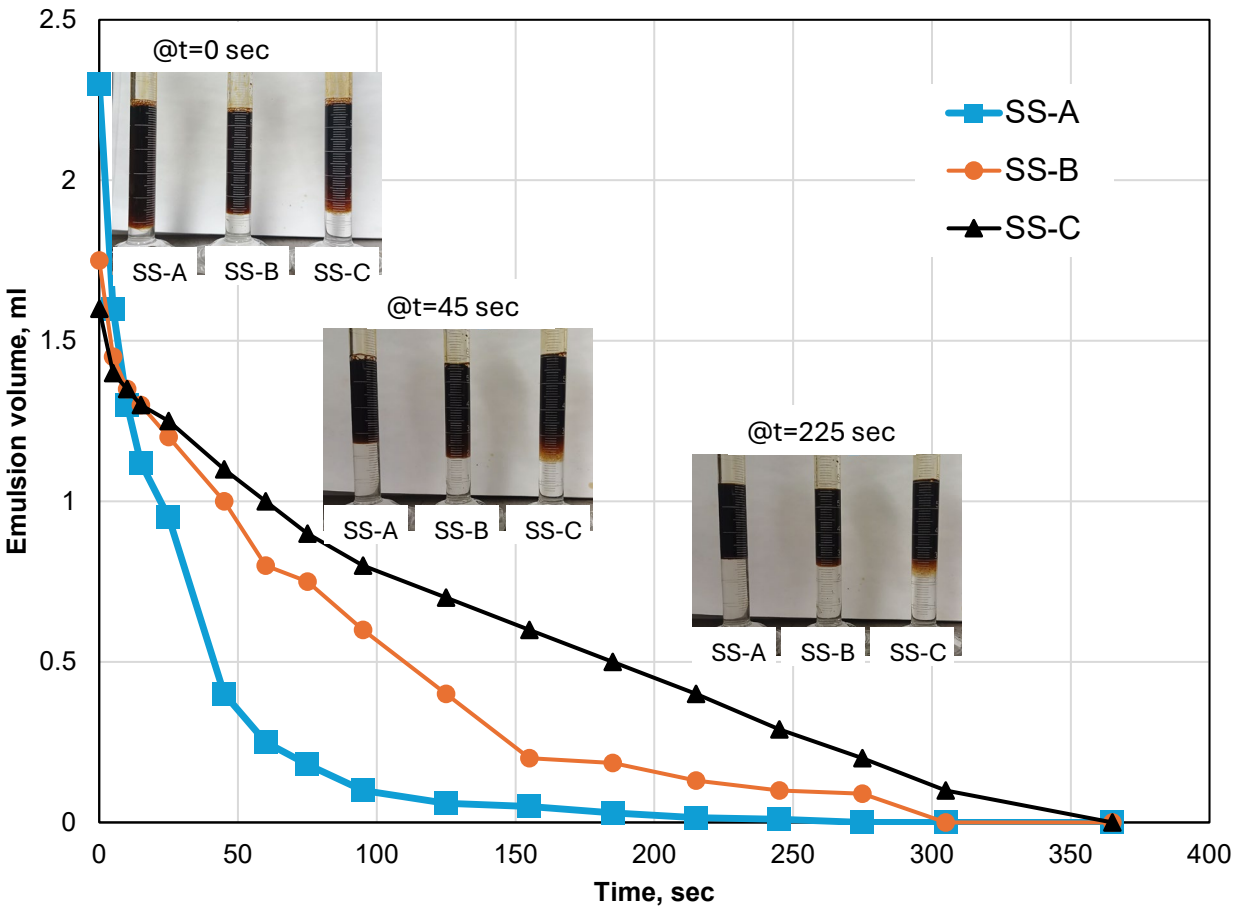

Figure A-8. Measurements of oil–surfactant emulsion volume for SS-A, SS-B, and SS-C.

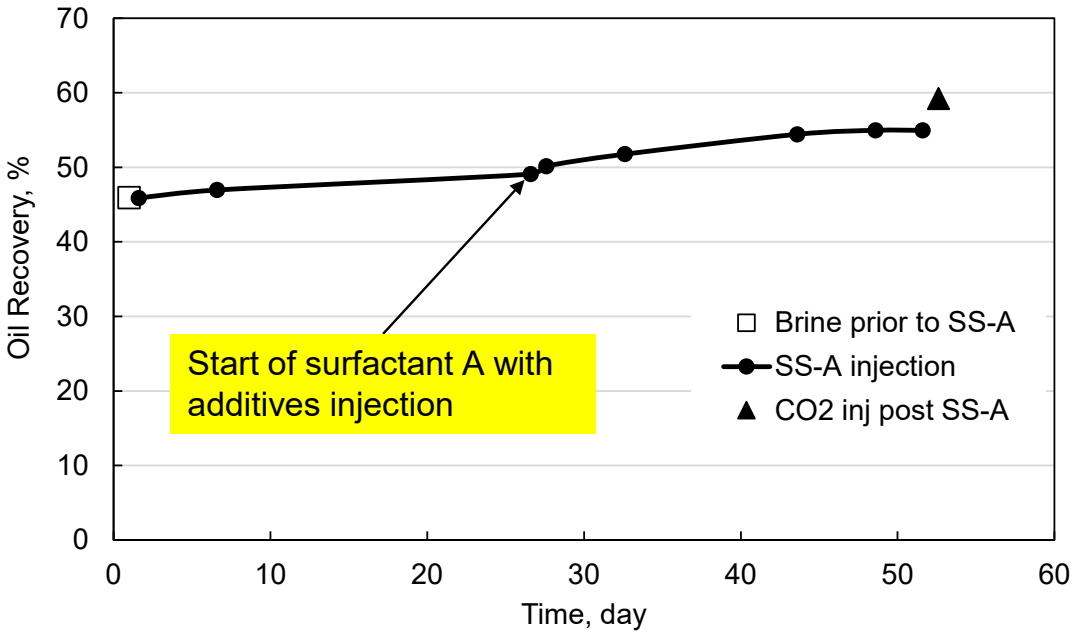

Figure A-9. Flow-through test results of Rock Sample 1 after brine injection, followed by SS-A at different soaking times, and finally by CO_2 injection.

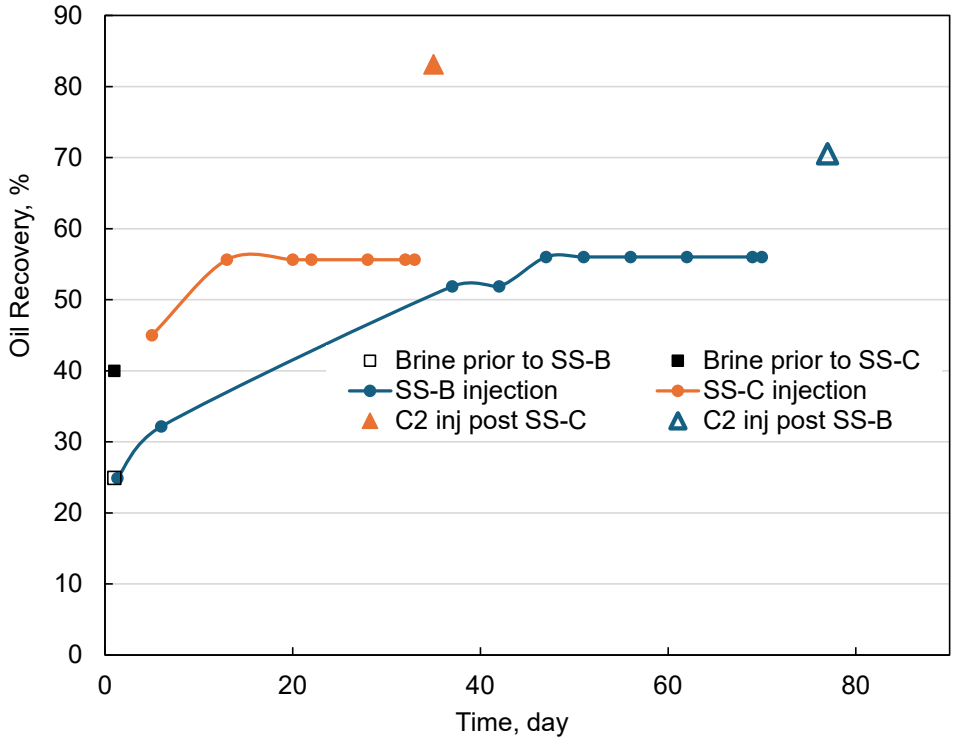

Figure A-10. Flow-through test results of Rock Samples 1 and 2 after brine injection, followed by SS-B and SS-C, respectively, at different soaking times, and finally by C2 injection.

1% of oil recovery. Increasing the soaking time by an additional 20 days resulted in an ultimate recovery factor of 49% up to this step. This multistage approach resulted in a notable improvement in the EOR performance of SS-A, leading to an additional displacement of almost 6% of oil after subsequent injections. Once surfactant injection ceased to yield further oil displacement, CO_2 was introduced, leading to an additional 4% increase in oil production.

Similar EOR schemes were tested to measure the oil recovery following the injection of SS-B and SS-C using Rock Samples 2 and 3, respectively. Brine injection tests conducted on Cores 2 and 3 resulted in oil recovery factors of 25% and 40%, respectively. Similarly to SS-A, SS-B was initially injected without preinjection soaking, resulting in no oil displacement. Allowing the rock sample to soak in SS-B for 5, 36, and 47 days resulted in an incremental oil recovery of 7.3%, 19.7%, and 4.2%, respectively. These results emphasize the influence of soaking duration on the EOR performance of surfactant injection. Following a 47-day soaking period, oil recovery using SS-B injection reached its peak at 56%, with no further oil displacement observed regardless of the duration of subsequent core soaking. Subsequently, ethane injection was initiated, leading to the displacement of an additional 14.5% of oil and resulting in a final recovery factor of 70.5%.

For Core 3, brine injection initially displaced 40% of the oil. After 5 days of soaking, SS-C injection led to a production of an additional 5%. Subsequent SS-C injection, following a 13-day soaking, resulted in displacing 10% more oil. At this stage, SS-C reached its peak and no more oil was produced. However, subsequent ethane injection helped displace 27.5% more oil, resulting in an ultimate recovery factor of 83.13%.

Formation Resistivity Tests

Formation resistivity testing was performed to increase the confidence level of water saturation calculations. Default values of 2.0 for both cementation and saturation exponents are commonly used in the Archie equation to calculate water saturation from log resistivity. Actual values were determined by core testing to provide higher precision in saturation calculations. The results of this testing are shown in Table A-2.

Table A-2. Results of Formation Resistivity Determination Using Core Plugs

					Archie Equation Variables		
Sample	Depth, ft	Permeability, mD	Porosity, %	Grain Density, g/cc	Formation Resistivity Factor, F	Cementation Exponent, M	Saturation Exponent, N
131811	9226.6	7.694	17.08	2.77	42.4	2.120	2.104
131834	9269.0	0.075	7.33	2.73	217.0	2.058	2.201
131841	9281.9	0.676	14.42	2.76	52.2	2.043	2.101
131846	9289.2	0.162	10.79	2.81	116.1	2.136	2.178

References

Ahmad, W., Vakili-Nezhaad, G., Al-Bemani, A.S., and Al-Wahaibi, Y., 2016, Experimental determination of minimum miscibility pressure: Procedia Engineering, v. 148, p. 1191–1198.

Bera, A., and Belhaj, H., 2016, A comprehensive review on characterization and modeling of thick capillary transition zones in carbonate reservoirs: Journal of Unconventional Oil and Gas Resources, v. 16, p. 76–89.

Chilingar, G.V., and Yen, T.F., 1983, Some notes on wettability and relative permeabilities of carbonate reservoir rocks, II: Energy Sources, v. 7, p. 67–75.

Dakhelpour-Ghoveifel, J., Shegeftfard, M., and Dejam, M., 2019, Capillary-based method for rock typing in transition zone of carbonate reservoirs. Journal of Petroleum Exploration and Production Technology, v. 9, p. 2009–2018.

Dindoruk, B., Johns, R., and Orr Jr, F.M., 2021, Measurement and modeling of minimum miscibility pressure—a state-of-the-art review: SPE Reservoir Evaluation and Engineering, v. 24, no. 2, p. 367–389.

Hawthorne S.B., Miller, D.J., Jin, L., and Gorecki, C.D., 2016, Rapid and simple capillary-rise/vanishing interfacial tension method to determine crude oil minimum miscibility pressure—pure and mixed CO_2, methane, and ethane: Energy & Fuels, v. 30, no. 8, p. 6365–72.

Jin, L., Kurz, B.A., Ardali, M., Wan, X., Zhao, J., He, J., Hawthorne, S.B., Djezzar, A.B., Yu, Y., and Morris, D., 2022a, Investigation of produced gas injection in the Bakken for enhanced oil recovery considering well interference: Paper presented at the SPE/AAPG/SEG Unconventional Resources Technology Conference, Houston, Texas, USA, June. URTEC-3723697-MS. https://doi.org/10.15530/urtec-2022-3723697.

Jin, L., Wan, X., Azzolina, N.A., Bosshart, N.W., Zhao, J., Yu, Y., Yu, X., Smith, S.A., Sorensen, J.A., and Gorecki, C.D., 2022b, Optimizing conformance control for gas injection EOR in unconventional reservoirs: Fuel, v. 324, p. 124523.

Kamari, A., Arabloo, M., Shokrollahi, A., Gharagheizi, F., and Mohammadi, A.H., 2015, Rapid method to estimate the minimum miscibility pressure (MMP) in live reservoir oil systems during CO_2 flooding: Fuel, v. 153, p. 310–319.

Masalmeh, S.K., Shiekah, I.A., and Jing, X.D., 2007, Improved characterization and modeling of capillary transition zones in carbonate reservoirs: SPE Reservoir Evaluation and Engineering, v. 10, no. 2, p. 191–204.

Shi, S., Belhaj, H., and Bera, A., 2018, Capillary pressure and relative permeability correlations for transition zones of carbonate reservoirs: Journal of Petroleum Exploration and Production Technology, v. 8, p. 767–784.

Taber, J.J., Martin, F.D., and Seright, R.S., 1997a, EOR screening criteria revisited—part 1—introduction to screening criteria and enhanced recovery field projects: SPE Reservoir Engineering, v. 12, no. 3, p. 189–98.

Taber, J.J., Martin, F.D., and Seright, R.S., 1997b, EOR screening criteria revisited—part 2—applications and impact of oil prices: SPE Reservoir Engineering, v. 12, no. 3, p. 199–206.

Yuan, D.Y., Pu, W.F., Wang, X.C., Sun, L., Zhang, Y.C., and Cheng, S., 2015, Effects of interfacial tension, emulsification, and surfactant concentration on oil recovery in surfactant flooding process for high temperature and high salinity reservoirs: American Chemical Society, v. 29 no. 10, p. 6165–6176.

Zhao, Y., Fan, G., Song, K., Li, Y., Chen, H., and Sun, H., 2021, The experimental research for reducing the minimum miscibility pressure of carbon dioxide miscible flooding: Renewable and Sustainable Energy Reviews, v. 145, p. 111091.

APPENDIX B

RECOMMENDED GEOLOGIC AND DYNAMIC FLOW SIMULATION MODELING WORKFLOW

RECOMMENDED GEOLOGIC AND DYNAMIC FLOW SIMULATION MODELING WORKFLOW

In this section, the steps in the recommended workflow for geoscience and reservoir engineering evaluation with the goal of revitalizing a Williston Basin oil field will be presented along with the illustrative applied case of Foreman Butte Field. An overview of the nine-step workflow (Figure B-1) will be presented first. Steps 1–9 will then be discussed in detail.

The process begins with Step 1, which involves defining the area of interest (AOI) and zone of interest (ZOI), setting the stage for the detailed investigations to follow. Step 2, data collection, is critical and involves gathering a wide array of data types from various sources, ensuring the data's maintenance and preparation for analytical use.

Step 3 involves the geological evaluation phase, emphasizing the depositional setting to understand the reservoir's geological framework. This is followed by Step 4, reservoir characterization, an integrated analysis that includes petrography, petrophysics, facies analysis, and faults characterization. An examination of historical reservoir performance is conducted in Step 5 to improve the reservoir characterization with results from production data, pressure data, and material balance analyses. These characterizations feed into Step 6, the construction of a comprehensive 3D geological model. This model integrates stratigraphy, structural formations, formation evaluation, and 3D models of facies and properties, providing a detailed representation of the reservoir.

The workflow then advances to Step 7, fracture characterization and modeling. This step addresses the complexities of fractures, including their density, orientation, and dip; porosity identification from geophysical well logs; fracture prediction using curvature mapping; and the development of an embedded discrete fracture model (EDFM). With the geological and fracture models in place, Step 8 focuses on setting up the dynamic model, which accounts for fluid and rock-fluid properties, establishes initial and boundary conditions, and integrates EDFM for dynamic simulations.

Finally, Step 9, reservoir simulation, involves applying the constructed models to simulate reservoir behavior through history matching, scenario analysis, optimization, and thorough results analysis. This step is crucial for predicting and optimizing reservoir performance under various operational scenarios and investigating the uncertainties in the geological model and simulation results. In the following sections, these steps and their application in the Foreman Butte Field case are described in detail.

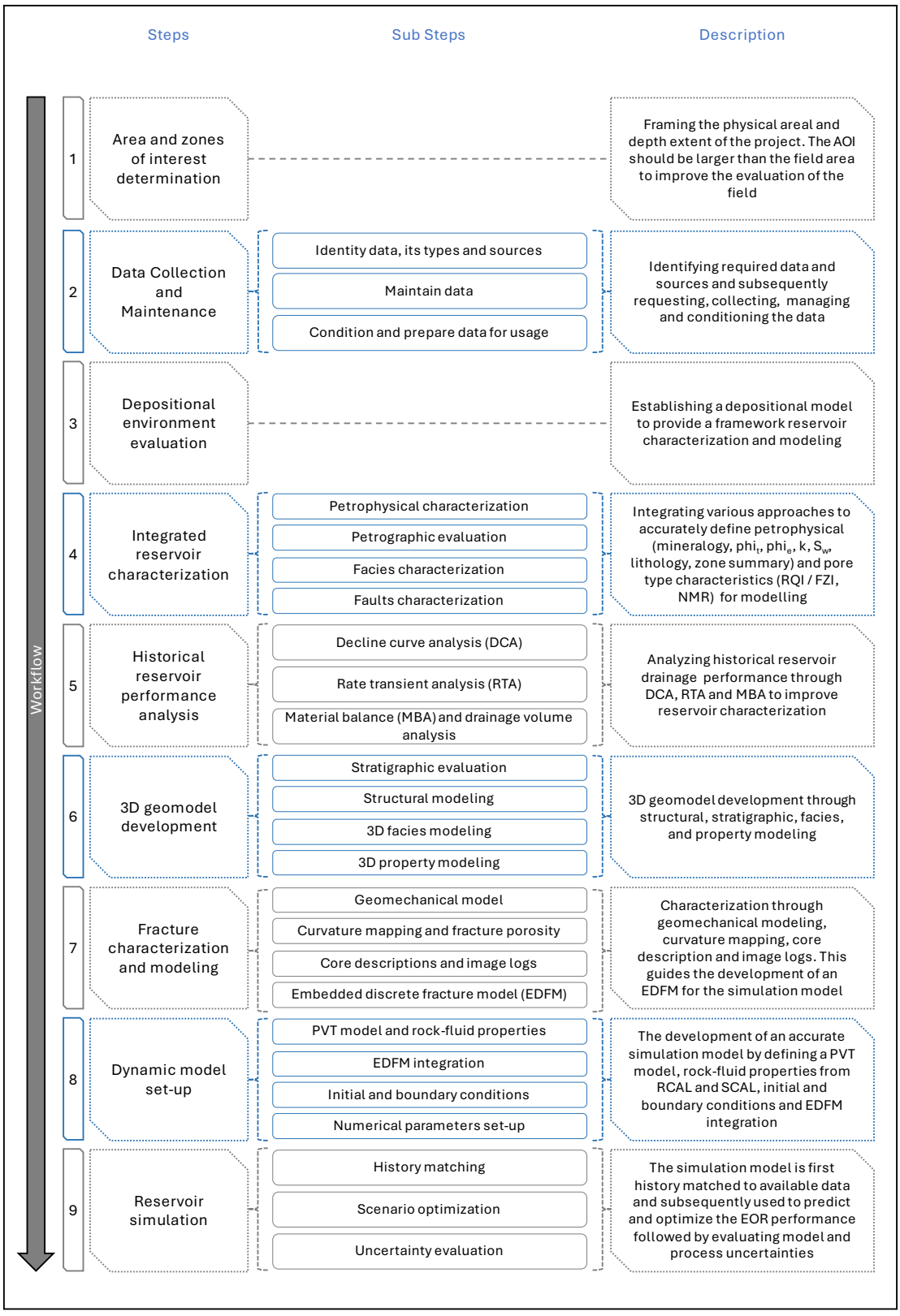

Figure B-1. Recommended evaluation workflow for legacy carbonate field revitalization studies.

Step 1: Define the AOI and ZOI

This step discusses the guidelines for defining the AOI and ZOI for the revitalization project. It represents the first step toward framing the lateral and vertical extent of the project.

Establish AOI

Determining an AOI for research and data to be collected needs to be sized to the planned work to be complete. The AOI should be assessed for expansion that allows for the adequate description of the subsurface with available data. Leased acreage or legally defined fields are often limited in expanse, and additional data outside the boundary will need to be collected. An AOI should be selected to provide a contiguous area with well data near the edges to limit the data extrapolation within the selected boundary. Wells with production data from the geologic interval being studied can assist with later calibration of the model. The natural boundaries identified from oil production trends or from available geologic information can help guide the AOI determination. It is suggested to have an AOI larger than needed for mapping and geological model development, since any model can be reduced later for numerical simulation to reduce computational cost if needed.

In the case of Foreman Butte, oil production trends and geologic data were used to determine the AOI (Figure B-2). The larger AOI surrounding the field allowed for more accurate mapping by maximizing geological and oil production data control along its edges. The determination of the AOI then allows for establishing the ZOI(s).

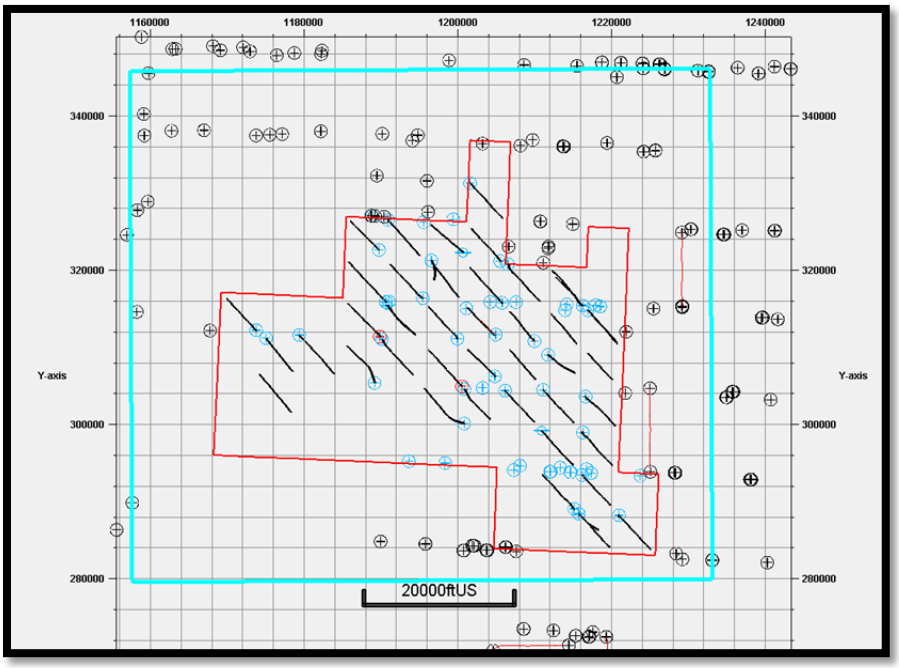

Figure B-2. AOI (blue line) used for data collection and modeling for Foreman Butte Field (red line).

Establish ZOI

Project requirements and questions will determine the target interval(s) that will be the project focus for the ZOI. With the aid of previous research and published sources, a final ZOI should be selected to include the primary target zones, thickness of confining cap rock above and below, and notable stratigraphic markers for correlation and mapping purposes. The target intervals for Foreman Butte were the Flat Lake and Alexander units, and the ZOI extended from the base of the last Charles Formation to the top of the Mission Canyon Formation (Figure B-3). Minor Mission Canyon production does occur around the fringe of the field, and a handful of wells have comingled Mission Canyon and Ratcliffe production. However, Mission Canyon production volumes were found to be insignificant compared with typical Mission Canyon wells. Therefore, the Mission Canyon Formation was excluded from the Foreman Butte project.

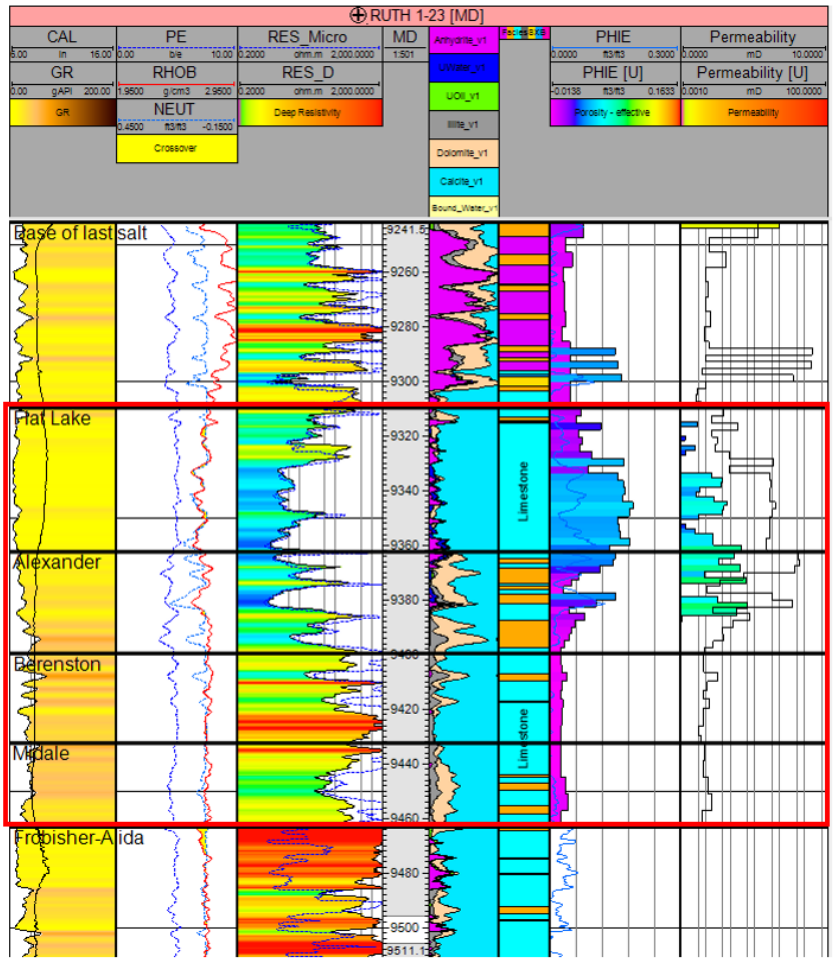

Figure B-3. Wireline and interpreted logs across the ZOI.

After data collection (Step 2), a final revision of the AOI and evaluation of available data types are needed to ensure the goals of the project are attainable. Reviewing the production for the field or acreage within the AOI can help determine reservoir quality or drainage area. Legal field boundaries often do not reflect subsurface realities. Therefore, adjusting the AOI to include additional data or removing area will need to be assessed against operator or project strategies (e.g., acquiring acreage). Identifying additional boundaries within the AOI for reviewing material balance or volumetric hydrocarbon in-place are useful for later integration between geologic modeling and numerical simulation.

From a previous interpretation of Foreman Butte, a porosity thickness map for porosity exceeding 4% for the Ratcliffe interval superimposed with a bubble map for Ratcliffe oil production was used to outline a boundary to be used for later volumetric calculation (see Figure B-4).

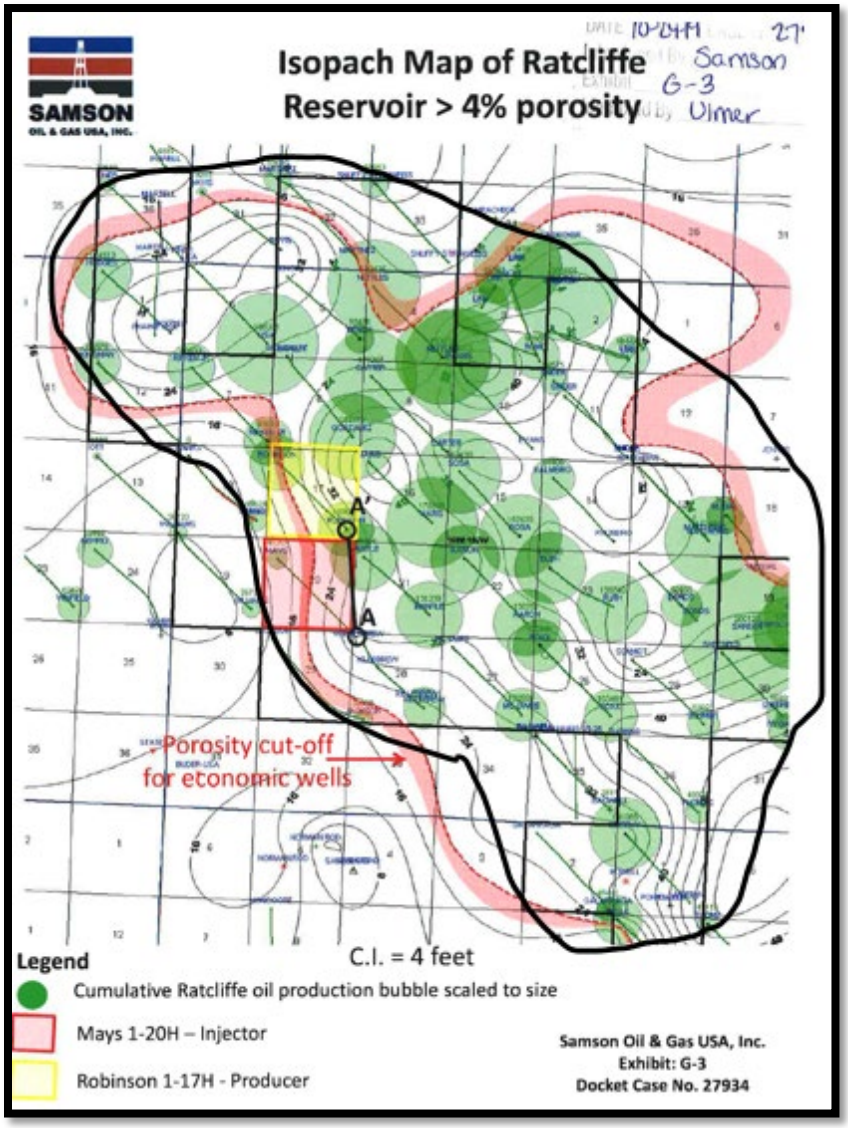

Figure B-4. Vintage map showing porosity height cutoff (pink line), cumulative Ratcliffe oil production (green bubbles), and volumetric boundary (black line).

Step 2: Data Types, Sources, Collection, Maintenance, and Conditioning

This step involves the process of identifying required data types and sources and how to collect, maintain, and condition them for proper use in the project. This step comes after the initial step of identifying the AOI and ZOI and involves several substeps and considerations. The data collected are different in types and sources, and a strategic plan to execute the data identification, collection, and maintenance is required for this project and similar projects. The details of this step were discussed in Section 3.2 of the report.

Step 3: Depositional Environment

Establishing a depositional model is a crucial step in the overall reservoir characterization process and provides the means to test hypotheses for reservoir and hydrocarbon system development. The characterization of carbonate systems using a sequence stratigraphic framework is a useful tool for understanding porosity and diagenesis through geologic time for later incorporation into a reservoir model. Using the carbonate platform depositional setting as an example depositional model, the depositional cycle within a sequence stratigraphic framework (Figure B-5) can be reviewed to make predictions for the data and interpretations expected from a field (Moore, 2001). Each sequence stratigraphic element (e.g., transgressive systems tract [TST], flooding surface, highstand systems tract [HST], sequence boundary, lowstand systems tract [LST], and platform drowning surface) represents stratigraphic geometries, erosional surfaces, and influences on the rock matrix and pore systems that should be considered in a reservoir model. A similar methodology can be applied in other dominant depositional settings, such as a reef.

Mississippian Mission Canyon and Charles Formation Depositional Model

Sheldon and Carter (1979) characterized the general depositional setting for the Mississippian and Charles Formations' carbonate systems (Figure B-6.) The Ratcliffe interval is described as primarily shallow-water limestones, transitioning to dolomite and evaporites on the margin of the basin. Foreman Butte Field is situated in part of the basin with lower amounts of dolomite across the sequence; for the same sequence north of Forman Butte, zones with higher levels of dolomite tend to be associated with elevated porosity (Burke, 2005). Burke (2005) also describes the wide variability in the Ratcliffe reservoir quality across the region, primarily due to diagenesis related to dolomitization and dissolution of grains associated with subaerial exposure. This variability demonstrates the importance of conducting carbonate sedimentology studies integrated with thin-section petrography and/or nuclear magnetic resonance (NMR) to understand the pore types, pore distribution, and diagenetic history.

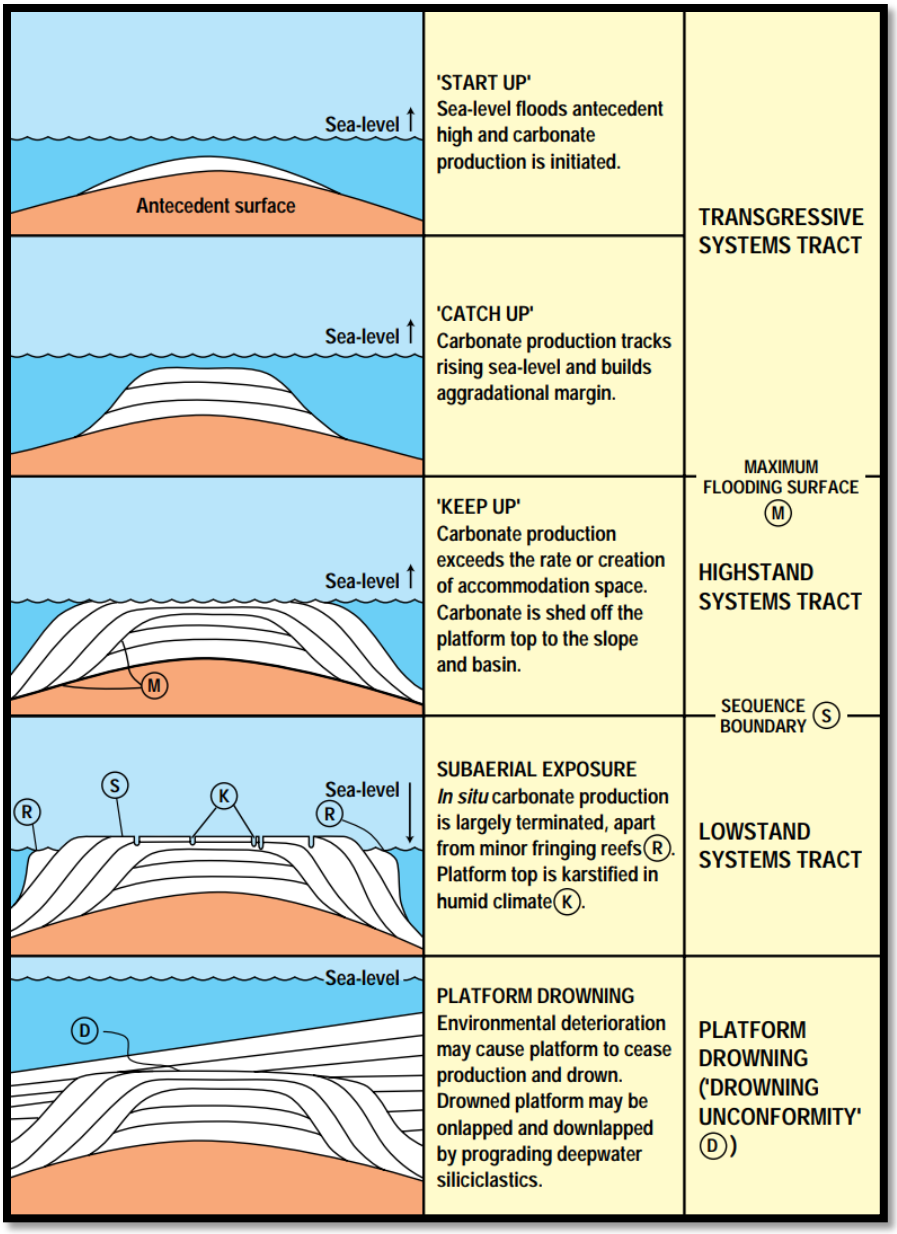

Figure B-5. Schematic model for an isolated carbonate platform, showing idealized system tract boundaries and platform drowning (Moore, 2001).

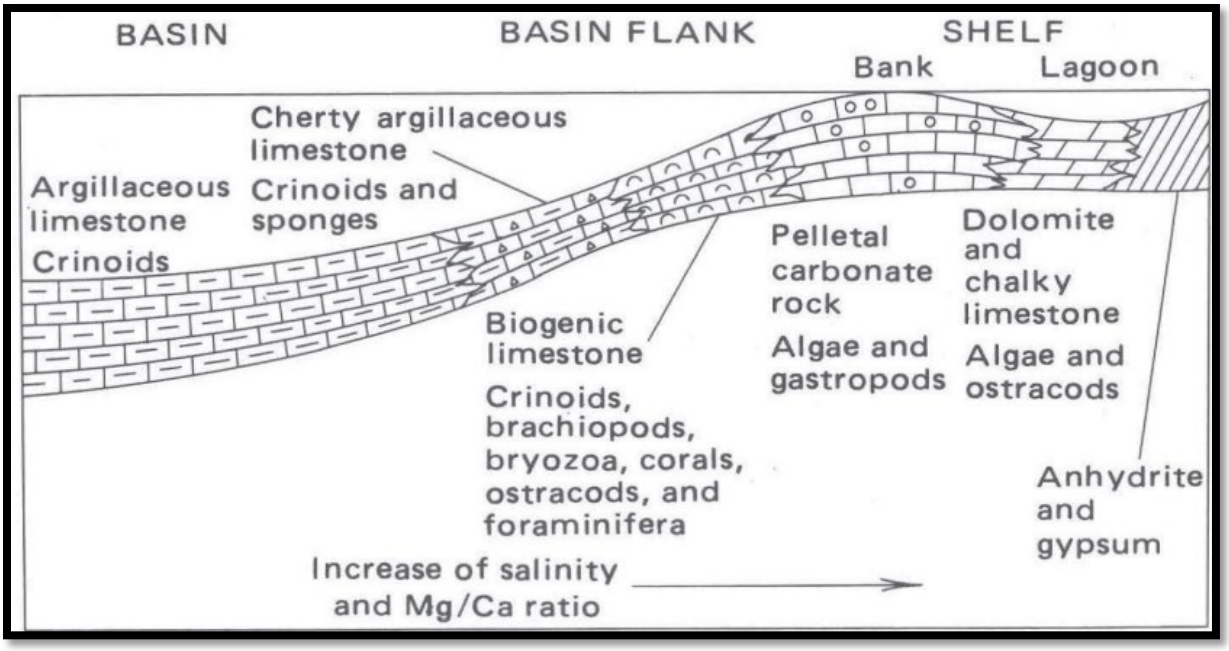

Figure B-6. Generalized model of sedimentation of the Mississippian and Charles Formations; includes Tilston, Frobisher-Alida, Midale, Ratcliffe, and Poplar intervals (Sheldon and Carter, 1979).

Carbonate Rock Classification

Two main schemes are used for classifying carbonate rocks. Folk (1959) is a detailed approach that encompasses a textural scale incorporating grainsize, roundness, sorting, and packing as well as grain composition. The complexity of the Folk classification (Figure B-7) makes it more applicable for use with a petrographic microscope in a research setting (Moore, 2001). Conversely, the Dunham classification is primarily textural in nature, simple, and easily used in the field and by wellsite geologists. Dunham's classification of major rock textures (Figure B-8) is based on the presence or absence of organic binding, presence or absence of carbonate mud, and the concept of grain versus matrix support. The four major rock classes, mudstone, wackestone, packstone, and grainstone, represent an energy continuum. The term boundstone emphasizes the significant role of organic binding and framework formation in carbonates and is a rock type unique to the carbonate realm (Moore, 2001). This document and recommended workflows are designed around the Dunham classification, including characterization of pore types, and integrated with other datasets such as NMR spectroscopy and whole-core calibrated petrophysical porosity and permeability analyses for the purposes of formulating geologically based hydraulic flow units. See Loucks (2003) for an additional reference regarding the application of Dunham's classification for carbonate system characterization.

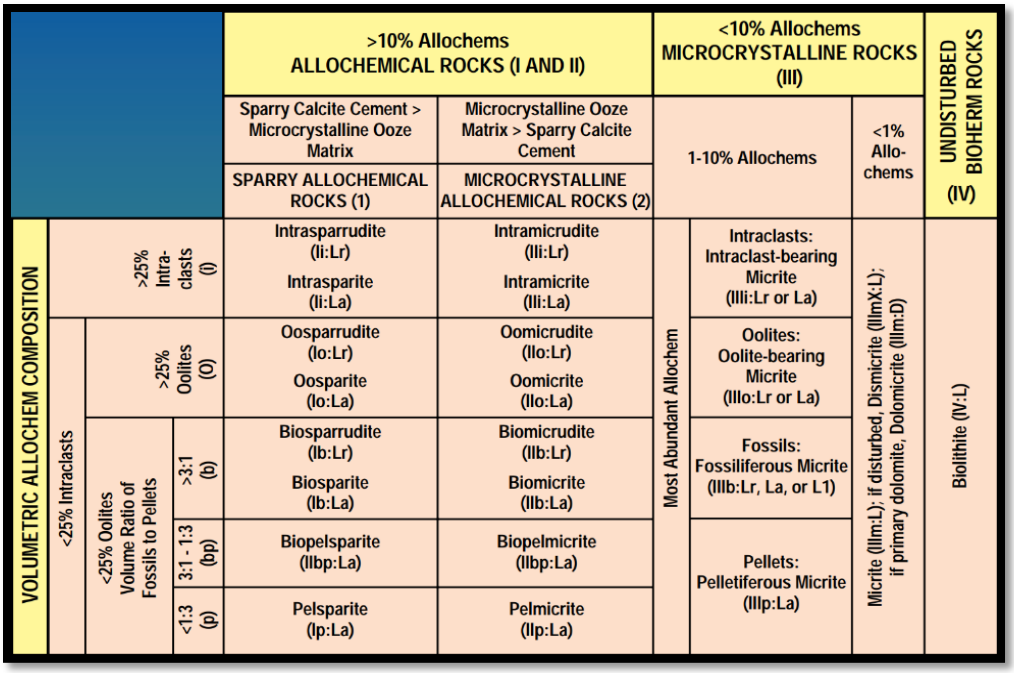

Figure B-7. Carbonate rock classification of Folk (1959). This classification is compositional and textural.

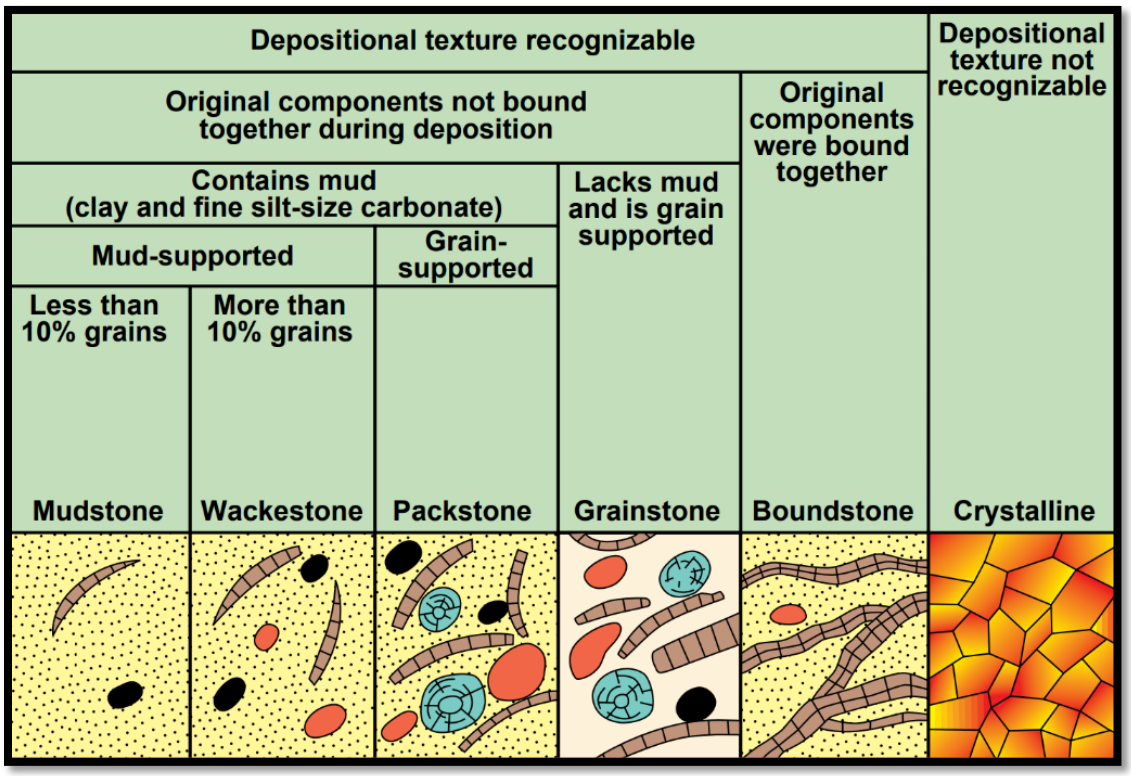

Figure B-8. Dunham carbonate classification (1962). This classification is primarily textural and depends on the presence of recognizable primary depositional elements.

Step 4: Integrated Reservoir Characterization

Accurate evaluation of carbonate reservoirs in the Williston Basin and other basins can be challenging because of the depositional environment and diagenetic heterogeneity of the reservoir rock. These challenges can lead to interpretation inaccuracies that affect oil-in-place calculations and oil–water contact determinations. To address these issues and enhance the predictive accuracy of static geological models and simulation outcomes, a comprehensive approach was adopted. This approach integrated geological facies descriptions, petrophysics, petrography, geophysical analyses (including NMR spectroscopy), and capillary pressure measurements to diminish uncertainty. The aim was to identify petrophysical and pore type characteristics specific to each geological facies, which were then predictively applied in the geological model. This process also encompassed identifying rock types and associated flow units that align with the depositional model across the ZOI. Such integration of petrophysical and facies interpretations, alongside flow unit calculations, highlights a comprehensive and coherent understanding of the data, framed within the depositional model, enhancing both static and dynamic model reliability.

Petrophysical Evaluation

Petrophysical calculation of total and effective porosity is carried out with higher certainty if all wells analyzed have a common vintage, vendor, and suite of geophysical well logs and adequate routine core analyses data are available to calibrate results. Geophysical well logs with modern suites of logs (generally post-early 1980s) provide additional tools for calibration to core and well tests. For carbonate reservoirs of the Williston Basin, density logs at a minimum proved to be vital to classify mineral components for porosity estimation. In Foreman Butte Field, most of the drilling took place after the field was discovered in 2003, and well log data contained at least density logs of similar vendor and vintage.

Obtaining core and analyzing data derived from core are fundamental in understanding the variations in reservoir quality and quantity, dominant pore types, and facies variations within the reservoir. Systematic whole-core descriptions by a carbonate sedimentologist are necessary to determine the overall process-based depositional setting(s) of the reservoir and depositional facies and to understand the stratigraphic cyclicity of the sequence. Core analysis data, integrated with process-based sedimentological core descriptions, and determination of dominant pore types from petrography and/or NMR data are essential to demonstrate the presence, quantity, distribution, and deliverability of hydrocarbons while providing a foundation for static and dynamic reservoir models. Core analysis and descriptions assist in reservoir performance predictions and the potential recovery from hydrocarbon systems.

To screen available core and determine if there are data gaps, review the following:

- Review of all field notes on the core collection and descriptions.
- Review of daylight, ultraviolet light, and x-ray photos of the core.
- Review of x-ray diffraction (XRD) and x-ray fluorescence (XRF) data.
- Review of previous sample selection locations and results based on routine core analysis (RCAL) and special core analysis (SCAL) results for all available rock types, geophysical

well log calibration, and sample density considering pay zones intraformational barriers, fractured zones, top seal, and basal seal.

If there are data gaps, recommended data acquisition programs should be directed toward addressing critical uncertainties of the reservoir or cap rock. If recommending the acquisition of additional whole or sidewall core, state the reasons for recommending the core program, the method of acquisition, the impact to the technical understanding of the field, and uncertainty reduction expected. See American Petroleum Institute (1998) for a complete summary for planning a coring program, procedures for wellsite core handling and preservation, core screening, core preparation, fluid saturation, porosity and permeability determination, and supplementary testing. For the latest laboratory procedures, partner with a laboratory technician to ensure maximum value extraction from the samples and that critical uncertainties are being addressed.

Petrophysical interpretations are updated based on previous models for the ZOI or from fit-for-purpose methods depending on available data, goals of the project, and critical uncertainties. Petrophysics tasks include normalization and harmonization of geophysical well log data, correction of bad hole and washout effects, quantification of mineral and lithological modeling calibrated with available core analyses data (e.g., XRD/XRF, porosity, permeability, fluid saturations), generation of petrophysical well log results (e.g., total porosity, effective porosity, permeability, water saturation, and lithology), and summarized zonal assessments using calculated properties and well correlations (e.g., stratigraphic tops).

If a new well or sidetrack well is to occur during a project across the ZOI, consideration should be given to obtaining new whole cores or open hole geophysical well logs. Reviewing the data audit from Step 2, coupled with ensuring new data, will impact the critical uncertainties. Foreman Butte initial well development was on 640-acre spacing and whole cores were available from five wells. A recommendation was made to collect core from Willy Miranda State 16-4 to reduce uncertainty. All available core data were used for the field study; see Table B-1 for a list of the wells and core intervals and Figure B-9 for core well locations.

Table B-1. List of Foreman Butte Wells with Whole Core

NDIC Well No.	Well Name	Cored Intervals, feet
15715	Evans 1-10H	9333–9350; 9350–9376; 9376–9448; 9448–9471
15803	McGriff Federal 1-22H	9362–9379; 9379–9414
15883	Bench 1-5H	9395–9427; 9427–9455
15766	Bagwell 1-35H	9459–9527.3
38630	Willy Miranda State 16-4	9212–9325; 9360–9401

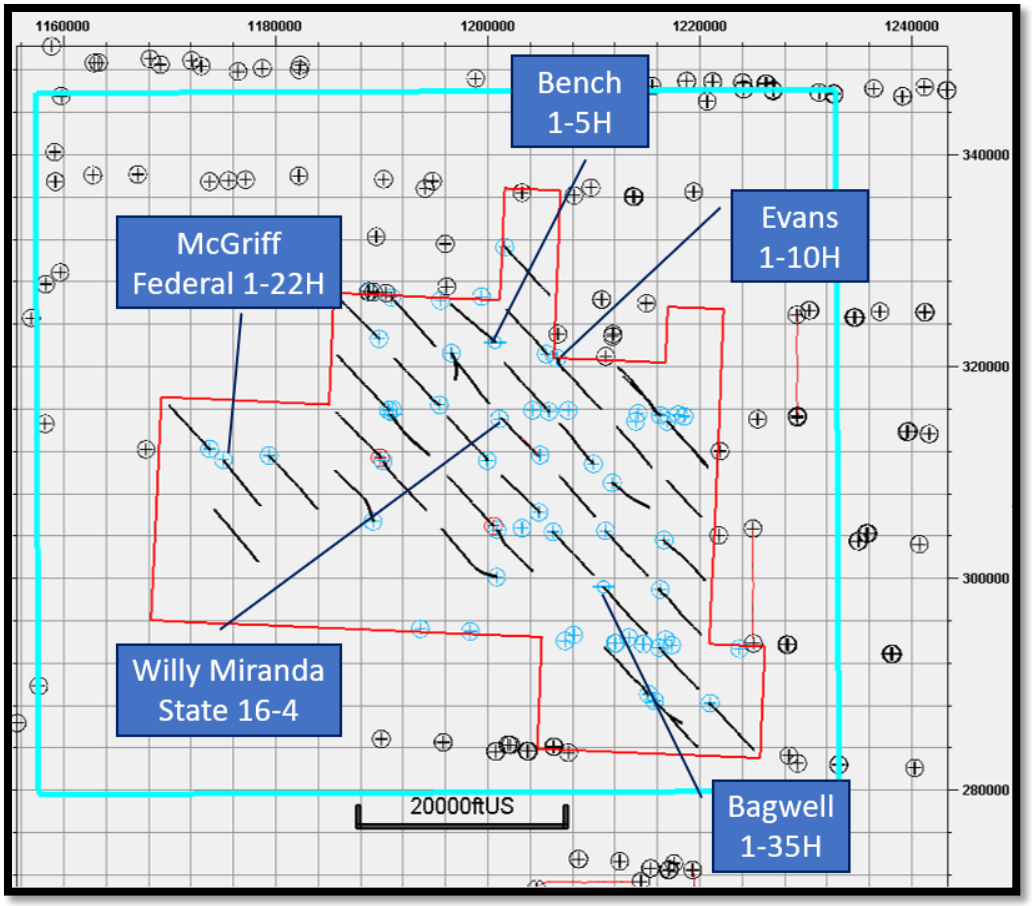

Figure B-9. Map showing locations of whole core of the Ratcliffe interval within Foreman Butte Field.

Using methods described by Amaefule and Others (1993), the core data can be used to develop rock quality index (RQI) relationships between porosity, permeability, rock types, and pore types to assist in predicting geophysical well log permeability and determining reservoir hydraulic flow units. The RQI approach provides the basis for delineation of hydraulic flow units using the flow zone index (FZI) model; however, the analysis should exclude outlying data points from samples where fracturing has impacted permeability measurements. By plotting RQI against the ratio of pore volume to grain volume (φ_z), points can be grouped into hydraulic flow units by FZI results, representing consistent pore geometries. While quantitative, this classification is independent of placement within the ZOI, so additional steps that account for deposition, diagenesis, and layering are needed to develop and define a meaningful group of hydraulic flow units (Amaefule and Others, 1993).

As part of a geologic evaluation, the process of depth shifting whole core data to appropriate geophysical well log depths allows for comparison and correlation and for calibration of petrophysical analyses (e.g., porosity, permeability, water saturation, XRD, etc.). Gamma ray logs taken from the whole core and compared to the wellbore gamma ray log are typically used for the

depth shift. A petrophysicist should assist in this process and can also ensure all geophysical logging runs have been depth-corrected.

Uncertainties with fluid saturations and characterization of the oil–water contact and free-water levels present challenges, particularly in lower-quality oil-bearing reservoirs that demonstrate long oil–water transition zones. Hydrodynamic studies of the Williston Basin suggested that some reservoirs have either a crescent-shaped or indistinct oil–water contact (White and Marchant, 1968). A more recent study has identified conditions that indicate the existence of a residual oil zone (ROZ) in the Madison section across much of the Williston Basin, where fluid contacts are impacted by hydrodynamic effects, and rock strata that were previously saturated with oil were later swept by movement of meteoric water (Advanced Resources International, 2006), creating a wide fluid saturation transition zone. This complicates the determination of fluid saturations and the nature of the oil-to-water transition zone and definition of the free-water level.

Petrographic Study

Depending on the availability of data, a petrographic study to characterize pore types should be considered. The integration of thin-section analysis, observations with petrophysics or high-tier geophysical logs (e.g., NMR), and capillary pressure data to characterize pore structure and porosity–permeability flow units (Figures B-10, B-11, and B-12) aids in the understanding of potential productivity of the carbonate reservoir and the FZIs that comprise the reservoir. The FZI characterization plot for Foreman Butte is shown in Figure B-13.

It is worth noting that the diagenesis of the Flat Lake and Alexander units is not well understood. Moldic and intercrystalline porosity resulting from dolomitization has been described in petrographic thin sections from one well in the field. Moldic and intercrystalline porosity is generally not connected and represents low permeability unless the porosity is connected via fractures. Petrographic diagenesis studies are important to consider, as results impact the definition of reservoir flow units that form the basis of static geological and dynamic simulation models.

Facies Characterization

Facies are described and characterized using available whole core based on the principles of process sedimentology and stratigraphy. Using the petrophysical interpretations, petrographic-based flow units, geophysical well log stacking pattern, and whole core-defined facies, predictive geologically facies and flow units can be classified. Machine learning methods can also be employed to determine classifications from the same data suite but require additional verification of the results. Facies results, correlated to FZIs, are useful in the static geological model to approximate the depositional model and help in the dynamic simulation model for assigning relative permeability values. Quantitative facies groupings should be reconciled with mineralogical analysis and qualitative review of core photographs, thin sections, x-ray analyses, capillary pressure data, and any pertinent knowledge of depositional environments, facies, and pore systems to establish the final description of the hydraulic flow units.

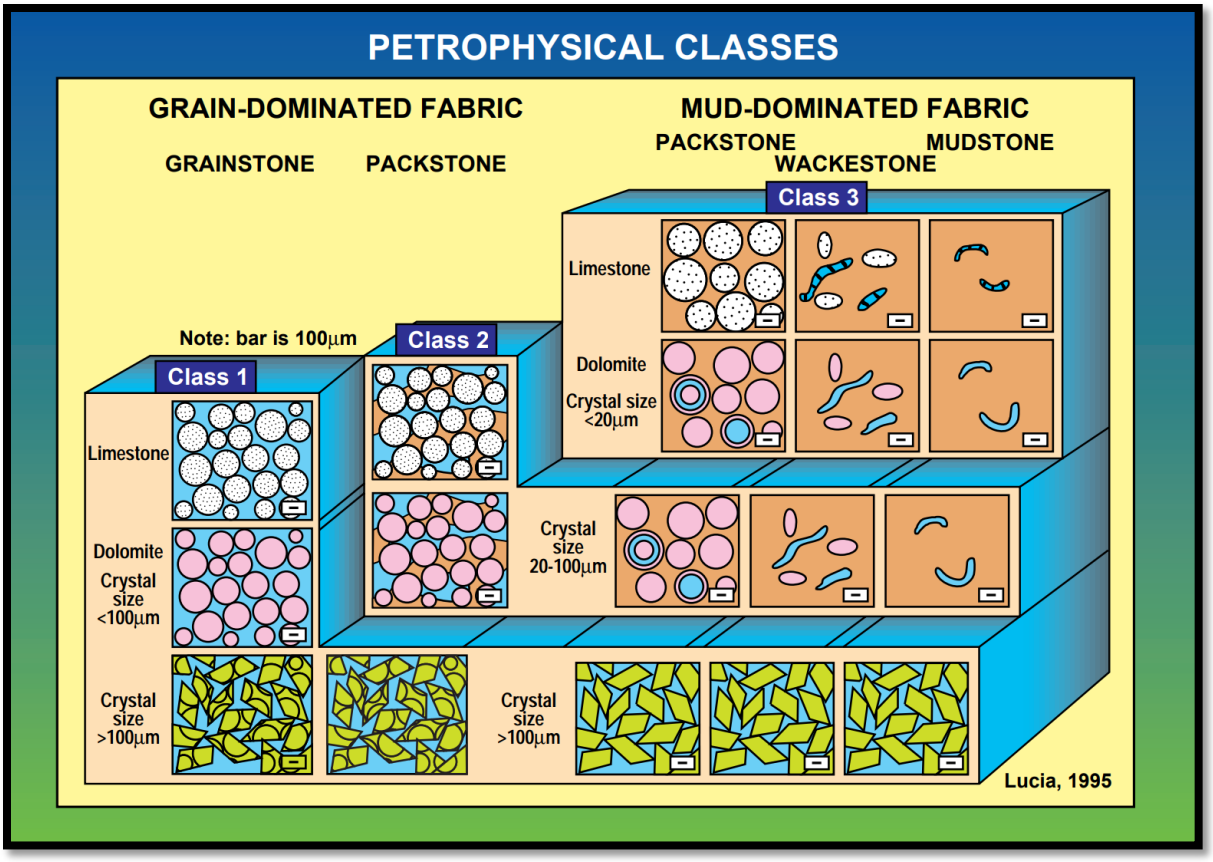

Figure B-10. Petrophysical and rock fabric classes based on similar capillary properties and interparticle porosity/permeability transforms (Lucia, 1995).

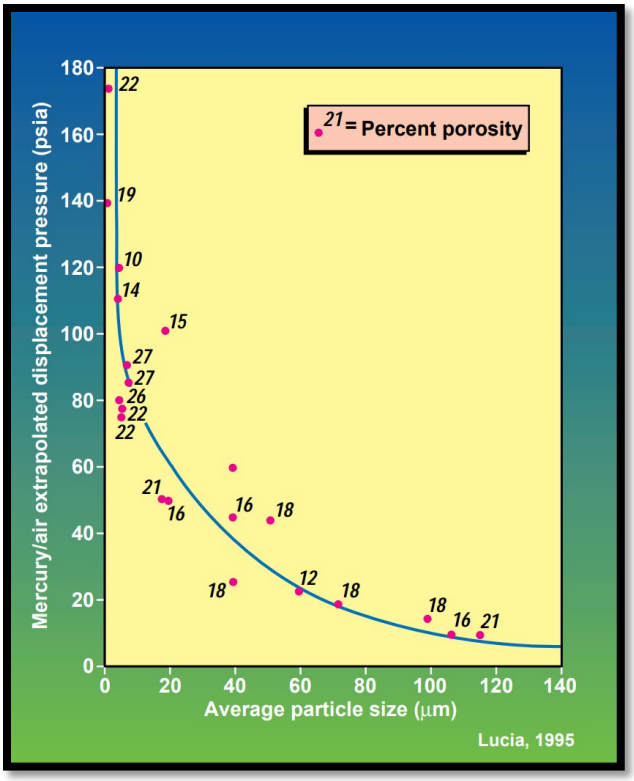

Figure B-11. Example relationship between mercury displacement pressure and average particle size for nonvuggy carbonates with >1mD (Lucia, 1995).

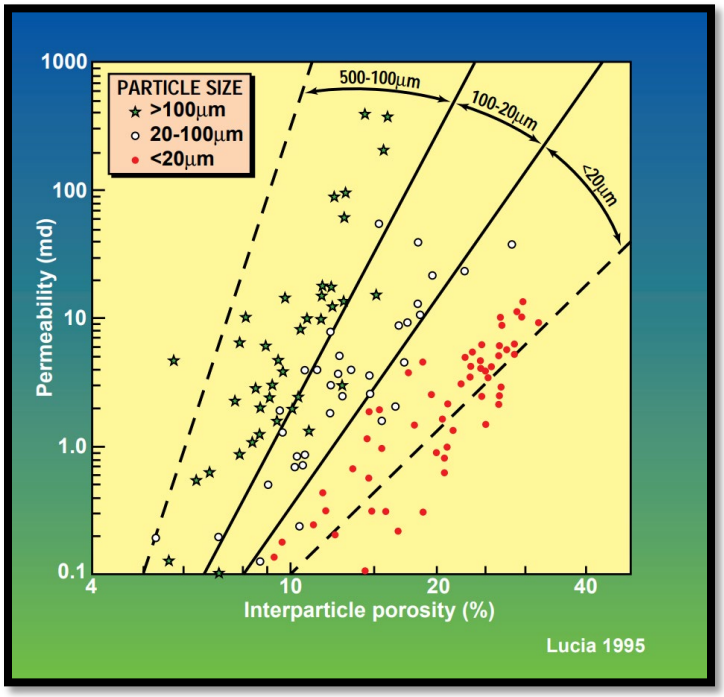

Figure B-12. Example porosity–air permeability relationship (transforms) for various particle-size groups in nonvuggy carbonate rocks (Lucia, 1995).

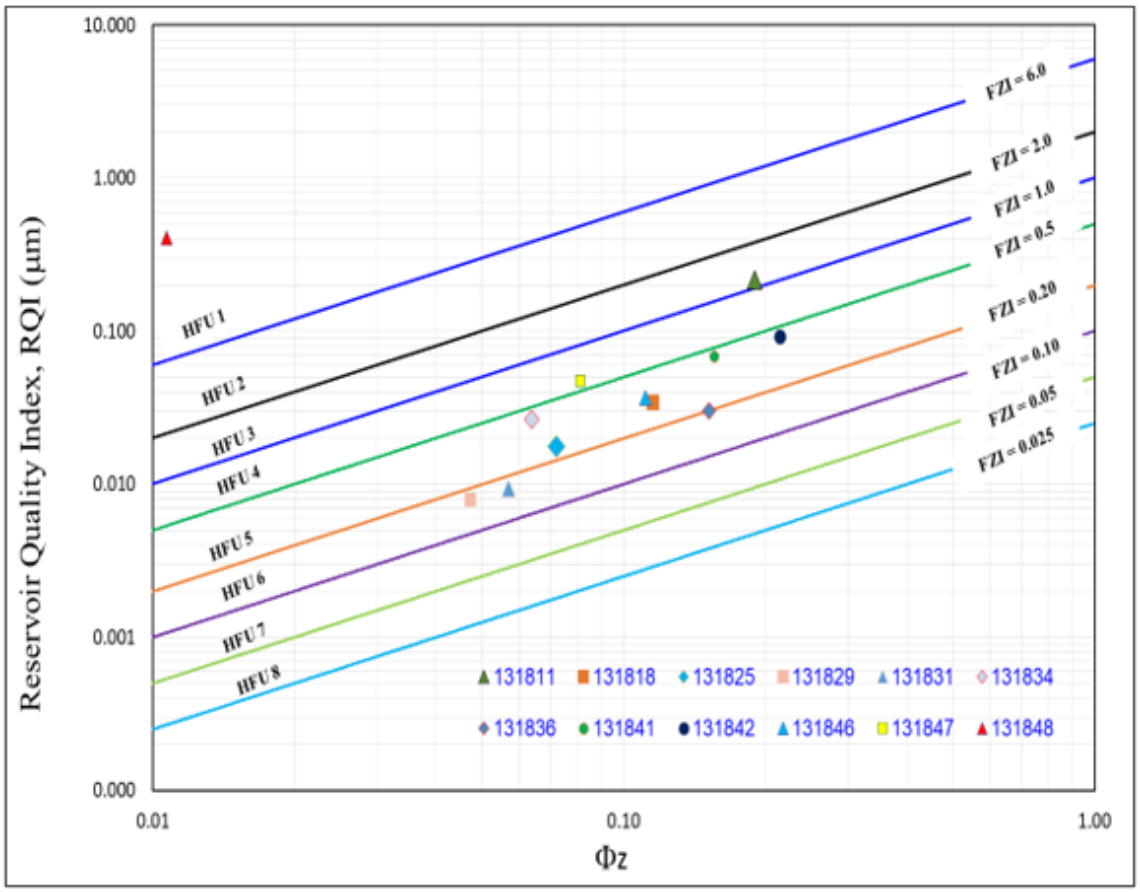

Figure B-13. FZI plot using Foreman Butte data from Willy Miranda State 16-4 well.

Faults

Faulting and tectonic history should be considered in the static geologic model. Potential impacts on the deposition of the interpreted facies (e.g., are faults post-depositional or syn-depositional) should be evaluated to ensure proper placement of the facies within the model. Integrated geologic, petrographic, petrophysical, and seismic inversion techniques can be used along with 3D static geological modeling techniques to create robust models of geologic-based flow units across the AOI.

Other Considerations

In the case that an adequate SCAL was not available in the field or well files, the need to acquire critical data through additional testing should be evaluated at this time, assuming physical core is available or attainable through drilling of wells that have been planned. The list of types of SCAL mentioned in Step 2 provides a comprehensive list of tests that are customary for an enhanced oil recovery (EOR) evaluation. Requests for additional SCAL tests at this point should be prioritized based on which properties have uncertainty bands that would cause the highest levels of uncertainty in the product (e.g., flow unit definition, fracture characterization, calculation of

original oil in place [OOIP]). This should be weighed against prior knowledge of the reservoir or data on analogous fields that can be used to reduce uncertainty in the geologic model and/or simulation while considering the time required for testing and the impact on the overall project timeline.

Step 5: Historical Reservoir Production Performance

This step is the precursor to developing the geologic model and simulation area model. Part of the process of developing an understanding of the reservoir is a review of production histories and well performance. It is important to understand the recovery factor by well or for specific repeatable areas such as land sections. Production for each of these portions of the reservoir should be broken out into primary and secondary production to understand how successfully the various areas were waterflooded. This will indicate where oil may have been bypassed and where there may be opportunities to increase recovery through stimulations, waterflood realignment, or infill drilling. In addition, this will be helpful information with which to frame projections of tertiary recovery, as oil may be inaccessible to displacement mechanisms because of geologic barriers. In the case of Foreman Butte, this does not apply since there was never a rigorous waterflood deployed.

This analysis should be done concurrently with analysis of the character of the oil production curves to look for evidence of fractured well behavior. Narr and others (2006) created a comprehensive list of production-, drilling-, geological-, and geophysical-related indicators of fractures. Geologic indications of fractures in Foreman Butte include visible open fractures in cores, brittle rock in the reservoir, and indications of fracturing in analogous fields in the Madison. Production-related indicators include higher production capacity from drillstem test (DST) results than is evident from core measurements (i.e., DST system permeability vs. permeability measured in a core plug); high initial production rates followed by rapid declines; and a rapid, early rise in gas–oil ratio (GOR) followed by stabilization at a level greater than solution GOR. The apparent ability of horizontal wells to drain layers above and below the lateral, which appear to be isolated from the lateral by low-permeability streaks, suggests that these fractures crosscut these low-permeability layers. These general indicators should be complemented by a quantitative and more detailed analysis to characterize the fractures in terms of the relative contributions of the matrix and the fractures to reservoir porosity and permeability. Grouping of core permeability data by fractured and nonfractured samples, normalized for similar porosity, will allow a rough quantification of the relative contributions of fractures and matrix to total permeability. A useful tool for determining the relative influences of each property on total permeability is to compare permeability k (or flow capacity, or kh, in millidarcy-feet) calculated from DST or other pressure transient tests to the k or kh calculated from core data. However, no single well in Foreman Butte has both core and DST data. By considering the values of kh from core data and from DSTs in different wells, it was concluded that fracture permeability is higher and more impactful to overall field performance than matrix permeability.

Step 6: 3D Geologic Model Development

The development of a 3D geological model is a crucial step in understanding the carbonate reservoir. This model provides input for reservoir simulation and helps engineers and geologists

in visualization of overall reservoir architecture, allowing more effective reservoir management and assessment of development opportunities. Two major steps were involved in the geological model development in Petrel: petrophysical/stratigraphic analysis and 3D structural and property modeling.

Petrophysical and Stratigraphic Interpretation

This involves integration of stratigraphic well correlation and petrophysical interpretation and computing petrophysical properties (porosity, permeability, and water saturation). The petrophysical interpretation workflow included log harmonization, log interpretation and calculation, reservoir identification, and mineralogy determination. Log harmonization is the process where the logs are depth-matched to reference curves, the units of the curves and the sampling are checked, and any anomalies such as missing data or bad hole are investigated and if possible, the curve or perform environmental corrections are predicted, if necessary. A quality check and calibration using core data were performed, as seen in Figure B-14.

After the lithology analysis and petrophysical logs were calibrated with the core data, the water saturation was calculated, and a quality check was performed. In the case of Foreman Butte, there was a high degree of uncertainty in saturation calculations. This needed to be addressed here, as the initial water saturations calculated in the Ratcliffe were higher than the irreducible water saturation, which was verified by both relative permeability tests and the fact that all wells produced water upon initial completion (with the average water cut being 50%). To narrow that range of uncertainty, lab experiments to measure Archie exponents “m” and “n” were conducted, and the results were incorporated into the log analysis.

Stratigraphic Analysis

Subsequently, stratigraphic analysis was performed to identify different intervals and subintervals and create structural maps that will represent the 3D geocellular model. Seven formation tops (Ratcliffe, base of Last Charles Salt, Flat Lake, Alexander, Berentson, Midale, and Frobisher-Alida) were interpreted, as depicted in Figure B-15.

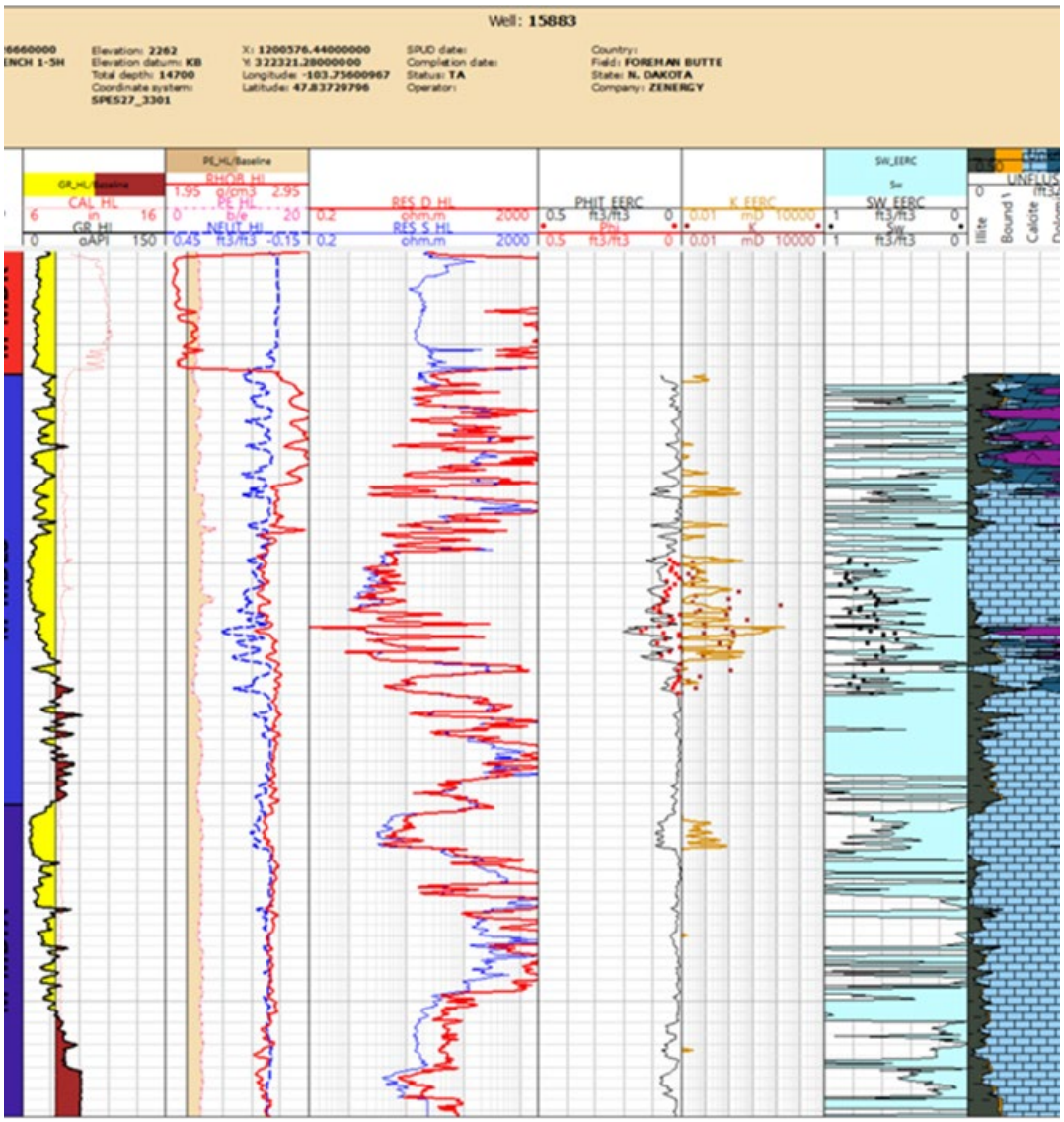

Figure B-14. Log display using Techlog®. Tracks from left to right include gamma ray and caliper, density, neutron and photoelectric, resistivities, porosity, permeability, calculated water saturation, and lithology.

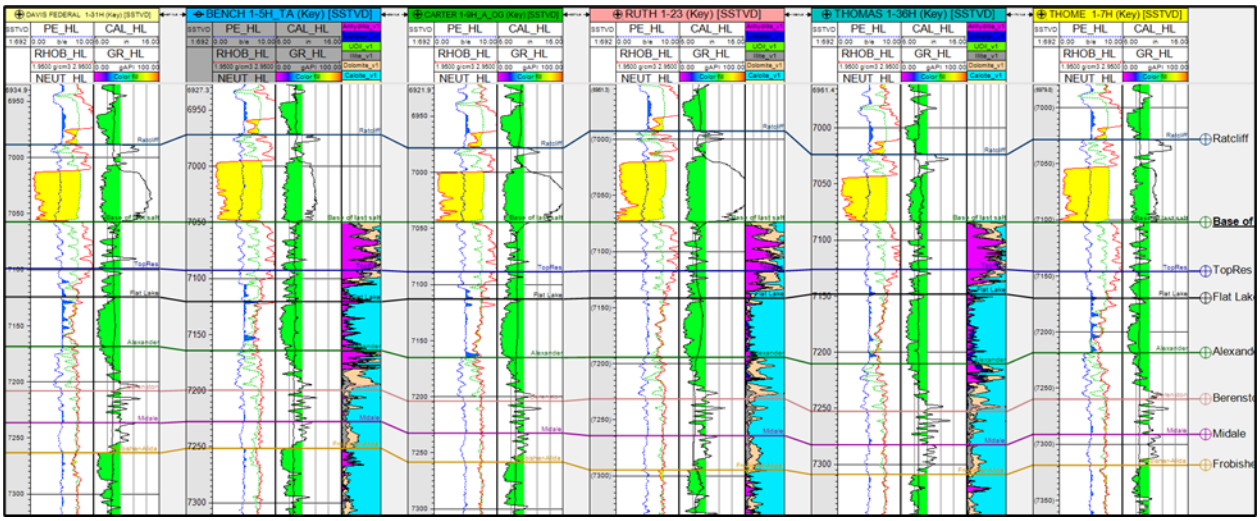

Figure B-15. Stratigraphic correlation displayed in Petrel. Tracks from left to right include density, neutron and photoelectric, gamma ray and caliper, and calculated mineralogy.

3D Structural and Property Modeling

The geological–petrophysical model was established by combining well data analyses and a conceptual geological model. After that, a 3D structural model was developed, followed by facies and property 3D modelling. Then the final model was exported for reservoir simulation using the industry-standard Computer Modelling Group (CMG) suite of software. The workflow for this step is depicted in Figure B-16 and is described in detail below.

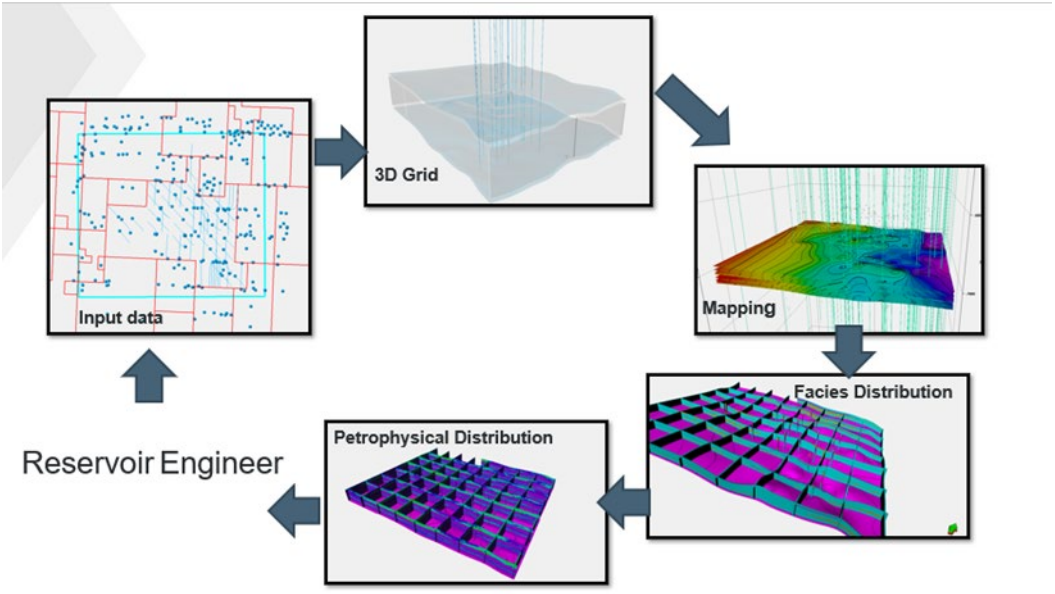

Figure B-16. 3D geological modeling workflow.

Structural Model

A 3D structural model was constructed using the identified formation top's well logs. Subsequently, the structural maps, as seen in Figure B-17, were generated from well log data that represent the control points at different horizons and faults. In this project, well control data were the primary focus. The workflow consisted of using thickness maps and structural surfaces as the main input for the geocellular model.

Property Model

The aim of this step was to evaluate the reservoir characteristics and create a facies and property model of the Ratcliff carbonate reservoir by using the available data and interpretations (petrophysical analysis and rock analysis).

The reservoir characterization of carbonate systems is much more difficult than for clastics because of the complexity of the pore network, facies characteristics, architecture, texture, and wider variety of mineral elements comprised in the matrix. Nevertheless, a realistic conceptual model can be created through a collaborative effort, such as the one described below.

1. Petrophysical analysis: The characterization of the petrophysical properties of carbonate is more challenging. Estimation of petrophysical parameters is challenging due to the porosity system that is more complex than a sandstone reservoir and scale variation (the pore size is highly variable, ranging from micropores to vugs).

2. Borehole images: The identification of fractures, lithology, and stratigraphy.

3. Core analysis: The description of this section and rocks analysis are fundamental in the lithofacies identification.

4. Lab measurement: The analysis of core samples is a major part of the carbonate study. The suggested core testing was previously presented in Section 3.4. Petrography description and mineralogy analysis described in that table give a better understanding of the sedimentology and depositional regime in which the reservoir was formed.

5. Outcrop studies: The integration of observations from analagous geological outcrops can be used to guide the facies characteristics of the 3D subsurface model (Zhanfeng, 2015; LaFontaine, 2021).

6. Seismic data: The use of seismic data, such as microseismic, 3D, or 2D datasets, is important for intepreting horizons, faults, and associated fracture systems, which are later integrated with well data. Seismic inversion data can also be used as conditioning for reservoir property modeling, and geophysical models can improve the reservoir characterization in terms of rock and fluid properties (Oumarou, 2021; Al Bin Hassan, 2003; Avseth, 2014).

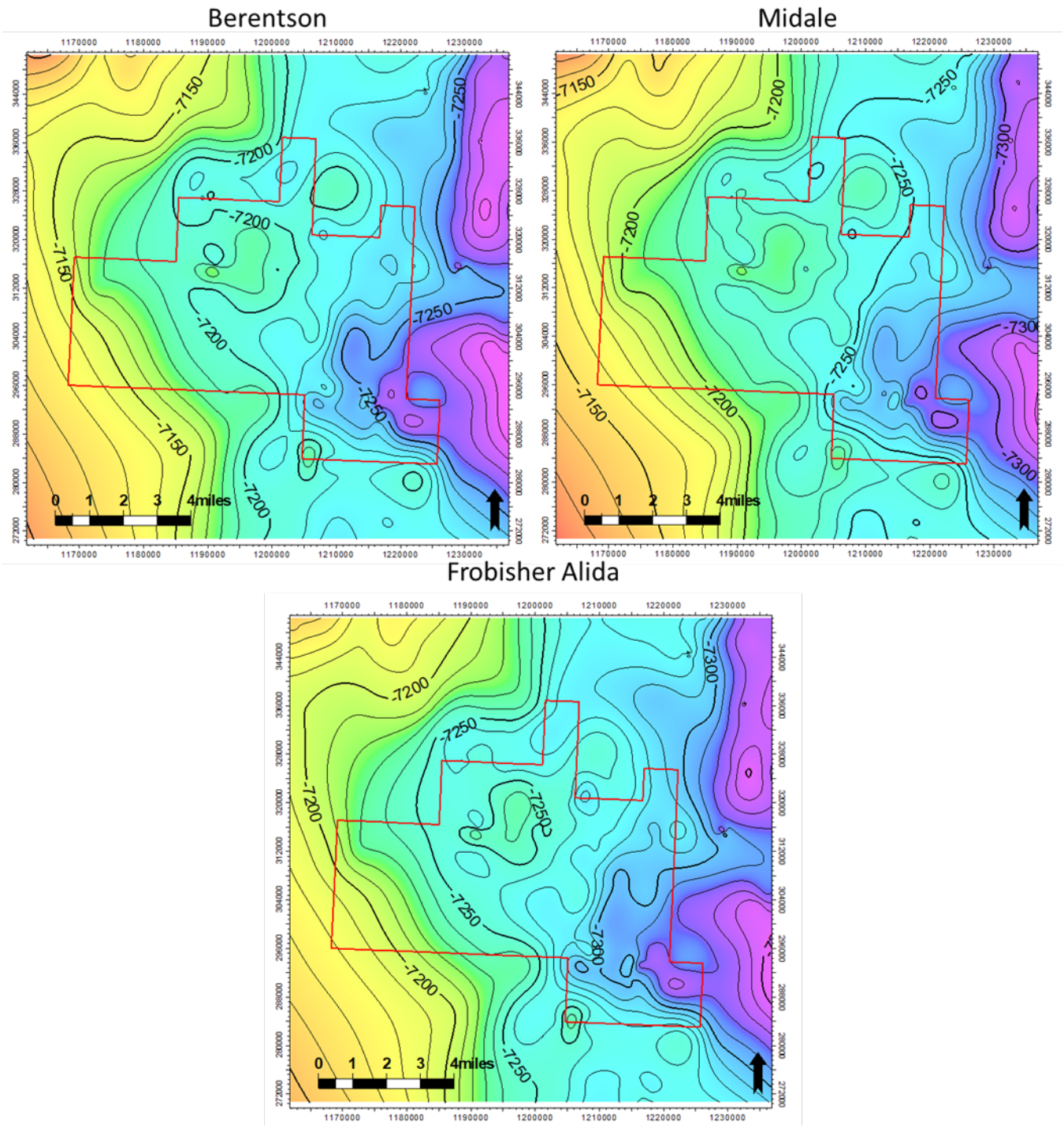

Figure B-17. Structural maps of members of the Ratcliffe reservoir (top of Frobisher-Alida marks the lower boundary of the Ratcliffe). Elevation is displayed in feet in subsea true vertical depth.

7. Log analysis and stratigraphic framework: Interpretation of a sequence stratigraphic framework can help to control the 3D reservoir property distribution (Harris and others, 1999; SEPM Strata, 2015).

8. Numerical model: The use of facies-calibrated geomodeling algorithms to populate the 3D model such as MPS (multiple point statistics) can improve the geomodel (Levy and others, 2006; Jung and others, 2012).

In the present work, the model was updated with rock types depending on the rock quality. The rock evaluation was based on a deterministic cutoff from several well logs, with combinations of values from the logs used to define a classification on mineral volume logs, as seen in Figure B-18.

The 41 wells with harmonized log suites were used to populate the 3D grid with petrophysical properties using the sequential indicator simulator algorithm. To preserve the log-based relationship, the porosity and permeability petrophysical properties in Figure B-19 were populated in the 3D model using rock typing as guidance (Figure B-20). These 41 wells are a subset of the wells that served as control points for structural mapping.

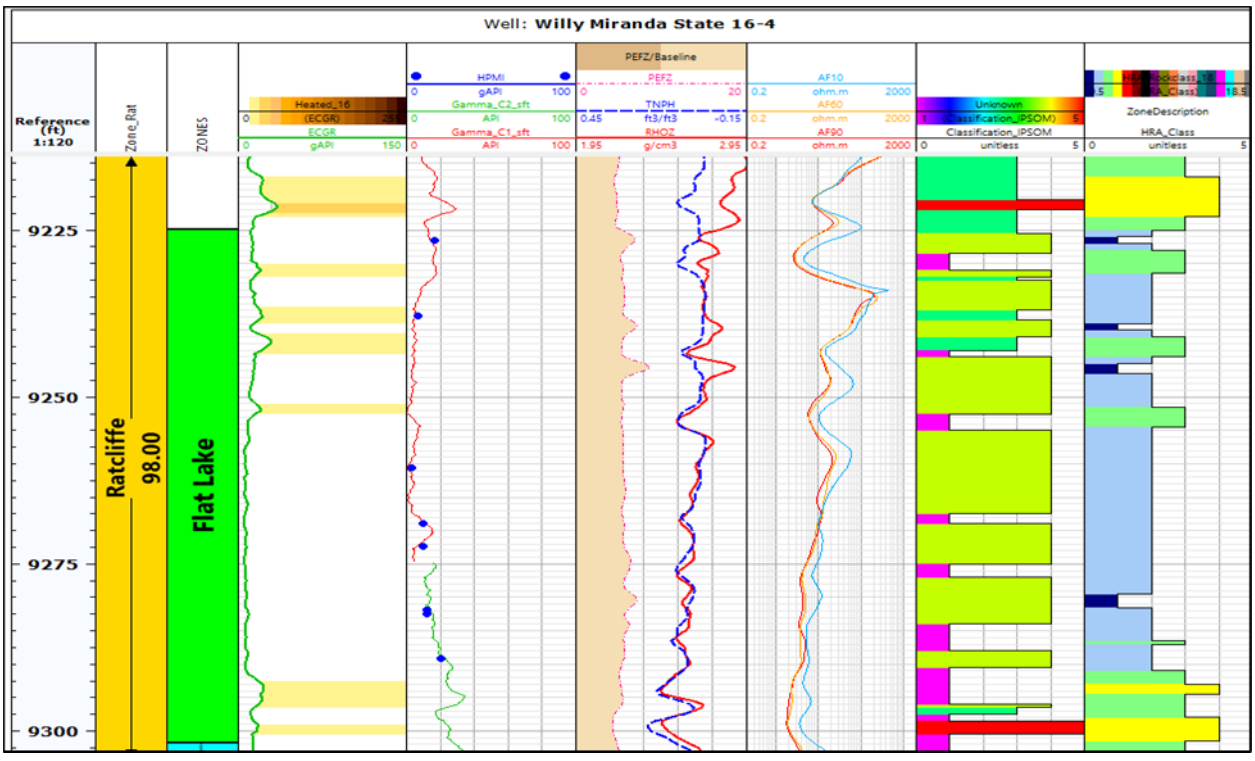

Figure B-18. Well log showing rock types based off deterministic cutoffs. Tracks from left to right: environmentally corrected gamma ray, gamma, and gamma from core, photoelectric, neutron, density, resistivity, classification, and rock type.

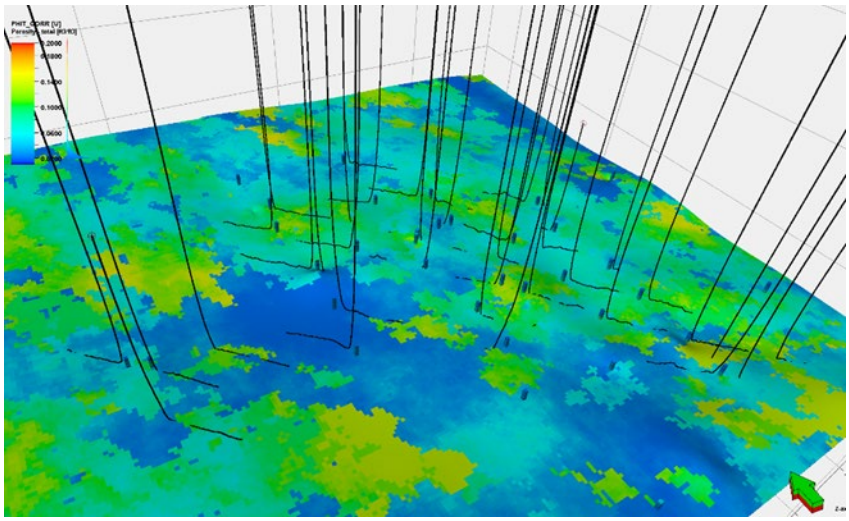

Figure B-19. 3D porosity map for the Ratcliffe Formation.

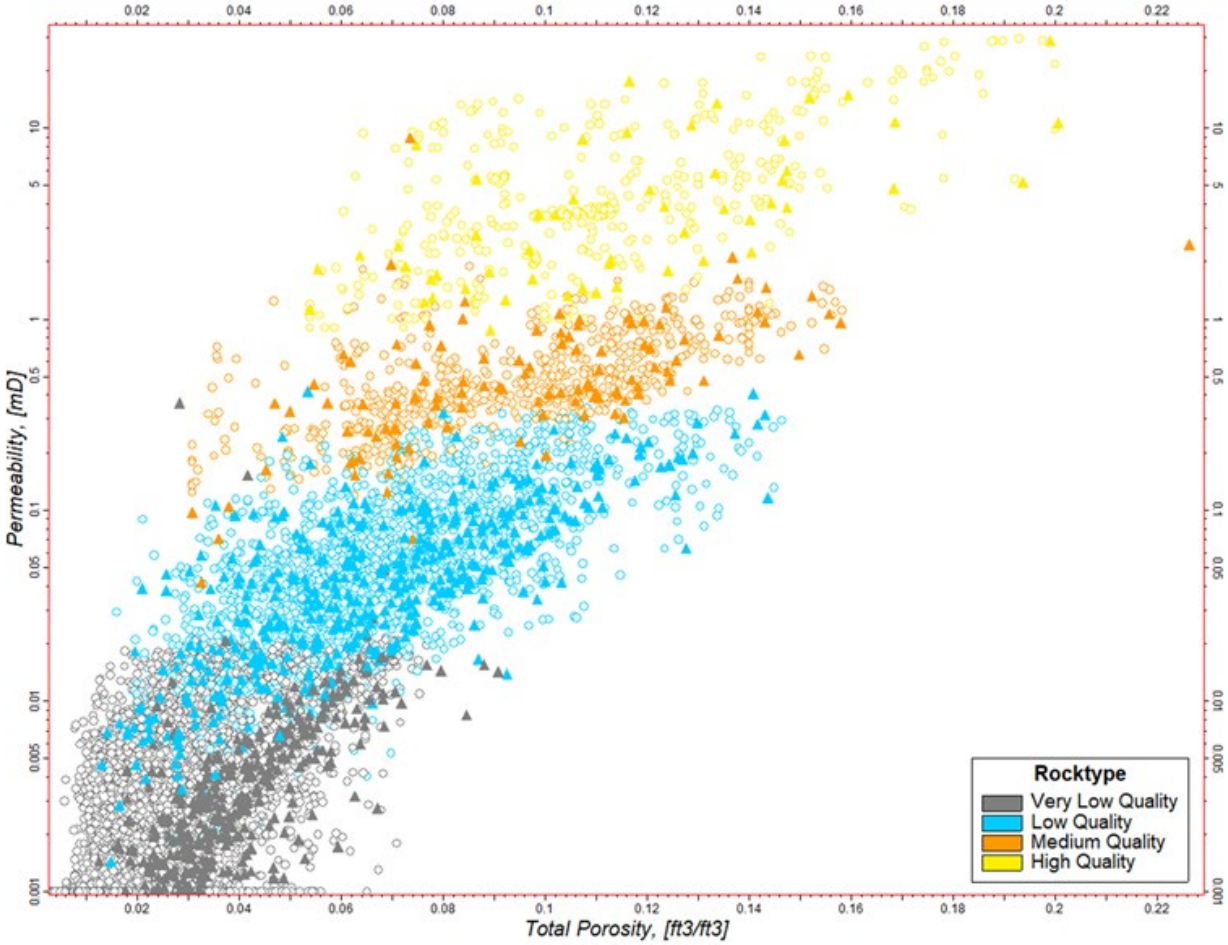

Figure B-20. Cross plot showing porosity vs. permeability for the Ratcliffe Formation, colored by rock type with the Y-axis in logarithmic. Upscaled well log point is displayed as filled triangles, with modeled cells displayed as circles.

Most of the ZOIs are characterized by low porosity in the 1%–4% range. However, better porosities exist in sweet spots, controlled by local facies. The geologic model not only provides three-dimensional distributions of reservoir properties for input into a simulation model, but it also provides engineers and geologists a tool to visualize reservoir architecture that can be used for various reservoir management tasks.

Once these steps are complete, everything is in place to create property maps. The most common series of maps to generate is a series including net pay (h), net porosity feet (φ-h), and net oil (φ-h-S_o). These maps were compared to identify inconsistencies or places where lack of data may affect accuracy. A review of all three maps, along with production data, improves reservoir understanding and is a key component of reviewing the field for additional workover or infill drilling opportunities. The φ-h-S_o map served as the starting point for calculating OOIP, and should the field ever undergo CO_2 flooding, the OOIP should be calculated for each injection well-centered pattern, as flood performance is a function of the reservoir volume of CO_2 injected relative to the OOIP in each pattern. Figure B-21 depicts maps of these three attributes for the Ratcliffe reservoir in Foreman Butte Field.

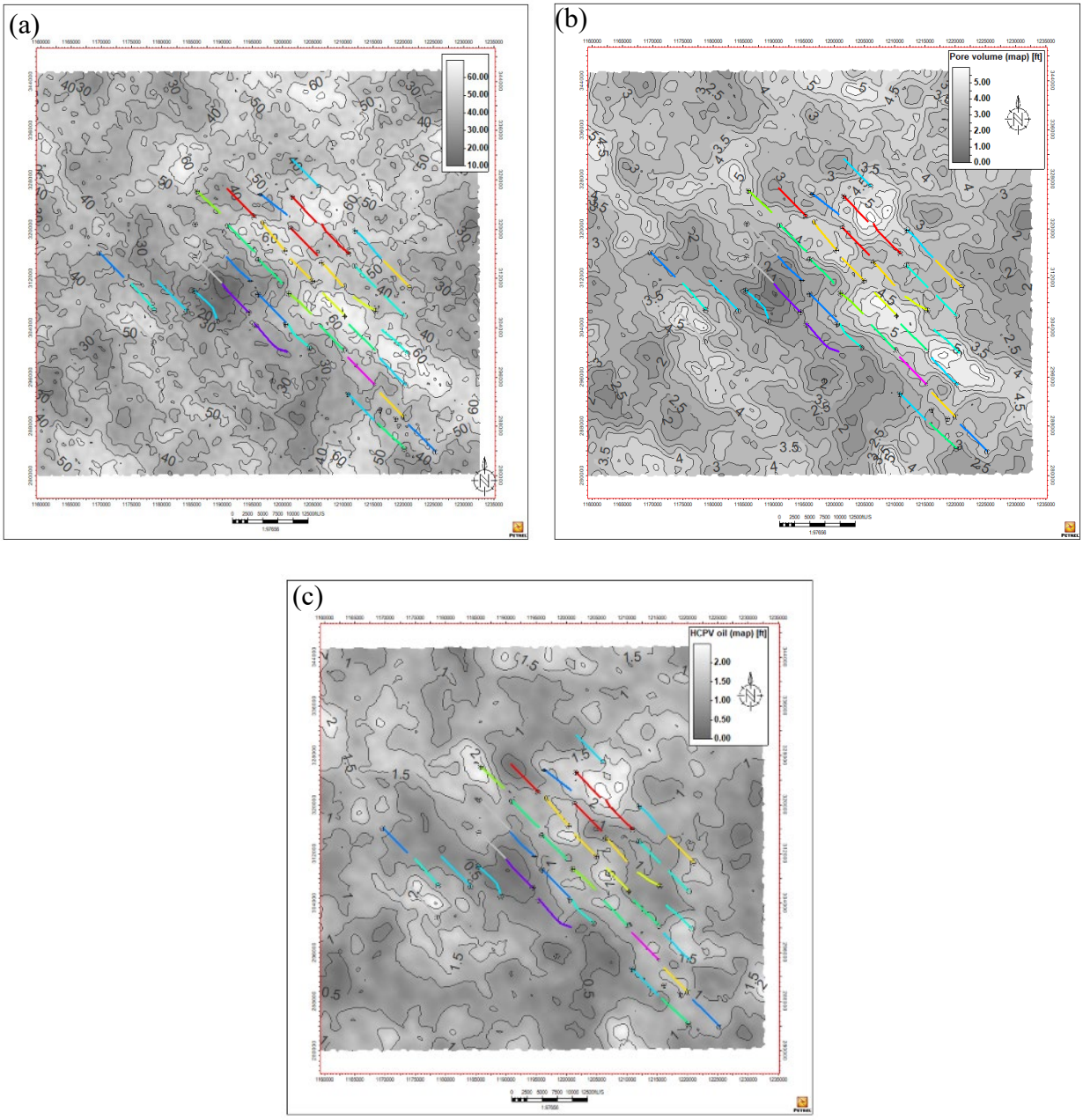

Figure B-21. Maps of (a) net pay, (b) net pore space thickness (φ*h), and (c) net hydrocarbon pore volume thickness (φ*h*S_o) for the Ratcliffe interval.

Step 7: Fracture Characterization and Modeling

The accurate characterization of natural fractures for a reservoir within an AOI ensures that the storage and flow of fluids within the reservoir are understood and can be captured for volumetric calculations and dynamic simulation. In this step, a general workflow for fracture characterization is presented, and later Foreman Butte Field fracture characterization results are discussed.

General Workflow

1. Conduct a regional assessment of the present and past tectonic regimes based on available literature, legacy studies, and previous work.

2. If possible, complete a 2D or 3D seismic interpretation, including structure and isopach mapping, curvature analysis, etc., and integrate data from well control.

3. Compare curvature analysis or related techniques with any potential fracture indications from DST and other pressure-transient data, core data (e.g., orientation, density, apertures), and production histories.

4. Interpret a 3D structural and fault framework, followed by development of a 3D kinematic solution, to aid an interpreter in validating a fault framework based on principles of structural geology. For reverse faulting, ensure interpretation software allows for Multi-Z solutions.

5. Develop a 1D geomechanical model to analyze rock deformation and behavior, based on Young's modulus and Poisson's ratio from the integration of wellbore acoustic data and static core lab data, resulting in a mechanical stratigraphy model. Determine zones that may be more prone to fracturing (stronger rocks) vs. zones that are weaker and less prone to fractures.

6. Use stress and strain values derived from the 3D kinematic modeling and/or 1D geomechanical modeling steps to develop proxies for fracture intensity and orientation to create a discrete fracture network (DFN) to estimate the major fracture systems for the ZOI. Calibrate results with direct borehole measurements, such as formation micro imager (FMI) image log interpretations or other underground measurements, to constrain the DFN characteristics (e.g., fracture apertures, orientations, and density). Develop a fracture network using software that allows the 3D characterization of fractures and fracture systems coupled with a range of realistic and data-constrained multiple scenarios for modeling.

7. In faulted fields where common oil–water contacts across fault blocks is suspected, consider conducting a fault juxtaposition analysis (Allan, 1989) to determine the likelihood of juxtaposition between the reservoir and across-fault permeable zones; use results to risk and rank the reservoir. Conversely, fault juxtaposition analysis can also be used to explain the occurrence of multiple oil–water contacts in fields with multiple fault blocks, where permeable zones are juxtaposed across the fault with an impermeable zone. Fault juxtaposition analysis is also referred to as Allan Mapping in the literature.

8. Conduct critical stress and risk analyses to determine if fracture/fault sets and orientations could be susceptible to failure conditions in response to elevated pore pressure associated with CO_2 injection, either storage or EOR (Fossum and others, in press). Software tools (e.g., Stanford University Fault Slip Potential [FSP] tool [Walsh and others, 2018], Rokdoc, Techlog, and MohrFrac) can be used in the analysis. The dominant SH_{max} direction is determined from available image log, microseismic, or geophysical data, or from the North America Stress map (Lund-Snee and Zoback, 2020). Faults that are oriented more favorably for slip in the stress field can be more permeable because of dilation (Barton and Zoback,

1995). The North America stress map, microseismic data, induced seismicity events, and regional structure can be used to calibrate the critical stress and risk analyses results.

9. To calibrate potential dual porosity–permeability systems from the matrix and fractures, the fracture characterization should be calibrated against petrophysical results, DST, and pressure-transient analysis.

10. Integrate the best technical-case-selected fracture model into the 3D static geological model for input into the dynamic simulation model. Consider the low- and high-case fracture models to drive the sensitivity analysis. The rule of thumb for porosity of a fracture system within a conventional reservoir generally ranges from 1% to 2%; given the low average matrix porosity of the Ratcliffe, oil storage within a fracture system could represent a significant portion of the stock tank original oil in place (STOOIP).

Foreman Butte Field Structural Setting and Fractures

Foreman Butte Field lies on the west flank of the Williston Basin within a broad eastward dipping homoclinal flexure. Production extends beyond the limits of this structure, suggesting that closure alone is not a prerequisite for production and hydrocarbons are stratigraphically trapped (Nordeng, 2007). The high-density well control of the field provides good control for mapping the structure. Without a 3D seismic survey in the field to confirm stratal relationships, well log stacking patterns are used to estimate the stratigraphy of the reservoir sequence and overlying sediments.

Begnaud and Claiborne (1983) observed that natural fractures played varying roles in oil production from reservoirs in the Mission Canyon and Ratcliffe units and that fracture properties might change with time as production went on. They reviewed the completions and production data of the wells in these geologic units and found that different methods were required to analyze the fractures depending on the rock properties and production history. They used seven field techniques, including zone testing, downhole pressure measurements, residual gel analysis, pump-in and swab tests, postfrac temperature logs, postfrac gamma ray logs, and a DST, and four stress measurements, including horizontal stress, vertical stress, in situ closure stress, and long-spaced sonic log stress, to analyze vertical fracture growth in the studied reservoirs. Based on the analysis of the data collected from the reservoirs, they proposed the following correlation (Equation B-1) to predict the fracture height during the production process:

$$P - P_o = \frac{K_{ic}}{\sqrt{\pi L}} \frac{1}{\sqrt{1+\varepsilon}} - 1 + \frac{2(\sigma_b - \sigma_a)}{\pi} cos^{-1}\left(\frac{1}{1+\varepsilon}\right) \quad \text{[Eq. B-1]}$$

Where P_o is the pressure as a fracture initially reaches the boundary, *psi*; P is the pressure above P_o, *psi*; L is half of the pay zone thickness, *ft*; ε is calculated as *(fracture half height/L-1)*, *ft*; K_{ic} is the critical stress intensity factor of the bounding layer; σ_b is the minimum horizontal stress in the pay zone, *psi*; and σ_a is the minimum horizontal stress in the boundary, *psi*.

Since the stresses changed with pore pressure (or reservoir pressure) in the production and injection process, the fracture height was not constant throughout the life cycle of a field. The production and injection history should be considered when estimating the fracture properties.

Begnaud and Claiborne (1983) estimated that the natural fracture height could vary between 0 and 100 feet in the studied reservoirs depending on the pressure conditions. Therefore, this factor needs to be specifically considered in the fracture simulation process when studying reservoirs in the Ratcliffe interval.

References

Advanced Resources International, 2006, Technical oil recovery potential from residual oil zones—Williston Basin: Report for the U.S. Department of Energy, Office of Fossil Energy, February. https://www.adv-res.com/pdf/ROZ_Williston_Document.pdf.

Al Bin Hassan, M., Marfurt, K., 2003, Fault detection using Hough transforms, 73rd Annual International Meeting: Society of Exploration Geophysicists Expanded Abstracts, p. 1719–1721. https://doi.org/10.1190/1.1817639.

Allan, U.S., 1989, Model for hydrocarbon migration and entrapment within faulted structures. AAPG Bulletin, v. 73, p. 803–811.

Amaefule, J.O., Altunbay, M., Tiab, D., Kersey, D.G., and Keelan, D.A., 1993, Enhanced reservoir description—using core and log data to identify hydraulic flow units and predict permeability in uncored intervals/wells: Paper presented at the SPE Annual Technical Conference and Exhibition, Houston, Texas, October 1993. https://doi.org/10.2118/26436-MS.

American Petroleum Institute, 1998, Recommended practices for core analysis, recommended practice 40 (2d ed.): February 1999. https://energistics.org/sites/default/files/2022-10/rp40.pdf.

Avseth, P., Veggeland, T., and Horn, F., 2014, Seismic screening for hydrocarbon prospects using rock physics attributes: The Leading Edge, p. 266–274

Barton, C.A., Zoback, M.D., and Moos, D., 1995, Fluid flow along potentially active faults in crystalline rock: Geology, v. 23, no. 8, p. 683–686. https://doi.org/10.1130/0091-7613(1995)023%3C0683:FFAPAF%3E2.3.CO;2.

Begnaud, W.J., and Claiborne, E.B., 1985, Vertical fracture growth considerations in the Mission Canyon/Ratcliffe Formations of the North Alexander Area: Paper presented at the SPE Annual Technical Conference and Exhibition, Las Vegas, Nevada, September 1985. https://doi.org/10.2118/14375-MS.

Burke, R.B., 2005, Evolving Mississippian Ratcliffe and Mission Canyon plays in North Dakota, Geologic Investigations No. 7, North Dakota Geological Survey. https://www.dmr.nd.gov/ndgs/Publication_List/pdf/geoinv/GI_7.pdf.

Dunham, R.J., 1962, Classification of carbonate rocks according to depositional texture, *in* Ham, W. E., ed., Classification of carbonate rocks: American Association of Petroleum, Geologists Memoir, p. 108–121.

Folk, R.L., 1959, Practical petrographic classification of limestones: American Association of Petroleum Geologists Bulletin, v. 43, p. 1–38.

Fossum, B.J., Jo, T.H., and Peck, W.H., 2023, Regional subsurface assessment for CO_2 storage in candidate basal reservoirs in the PCOR region: Report for the U.S. Department of Energy, Subtask 2.1, Part D11, 90 p. [in press].

Harris, P., and Simo, J., 1999, Advances in carbonate sequence stratigraphy—applications to reservoirs, outcrops and models: Society of Exploration Petrologists and Mineralogists Special Publication, v. 63.

Jung, A., Aigner, T., Palermo, D., Nardon, S., and Pontiggia, M., 2012, A new workflow for carbonate reservoir modeling based on MPS—shoal bodies in outcrop analogues (Triassic, SW Germany): Advances in Carbonate Exploration and Reservoir Analysis v. 370.

LaFontaine, N., Le, T., Hoffman, T., and Hoffman, M., 2021, Integrated outcrop and subsurface geomodelling of the Turonian Wall Creek Member of the Frontier Formation, Powder River Basin, Wyoming USA: Marine and Petroleum Geology, v. 125, no. 3, p. 104795.

Levy, M., Harris, P., and Strebelle, S., 2006, Carbonate reservoir modeling using multiple-point statistics (MPS)/facies distribution modeling(FDM): Adapted from poster presentation at American Association of Petroleum Geologists Annual Convention, Houston, Texas, April 9–12.

Loucks, R.G., Kerans, C., and Janson, X., 2003, Introduction to carbonate environments, facies and facies tracts: Bureau of Economic Geology Online Learning Modules, American Geological Institute and American Association of Petroleum Geologists, https://www.beg.utexas.edu/lmod/_IOL-CM01/cm01-step03.htm (accessed August 2023).

Lucia, F.J., 1995, Rock-fabric petrophysical classification of carbonate pore space for reservoir characterization: American Association of Petroleum Geologists Bulletin, v. 79, p. 1275–1300.

Lund Snee, J.E., and M.D., Zoback, 2020, Multiscale variations of the crustal stress field throughout North America: Nature Communications, v. 11, p. 1951. https://doi:10.1038/s41467-020-15841-5.

Moore, C.H., 2001, Carbonate reservoirs—porosity evolution and diagenesis in a sequence stratigraphic framework: Developments in Sedimentology, Elsevier, v. 55, 444 p.

Narr, W., Schechter, D.S., and Thompson, L.B., 2006, Naturally fractured reservoir characterization, Richardson, TX, Society of Petroleum Engineers, 112 p.

Nordeng, S.H., 2007, Stratigraphic and structural framework of the recent Ratcliffe (Mississippian, Charles Formation) production in western North Dakota: North Dakota Geological Survey Geologic Investigations, no. 41. https://www.dmr.nd.gov/ndgs/documents/Publication_List/pdf/geoinv/GI_41.pdf.

Oumarou, S., Mabrouk, D., Tabod, C., Marcel, J., Ngos III, S., Essi., A., and Kamguia, J., 2021, Seismic attributes in stress characterization—an overview: Arabian Journal of Geosciences, v. 14.

SEPM Strata, 2015, Carbonate Sequence Stratigraphy, February 2, p. 131.

Sheldon, R.P., and Devereux, C.M., 1979, Paleotectonic investigations of the Mississippian System in the United States, Part 1—introduction and regional analysis of the Mississippian System, Williston Basin region: U.S. Department of the Interior Geological Survey Professional Paper 1010.

Walsh, F.R., Zoback, M.D., Lele, S.P., Pais, D., Weingarten, M., and Tyrell, T., 2018, FSP 2.0—a program for probabilistic estimation of fault slip potential resulting from fluid injection: User Guide from the Stanford Center for Induced and Triggered Seismicity. SCITS.Stanford.edu/software.

Zhanfeng, Q., Anjiang, S., Jianfeng, Z., Shaoying, C., and Yana, C. 2015, Three-dimensional carbonate reservoir geomodeling: Petroleum Exploration and Development, v. 42, no 3.

APPENDIX C

PREDICTIVE SIMULATION SCENARIOS FOR FOREMAN BUTTE FIELD

PREDICTIVE SIMULATION SCENARIOS FOR FOREMAN BUTTE FIELD

Water Injection Scenario 1 – Skin Factor Effect on Offset Well Production

The production wells had apparent skin damage near the wellbore after years of production because of scale decomposition, salt precipitation, etc., leading to minimal oil production in many wells. The reservoir model took skin damage into account by assigning different skin factor values to each well to achieve a satisfactory history matching result. The estimated skin factor values for Wells 9 and 10 were +3 and +10, respectively, at the end of the production history.

Five predictive cases were designed to assess the skin effects on the liquid, oil, and water production in Wells 9 and 10. Simulated water was injected using tracer function through Well 5 with a constant injection rate of 500 bpd for 10 years. The injection and production constraints of Wells 5, 9, and 10 are summarized in Table C-1.

Table C-1. Constraints Setup of the Injection and Production Wells for Scenario 1

	Well 5	Well 9			Well 10		
Case No.	Injection Rate, bpd	Skin	Max. Production Rate, bpd	Min. Pressure, psi	Skin	Max. Production Rate, bpd	Min. Pressure, psi
1		3			10		
2		1.5			5		
3	500	0	700	500	0	700	500
4		−1			−1		
5		−2			−2		

Case 1 was the baseline case that Wells 9 and 10 had skin factors of 3 and 10, respectively. Simulation results showed that 1957 and 4105 bbl of oil could be produced from Wells 9 and 10, respectively, in 10 years. In the meantime, the water production could reach 573,043 and 399,525 bbl in Wells 9 and 10, respectively, as shown in Figure C-1.

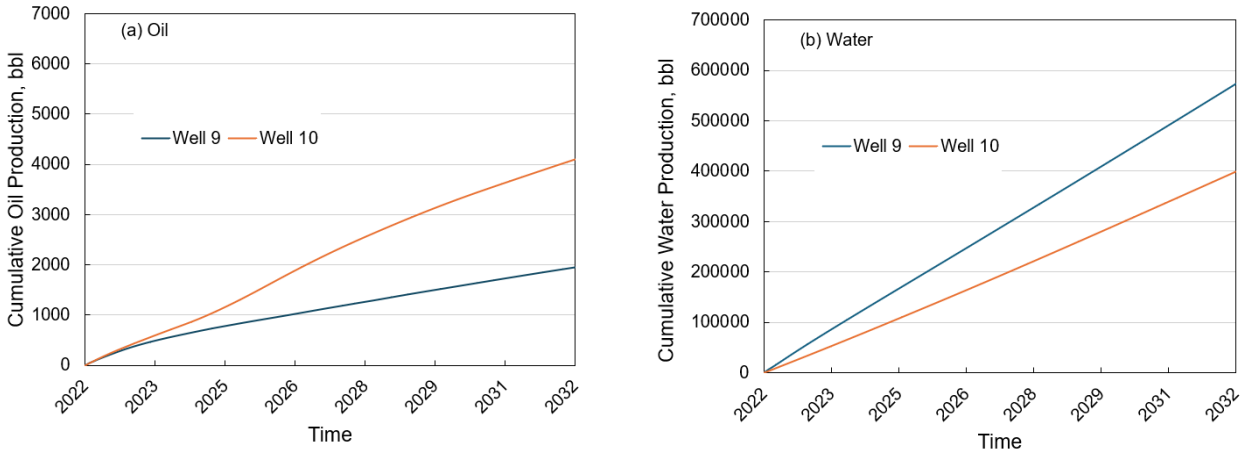

Figure C-1. Simulation results of Case 1: (a) cumulative oil production and (b) cumulative water production during 10-year predictive period.

Cases 2–5 applied smaller skin factors, as shown in Table C-1, to analyze the effect of reduced skin factors on oil and water production. The results showed that reducing skin factors contributed to a greater liquid production for both Wells 9 and 10 during the predictive period. Reducing skin to -2 yielded incremental liquid production of 89,936 bbl and 234,217 bbl for Wells 9 and 10, respectively, as shown in Figure C-2a. An increase in oil production of up to 5995 bbl was observed in Well 10, whereas a decrease in oil production was observed in Well 9. Despite an increase in oil production with reducing skin was observed in Well 10, Wells 9 and 10 show significant increase in water production of up to 90,180 bbl and 228,221 bbl with reducing skin factors, as shown in Figure C-2c. The water cut reached approximately 99.7% and 99.0% for Wells 9 and 10, respectively, after 10 years of water injection treatment regardless of changing skin factor values. The modeling results indicated that removing skin damage could allow more liquid to be produced from the reservoir. However, removing skin may not relieve the issue of high water cut and may not necessarily contribute to meaningful incremental oil production in all the production wells. The decrease of oil production in Well 9 with reducing skin was influenced by the production in Well 10.

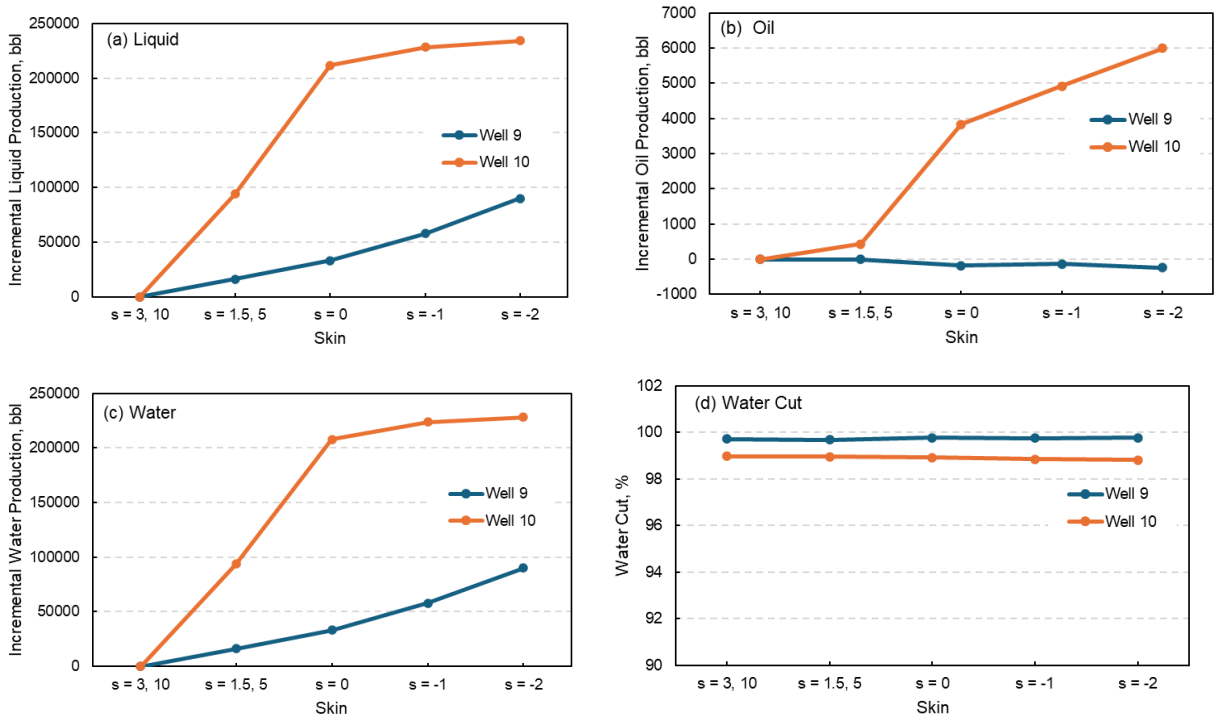

Figure C-2. Effects of reduced skin factor on Wells 9 and 10 during the predictive period: (a) cumulative liquid production, (b) cumulative oil production, (c) cumulative water production, and (d) water cut.

Water Injection Scenario 2 – Water Injection Rate Effect on Offset Well Production

To investigate the effect of water injection rate on production of offset wells, five additional cases with different water injection rates were designed to be compared with Case 1. The injected water was marked with a tracer to track the dynamic distribution of injection water. The injection and production constraints setup for Wells 5, 9, and 10 are summarized in Table C-2.

Table C-2. Constraints Setup of the Injection and Production Wells for Scenario 2

	Well 5	Well 9			Well 10		
Case No.	Injection Rate, bpd	Skin	Max. Production Rate, bpd	Min. Pressure, psi	Skin	Max. Production Rate, bpd	Min. Pressure, psi
1	500	3	700	500	10	700	500
6	0						
7	800						
8	1000						
9	1230						
10	1500						

The results suggest that increasing water injection rate contributed to higher liquid, oil, and water production in both Wells 9 and 10, as shown in Figure C-3 also shows that increasing the water injection rate generally resulted in a greater increase in liquid, water, and oil production for Well 9 than for Well 10. One possible explanation is that more injected water flowed to Well 9 than to Well 10 as the injection rate increased, sweeping more liquids (oil and water) from the reservoir to Well 9.

With a water injection rate of 1500 bpd, cumulative oil production increased 5908 and 4770 bpd for Wells 9 and 10 respectively, compared to Case 6 (no water injection case) after 10 years of simulation. Compared to the insignificant increase in oil production, the increase in water production was as high as 1488,111 bbl and 628,867 bbl, respectively, for Wells 9 and 10. The water cut maintained above 99.6% and 99.2%, respectively, for Wells 9 and 10 after 10 years of water injection and production for all the cases with water injection rates of no less than 500 bpd, as shown in Figure C-4d. The results suggest that although incremental oil production could be achieved by increasing the water injection rate, that is at the cost of maintaining a high water cut and producing a significant amount of water.

As shown in Figure C-5, with an increasing injection rate from 500 to 1500 bpd, the tracer concentration increases for both paths to Well 9 and Well 10, leading to higher oil and water production in both wells. For all cases, tracer concentration is higher for the path to Well 9 than that to Well 10. The results confirmed that more injected water flowed from Well 5 to Well 9 than to Well 10 as injection rate increased.

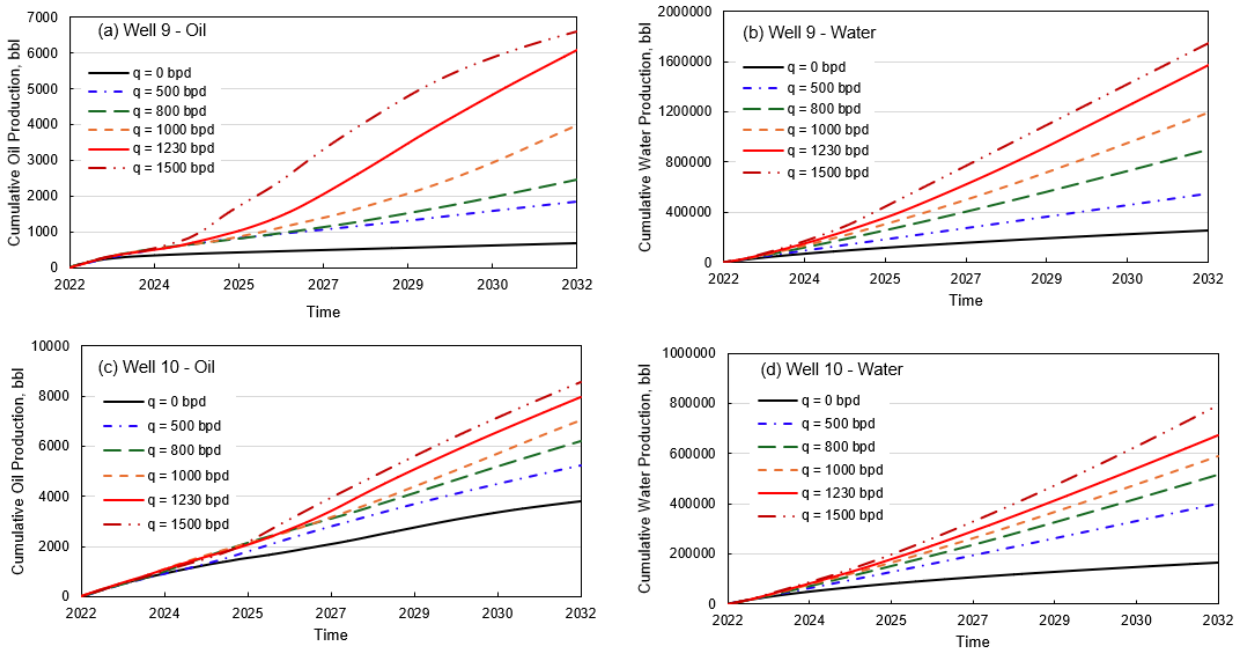

Figure C-3. Cumulative oil production of (a) Well 9 and (c) Well 10 and additional cumulative water production of (b) Well 9 and (d) Well 10 during 10 years of prediction for Case 1 and Cases 6–10 of Scenario 2. Cumulative production excludes the cumulative production by the end of the production history and counts the total production during the prediction period.

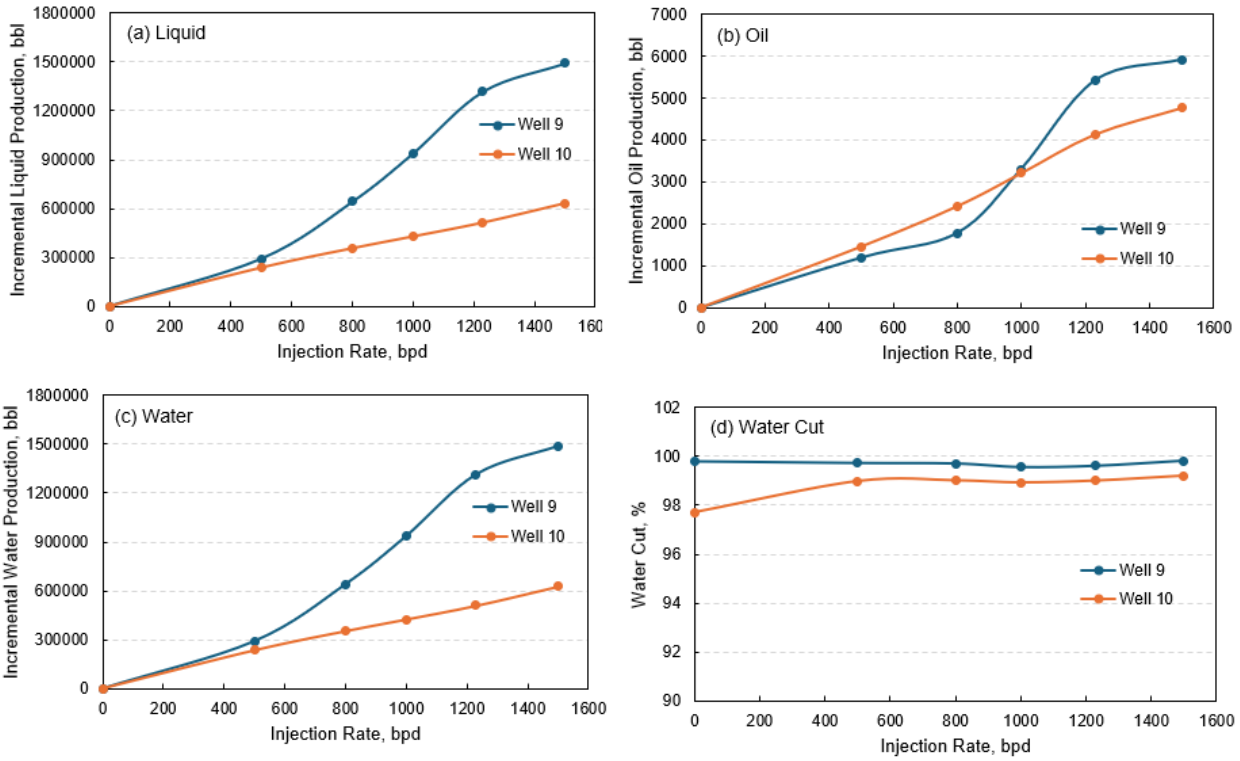

Figure C-4. (a) Incremental liquid production, (b) incremental oil production, (c) incremental water production, and (d) water cut of production for Wells 9 and 10 after 10 years of prediction for Case 1 and Cases 6–10 of Scenario 2. The incremental production represents the cumulative production of each case at the end of prediction subtracted by that of Case 6 (no water injection).

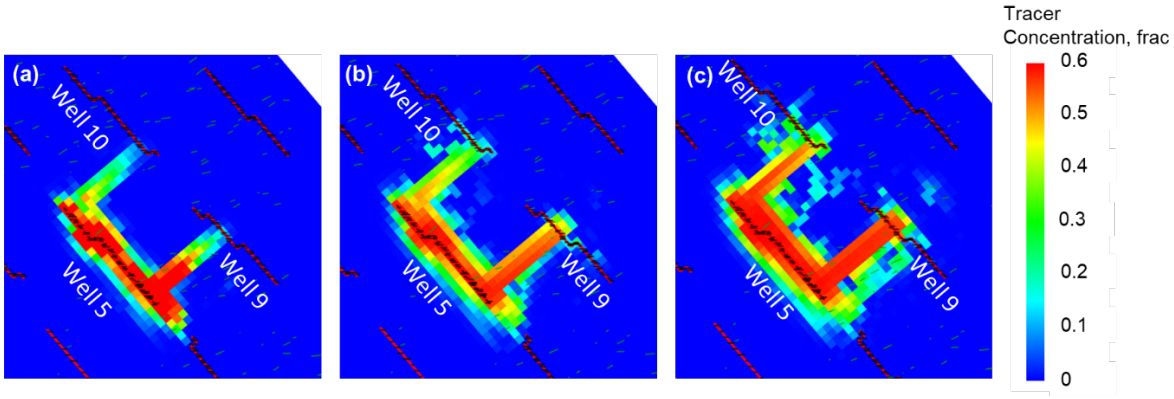

Figure C-5. Distribution of tracer concentration after 10 years of water injection treatment for water injection rate of (a) 500 bpd, (b) 1000 bpd, and (c) 1500 bpd.

Water Injection Scenario 3 – Minimum Bottomhole Pressure (BHP) Effect on Offset Wells Production

During the treatment of water injection, the production performance of Wells 9 and 10 was also affected by their operational status. Three additional prediction models were built with different minimum BHP in Wells 9 and 10. The injection and production constraints setup of Wells 5, 9, and 10 for Scenario 3 are summarized in Table C-3.

Table C-3. Constraints Setup of the Injection and Production Wells for Scenario 3

	Well 5	Well 9			Well 10		
Case No.	Injection Rate, bpd	Skin	Max. Production Rate, bpd	Min. Pressure, psi	Skin	Max. Production Rate, bpd	Min. Pressure, psi
1	500	3	700	500	10	700	500
11				1000			1000
12				1500			1500
13				2000			2000

The simulation results of Cases 11, 12, and 13 were compared with that of Case 1. As shown in Figure C-6, reducing minimum BHP resulted in an increase in liquid, oil, and water production. When minimum BHP reduced from 2000 psi to 500 psi, the incremental oil production in Wells 9 and 10 was up to 1042 and 2174 bbl, respectively, while the incremental water production was up to 255,715 and 159,265 bbl, respectively, as shown in Figure C-7. The final water cut after 10 years of injection and production was not significantly different with reducing minimum BHP. The results implied that the production wells could maintain a low BHP to ensure more oil production.

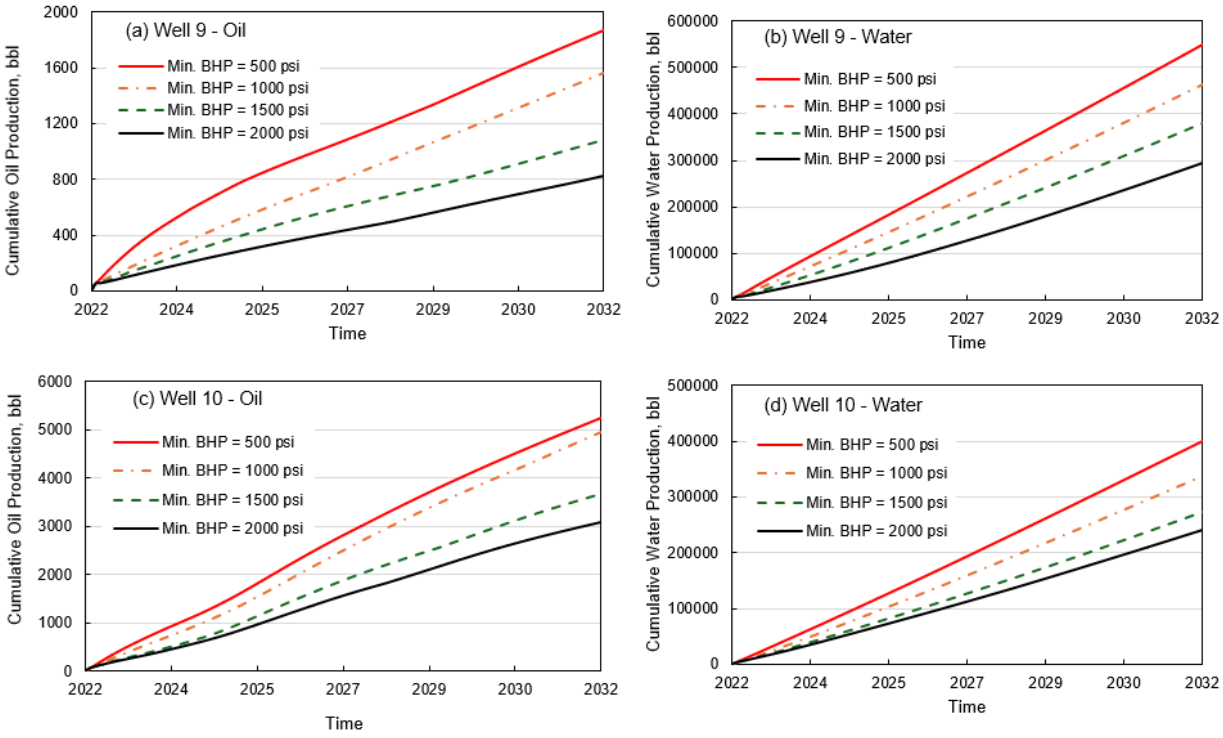

Figure C-6. Cumulative oil production of (a) Well 9 and (c) Well 10 and additional cumulative water production of (b) Well 9 and (d) Well 10 during 10 years of prediction for Case 1 and Cases 11–13 of Scenario 3. Cumulative production excludes the cumulative production by the end of the production history and counts the total production during the prediction period.

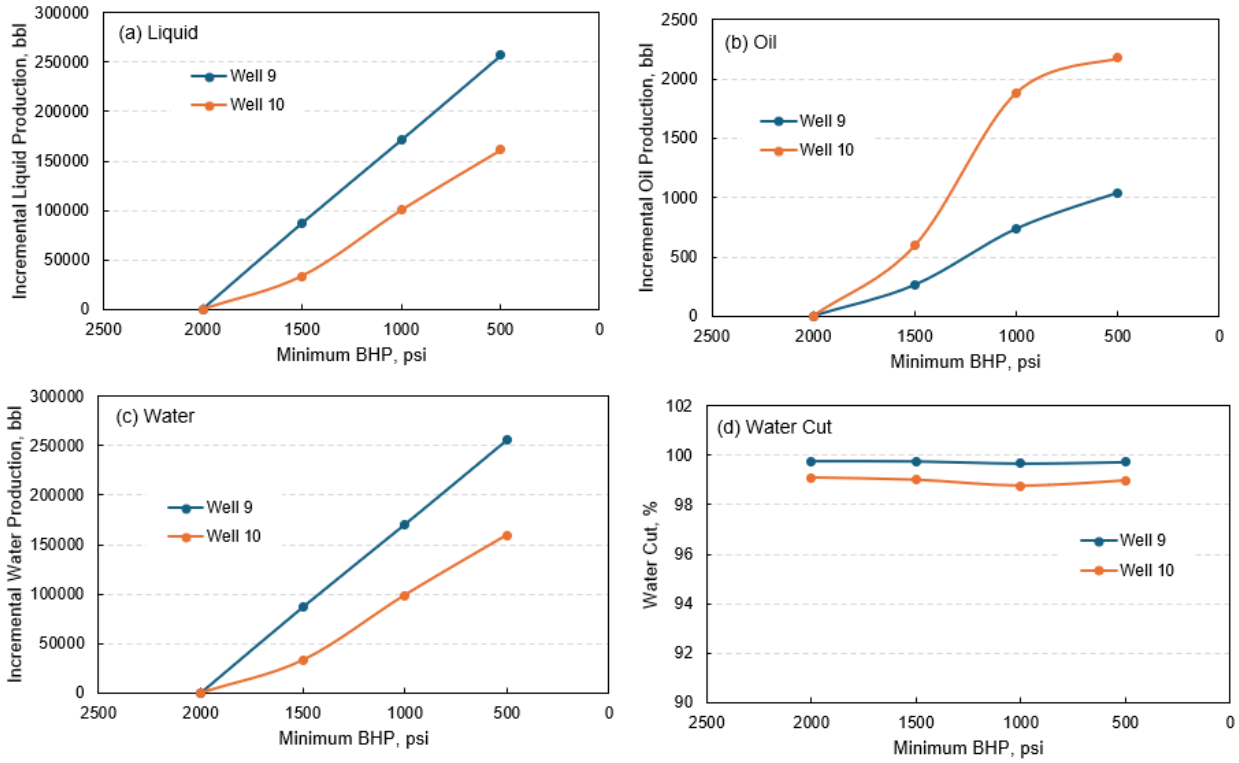

Figure C-7. (a) Incremental liquid production, (b) incremental oil production, (c) incremental water production, and (d) water cut of production for Wells 9 and 10 after 10 years of prediction for Case 1, 11, 12, and 13 of Scenario 3. The incremental production represents the cumulative production of each case at the end of prediction subtracted by that of Case 13 (minimum BHP of 2000 psi).

Changing minimum BHP has a critical impact on gas production. As illustrated in Figure C-8, both Wells 9 and 10 show exponential increase in incremental gas production and production GOR. This is because producing with lower minimum BHP constraint results in greater reservoir pressure reduction. As reservoir pressure falls below the bubble-point pressure, more gas is liberated from oil.

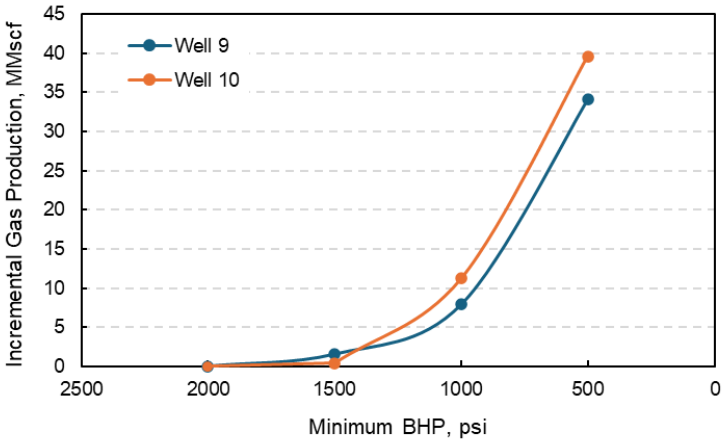

Figure C-8. Incremental gas production of production Wells 9 and 10 after 10 years of prediction for Case 1, 11, 12, and 13 of Scenario 3. The incremental gas production represents the cumulative gas production of each case at the end of prediction subtracted by that of Case 13 (minimum BHP of 2000 psi).

Simulations of different strategies to optimize water injection treatment suggested that reducing skin, increasing water injection rate, and reducing well BHP are approaches to ensure incremental oil production in the production wells. However, the increase in oil production was not significant and at the expense of increasing water production. These results imply that the operators need to improve the ability of the equipment to process large amounts of water to achieve incremental oil production during water injection treatments. Alternative strategies should be analyzed and applied to achieve greater increase in oil production and minimize water cut in offset production wells.

CO_2 Enhanced Oil Recovery (EOR) Performance

Compared to water, CO_2 has more advantages as an injectant in enhancing oil recovery, including higher solubility in oil, lower interfacial tension, and higher mobility than water. In addition, CO_2 can dissolve in oil, reduce oil viscosity, and swell the oil, thus contributing to more oil production in the production wells (Dellinger and others, 1984; Grigg and Schechter, 1997; Davarpanah and others, 2019).

Five cases were designed and compared with Case 6 (no injection case) to investigate the effect of increasing the CO_2 injection rate on the improvement of oil production. Well 5 was converted into a gas injection well to inject CO_2 for 10 years. Wells 9 and 10 were produced and monitored. The injection and production well constraints setup is summarized in Table C-4.

As shown in Figure C-9, increasing the CO_2 injection rate contributed to greater increase in liquid, oil, and water production. Compared to the no-injection model, increasing the CO_2 injection rate from 0 to 5 MMscf/d resulted in 248,032 bbl and 56,782 bbl of incremental oil production from Well 9 and Well 10, respectively. Increasing the CO_2 injection rate also resulted in reduction in water cut from the production wells. With a CO_2 injection rate of 5 MMscf/d, the reduction of

water cut was 28% and 21%, respectively, for Wells 9 and 10 compared to the no-injection model. Compared to all the water injection optimization strategies, the performance of CO_2 flooding is better from the improving oil production perspective: higher incremental oil production and significant reduction in water cut can be achieved for Wells 9 and 10 by applying CO_2 EOR. Comparison of the CO_2 EOR performance between Wells 9 and 10 suggests that Well 9 could achieve higher incremental oil production and greater reduction in water cut than Well 10, as shown in Figure C-10 (b) and (d).

Table C-4. Constraints Setup of the Injection and Production Wells for the CO_2 EOR Scenario

	Well 5	Well 9			Well 10		
Case No.	Injection Rate, MMscf/d	Skin	Max. Production Rate, bpd	Min. Pressure, psi	Skin	Max. Production Rate, bpd	Min. Pressure, psi
6	0	3	700	500	10	700	500
14	1						
15	2						
16	3						
17	4						
18	5						

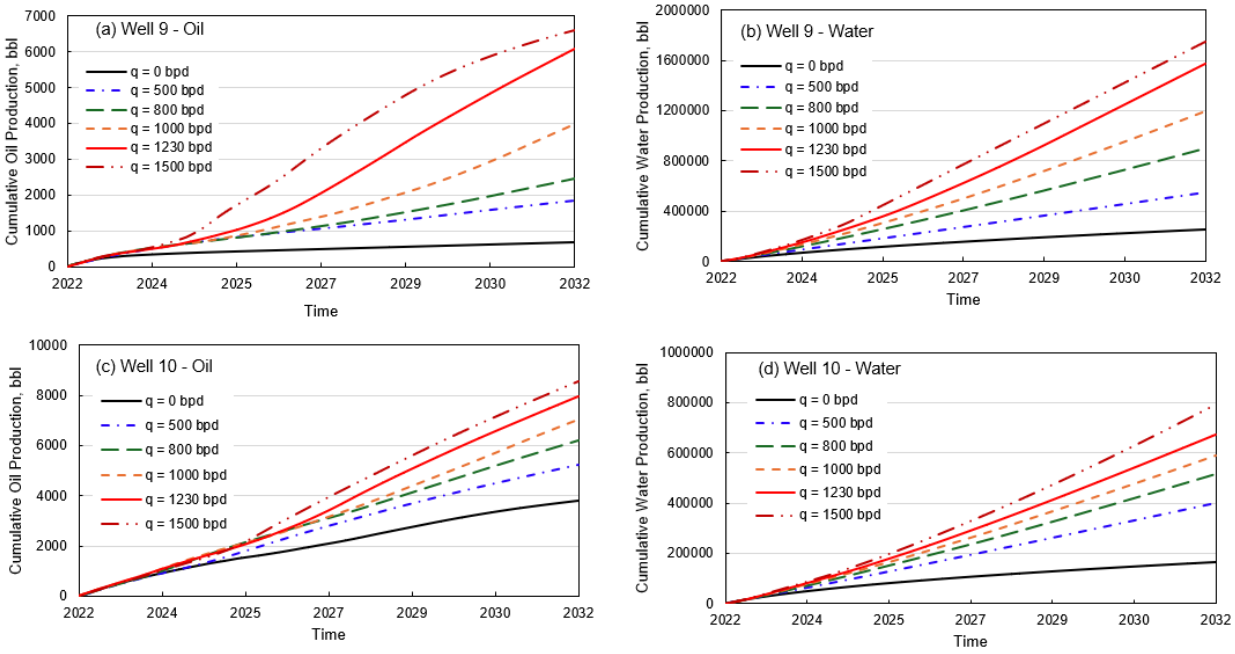

Figure C-9. Cumulative oil production of (a) Well 9 and (c) Well 10 and cumulative water production of (b) Well 9 and (d) Well 10 during 10 years of prediction for Case 6 and Cases 14–18 of the CO_2 EOR scenario.

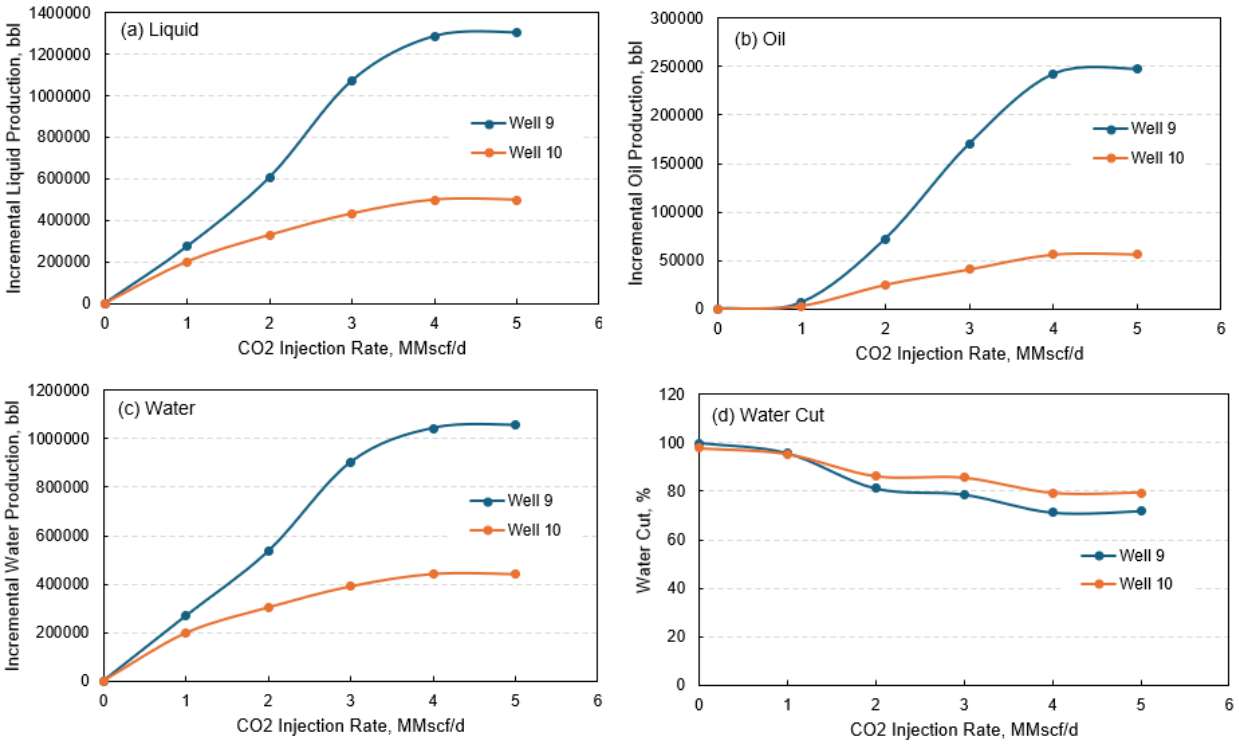

Figure C-10. (a) Incremental liquid production, (b) incremental oil production, (c) incremental water production, and (d) water cut of production for Wells 9 and 10 after 10 years of prediction for Case 6 and Cases 14–18 of the CO_2 EOR scenario. The incremental production represents the cumulative production of each case at the end of prediction subtracted by that of Case 6 (no water injection).

The movement and behavior of the injected CO_2 under different CO_2 injection rates is visualized in Figures C-11–C-14. The results show that with a higher CO_2 injection rate, the injected CO_2 flooded a larger area, as shown in Figure C-11. Comparison between Figure C-11 and Figure C-12 shows that a portion of the CO_2 flooded area was filled with CO_2 in the oil phase. With increasing the CO_2 injection rate, the area with CO_2 mole fraction in oil phase was larger, implying that more CO_2 could mix with oil and swell the oil with a higher CO_2 injection rate. Comparison among the subfigures (a), (b), and (c) for Figure C-11 and Figure C-12 suggests that more CO_2 flowed to Well 9 than to Well 10 and more CO_2 was in the oil phase from Well 5 to Well 9 than from Well 5 to Well 10. The results were comparable to the tracer concentration distribution for water injection (Figure C-5) that shows more water flowed to Well 9 than to Well 10. The results also confirmed the findings from Figure C-10 that greater incremental oil production was achieved in Well 9 compared to Well 10.

When CO_2 injection was performed for a longer time, the injected CO_2 swept a larger area in the reservoir, as shown by comparing Figure C-13 and Figure C-11. Comparison between Figure C-14 and Figure C-12 showed that with longer injection time, the injected CO_2 turned into the oil phase in a larger area because CO_2 entered more porous media of the reservoir matrix and became miscible with more residual oil.

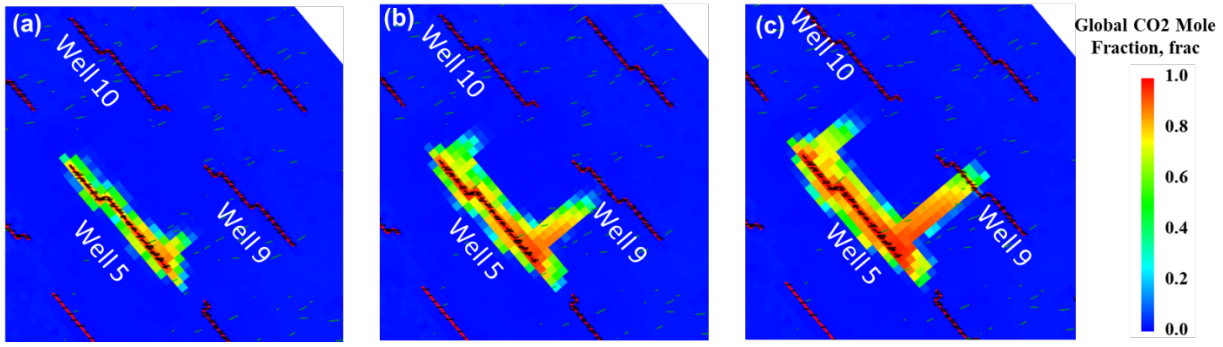

Figure C-11. Distribution of CO_2 global mole fraction after 2.5 years of CO_2 injection treatment for CO_2 injection rate of (a) 1 MMscf/d, (b) 2 MMscf/d, (c) 3 MMscf/d.

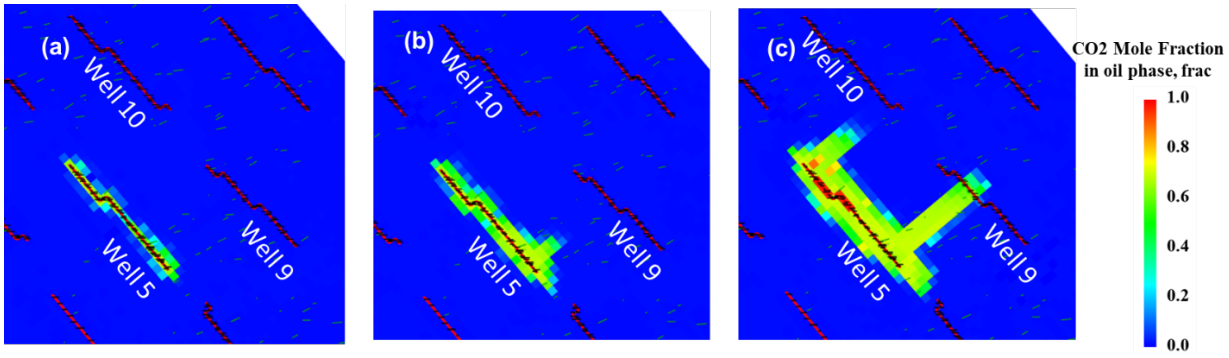

Figure C-12. Distribution of CO_2 mole fraction in oil phase after 2.5 years of CO_2 injection treatment for CO_2 injection rate of (a) 1 MMscf/d, (b) 2 MMscf/d, (c) 3 MMscf/d.

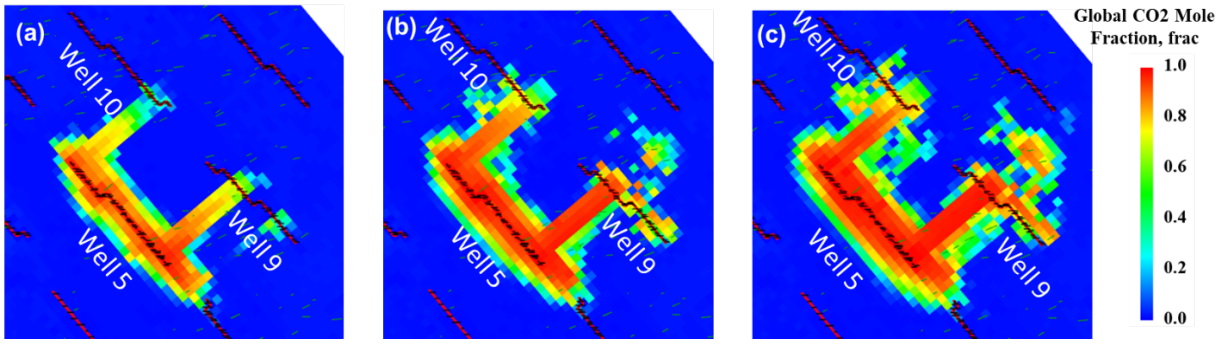

Figure C-13. Distribution of CO_2 global mole fraction after 10 years of CO_2 injection treatment for CO_2 injection rate of (a) 1 MMscf/d, (b) 2 MMscf/d, (c) 3 MMscf/d.

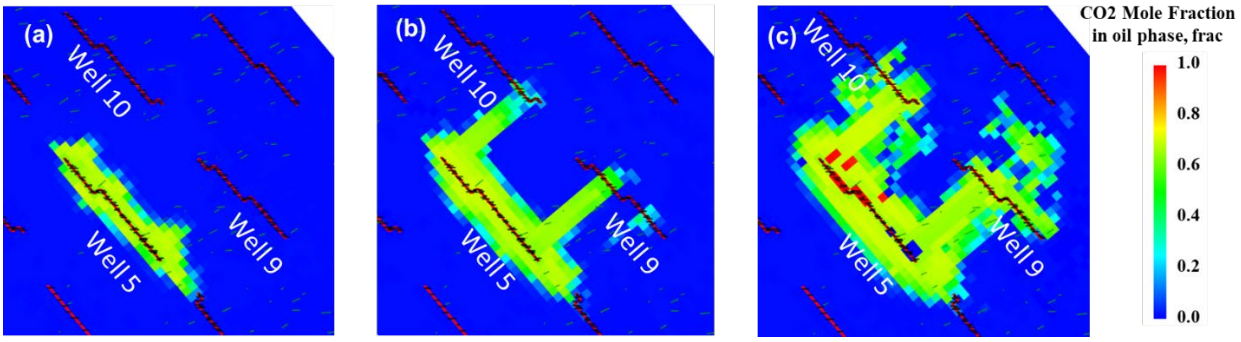

Figure C-14. Distribution of CO_2 mole fraction in oil phase after 10 years of CO_2 injection treatment for CO_2 injection rate of (a) 1 MMscf/d, (b) 2 MMscf/d, (c) 3 MMscf/d.

The injection of CO_2 causes a portion of the CO_2 to be stored in the reservoir and the other portion of CO_2 produced from the offset wells. With increasing the CO_2 injection rate, an increase in both CO_2 production and CO_2 storage was observed, as shown in Figure C-15a. Injecting CO_2 with an injection rate of 4 MMscf/d for 10 years contributes to 11,095 MMscf of CO_2 stored in the reservoir and 2470 MMscf of CO_2 produced from the nearby wells. Increasing the CO_2 injection rate causes a reduction in CO_2 retention rate. An explanation is that CO_2 saturation increases as more CO_2 is injected into the reservoir, leading to an increase in gas relative permeability, thus CO_2 could further enter the porous media and be stored in the reservoir.

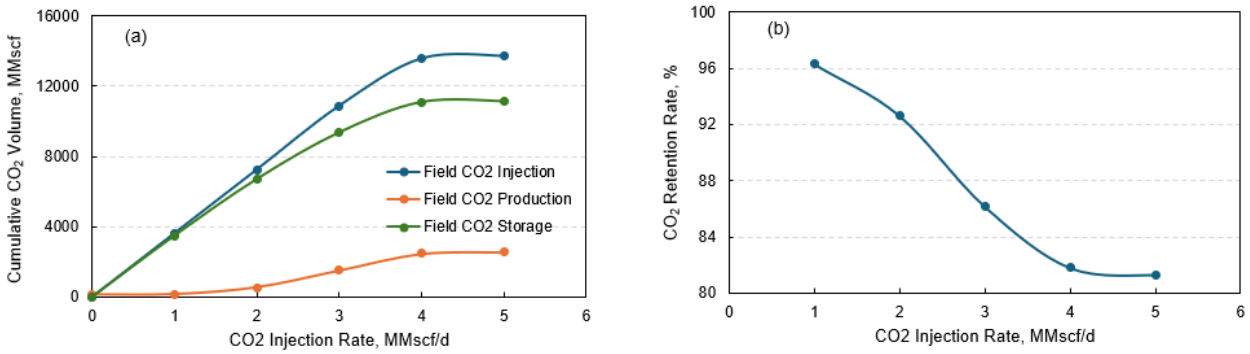

Figure C-15. (a) Cumulative CO_2 injection, production, and storage volumes and (b) CO_2 retention rate of the field at different CO_2 injection rates.

Surfactant EOR Investigation

Surfactant EOR was also evaluated as a potential method for improving field performance. Surfactants improve oil recovery by various mechanisms including the creation of microemulsion due to a decrease in the interfacial tension between the oil and water phases and the reservoir rock wettability alteration toward more favorable water-wet conditions (Sheng 2010). In this work, we focus on the wettability alteration mechanism as it was observed to be the prevailing mechanism

in this study based on the conducted experiments. Four cases were designed for modeling the surfactant effect. These four cases represented the utilization of surfactants with varying strength and effectiveness in altering the reservoir wettability for improving the oil production and recovery. The wettability alteration process was adopted in the simulation by adjusting the relative permeability curves based on the surfactant strength as observed from the results of the core-flooding experiments in the core samples. The adopted relative permeability curves for each case (no surfactant, weak surfactant, normal surfactant, and strong surfactant) are shown in Figure C-16. It can be observed that as the surfactant strength increases, the oil phase relative permeability curves shift higher and the water phase curves shift lower. The shifts reflect the expected more favorable wetting conditions inside the reservoir. Figure C-16 shows the relative permeability curves adopted for the area around each respective well—Well 9, Well 10, and Well 5—employing surfactants with different strengths. The setup of the injection and production constraints is the same as Case 1 (Table C-1).

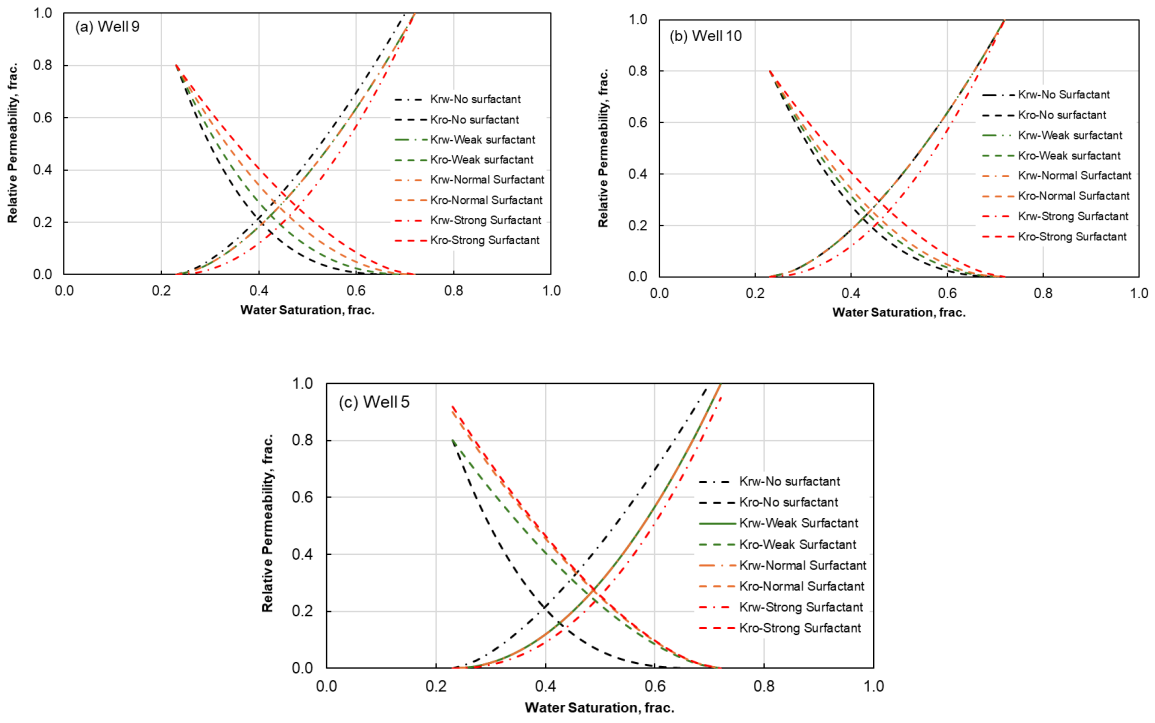

Figure C-16. Relative permeability curves for various surfactant EOR cases representing no surfactant, weak surfactant, normal surfactant, and strong surfactant cases near (a) Well 9, (b) Well 10, and (c) Well 5.

The results of the four simulated surfactant cases in terms of cumulative liquid, oil, and water production from Well 9 and Well 10 are shown in Figure C-17 and Figure C-18, respectively. Results distinctly showed that the liquid and water production remained almost unchanged between the four cases using no surfactant or surfactants with varying strengths. However, the

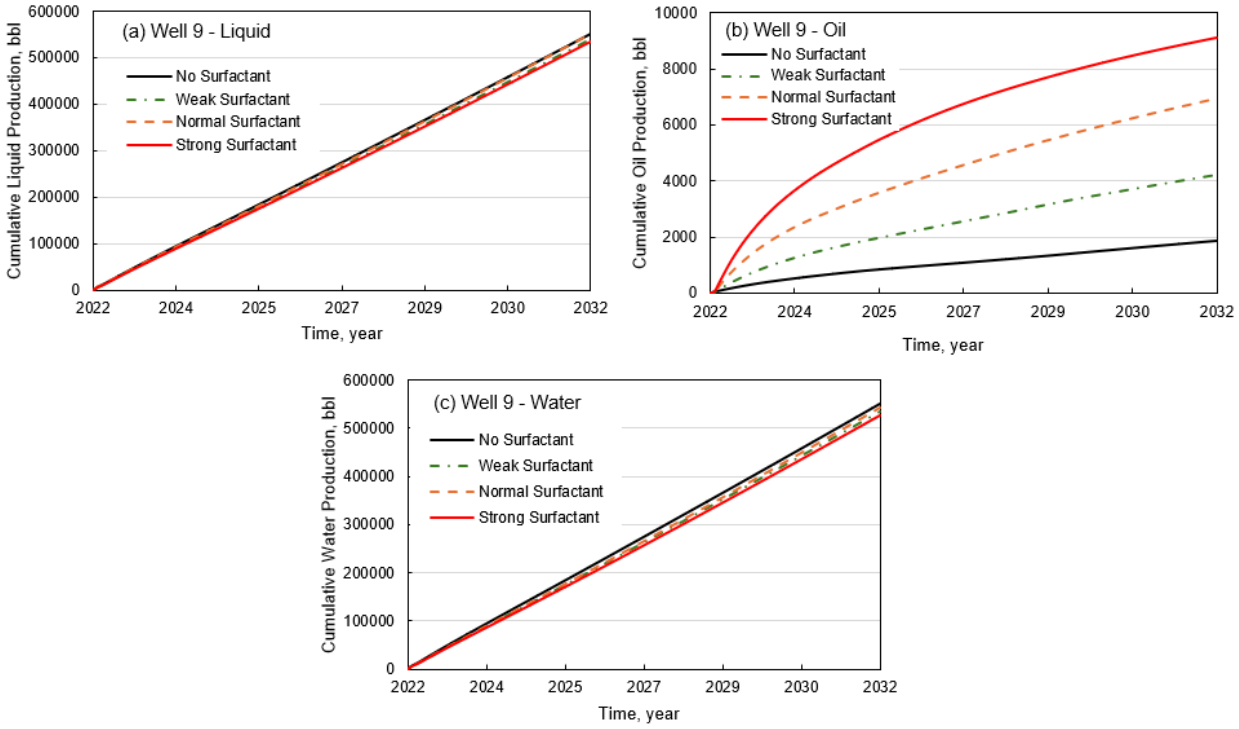

Figure C-17. (a) Cumulative liquid production, (b) cumulative oil production, and (c) cumulative water production of Well 9 for the various surfactant EOR cases.

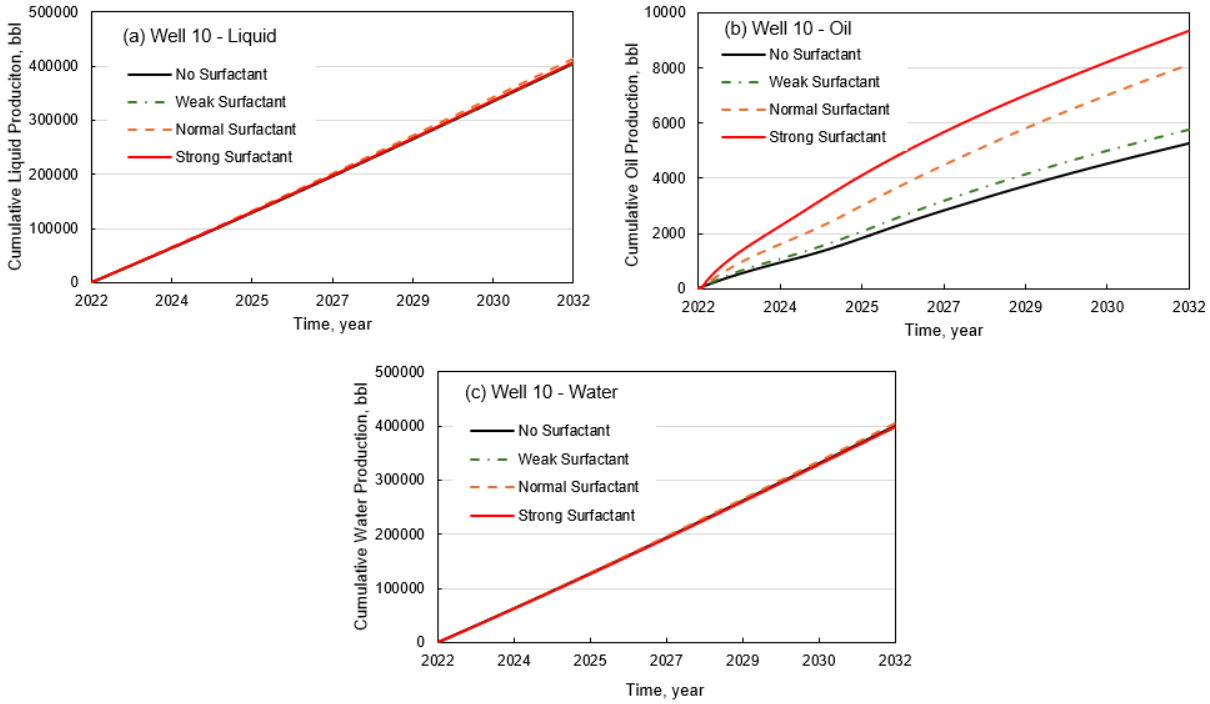

Figure C-18. (a) Cumulative liquid production, (b) cumulative oil production, and (c) cumulative water production of Well 10 for the various surfactant EOR cases.

cumulative oil production from both wells, Well 9 and Well 10, witnessed an increase directly dependent on surfactant utilization. The case in which no surfactant was used resulted in the lowest cumulative oil production, 1866 bbl from Well 9 and 5254 bbl from Well 10, followed by the weak surfactant case that yielded additional cumulative oil production of 2376 bbl from Well 9 and 506 bbl from Well 10 compared to the no-surfactant case. In a similar trend, the normal surfactant case showed higher oil production than the weak surfactant case, and the strong surfactant case resulted in the highest oil production. 7234 bbl and 4071 bbl of incremental oil production was observed from Well 9 and Well 10, respectively, as a result of using the strong surfactant compared to the no-surfactant case. This corresponds to a 388% increase from Well 9 and 77% from Well 10 in terms of the cumulative oil produced compared to the no-surfactant case. Similar increases in oil production and decrease in water have been noted in the literature from field application observations. For example, in Semoga Field in Indonesia, the average oil production increased from 425 bpd to 928 bpd and the water cut dropped from 96% to 88% as a result of surfactant flooding (Rilian and others, 2010). Cheng and Kwan (2012) reported an incremental oil production between 29% and 71% from the application of an anionic surfactant in a dolostone reservoir of Yates Field. Therefore, the results of surfactant experimental and simulation work conducted in this study could be considered for a field pilot in the Foreman Butte Field through a proper design.

Infill Well Drilling

Infill well drilling is a commonly adopted industrial practice to improve oil recovery in heterogeneous reservoirs. This technique could be applied to any stage of reservoir development, especially in legacy fields with years of waterflood treatment (Fuller and others, 1992; Syed and others, 2021). Incremental oil production could be accomplished by infill well drilling via improving sweep efficiency, lateral formation connectivity, and recovery of “wedge-edge” oil (Driscoll, 1974; Gould and Munoz, 1982; Syed and others, 2021).

A prediction model was built to evaluate the oil production performance of assumed infill wells in Foreman Butte Field. Four assumed infill wells—Infill1, Infill2, Infill3, and Infill4—were added to the model at different locations. The locations of added infill wells are shown in Figure C-19. All the infill wells were produced with the maximum liquid rate constraint of 300 bpd and minimum bottomhole pressure of 500 psi for 10 years. The cumulative oil production of each infill well during the 10-year prediction period is shown in Figure C-20a and is compared with the average cumulative oil production of their nearby two wells during the production history, as shown in Figure C-20b. The results suggest that the infill wells with higher average cumulative oil production in their nearby two existing wells produce more oil during the prediction period. This can be observed from comparing the expected cumulative oil production from Infill1 and Infill2 to Infill3 and Infill4. The predicted cumulative oil produced from Infill1 and Infill2 were 15,591 bbl and 9647 bbl, respectively, and they correspond to the existing nearby well pairs with highest production, which are Wells 11 and 16 for Infill1 and Wells 8 and 13 for Infill2. Infill3 and Infill4 resulted in lower expected cumulative oil production similar to the relatively lower cumulative oil produced by the nearest well pairs, Wells 1 and 7 for Infill3 and Wells 3 and 5 for Infill4. The results imply that drilling infill wells could be an effective approach to improve oil recovery for the tight legacy oil field. The locations of infill wells should be selected close to the existing wells with high cumulative oil production to potentially achieve meaningful oil production in the infill wells.

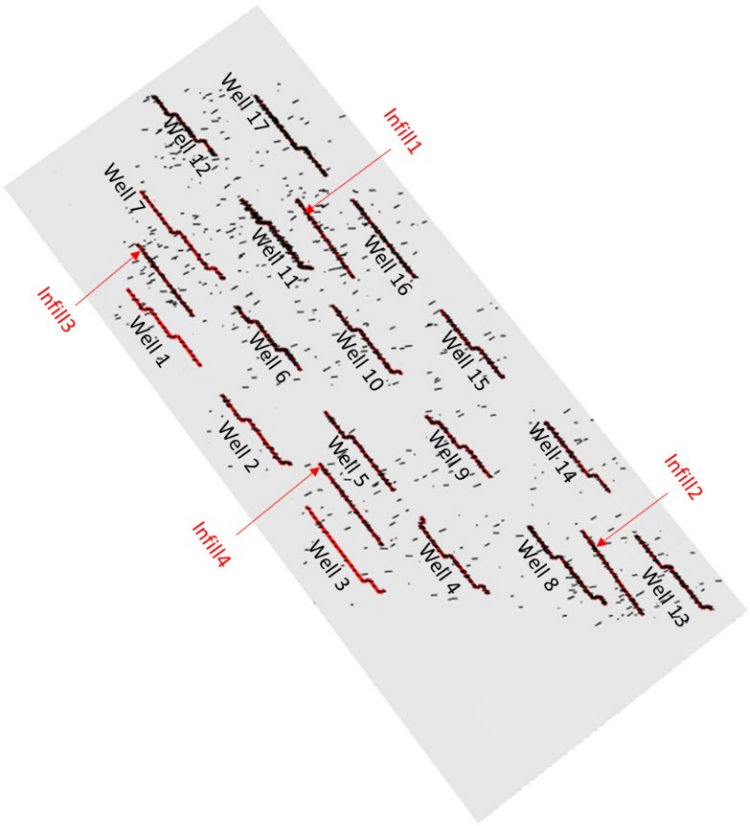

Figure C-19. Distribution of wells and natural fractures for the model with four infill wells.

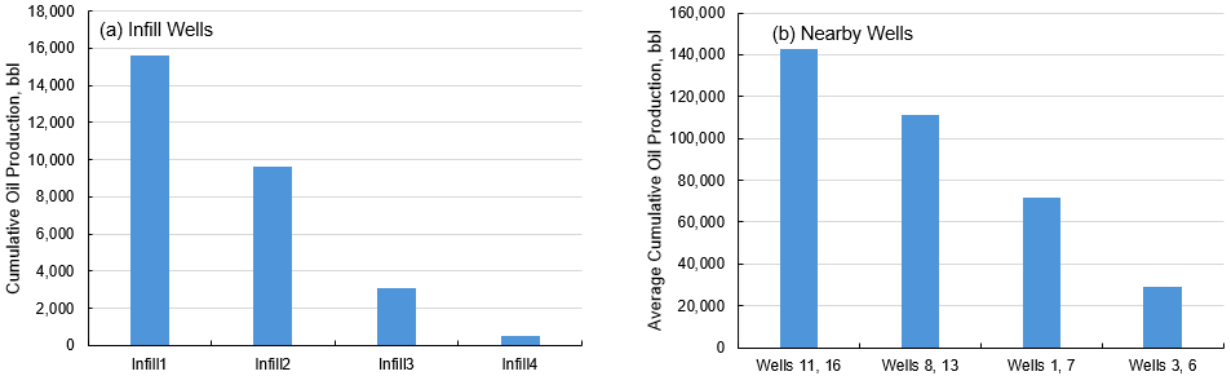

Figure C-20. Cumulative oil production of the infill wells (a) during the 10-year prediction period and average oil production of their nearby two existing wells (b) before adding infill wells.

References

Cheng, A.M., and Kwan, J.T., 2012, Optimal injection design utilizing tracer and simulation in a surfactant pilot for a fractured carbonate Yates Field: Paper presented at the SPE Improved Oil Recovery Conference, Tulsa, Oklahoma, USA, April 2012. https://doi.org/10.2118/154270-MS.

Davarpanah, A., Mirshekari, B., and Razmjoo, A.A., 2019, A simulation study of water injection and gas injectivity scenarios in a fractured carbonate reservoir—a comparative study: Petroleum Research, v. 4, no. 3, p. 250–256.

Dellinger, S.E., Patton, J.T., and Holbrook, S.T., 1984, CO_2 mobility control: Society of Petroleum Engineers Journal, v. 24, no. 2, p. 191–196.

Driscoll, V.J., 1974, Recovery optimization through infill drilling concepts, analysis, and field results: Paper presented at the Society of Petroleum Engineers of AIME, Houston, Texas, October 1974. https://doi.org/10.2118/4977-MS.

Fuller, S.M., Sarem, A.M., and Gould, T.L., 1992, Screening waterfloods for infill drilling opportunities: Paper presented at the SPE International Oil and Gas Conference and Exhibition in China, Beiging, China, March 1992. SPE-22333. https://doi.org/10.2118/22333-MS.

Gould, T.L., and Munoz, M.A., 1982, An analysis of infill drilling: Paper presented at the SPE Annual Technical Conference and Exhibition, New Orleans, Louisiana, September 1982.

Grigg, R.B., and Schechter, D.S., 1997, State of the industry in CO_2 floods: Paper presented at the SPE Annual Technical Conference and Exhibition, San Antonio, Texas, October 1997. https://doi.org/10.2118/38849-MS.

Rilian, N.A., Sumestry, M., and Wahyuningsih, _, 2010, Surfactant stimulation to increase reserves in carbonate reservoir: a case study in Semoga Field: Paper presented at the SPE EUROPEC/EAGE Conference and Exhibition, Barcelona, Spain, June 2010. https://doi.org/10.2118/130060-MS.

Sheng, J.J., 2010. Modern chemical enhanced oil recovery—theory and practice. Gulf Professional Publishing, 648 p.

Syed, F.I., Negahban, S., and Dahaghi, A.K., 2021, Infill drilling and well placement assessment for a multi-layered heterogeneous reservoir: Journal of Petroleum Exploration and Production, v.11, no. 1, p. 901–910.

APPENDIX D

REVITALIZATION OF A CARBONATE RESERVOIR FROM THE RED RIVER FORMATION IN NORTH DAKOTA

REVITALIZATION OF A CARBONATE RESERVOIR FROM THE RED RIVER FORMATION IN NORTH DAKOTA

Reservoir and Well Description

Another conventional oil field located in southwest North Dakota was used for this evaluation through publicly available data from the North Dakota Industrial Commission (NDIC). The main pay zone is a carbonate reservoir in the Ordovician Red River Formation consisting of dolomitized laminated carbonate with permeable intervals (Montgomery, 1997). Five wells (A, B, C, D, E, as shown in Table D-1) with production history dating back to as early as 1960 were selected to optimize strategies to revitalize this legacy oil field. To improve oil production, all the wells were stimulated by matrix acidizing or acid frac treatments. All the wells were drilled vertically during the initial completion. Wells A, D, and E were recompleted with lateral sections. Well B was treated with water injection from 1970 to 1985. Wells A and E have been treated with water injection and high-pressure air injection to improve oil production in this section. The production performance and injection operation details are summarized in Table D-1.

Table D-1. Production and Injection Statistics of the Selected Five Wells in the Field

		Water Injection	Gas Injection	Cumulative Production				Cumulative Injection	
Well	Completion Type	yy.mm-yy.mm	yy.mm-yy.mm	Liquid, bbl	Oil, bbl	Water, bbl	Gas, MMscf	Water, bbl	Gas, MMscf
A	Horizontal Reentry	10.03–23.12	04.03–09.12	822,619	260,083	562,536	36.2	500,484	2205.72
B	Vertical	70.06–85.04	–	129,709	125,145	4,564	13.9	2,265,559	0
C	Vertical	–	–	3,502,098	1,089,358	2,412,740	176.6	0	0
D	Horizontal Reentry	–	–	2,521,178	1,024,946	1,496,232	2796.7	0	0
E	Horizontal Reentry	10.03–23.12, 01.09–04.04	04.08–09.12	24,228	2,373	21,855	0.068	1,059,474	2754.2

Simulation Model Development

Baseline Reservoir Model

To reproduce the history of the wells, a compositional reservoir simulation model was developed using Computer Modelling Group Ltd.'s (CMG's) GEM®. The width, length, and height of the reservoir model were approximately 7000, 7500, and 192 feet, with 70, 75, and 35 cells in the X, Y, and Z directions, respectively. The location and trajectories of the selected five wells are presented in Figure D-1a. Natural fractures were included in the reservoir model using a high-efficiency fracture simulation approach, embedded discrete fracture model (EDFM), as shown in Figure D-1b. The reservoir structure and properties, including permeability, porosity, and initial oil saturation, were initialized by Petrel® based on available well log and core data and imported into the baseline reservoir model. As shown in Figure D-2, the distribution of permeability, porosity, and initial oil saturation suggests that the reservoir is heterogeneous. A large area of a permeable and productive layer consists of rocks with permeability greater than 1 mD, porosity greater than 10%, and initial oil saturation greater than 0.5, as shown in Figure D-2.

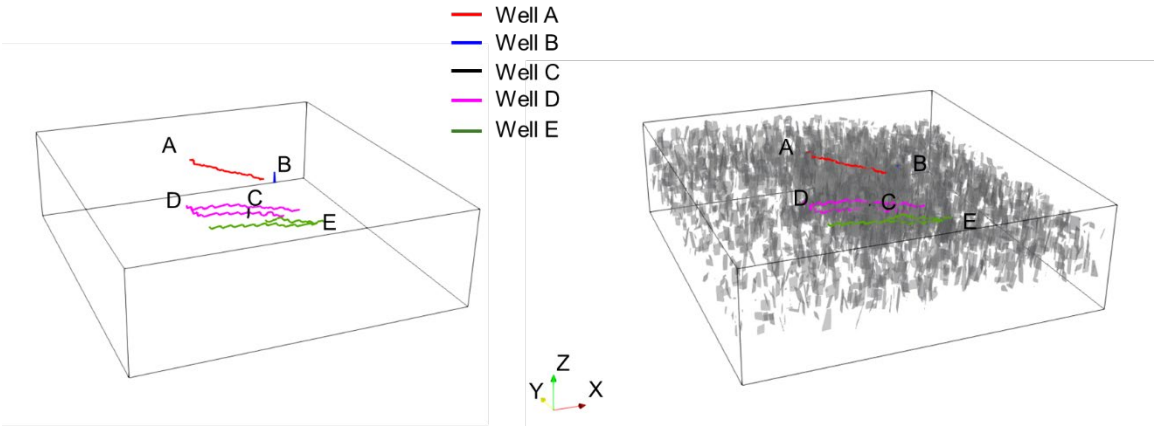

Figure D-1. Schematic of three-dimensional (3D) baseline reservoir model framework (left) and distribution of natural fractures (right).

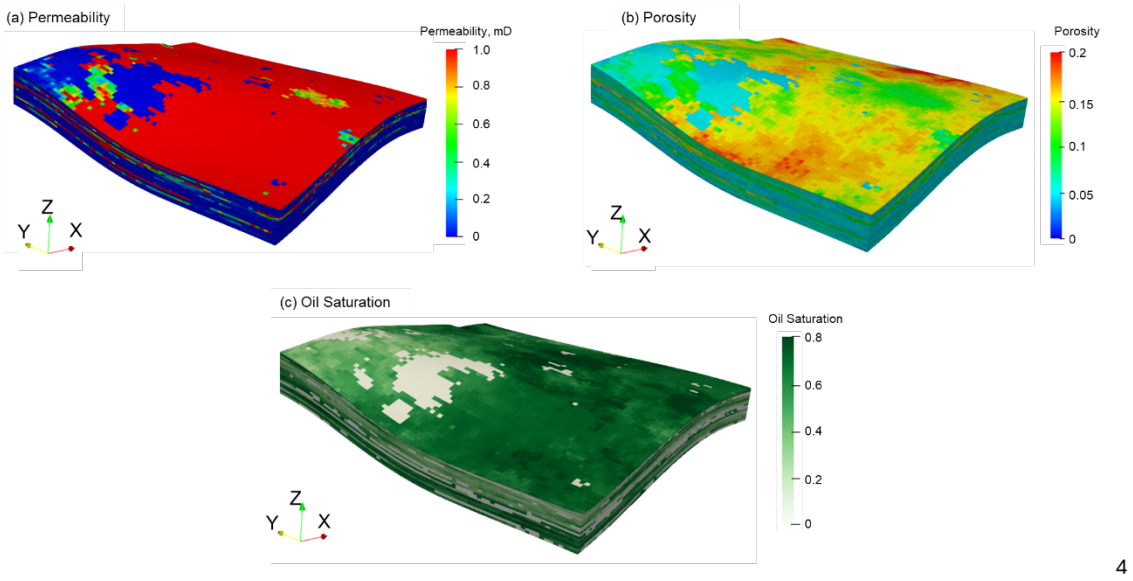

Figure D-2. 3D top view of the (a) permeability, (b) porosity, and (c) oil saturation distribution for the permeable and productive layers of the baseline reservoir model.

History Matching

History matching was performed for the five selected wells in the model. Reasonable history-matching results for liquid, water, oil, and gas production rates were achieved, as shown in Figure D-3. The water and gas injection rates were also matched satisfactorily, as illustrated in Figure D-4.

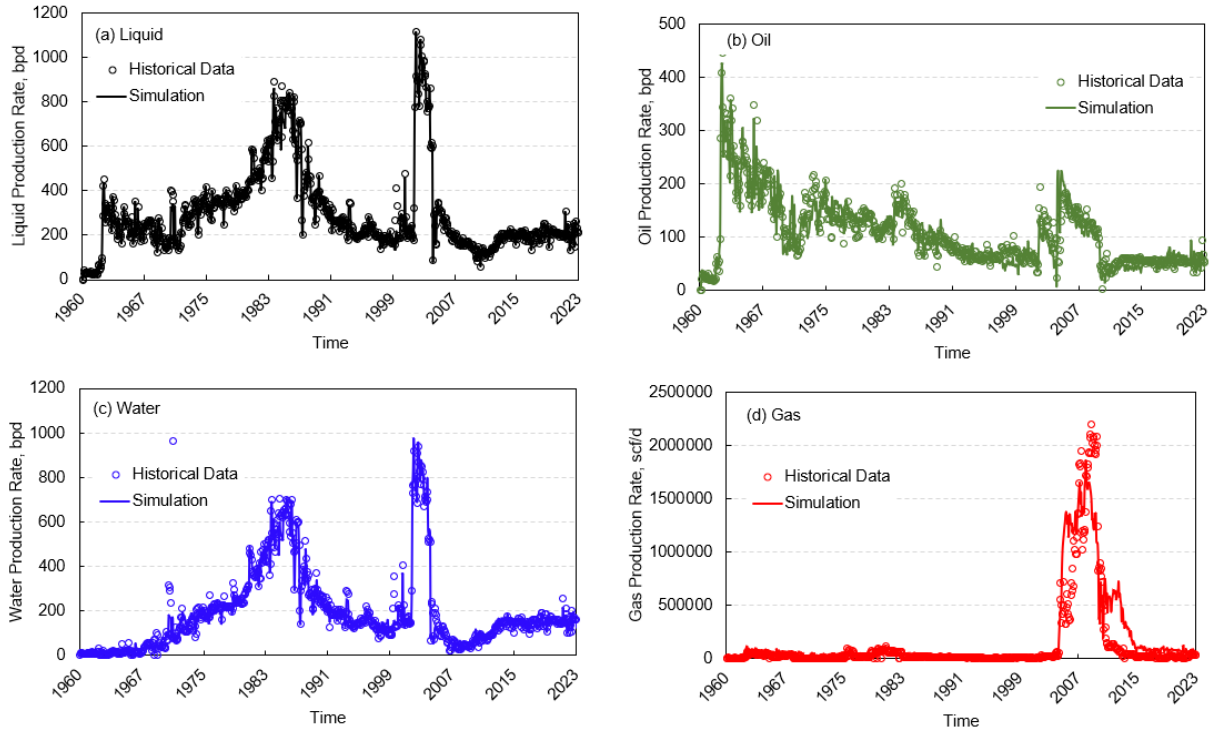

Figure D-3. History-matching results for production rates of all the wells in the model: (a) liquid rate, (b) oil rate, (c) water rate, and (d) gas rate.

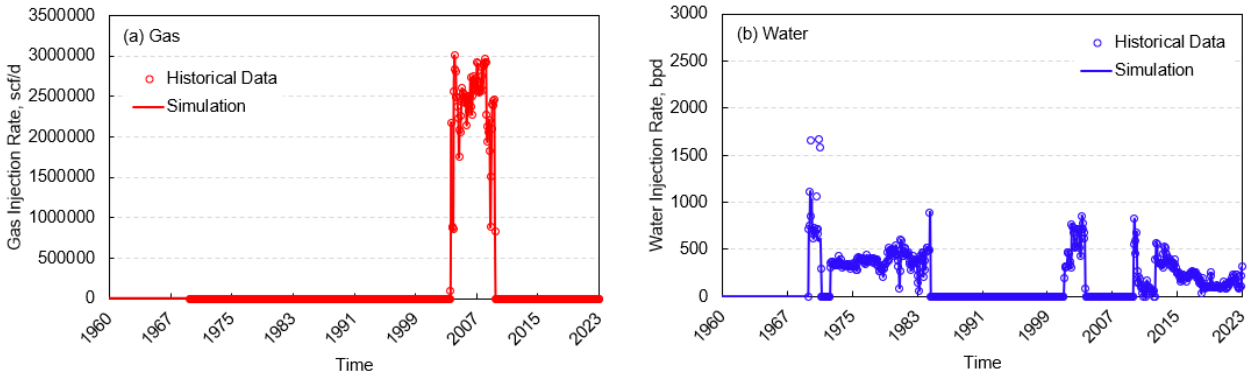

Figure D-4. History-matching results for injection rates of all the wells in the model: (a) gas injection rate and (b) water injection rate.

The reservoir model also captured the behavior of reservoir pressure due to water and gas injection, as shown in Figure D-5. The results suggest that water injection maintained or slowed down the depletion trend of reservoir pressure but did not significantly increase reservoir pressure. This is because the production wells were produced with similar rates as water injection rates during the water injection period. In comparison, reservoir pressure increased clearly during the high-pressure air injection period because the amount of injected gas was significant and the injected gas migrated fast through the reservoir to increase the overall pressure in the pore space.

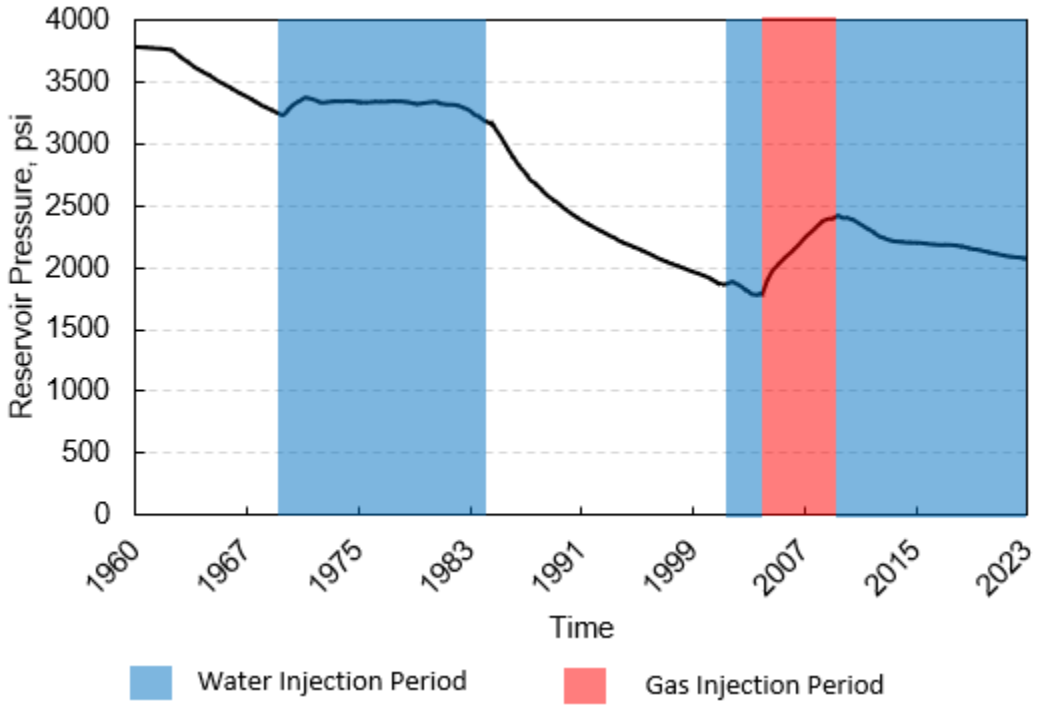

Figure D-5. Simulation results of reservoir pressure in the model.

The development of reservoir pressure and oil saturation during the simulated history is visualized in Figure D-6 and Figure D-7, respectively. Water injection in Well B from June 1970 to January 1975 increased reservoir pressure in its near-wellbore region, as shown in Figure D-6 (a) and (b). A decrease in oil saturation near Well B was observed during this period by comparing Figure D-6 (a) and (b). The results indicate that a portion of the oil near Well B was swept by injected water to flow to production Wells A, C, and D. From April 1985 to January 2000, the reservoir pressure declined because wells A, C, and D were producing while water or gas injection was not conducted, as illustrated in Figure D-5 and visualized by comparing Figure D-6 (b) and (c). Water injection and high-pressure air injection in Wells A and E from September 2001 to December 2010 restored reservoir pressure, as illustrated in Figure D-5 and visualized by comparing Figure D-6 (c) and (d). The areas near the two injection wells show a decrease in oil saturation, as observed by comparing Figure D-7 (c) and (d), implying that the injected water and air swept the oil in the reservoir and contributed to oil production in the production Well D.

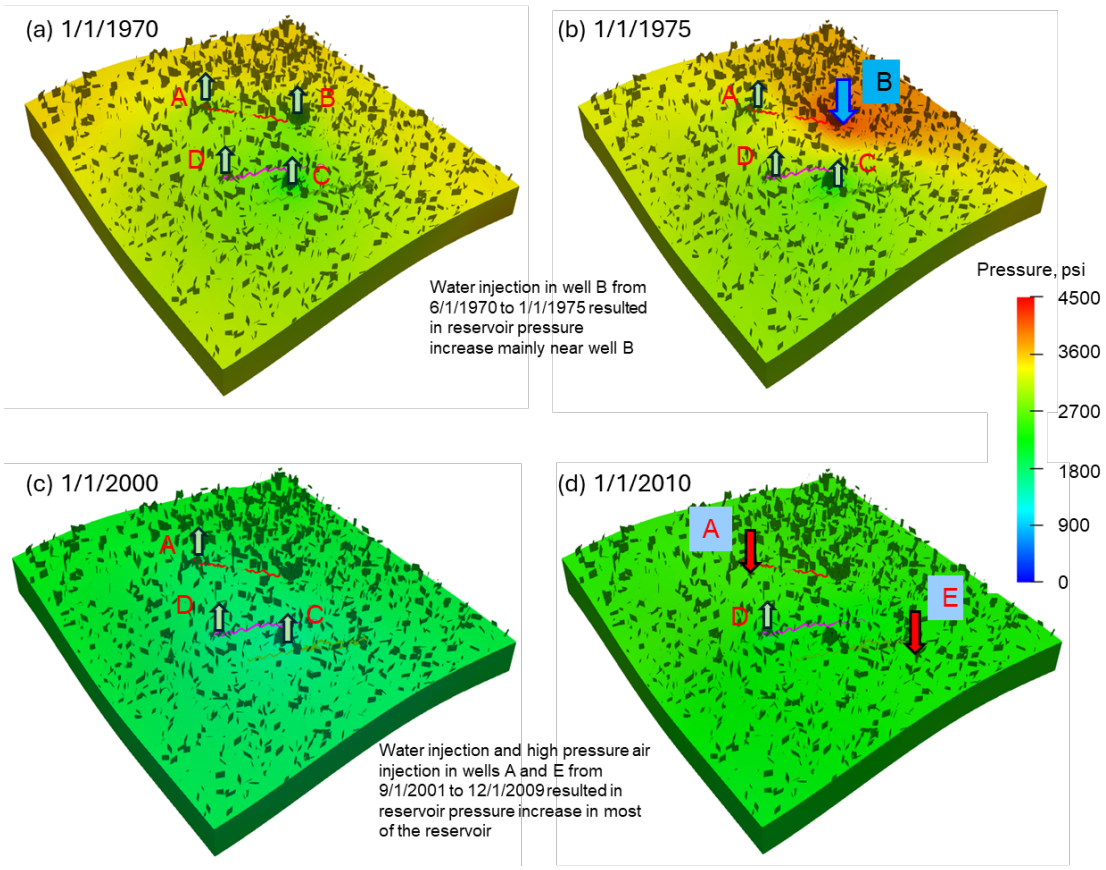

Figure D-6. 3D top view of reservoir pressure distribution at the production layer at different times: (a) 1/1/1970, (b)1/1/1975, (c) 1/1/2000, and (d) 1/1/2010.

Water-Flooding Investigation

Five predictive cases were designed to investigate the oil production performance of different water-flooding strategies in the field. For all cases, the reservoir was repressurized by injecting water with the maximum water injection rate of 1500 bpd in both Wells A and E and shutting in production Wells B, C, and D for 2 years. Then, the constraints of injection and production wells were changed for the five cases according to Table D-2, and the prediction simulation was performed for another 28 years. The total maximum water injection rates and total maximum liquid production rates were equal, to maintain the reservoir pressure during 28 years of prediction.

During 2 years of repressurization, the BHP of the three wells increased to above 3000 psi. Then, the BHPs of the three wells were reduced and stabilized during the 28 years of injection and production, as shown in Figure D-8. The water injection also resulted in an increase in average reservoir pressure to above 3000 psi. During the subsequent 28 years of injection and production, the average reservoir slightly decreased but maintained close to the magnitude of 3000 psi, as shown in Figure D-9. The oil production performance in the field of all cases is shown in

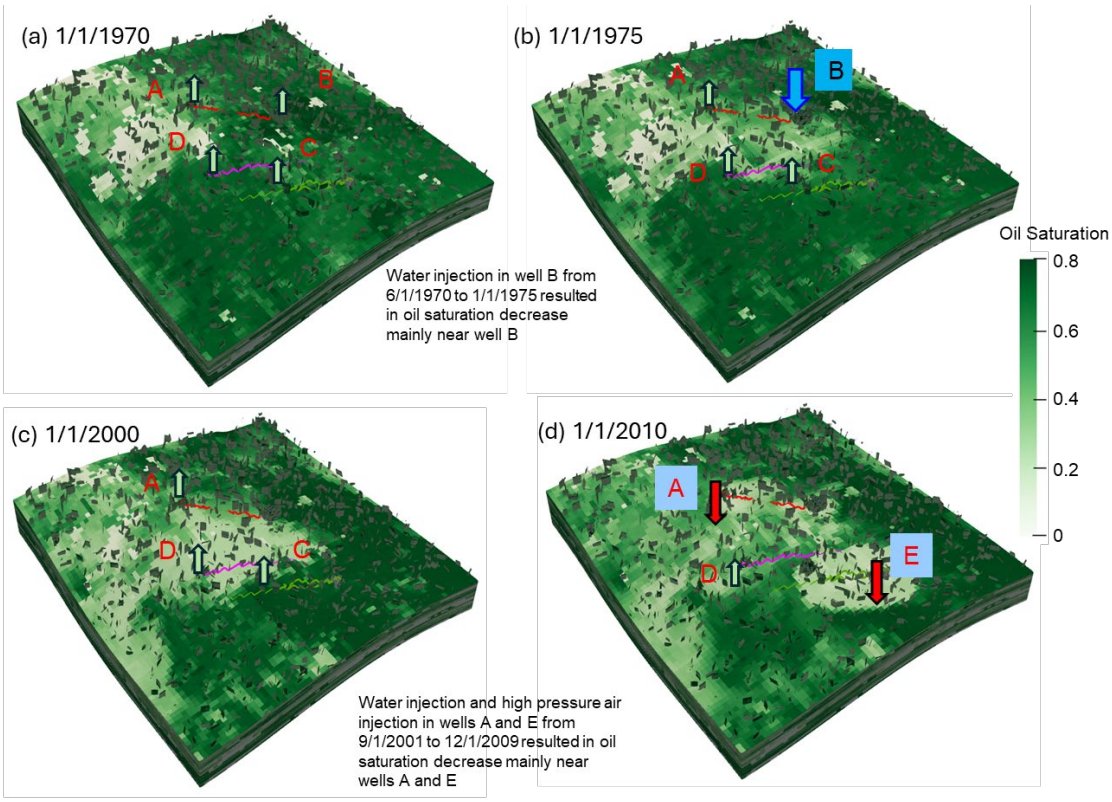

Figure D-7. 3D top view of oil saturation distribution at the production layer at different times: (a) 1/1/1970, (b)1/1/1975, (c) 1/1/2000, and (d) 1/1/2010.

Table D-2. Constraints Setup of the Injection and Production Wells in 28 years of Prediction for Water-Flooding Operations

Case No.	Injection Wells			Production Wells				Minimum Bottomhole Pressure (BHP), psi
	Maximum Water Injection Rate, bpd			Maximum Liquid Production Rate, bpd				
	Well A	Well E	Total	Well B	Well C	Well D	Total	
1	100	100	200	25	40	135	200	500
2	300	300	600	75	120	405	600	
3	500	500	1000	125	200	675	1000	
4	700	700	1400	175	280	945	1400	
5	900	900	1800	225	360	1215	1800	

Figure D-10. With increasing water injection rates, the additional cumulative liquid, oil, and water production of all the production wells in the field increased. 28 years of water injection with an injection rate of 900 bpd in Wells A and E contributed to additional cumulative oil production of 1,309,472 bbl in the three production wells.

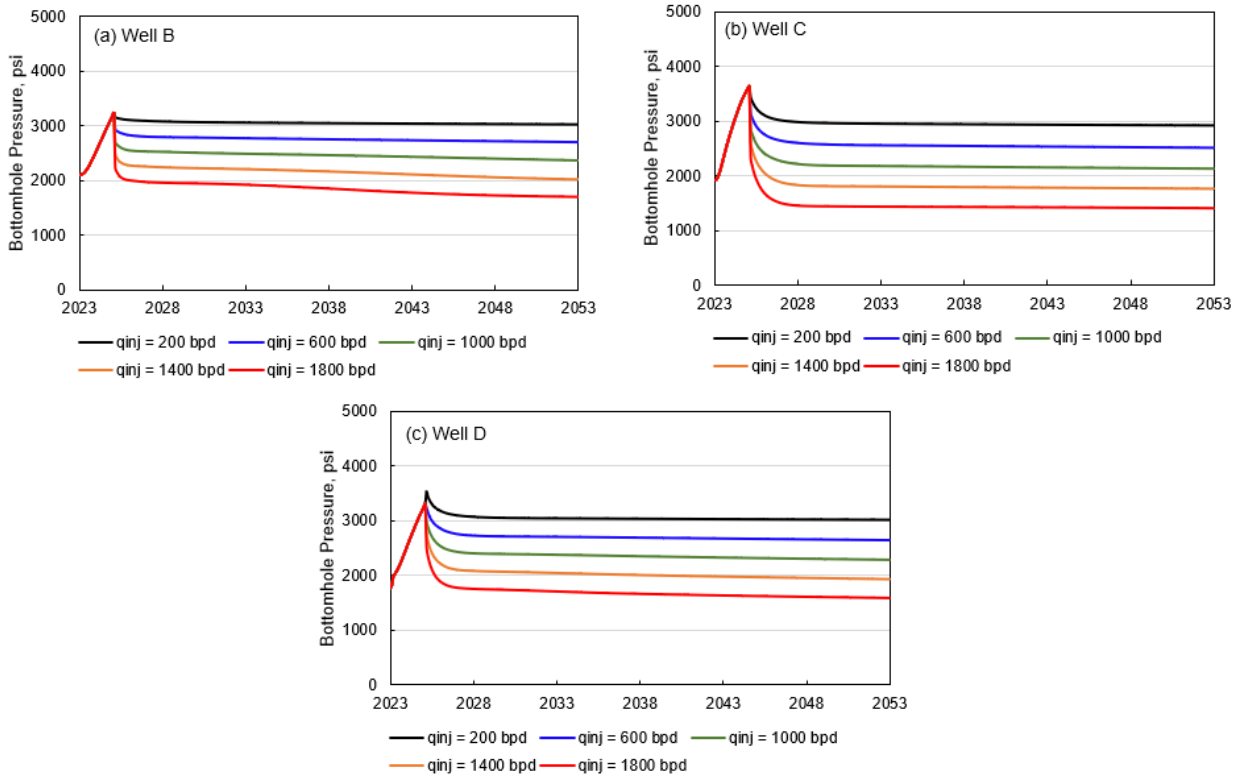

Figure D-8. BHP behavior in Wells (a) B, (b) C, and (c) D during 30 years of water-flooding prediction for Cases 1–5; qinj is the total water injection rate of Wells A and E.

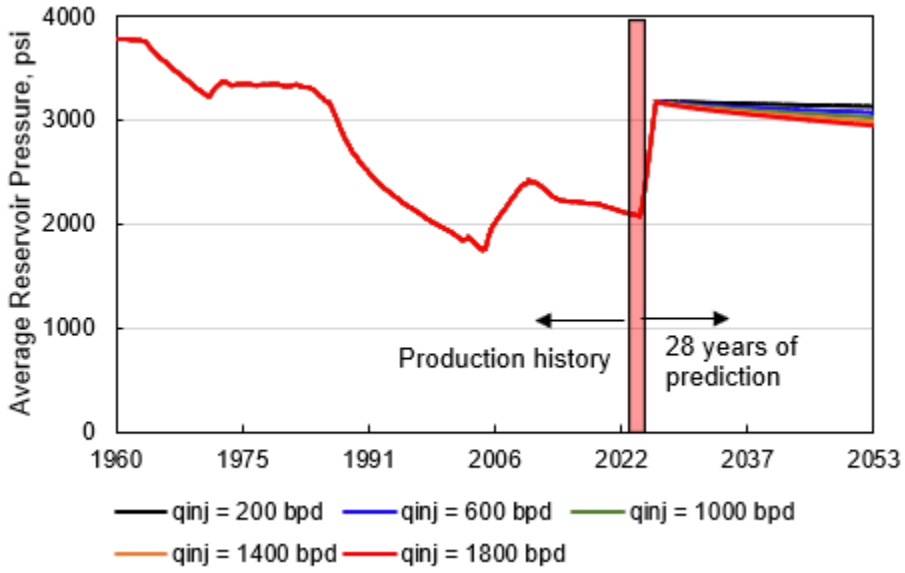

Figure D-9. Development of average reservoir pressure during the production history and 30 years of the water-flooding prediction period. The red box represents 2 years of injecting water and suspending production.

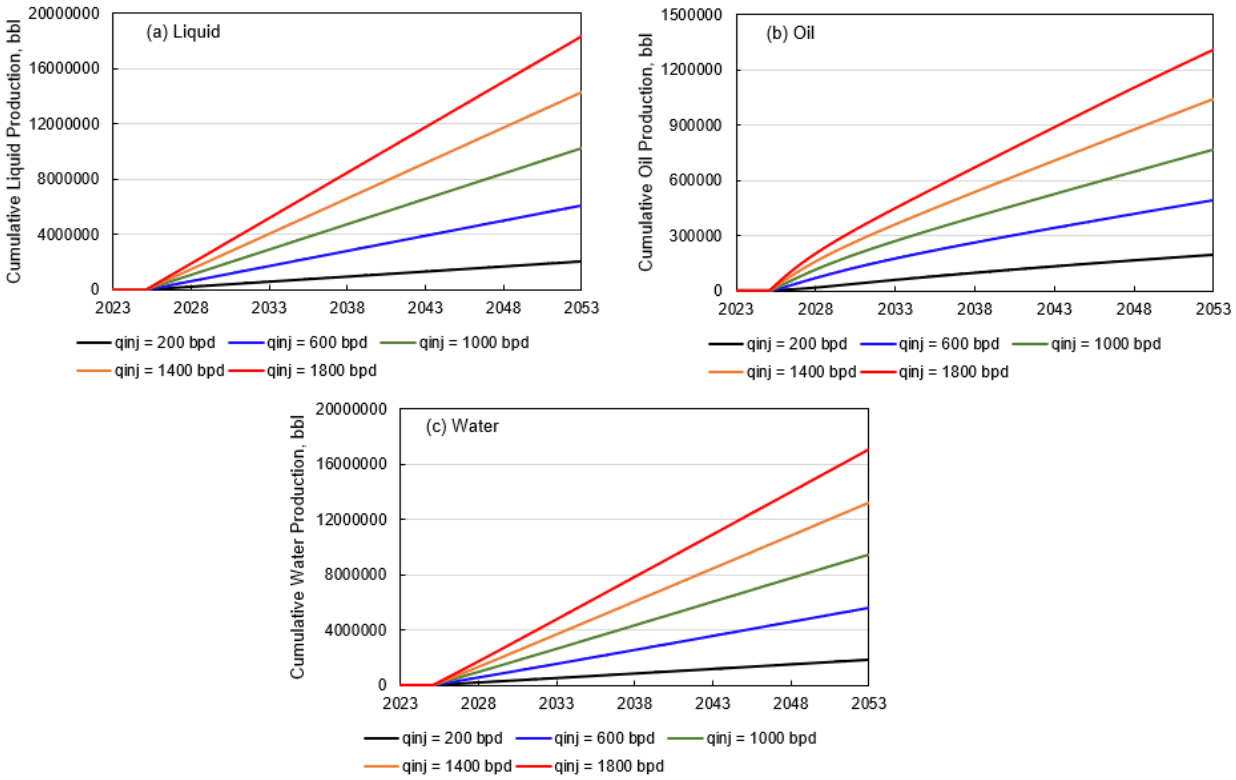

Figure D-10. Comparison of (a) additional cumulative liquid production, (b) additional cumulative oil production, and (c) additional cumulative water production during 30 years of water-flooding prediction. Field additional cumulative production represents the total production accumulated since 7/1/2023 in the prediction period; qinj is the total water injection rate of Wells A and E.

Continuous CO_2 Injection Enhanced Oil Recovery (EOR)

Four predictive cases were designed to investigate the performance of CO_2 EOR in the model. To restore the reservoir pressure, CO_2 was injected with the maximum injection rate of 3 MMscf/d in both Wells A and E, and the production Wells B, C, and D were shut in for 2 years. Then, the CO_2 injection rate was adjusted to 1, 2, 3, and 4 MMscf/d in Wells A and E, and the production wells were open for production with different maximum liquid rate constraints, as shown in Table D-3. All four predictive cases were simulated for another 28 years to be comparable with the water-flooding scenarios.

Table D-3. Constraints Setup of the Injection and Production Wells in 28 years of Prediction for CO_2 Injection Optimization

Case No.	Injection Wells			Production Wells				Minimum BHP, psi
	CO_2 Injection Rate, MMscf/d			Maximum Liquid Production Rate, bpd				
	Well A	Well E	Total	Well B	Well C	Well D	Total	
6	1	1	2	28	21	95	144	2500
7	2	2	4	40	30	135	205	
8	3	3	6	52	39	175	266	
9	4	4	8	64	48	215	327	

With the adjusted well operation constraints, the BHP was maintained between 2500 and 4200 psi for the production wells during most of the EOR period, as shown in Figure D-11. The average reservoir pressure was maintained between 3000 and 4500 psi during the EOR period, as shown in Figure D-12b. The minimum miscibility pressure (MMP) between CO_2 and crude oil is estimated to be a little bit above 3000 psi. Maintaining reservoir pressure above 3000 psi ensured that most of the injected CO_2 was at the miscible or near-miscible condition in the reservoir during the 28-year prediction period so that more residual oil could be produced. The injection and production setup of the four cases also ensured that the production gas oil ratio was below 1 MMscf/bbl in 28 years of production, as shown in Figure D-12a. The production performance of the continuous CO_2 injection cases is shown in Figure D-13. The results showed that the cumulative production of liquid, oil, water, and gas increased with CO_2 injection rates in the field. A total CO_2 injection rate of 8 MMscf/d contributed to the maximum additional cumulative oil production of 1,486,622 bbl.

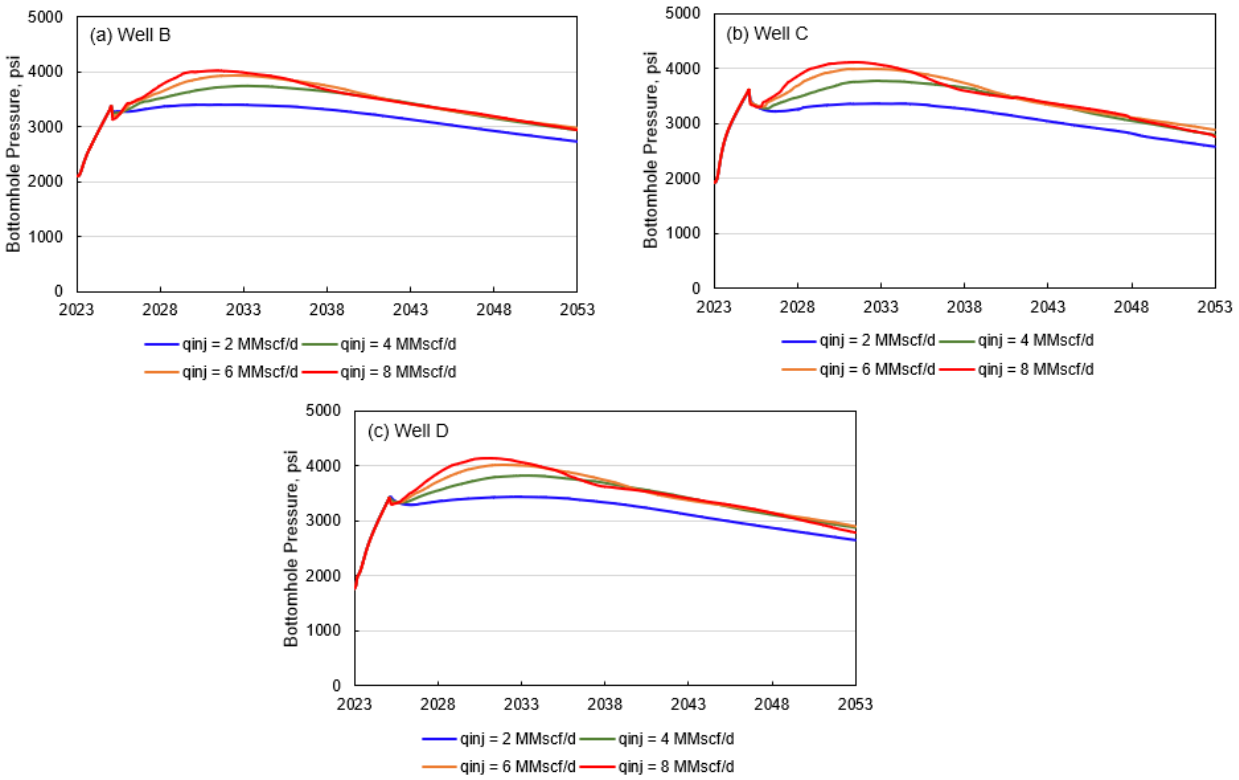

Figure D-11. BHP behavior in (a) Well B, (b) Well C, and (c) Well D during 30 years of injection and production prediction for Cases 6–9; qinj is the total CO_2 injection rate of Wells A and E.

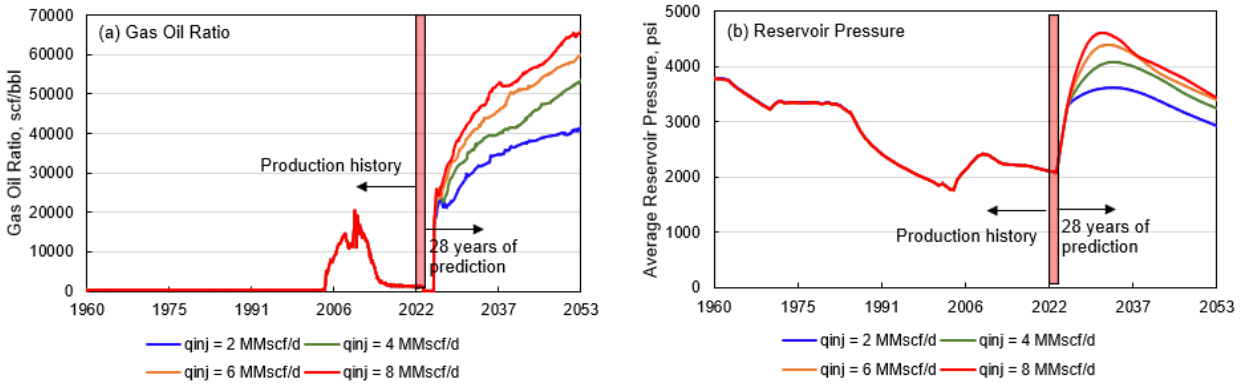

Figure D-12. Development of (a) production gas oil ratio and (b) average reservoir pressure during the production history and 30-year prediction period. The red box represents 2 years of injecting CO_2 in Wells A and E and suspending production in other production wells.

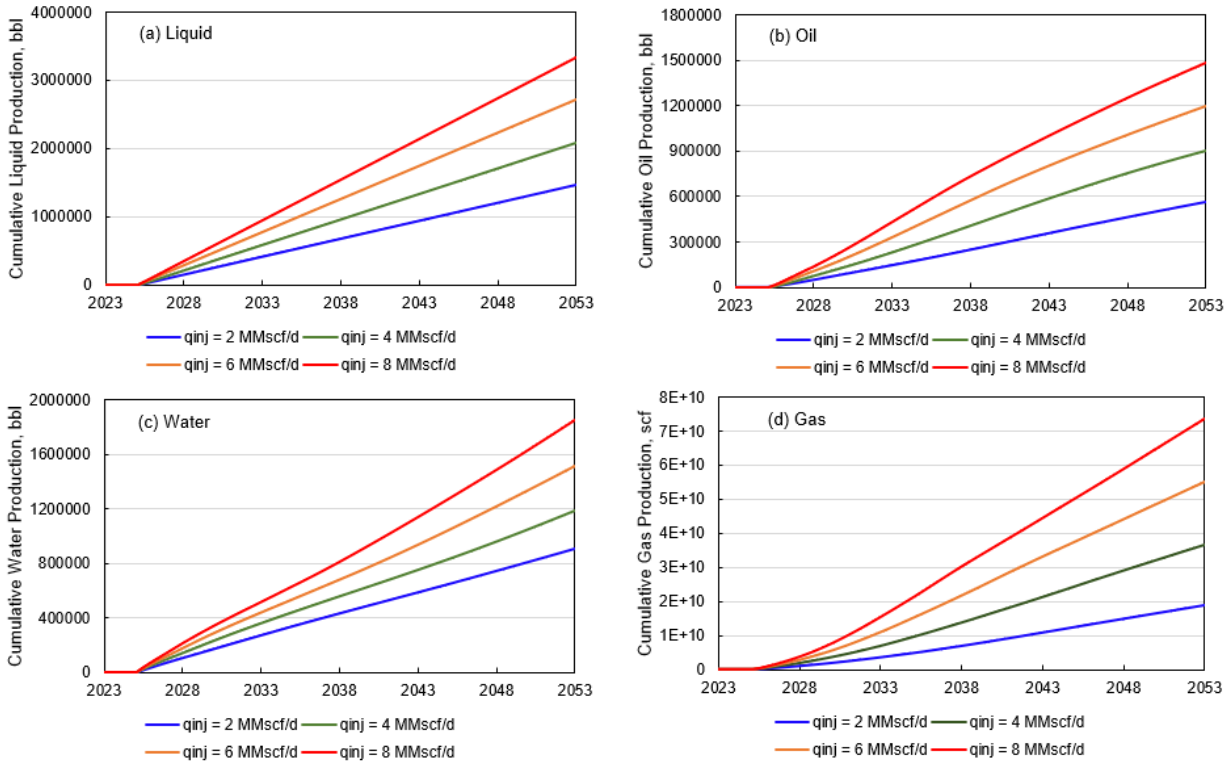

Figure D-13. Comparison of (a) cumulative liquid production, (b) cumulative oil production, (c) cumulative water production, and (d) cumulative gas production during 30 years of continuous CO_2 injection prediction for Cases 6–9. Cumulative production represents the total production accumulated since 7/1/2023 in the prediction period; qinj is the total CO_2 injection rate of Wells A and E.

CO_2 Water Alternative Gas EOR

Although continuous CO_2 injection could be an effective method to improve oil production in the model, this method requires a large volume of CO_2 to maintain the injection rate through the EOR period. CO_2 water alternative gas (WAG) is an alternative approach that avoids injecting excessive volume of CO_2 while increasing the amount of contacted oil (Lake, 1989; Ghaderi and others, 2012). The WAG process takes advantage of sweep efficiency enhancement during water flooding and displacement efficiency improvement during CO_2 flood to achieve incremental oil production (Kulkarni and Rao, 2005).

Six cases were designed to investigate the EOR performance of CO_2 WAG in the model. The reservoir pressure was restored using the same approach as the continuous CO_2 cases by continuously injecting CO_2 with the maximum rate of 3 MMscf/d in both Wells A and E and shutting the production Wells B, C, and D for 2 years. Then, the production wells were opened, and the injection wells were switched to a cyclic CO_2 and water injection mode with 1 month of CO_2 injection followed by 1 month of water injection. The simulations of the six cases ran for an additional 28 years. Detailed constraints setup for the injection and production wells are summarized in Table D-4.

Table D-4. Constraints Setup of the Injection and Production Wells for CO_2 WAG Investigation

Case No.	Injection Wells						Production Wells				
	CO_2 Injection Rate, MMscf/d			Water Injection Rate, bpd			Maximum Liquid Production Rate, bpd				Minimum BHP, psi
	Well A	Well E	Total	Well A	Well E	Total	Well B	Well C	Well D	Total	
10	3	3	6	500	500	1000	97	93	380	570	2500
11	4	4	8	560	560	1120	110	106	434	650	
12	5	5	10	620	620	1240	124	120	488	732	
13	6	6	12	680	680	1360	137	133	542	812	
14	7	7	14	740	740	1480	151	147	596	894	
15	8	8	16	800	800	1600	164	160	650	974	

All the CO_2 WAG cases showed BHP no less than 2500 psi in all the production wells during the 28-year prediction period, as shown in Figure D-14. The average reservoir pressure was maintained above MMP of 3150 psi for 28 years, as shown in Figure D-15b. The pressure made CO_2 miscible with crude oil in the reservoir. The production gas oil ratio was below 0.5 MMscf/bbl during 28 years of production, as shown in Figure D-15a.

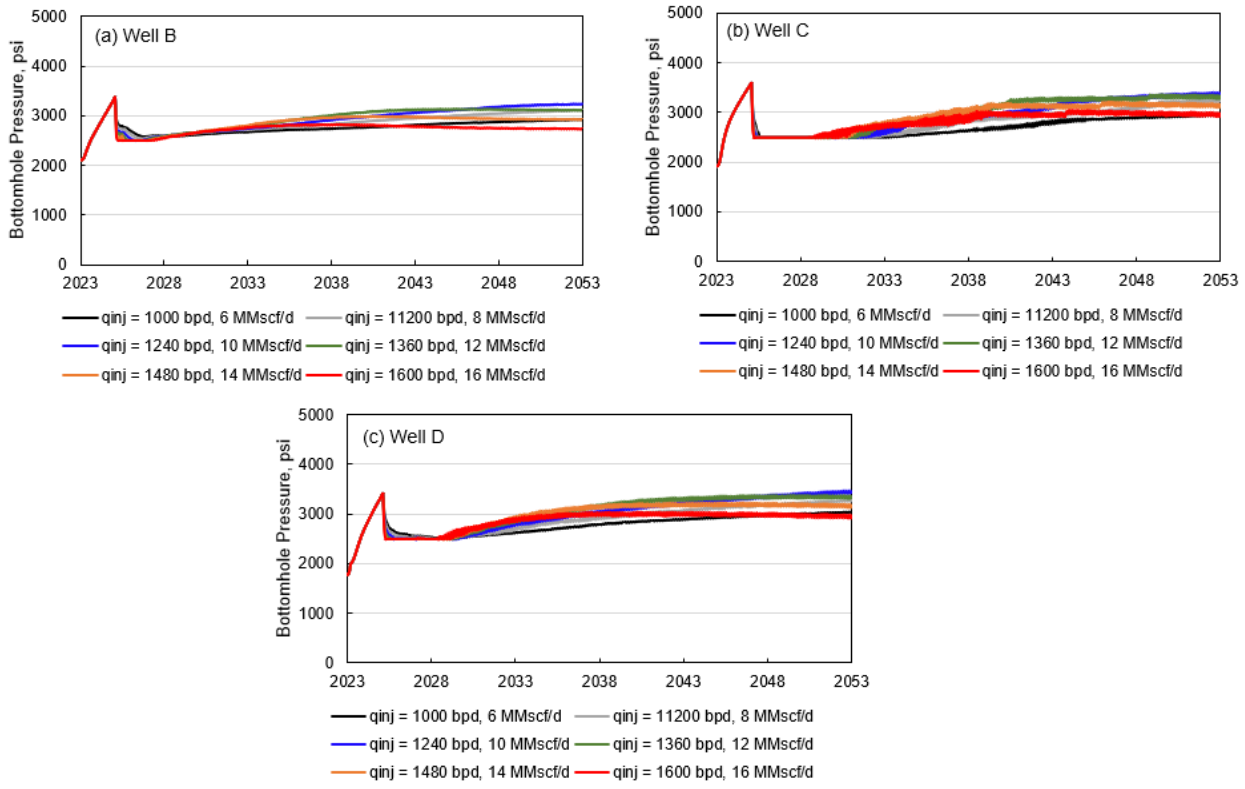

Figure D-14. BHP behavior in Wells (a) B, (b) C, and (c) D in CO_2 WAG operations. qinj provides the total CO_2 injection rates and the total water injection rates of Wells A and E during each CO_2 and water injection cycle.

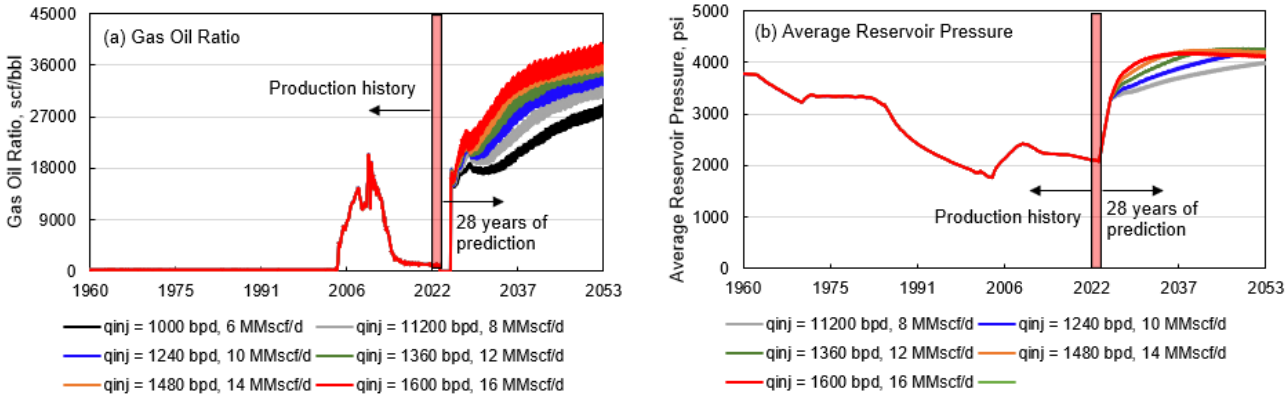

Figure D-15. Development of (a) production gas oil ratio and (b) average reservoir pressure during the production history and 30-year prediction period for Cases 10–15. The red box represents 2 years of injecting CO_2 injection in Wells A and E with all production wells shut-in.

The production performance of the CO_2 WAG cases is shown in Figure D-16. The results showed that with increasing CO_2 and water injection rates in the injection wells, the additional cumulative production of liquid, oil, water, and gas during the 30-year prediction period increased. Injecting with a total CO_2 injection rate of 16 MMscf/d and a total water injection rate of 1600 bpd contributed to the maximum additional cumulative oil production of 2,257,019 bbl.

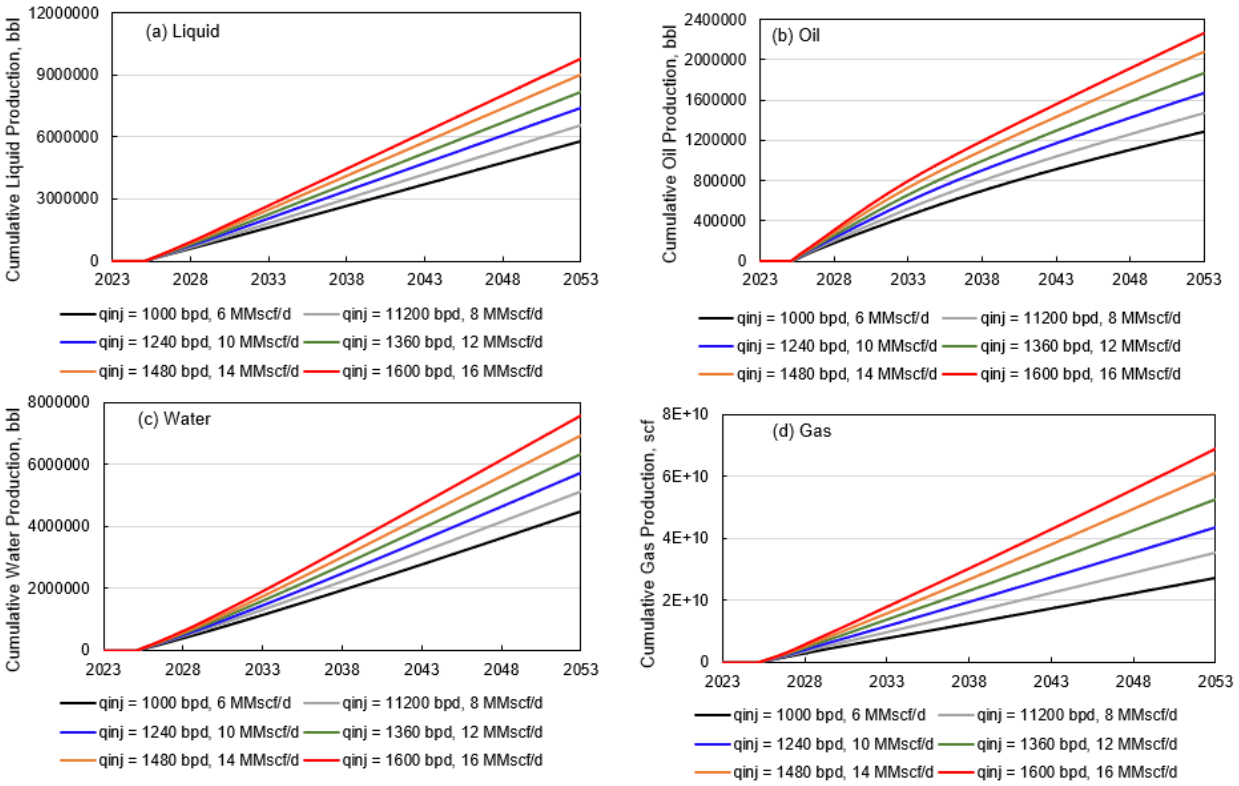

Figure D-16. Comparison of (a) cumulative liquid production, (b) cumulative oil production, (c) cumulative water production, and (d) cumulative gas production during 30 years of continuous CO_2 WAG prediction for Cases 10–15. Cumulative production represents the total production accumulated since 7/1/2023 in the prediction period; qinj is the total CO_2 injection rate of Wells A and E.

Comparison of Oil Production Strategies

In order to have a better evaluation of the improved oil production performance through water and/or CO_2 flooding, a no-injection scenario (Case 16) was designed to predict the oil production behavior by pressure depletion only in the target section. Wells A and E were shut-in in Case 16 during the 30 years of prediction, while Wells B, C, D were shut-in for 2 years and reopened with a minimum BHP of 500 psi and maximum liquid rates of 1215 bpd, respectively, in the remaining 28 years. Table D-5 shows the comparison of the cases with the maximum oil production from water flooding (Case 5), continuous CO_2 flooding (Case 9), CO_2 WAG (Case 15), to the no-injection scenario (Case 16).

Table D-5. Injection and Production Performance the Water Injection, Continuous CO_2 Injection, and CO_2 WAG, as well as the No-Injection Cases in 30 years of Prediction

	Total Amounts of Injection		Total Amounts of Production				Final Reservoir Pressure, psi
Scenario	Water, bbl	CO_2, MMscf	Liquid, bbl	Oil, bbl	Water, bbl	Gas, MMscf	
Water Inj.	20,422,840	0	18,353,961	1,309,472	17,044,490	704	2,942
Continuous CO_2	0	85,954	3,337,751	1,486,622	1,851,129	73,890	3,434
CO_2 WAG	7,517,540	82,870	9,830,433	2,257,019	7,573,415	69,109	4,135
No Inj.	0	0	4,453,219	1,020,869	3,432,350	1566	896

The table shows that both water and CO_2 injection could yield more oil production and maintain pressure in the reservoir. The CO_2 WAG case generated the greatest amount of oil during the prediction period and resulted in the highest average reservoir pressure at the end of production operations. Compared to the water-flooding scenario, CO_2 WAG required less water injection and production. CO_2 WAG also required less volume of CO_2 for injection when compared with the continuous CO_2 injection scenario.

Compared to the continuous CO_2 injection case, the CO_2 WAG case maintained a lower production gas oil ratio during the 28-year prediction period, as shown in Figure D-17a. Since more CO_2 was injected in the continuous CO_2 injection case than the CO_2 WAG case, the results indicated that CO_2 could be used more effectively for improving oil production through WAG operations. Two years of water and CO_2 injection yielded a similar reservoir pressure build-up trend, and the pressure maintained above 2500 psi in the remaining 28 years, as shown in Figure D-17b. For the no-injection case, the reservoir pressure was maintained when no production was conducted in the initial 2 years, but the pressure gradually declined in the remaining 28 years as the production wells were reopened for production, as indicated by the black line in Figure D-17b.

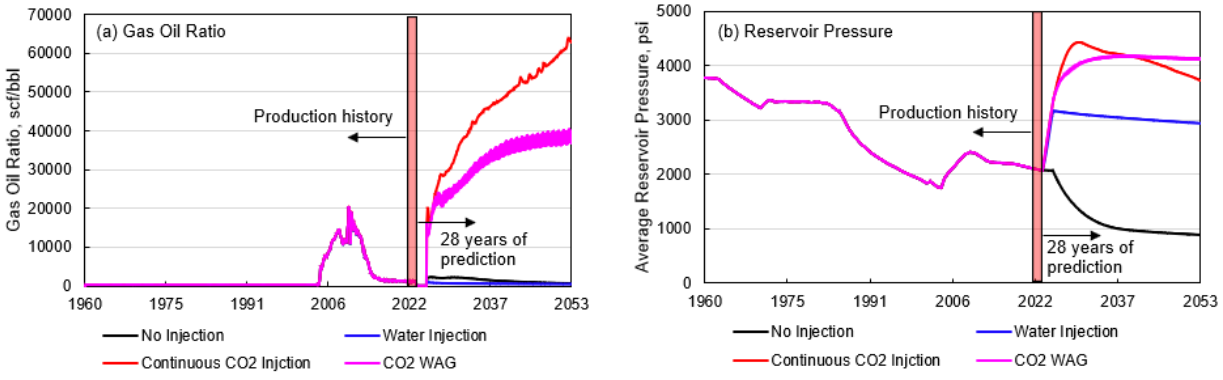

Figure D-17. Development of (a) production gas oil ratio and (b) average reservoir pressure during the production history and 30-year prediction period for different production scenarios. The red box represents the 2 years of reservoir pressure stabilization or build-up period.

Despite the no-injection case having the same liquid production rate constraint set up as the water injection case, the total liquid production of the no-injection case is much less because of rapid reservoir depletion, as shown in Figure D-18a. Water injection ensures that the production wells produced with total liquid rate of 1800 bpd throughout the 28 years of prediction, contributing to 28% higher oil production than the no-injection case, as shown in Figure D-18b, but at the expense of producing excessive amounts of water, as shown in Figure D-18c. The continuous CO_2 injection case was conservative compared to other selected cases by limiting the maximum total liquid production rate to 327 bpd to maintain high reservoir pressure. Continuous injection of CO_2 resulted in more oil production compared to the optimum water injection and no-injection cases at the end of the prediction period, as shown in Figure D-18b, but led to the highest volume of gas production at the end of the prediction period, as shown in Figure D-18d, although the liquid production was the least among the selected cases. The CO_2 WAG case took advantage of the benefits of both water and CO_2 flooding operations. WAG allowed the production wells to produce with a maximum liquid rate of 974 bpd while maintaining high reservoir pressure, as shown in Figure D-17b. The CO_2 WAG case achieved total oil production improvements of 52% compared to the continuous CO_2 injection case and 72% compared to the water-flooding case at the end of the prediction period.

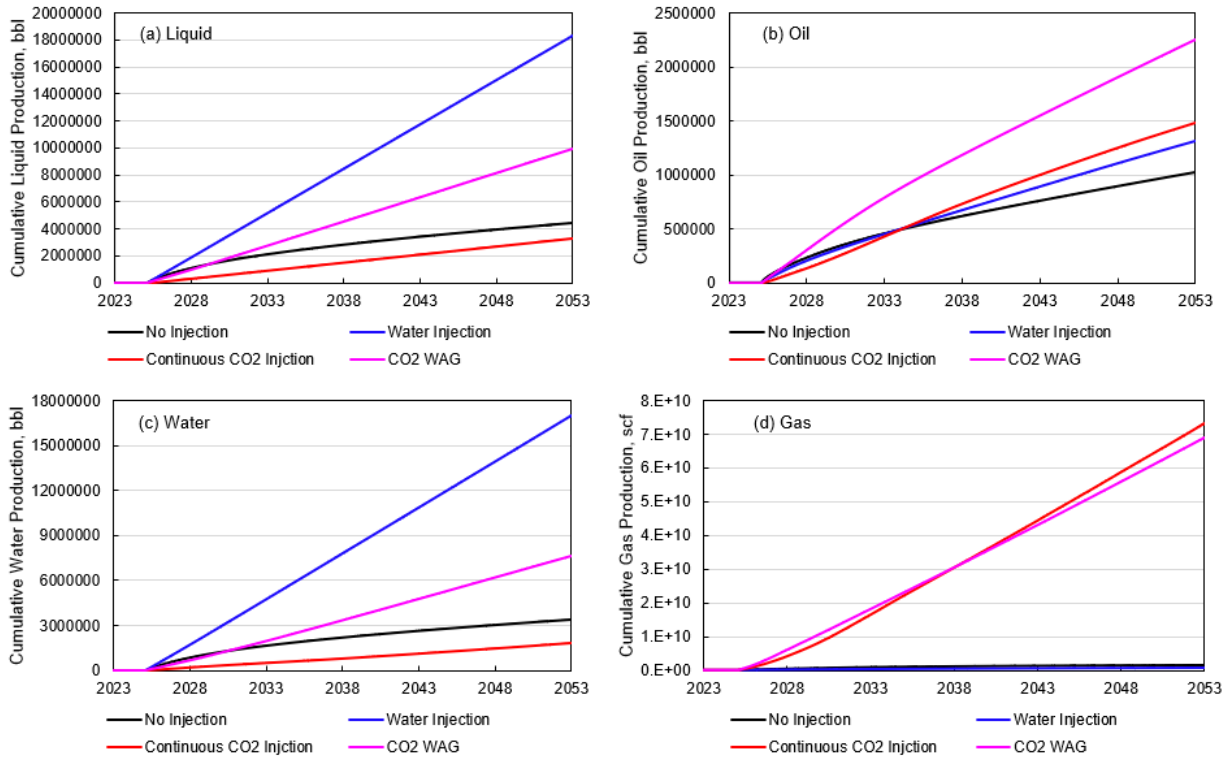

Figure D-18. Comparison of (a) cumulative liquid production, (b) cumulative oil production, (c) cumulative water production, and (d) cumulative gas production during 30-year prediction period for different production scenarios. Cumulative production represents the total production accumulated since 7/1/2023 in the prediction period.

Infill Well Drilling

The previous production strategy case showed that a proper design of CO_2 WAG could produce 2,257,019 bbl of oil in 28 years of prediction, which was equivalent to an average of 221 bpd using the three existing production wells. The results implied that a significant amount of oil was left in the reservoir and drilling infill wells could be an alternative strategy to produce oil from the model. An infill well drilling prediction model was developed by adding three infill wells (Infill1, Infill2, and Infill3) to the existing reservoir model, as shown in Figure D-19. By the end of the production history, the oil saturation surrounding the existing injection wells A and E was low (<0.4) due to years of water injection. However, other areas were less impacted by water injection because of strong heterogeneity. Therefore, two infill wells (Infill1 and Infill2) were selected to be drilled in the high oil saturation areas; another infill well (Infill3) was placed to the low oil saturation area for oil production performance comparison.

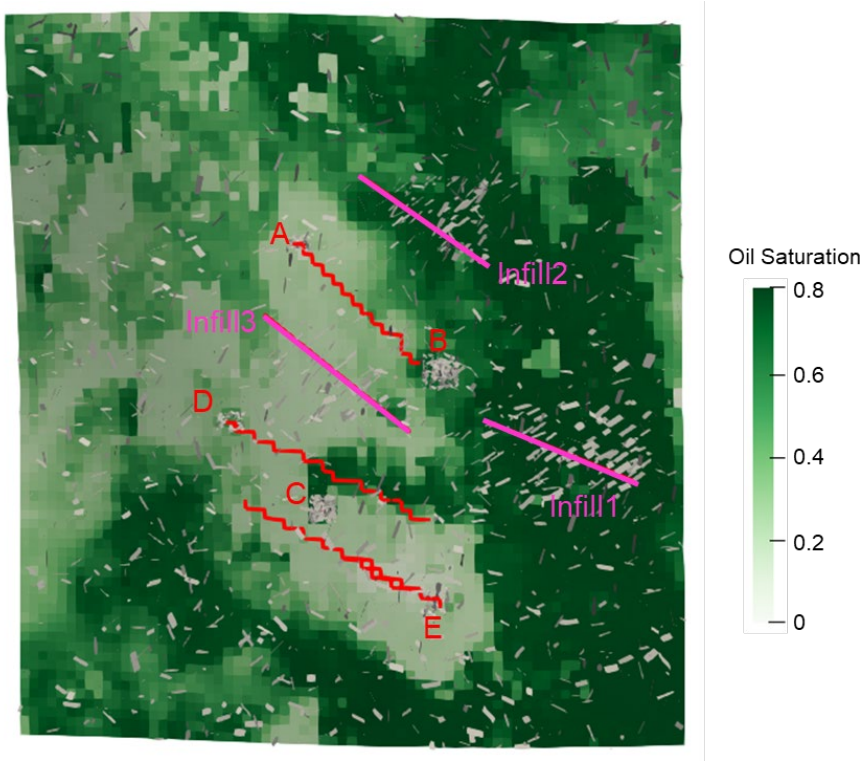

Figure D-19. Distribution of oil saturation in a layer of the pay zone in the model at the end of production history with both existing and infill wells.

To investigate the production performance of the added infill wells, five predictive cases (Cases 17–21) were developed, as shown in Table D-6. The existing injection and production were open with fixed water injection rates and maximum liquid production rates in the 30-year prediction period. The total volume of water injection is equal to the total volume of liquid production in the existing wells for the five cases to investigate the production performance of infill well drilling in the following situations:

Table D-6. Constraints Setup of the Injection and Production Wells in 30 years of Prediction for the Infill Well Drilling Model

	Injection Wells			Production Wells							
	Water Injection Rate, bpd			Maximum Liquid Production Rate, bpd							Minimum
Case No.	Well A	Well E	Total	Well B	Well C	Well D	Infill1	Infill2	Infill3	Total	BHP, psi
17							0	0	0	200	
18							100	0	0	300	
19	100	100	200	50	50	100	100	0	100	400	500
20							100	100	0	400	
21							100	100	100	500	

- Case 17: all infill wells were closed.
- Case 18: one infill well at the high oil saturation area was open.
- Case 19: two infill wells at the low and high oil saturation areas were open.
- Case 20: two infill wells at the high oil saturation area were open.
- Case 21: all infill wells were open.

The production performance of the five infill well drilling cases is shown in Figure D-20. The results suggest that opening more infill wells contributed to higher additional oil production in 30 years of prediction. Opening all infill wells could generate an additional 1,576,075 bbl of oil production in 30 years. A comparison of Cases 19 and 20 suggested that opening Infill1 and Infill2, which were located at the high oil saturation areas, could yield better oil production performance in the studied area. The results implied that the location for infill well drilling should be selected at the high oil saturation areas and be away from the existing water injection wells.

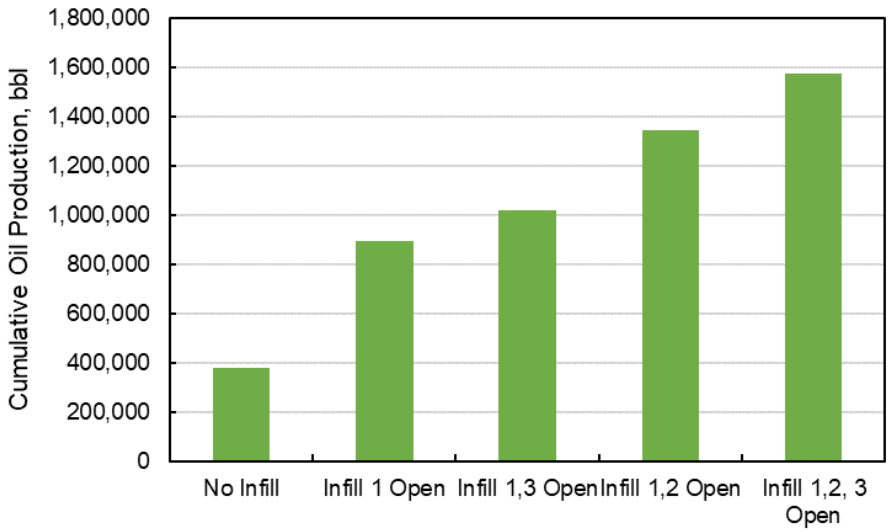

Figure D-20. Comparison of field additional cumulative oil production for Cases 17–21 of the infill well drilling scenario. Cases 17–21 represent the following situations: all infill wells are closed; one infill well at the high oil saturation area is open; two infill wells at the low and high oil saturation areas are open; two infill wells at the high oil saturation area are open; and all infill wells are open.

Summary of the Results

This section investigated potential strategies for revitalizing a legacy carbonate oil field producing from the Red River Formation using the fractured reservoir modeling and simulation workflow developed in this project. A baseline reservoir model was developed based on the available well data and geological information using the embedded discrete fracture model (EDFM) method, which enabled natural fractures to be included in the model. History matching was performed to ensure that the simulation results captured the injection and production performance of wells and reproduced the flow behaviors in the reservoir. 16 prediction cases were designed based on the baseline reservoir model to analyze, compare, and improve strategies including water injection, continuous CO_2 injection, and CO_2 WAG. These cases were simulated by repressurizing the reservoir with water or CO_2 injection and production suspension for 2 years, then resuming production with changing injection and production constraints for another 28 years. Five additional prediction cases were developed by adding three infill wells to the existing reservoir model to investigate the potential oil production improvement via production from different numbers of infill wells. The findings for this evaluation are summarized as follows:

- Injecting water or CO_2 while suspending production ensured that the reservoir pressure was restored so that the target liquid production rate could be achieved when production was resumed.

- The improved cases of the water injection, continuous CO_2 injection, and CO_2 WAG showed better oil production and reservoir pressure responses than the no-injection case.

- Increasing the water injection rate contributed to improvement in oil production. Injecting water with a total water volume of 20,422,840 bbl resulted in 1,309,472 bbl of oil production in 30 years.

- Increasing the CO_2 injection rate resulted in an increase in oil production. Continuously injecting 85,954 MMscf of CO_2 contributed to 1,486,622 bbl of oil production in 30 years.

- High-rate water injection could yield more oil production at the expense of treating significant amounts of produced water.

- CO_2 WAG had benefits of both water injection and CO_2 injection to achieve better EOR performance. By cyclically injecting 82,870 MMscf of CO_2 and 7,517,540 bbl of water, 2,257,019 bbl of oil production was achieved in 30 years.

- Drilling new infill wells could contribute to additional oil production. The simulation results showed that 1,576,075 bbl of oil production could be achieved via production from all the existing production wells and the added infill wells.

References

Ghaderi, S.M., Clarkson, C.R., and Chen, S., 2012, Optimization of WAG process for coupled CO_2 EOR-storage in tight oil formations—an experimental design approach, *in* SPE Canada Unconventional Resources Conference: Calgary, Alberta, Canada, p. SPE-161884.

Kulkarni, M.M., and Rao, D.N., 2005, Experimental investigation of miscible and immiscible water-alternating-gas (WAG) process performance: Journal of Petroleum Science and Engineering, v. 48, nos. 1–2, p. 1–20.

Lake, L.W., 1989, Enhanced oil recovery: Englewood Cliffs, New Jersey, Prentice-Hall, 550 p.

Montgomery, S.L., 1997, Ordovician Red River "B"—horizontal oil play in the southern Williston Basin: AAPG Bulletin, v. 81, no. 4, p. 519–532.

Sheng, J.J., 2010. Modern chemical enhanced oil recovery: theory and practice. Gulf Professional Publishing, 648 p.

APPENDIX E

GEOENERGY SCIENCE ARTICLE DEVELOPMENT OF A NEW CO_2 EOR SCREENING APPROACH FOCUSED ON DEEP-DEPTH RESERVOIRS

GEOENERGY SCIENCE ARTICLE DEVELOPMENT OF A NEW CO_2 EOR SCREENING APPROACH FOCUSED ON DEEP-DEPTH RESERVOIRS

Development of a New CO_2 EOR Screening Approach Focused on Deep-Depth Reservoirs
https://doi.org/10.1016/j.geoen.2023.212335